# ENERGY AND EXERGY STUDIES ON RECOVERY FROM WET-ETHANOL FUELLED HCCI ENGINE FOR PERFORMANCE ENHANCEMENT AND AIR CONDITIONING

*A thesis submitted in partial fulfillment*

*of the requirement of the degree of*

***Doctor of Philosophy***

*In*

***Mechanical Engineering***

By

**MOHD ASJAD SIDDIQUI**

**(2K18/PhD/ME/17)**

***Under Supervision of***

**Dr. Rajesh Kumar**
**Professor**
Department of Mechanical Engineering,
Delhi Technological University, Delhi

**Dr. Abdul Khaliq**
**Professor**
Department of Mechanical Engineering,
Taibah University, Government of Saudi Arabia


**DEPARTMENT OF MECHANICAL ENGINEERING**

**DELHI TECHNOLOGICAL UNIVERSITY**

**Delhi-110042**

**February- 2022**

*Dedicated to*

*My Family*

# CERTIFICATE

This is to certify that the work embodied in the research plan entitled **"Energy and Exergy Studies on Recovery from Wet-Ethanol Fuelled HCCI Engine for Performance Enhancement and Air Conditioning"** has been completed by Mr. **Mohd Asjad Siddiqui (Roll No.- 2K18/PhD/ME/17)** under the guidance of Prof. Rajesh Kumar, Professor, Department of Mechanical Engineering, DTU and Prof. Abdul Khaliq, Professor, Department of Mechanical Engineering, Taibah University, Government of Saudi Arabia, towards partial fulfilment of the requirements for the degree of Doctor of Philosophy of Delhi Technological University, Delhi. This work is based on original research and has not been submitted in full or in part for any other diploma or degree of any university.

**Prof. Rajesh Kumar**

Professor

Dept. of Mechanical Engineering

DTU, Delhi

**Prof. Abdul Khaliq**

Professor

Dept. of Mechanical Engineering

Taibah University,

(Government of Saudi Arabia)

# ACKNOWLEDGEMENT

First of all, I am highly indebted and thankful, Almighty Allah, the most merciful and benevolent to all, who thought man that which he knew note and bestowed the man with epistemology and gave him the potential to ameliorate the same. It is his blessing, which inspired and enabled me to complete this work. It is my pleasant duty to acknowledge the help received from several individuals during this work.

It is my great pleasure to express my profound gratitude to my guide **Prof. Rajesh Kumar**, Professor, Department of Mechanical Engineering, DTU and **Prof. Abdul Khaliq**, Professor, Dept. of Mechanical Engineering, Taibah University, Government of Saudi Arabia, for their illuminative and precious guidance, constant supervision, critical opinion and timely suggestion, constant beneficial encouragement and technical tips which have always been a source of inspiration during the preparation of the thesis. Their valuable comments and advice gave me the confidence to overcome the challenges in formulating this thesis.

I pay my sincere thanks to **S.K. Garg**, Head of Department and DRC Chairman (Dept. of Mechanical Engineering), for giving me an opportunity to do research. I am thankful to all faculty members and technical staff of the department for their guidance and help.

Last but not least, I would like to express my special thanks to my parents for their tremendous support, continuous motivation, unconditional love and encouragement throughout the years.

**MOHD ASJAD SIDDIQUI**

(Roll No.- 2K18/PhD/ME/17)

Delhi Technological University,

Delhi-110042

# ABSTRACT

Blending of ethanol especially with gasoline has become quite common in developing countries like India but the barriers for its application as a primary fuel to internal combustion engines have not been overcome yet. Detailed study on ethanol production from corn shows a slightly energetic advantage and estimated the net energy gain of 20%. In order to obtain further net-energy gain and hence to lower the energetic cost of changing ethanol to utilizable form, development of new utilization techniques needed. Utilization of ethanol-water mixture (wet-ethanol) in combustion engines by eliminating the energy spent in removal of water may significantly increase the net energy gain, from 21% to 55%. HCCI engines can exploit wet-ethanol more effectively than the traditional engines and hence can be considered as a suitable mode of combustion for the direct utilization of wet-ethanol as a primary fuel.

Renewable fueled HCCI engines have been analyzed using a traditional method of analysis based on first law of thermodynamics which cannot show how or where the irreversibilities in the system or process occur and hence it does not provide further insight into the overall thermodynamics of the phenomena. On the other hand, second law of thermodynamics allows the identification of various processes where most exergy destruction of working medium occurs. Reduction of those irreversibilities and exergy losses can lead to an effective exploitation of a renewable fuel in HCCI engines. Second law investigations carried out on HCCI engines shows that a majority of thermodynamic losses occurs during the HCCI combustion process and thermal energy exhaust to the ambient. It is calculated that a larger portion of the fuel energy is expelled as waste enthalpy in the hot exhaust gases, resulting in a substantial quantity of exergy being emitted from the system. It has been determined that recovering part of the thermal energy contained in exhaust gases is worthwhile in the development of more effective and environmentally friendly combustion engines.

In this regard, present thesis provides a two-folded methodology to increase the work output and fuel conversion efficiency of HCCI engine fueled by wet-ethanol. First, a detailed exergy analysis of HCCI engine was developed and performed operating on an advanced combustion strategy with wet-ethanol. Second, a theoretically driven, computational exergy analysis methodology of exhaust flows to characterize the exhaust exergy was introduced and implemented on a HCCI engine. In this regard, an exergy analysis framework is developed to quantify fuel exergy transformations in HCCI engine combined with the waste heat driven cooling systems. Then, the study leading to variation of exergy components and the effect of operating conditions on exergy distribution and irreversibilities were conducted. A detailed investigation was made first, to recover the energy and exergy accompanied by engine exhaust gases to drive the novel thermodynamic cycles producing the cogeneration of power and cooling. Additional generation of cooling and power through engine exhaust heat is expected to provide the economic benefits and improves the engine overall efficiency without supplying the additional fuel. Obligatory standards concerning the weight of the empty vehicle disregard the use of absorption refrigeration cycles (ARC) as they are bulky, expensive and complex in design. To surmount this limitation, ERC (ejector refrigeration cycle) is found to be a promising option as it avoids the use of mechanical compressor and CFC's. Moreover, ejectors are more compact and easier to maintain than compression and absorption cooling systems. In this context, a novel configuration consists of an organic Rankine cycle combined with the ejector is applied as the most potential means to recover the wet-ethanol fueled HCCI engine exhaust heat to produce cooling and power in an energy efficient, less expensive and eco-friendly manner. The developed combined system of cooling-power cogeneration was simulated by Engineering Equation Solver (EES) software. Combined system responses to altering the operative conditions on the energy and exergy performances are ascertained to obtain guidance for system design. The results are computed for R134a, R290, and R600a working fluids. Increase in turbocharger pressure ratio from 2.5 to 3.5

raises the thermal efficiency of cooling-power cogeneration from 47.87% to 50.09% when R134a is used as working fluid. Cooling capacity and exergy of refrigeration are decreased by greater than 2.0% in case of R134a operated system when the vapor generator pressure is elevated from 1800 kPa to 2200 kPa. Increase in evaporator pressure of ERC from 327.4 kPa to 348.7 kPa is greatly beneficial to thermodynamic performance of cogeneration and its cooling capacity is improved by 11.34% when R134a is utilized as the working. When $P_{Evap}$ rises from 175.7 kPa to 186.9 kPa and R600a is employed as the working fluid, the cooling capacity is increased by 12.58%.

In order to determine the comparative waste heat recovery potential of heat driven cooling systems an HCCI engine fueled by wet-ethanol was proposed to be bottomed with the ERC and ARC, separately, to recover the exhaust heat for refrigerating the thermal load of vehicle air conditioning. A comparative thermodynamic analysis of proposed cooling-power cogeneration was conducted by considering the quality and quantity of energy transfers during the energy conversion processes of the cycle. Energetic and exergetic performances of cogeneration cycle was assessed by altering the following parameters; turbocharger pressure ratio, turbocharger compression efficiency, and ambient temperature. In addition, the distribution of fuel energy supplied in terms of energy produced and energy lost as well as the breaking down of exergy of fuel supplied into the exergy produced, exergy destruction in the major components of cogeneration cycle, and the loss of exergy due to thermal exhaust to ambient is also computed, graphed, and discussed. The contribution of exergy destruction is scrutinized and debated in regard of cycle performance improvement. Results are derived for the employment of R134a as the refrigerant of ERC and LiBr-$H_2O$ mixture as the working fluid pair for the ARC. Further, the COP of both ERC and ARC were computed with the variation in the entrainment ratio and generator temperature, respectively.

Results show that elevated pressure of turbocharger results in the enhancement of HCCI engine power and increase of the refrigeration of thermal load, simultaneously. However, ambient

temperature rising shows the decline of HCCI engine efficiencies and energy efficiency of cogeneration while the cogeneration cycle exergy efficiency is found increasing. Furthermore, the results are reported for the refrigeration performed by LiBr-$H_2O$ operated ARC, and R134a and R290 operated ERC, respectively. Mapping of exergy destruction for the cogeneration cycle studied discovered HCCI engine, boiler of ERC, generator of ARC, and catalytic convertor as the components of significant exergy destruction. Entrainment ratio and type of refrigerant employed in ERC and the generator temperature of ARC shows a marginal impact on the COPs of these cycles. It was noticed that an increase in pressure ratio across the turbocharger from 2.5 to 3.5 raises the HCCI engine first law efficiency from 44.09% to 46.32%, and for cogeneration it is increased from 47% to 49.21% when R134a is used as ERC refrigerant and from 46.06% to 48.29% when R290 is the ERC refrigerant, and in case of ARC bottoming it is increased from 55.08% to 57.25%.

Furthermore, a relatively new thermodynamic model was also developed in EES to compare the performance of HCCI engine operating on natural gas and wet-ethanol, and a new type of ejector technology was employed to recover the exhaust heat of a natural gas fueled HCCI engine to simultaneously refrigerate the thermal load of air conditioning and low temperature refrigeration. A shaft power driven two-phase ejector which consists of a hermetic reciprocating compressor, an air cooled condenser, a separator, and two evaporators for combined production of refrigeration and air conditioning and integrated to HCCI engine operated on natural gas engine was employed as it was found novel for current investigation. The development of such a cooling-power cogeneration has been found to possess three fold benefits; cooling produced by low temperature evaporator will refrigerate a thermal load for food and vaccine preservations and the cooling produced by high temperature evaporator will provide cabin cooling or air conditioning of vehicle, and decrease in exhaust temperature due to waste heat recovery will reduce the thermal pollution. Energetic and exergetic investigations were carried out to study the role of equivalence ratio,

engine speed, condenser temperature, refrigeration evaporator temperature, air conditioning evaporator temperature, and ejector nozzle efficiency on the thermodynamic performance parameters of the combined cycle. The analysis of two-phase ejector cooling cycle using three working fluids including R717, R290, and R600a is conducted. Results reveal that the thermal efficiency of HCCI engine is increased from 47.44% to 49.94%, and for the R600a operated combined cycle it is increased from 60.05% to 63.26% when the equivalence ratio is promoted from 0.3 to 0.6. Distribution of fuel exergy results show that out of 100% exergy input, in case of R717 operated combined cycle, 139.79 kW (38.72%) is the total exergy output and 164.21 kW (45.49%) and 57 kW (15.79%), are the values for exergy destruction and exergy losses. It is further shown that change in refrigerant minorly influence the percentages of exergy distribution.

Finally, an important existing knowledge gap was covered by introducing a methodology for performing a detailed exergy analysis of exhaust flows from the perspective of exhaust waste energy recovery in HCCI engine for cooling production. The physical exergy of a flowing stream and its thermal and mechanical components along with the chemical exergy of fuel and the subsequent mixture of gases are computed by combining the thermodynamic formulations developed in this study.

# LIST OF PUBLICATIONS

1. **Mohd Asjad Siddiqui,** Abdul Khaliq, Rajesh Kumar. Proposal and analysis of a novel cooling-power cogeneration system driven by the exhaust gas heat of HCCI engine fuelled by wet-ethanol, Energy, Vol. 232, pp. 120954, 2021. https://doi.org/10.1016/j.energy.2021.120954 **(Published) (SCIE indexed)**
2. **Mohd Asjad Siddiqui,** Abdul Khaliq, Rajesh Kumar. Thermodynamic and comparative analysis of ERC and ARC integrated wet-ethanol fueled HCCI engine for cogeneration of power and cooling, **ASME Transactions J. Thermal Sci. Eng. Appl.,** Vol. 14(4) pp. 041003, 2022. https://doi.org/10.1115/1.4051632 **(Published) (SCIE indexed)**
3. Abdul Khaliq, Bandar A. Almohammadi, Mathkar A. Alharthi, **Mohd Asjad Siddiqui**, Rajesh Kumar. Investigation of a combined refrigeration and air conditioning system based on two-phase ejector driven by exhaust gases of natural gas fueled homogeneous charge compression ignition engine, **ASME Transactions J. Energy Resour. Technol.,** Vol. 143 pp. 120911, 2021. https://doi.org/10.1115/1.4052248 (**Published**) (**SCIE indexed**)
4. **Mohd Asjad Siddiqui**, Abdul Khaliq, Rajesh Kumar. Thermodynamic analysis of exhaust waste heat recovery from turbocharged HCCI engine fueled by wet-ethanol using an Absorption Refrigeration Cycle (ARC), *Paper presented at*: 1st International conference on Technology Innovation in Mechanical Engineering; 2021 May 10-11; Bhopal, India.
5. **Mohd Asjad Siddiqui**, Abdul Khaliq, Rajesh Kumar. Thermodynamic investigations of a turbocharged homogeneous charge compression ignition (HCCI) engine running on wet-ethanol, *Paper presented at*: 1st International conference on Technology Innovation in Mechanical Engineering; 2021 May 10-11; Bhopal, India

# TABLE OF CONTENTS

# LIST OF FIGURES

# LIST OF TABLES

# NOMENCLATURE

**Abbreviations**

| | |
|---|---|
| ARC | Absorption Refrigeration Cycle |
| ARS | Absorption refrigeration system |
| ERC | Ejector refrigeration cycle |
| HCCI | Homogeneous charge compression ignition |
| LiBr-$H_2O$ | Lithium Bromide-Water |

**Symbols**

| | |
|---|---|
| $A_{ch}$ | surface of cylinder head ($m^2$) |
| $A_{cyl}$ | surface of the cylinder ($m^2$) |
| $c_p$ | specific heat at constant pressure (kJ/kg) |
| $\dot{E}_x$ | exergy rate (kW) |
| $e_x$ | specific flow exergy (kJ/kg) |
| $e_x^{ch}$ | chemical exergy (kJ/kg) |
| $e_x^{ph}$ | physical exergy (kJ/kg) |
| $g$ | specific Gibbs function (kJ/kg) |
| $\bar{h}_f^\circ$ | enthalpy of formation on molar basis (kJ/kmol) |
| $H$ | enthalpy (kW) |
| $h$ | specific enthalpy (kJ/kg) |
| $\dot{m}$ | mass flow rate (kg/s) |
| $M$ | molar mass (kg/kmol) |
| $p_{mot}$ | pressure at motored condition (kPa) |
| $p$ | pressure (kPa) |
| $\dot{Q}$ | heat transfer per unit time (kW) |

| | |
|---|---|
| $R$ | molar gas constant (J/K mol) |
| s | specific entropy (kJ/kg-K) |
| T | temperature (K) |
| V | volume ($m^3$) |
| $\dot{W}$ | output power (kW) |

**Greek symbols**

| | |
|---|---|
| $\eta_{en}$ | energy efficiency (%) |
| $\eta_{ex}$ | exergy efficiency (%) |
| $\eta$ | efficiency (%) |
| $\mu$ | chemical potential (kJ/kg) |
| $\omega$ | mean gas velocity (m/s) |
| $\emptyset$ | equivalence ratio |

**Subscript**

| | |
|---|---|
| a | air |
| Abs | absorber |
| AC | air-conditioner |
| avr | average |
| Boi | boiler |
| BT | brake thermal |
| C | compressor |
| C1 | compressor 1 |
| C2 | compressor 2 |
| cat | catalytic |
| CC | combined cycle, catalytic convertor |
| CC1 | catalytic converter of ERC |

| | |
|---|---|
| CC2 | catalytic converter of ARC |
| ch | chemical |
| comb | combustion |
| comp | compression |
| Comp1 | compressor of ERC |
| Comp2 | compressor of ARC |
| Cond | condenser |
| Cond1 | condenser of ERC |
| Cond2 | condenser of ARC |
| D | destruction |
| Eje | ejector |
| EV | expansion valve |
| EV1 | expansion valve 1 |
| EV2 | expansion valve 2 |
| Evap | evaporator |
| Evap1 | evaporator of ERC |
| Evap2 | evaporator of ARC |
| ex | exergy |
| exh | exhaust |
| exp | expansion |
| f | fraction of residual gases |
| f | fuel |
| FM | fuel mixer |
| FV | fuel vaporizer |
| FV1 | fuel vaporizer of ERC |

| | |
|---|---|
| FV2 | fuel vaporizer of ARC |
| Gen | generator |
| HE | heat exchanger |
| HX | heat exchanger |
| i | inlet |
| LHV | Lower Heating Value |
| *n* | polytropic index, number of moles |
| o | Outlet |
| ORC | Organic Rankine cycle |
| P1 | pump of ERC |
| P2 | pump of ARC/ ORC pump |
| ph | physical |
| ref | refrigerator, reference, cooling capacity |
| Reg | regenerator |
| Reg1 | regenerator of ERC |
| Reg2 | regenerator of ARC |
| rg | residual gas |
| Sep | separator |
| sol | solution |
| surr | surrounding |
| T | turbine |
| T1 | turbine of ERC, power turbine |
| T2 | turbine of ARC, ORC turbine |
| th | thermal |
| VG | vapor generator |

| | |
|---|---|
| $x$ | mass fraction |
| $y$ | mole fraction |

# Chapter 1

# Introduction and Literature review

## 1.1 Energy demand

Human life has changed dramatically as a result of the Industrial Revolution. Steam engines, followed by IC (Internal combustion) engines and gas turbines, revolutionized industry and transportation. This has resulted in a phenomenal increase in the global population, which has risen from 700 million people at the start of the industrial age to 7.87 billion now. According to the United Nations, this population will grow to 9.7 billion in 2050 and then to 10.9 billion in 2100 [1]. The energy demand is rising throughout the world to keep up with the increasing population and improved living standards. Between 2018 and 2050, according to the International Energy Agency, energy consumption will increase by 50% [2]. According to a report published by IEA, global energy demand is expected to rise by 4.6 % in 2021, more than offsetting the 4% decline in 2020 and boosting demand above 2019 levels, as illustrated in Fig.1.1 [3].

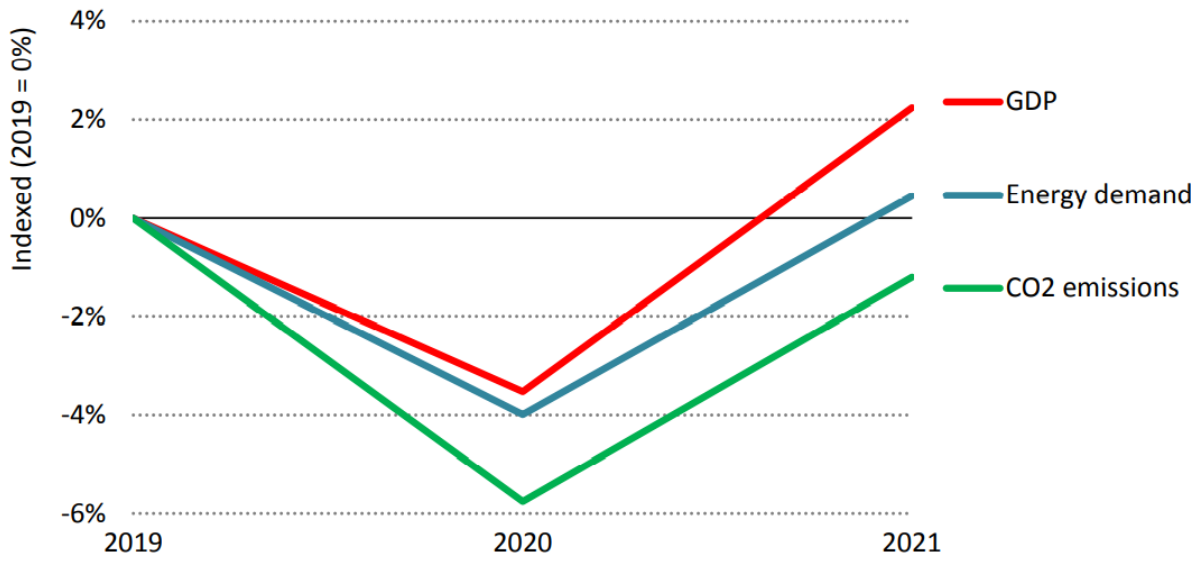


**Fig. 1.1.** In comparison to 2019, the evolution of total primary energy demand, global GDP and energy-related $CO_2$ emissions.[3]

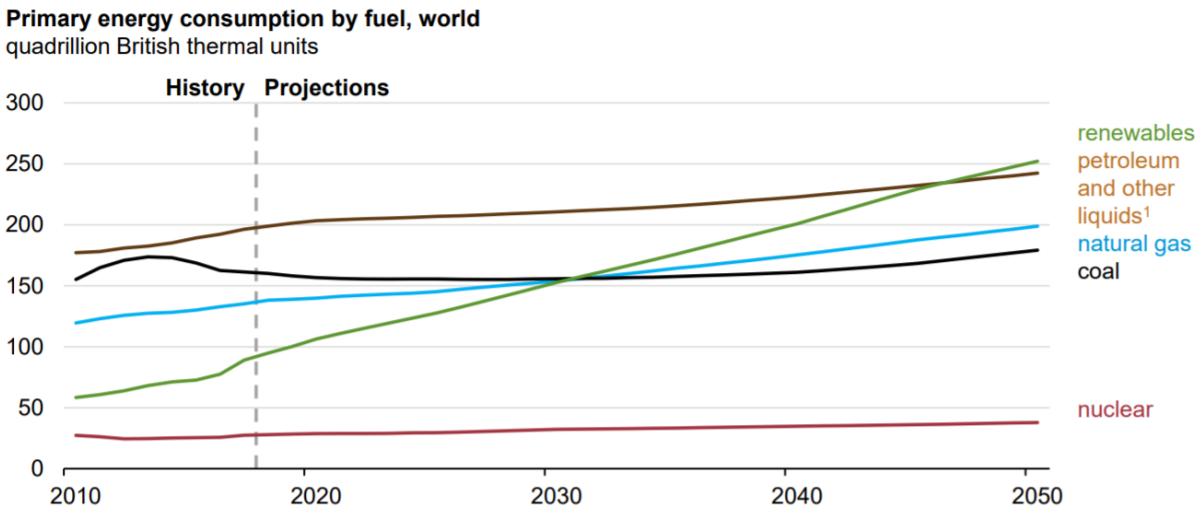


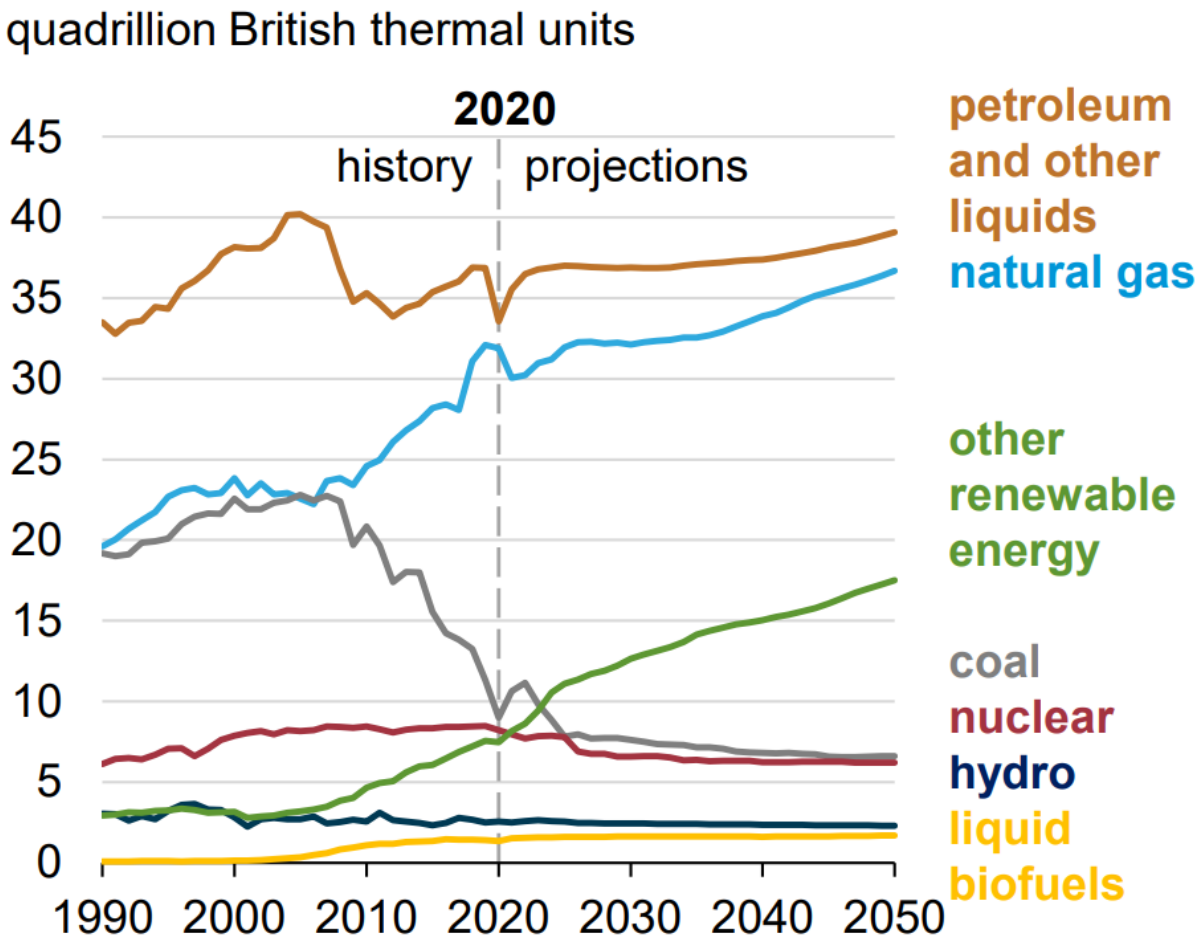


**Fig. 1.2 a)** World energy consumption by energy source [2], **b)** U.S. energy consumption by fuel [4].

Fig. 1.3 illustrates that oil demand peaks in the late 2020s and gas demand peaks in the 2030s, whilst coal demand declines steadily and is also described as [5]:

- Oil demand growth slows significantly, with a forecast peak in the late 2020s and a 10% drop by 2050, owing to slower car-park development, improved engine efficiency in road transportation, and more electrification.
- In the next ten to fifteen years, gas will continue to expand its share of global energy demand—the only fossil fuel to do so—before peaking in the late 2030s. Nonetheless, gas demand in 2050 will be 5% more than it is now.
- Between 2019 and 2050, coal consumption falls nearly 40%, owing to the phaseout of coal plants in the power industry in various zones.

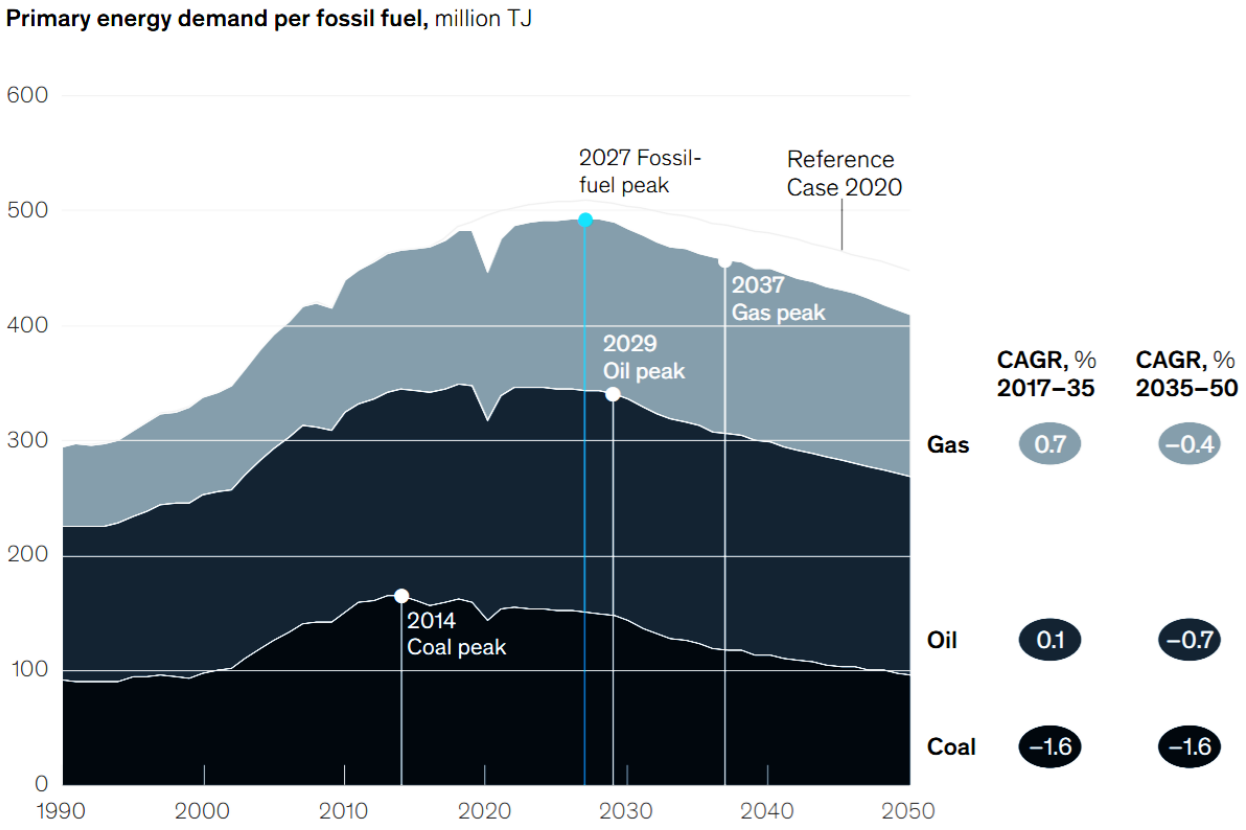


**Fig. 1.3**. Fossil fuels are still a primary source of energy for an energy system. [5]

Global demand for transportation energy is expected to elevate at a rate of 1–1.5 % annually at least 2050 [6-9] due to fast growth in population and standard of living in developing countries. Gasoline, diesel, and jet fuel are likely to dominate the transportation energy portfolio, both for

light-duty and heavy applications despite considerable development in alternative energy sources [7-9]. Furthermore, there is much evidence that there are enough crude reserves to supply this growing need [9, 10]. Global greenhouse gas emissions are a result of fossil fuel consumption, which has a negative influence on public health and climate change. As a consequence, government bodies impose strict efficiency and emissions limitations on the transportation industry. Global energy consumption and greenhouse gas emissions reduction can be achieved by improving fuel economy in the transportation sector.

Three main sources of energy supply are used to meet this high demand. Fossil fuels, nuclear power plants, and renewable energy sources are the three options. Fossil fuels are still the primary source of energy for practically all sectors, including household, transportation, and industry. Transportation is one of the world's major consumers of fossil fuels, owing to the vast number of vehicles produced globally. The production of greenhouse gases, which have a considerable negative impact on the environment, is a key concern associated with the consumption of fossil fuels. The employment of IC engines in transportation, power generation, and the commercial sector is the major source of both emissions and consumption of fuel. Cleaner fuels and more efficient combustion technology in IC engines are major solutions for reducing fuel consumption and emission in the transportation sector.

In both established and emerging countries, hybrid electric vehicles [11,12], pure electric vehicles [13–15], and fuel cell vehicles [16,17] are evolving rapidly and aggressively. Nevertheless, unless a full infrastructure is in place, some users may be turned off by the battery life, charging stations, and mileage range restrictions. Fig.1.4 shows various power units and fuel economy of a new passenger car in the recent 20 years and the next 20 years [18].

In the coming decades, the IC engine will continue to be the primary power source in passenger cars, especially in heavy-duty passenger cars [19, 21]. Furthermore, in the coming decades, fuel usage will be significantly reduced [22,23].

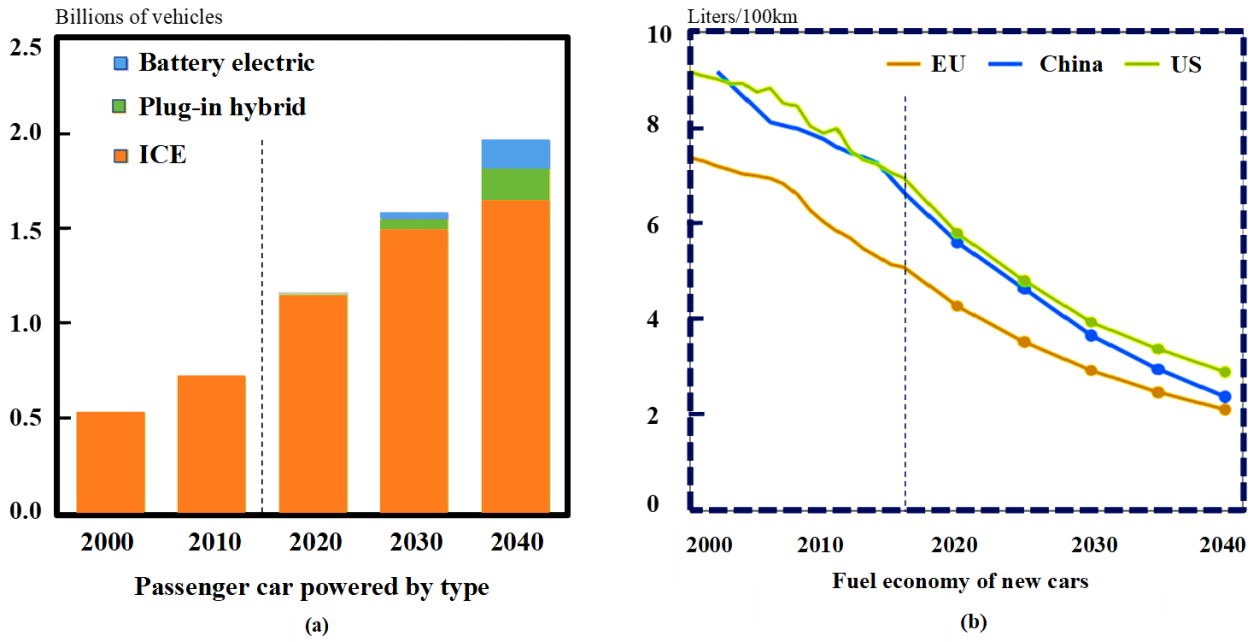


**Fig. 1.4.** The main power units and fuel economy of a passenger car.[18]

## 1.2 IC Engine

IC engines are commonly utilized in vehicles that we use on a daily basis, such as cars, motorbikes, and buses. These are also an important source of energy for the transportation of cargo and agricultural goods. As a consequence of their use in the automobile and stationary power production industries, the IC Engine has become the most widely used device or an essential component of life. The cause for its popularity could be described by its entire appearance in terms of features such as economy, performance, controllability, and durability, also the scarcity of other competing options. Internal combustion happens when a fuel is burned inside a combustion chamber with the help of an oxidizer. The piston converts the heat released by the combustion into usable mechanical power. A large number of automobiles are powered by IC engines, which consume large amounts of fossil fuel.

An increasingly efficient and easy living standard made possible by IC engines has also contributed to the environmental degradation due to the emissions from IC engines. Unburned hydrocarbons (UHC), carbon dioxide ($CO_2$), nitrogen oxides (NOx), and particulate matter (PM) are some of the harmful exhaust pollutants produced by engines after they have generated power by combusting a large amount of fuel [24]. IC engine exhaust are still a major cause of air

pollution and energy waste, despite the growing use of renewable energy for power. As a result, there is a strong need to enhance the efficiency of IC engines.

The IC engine runs in a wide range of situations, also it is crucial to study the performance of the engine at a variety of rotational loads and speeds in order to simulate a variety of real-world conditions. Studies on IC engines have been ongoing since 1876 when they were first invented. It is possible to predict engine performance using computer-aided approaches, which can contribute to the development of more efficient engines. Therefore, in order to design appropriate progress in improving IC engine performance, researchers must continue to employ basic methods is used to predict the link between the thermal fluid variables in IC engines.

Spark Ignition (SI) and Compression Ignition (CI) engines are the two most common forms of IC engines nowadays. In terms of efficiency and pollutant emissions, both methods have their benefits and drawbacks.

### 1.2.1 Spark Ignition (SI) engines

The combustion of a homogenous air-fuel mixture defines SI engines, often known as Otto or gasoline engines. The near-stoichiometric fuel-air mixture is compressed in the actual Otto cycle. A carburetor has traditionally been used to add gasoline to the inducted air, but current SI engines use a fuel injection system to transfer fuel into the combustion chamber. In the most usual condition, compression ratios are around 10:1, with pre-ignition cylinder pressures around 700 kPa and maximum pressures around 2000 kPa [25]. Before the piston compresses the fuel, it is premixed with air and injected into the inlet port. Due to the extreme volatility of the liquid fuel used in SI engines, a spark plug is employed to ignite the mixture near the Top Dead Center (TDC), resulting in premixed turbulent flame combustion. Because of this combustion approach, it is susceptible to self-ignition, or "knocking," that can cause damage to the structure, particularly to the piston. The SI engine's compression ratio is limited as a result of this phenomena, which reduces thermal performance. The octane number of the fuel determines the degree of knocking resistance of the fuel for the SI engines.

Because the pressures are limited, the SI engine may use higher rpm's to achieve high specific power because the compression ratio is lower. As a result, a more lightweight design that permits greater rpm's could be used. Throttling is used to control load, which implies that a restriction,

usually a butterfly valve, controls the inlet pressure and hence the air mass flow through the engine. At part load, the engine is forced to function as a compressor, lowering efficiency.

The main working point of the engine in automotive applications is low to medium load, which indicates the overall efficiency drops significantly. In the case of the CI engine, the situation is almost the complete reverse. As a result, the number of diesel-powered vehicles has increased. It utilizes stoichiometric mixtures, which provides the possibility of using a three-way catalyst to treat exhaust gases. As a result, NOx emissions can be reduced while CO and UHC are oxidized at the same time. In this way, the SI engine with a three-way catalyst is the most environmentally acceptable option for IC engines. It gets much better if biofuels are employed, which, unlike fossil fuels, do not contribute to a net $CO_2$ rise in the environment over time.

### 1.2.2 Compression Ignition (CI) engine

High compression ratios and low octane number fuels are used in CI engines, often known as diesel engines, to start combustion through compression ignition. The CI engine has a higher thermal efficiency due to its high compression ratio, but it generates a lot of nitrogen oxide (NOx) emissions due to its combustion mechanism (diffusion flame). Furthermore, the diesel engine load is limited by high peak pressures and soot generation. Self-ignition is the ignition principle, and great ignitability is desired for precise combustion timing. The fuel's ignitability is determined by its cetane number. High peak pressures are caused by the high compression ratio, which requires a robust engine structure, that increases the mass of the design. The piston compresses only air to high temperatures in this engine, and the fuel is injected into the hot air at the end of the compression, resulting in its self-ignite. At extremely high temperatures, NOx is generated in the presence of oxygen and nitrogen. The fuel-air mixture is non-homogeneous in the absence of premixing, resulting in charge stratification in CI engines due to a diffusion process in very lean and hot regions where NOx is generated. As a result, diesel engines are known for their higher NOx emissions. Moreover, CI engines have superior thermal efficiency than SI engines due to higher compression ratios and typical fuel-air equivalence ratios just under 0.6, leading to reduced fuel usage and $CO_2$ emissions.

However, due to its combination of fuel economy, durability, and the reality that engine mass plays a minor factor in many applications, this engine has discovered significant usage in trucks, trains,

industrial, agriculture, and forestry apparatus. Turbocharging has made it possible for diesel engines to be used in lightweight vehicles. In the CI engine, just the amount of fuel that is injected is regulated, which makes it incredibly simple.

## 1.3 Use of potential fuel in IC engines

For IC engines, fossil fuel is without a dispute the largest source of energy. Moreover, due to a large number of vehicles produced worldwide, rapid depletions of fossil fuels and pollutant emissions within their combustion products, causing environmental degradation, and concern regarding supply safety due to the uneven distribution of fossil fuel resources worldwide, about half of which are located in the Middle East, encourages significance, relevance and adoption of renewable fuels in IC engines [26].

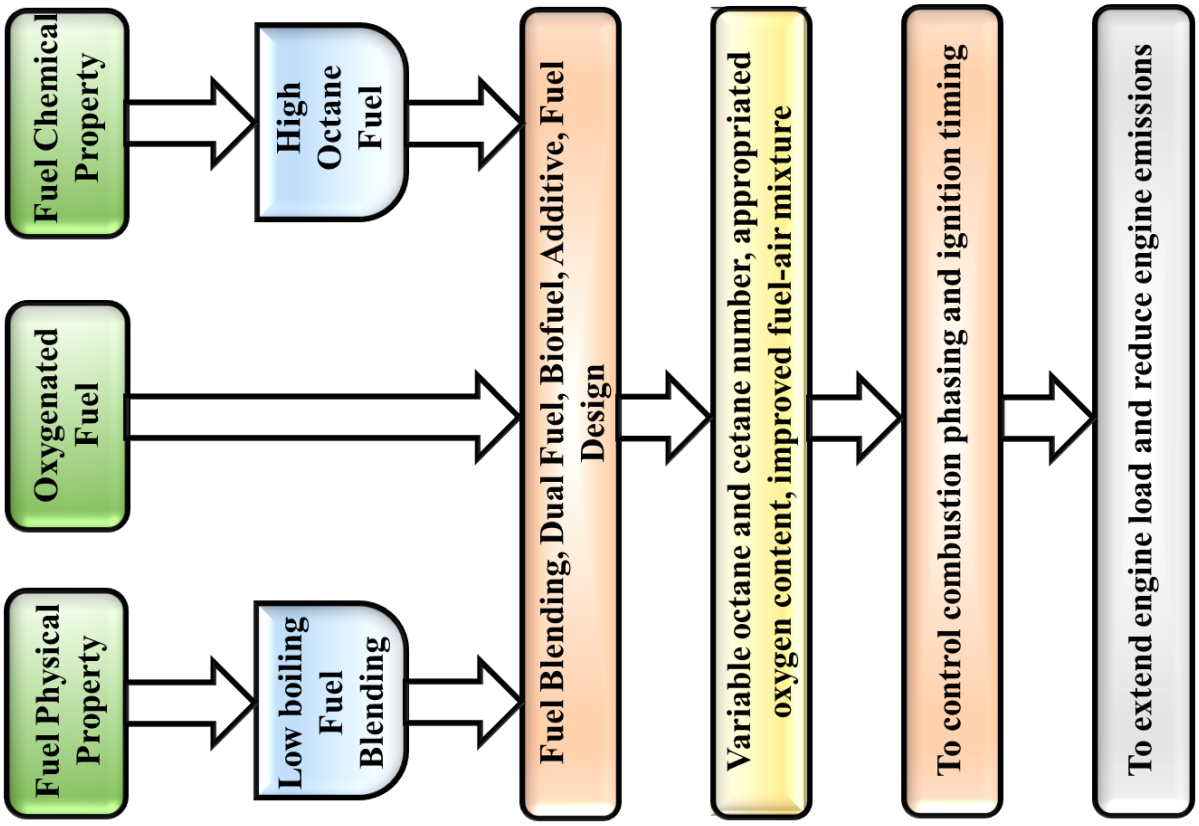


**Fig. 1.5.** Fundamental principles of fuel design for internal combustion engine [27].

The ever-increasing density and fuel requirement of transportation vehicles forced investigators and experts to look for new transportation fuel sources. Many strategies and procedures have been created and are constantly being developed throughout the years to improve yield, cost economy,

and sustainable development. The essential principles of fuel design for IC engines, as shown in Fig. 1.5, are used to conduct a comprehensive investigation of the numerous sources of alternative fuels and their manufacturing processes.

Biodiesel, methanol, ethanol, and natural gas are among the most regularly used liquid alternative fuels in the transportation industry, as discussed in the following paragraphs. Today, “renewable” fuels are beginning to come on the market, that indicates that, unlike fossil fuels, they do not cause to a net increase in $CO_2$ in the environment.

### 1.3.1 Biodiesel

Biodiesel is a renewable fuel created biologically that is similar to conventional or "fossil" diesel. It is domestically produced non-petroleum-based diesel fuel from animal fats (pork lard, beef tallow), plant oils (Jatropha, canola oil, corn oil, soybean oil, cottonseed oil), or recycled and renewable cooking oils using a Transesterfication process to remove glycerin and yield methyl or ethyl esters optimized for combustion. It can be used in unmodified diesel-engine vehicles (pure, or blended with conventional fuel). The commonly adapted processes for converting those vegetable oils to biodiesel to be used as a fuel in CI engines include transesterification, thermal cracking, microemulsification, and blending/dilution. The esterification process is depicted in simplified form in Fig. 1.6. Biodiesel is defined as mono-alkyl esters of long-chain fatty acids, commonly known as fatty acid methyl esters (FAME), according to the American Society for Testing and Materials (ASTM) [28].

It is believed to be a stable fuel that can be stored for a long period of time, and it has less sulfur and no aromatic chemicals, resulting in low PM emissions [29]. As demonstrated in Table 1.1, biodiesel has similar physical attributes to traditional or "fossil" diesel. Biodiesel produces more complete combustion due to its high oxygen content and substantially higher cetane ratings [30]. Biodiesel is also a suitable lubricant additive because of its high viscosity.

Biodiesel is a non-petroleum fuel that can be used directly in CI engines without modification and may be blended with conventional diesel to make a biodiesel blend. It is also known as B100 or neat biodiesel.

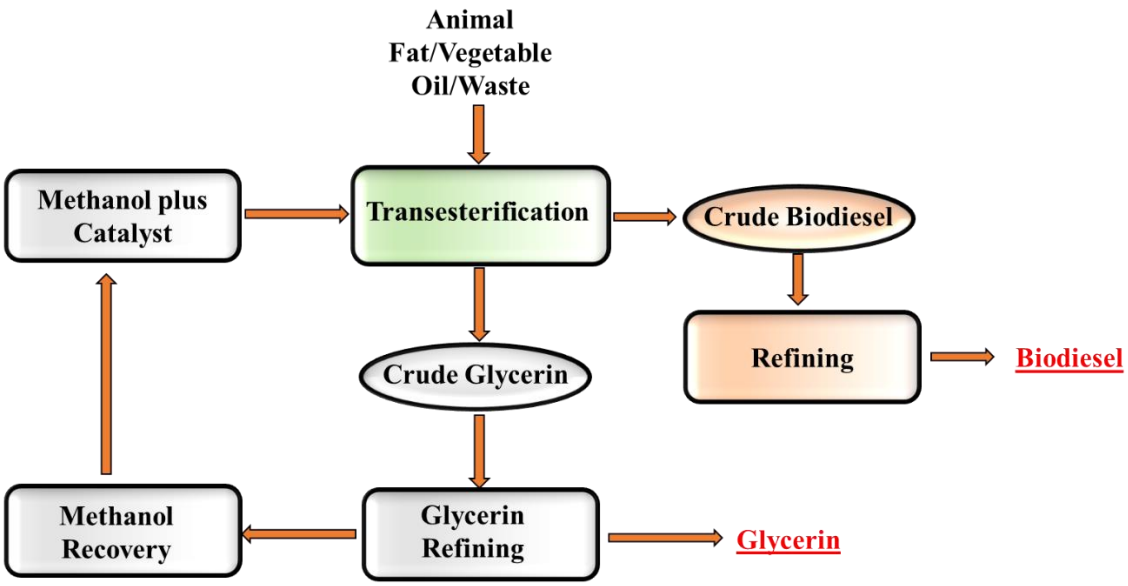


**Fig. 1.6. Basic Transesterification Process**

Biodiesel is a non-petroleum fuel that can be used directly in CI engines without modification and may be blended with conventional diesel to make a biodiesel blend. It is also known as B100 or neat biodiesel. Biodiesel is safe to handle and store because it is non-toxic, non-flammable, and non-volatile. Furthermore, because it has a lower calorific value, is less volatile, and thickens in cold conditions, anti-freeze additives are required [31-34]. Clean, dry, dark storage is recommended for biodiesel. Aluminum, steel, fluorinated polyethylene, fluorinated polypropylene, and Teflon are all acceptable materials for storage tanks. Avoid copper, brass, lead, tin, and zinc. Because of the high concentration of oxygen and unavailability of aromatics in biodiesel, it leads to more complete combustion in CI engines, resulting in significant reductions in UHC, CO, and PM levels when compared to traditional diesel fuel emissions.

**Table. 1.1** Physical properties of biodiesel produced from different feedstocks [34-41]

| **Feedstock Type** | **Calorific Value (MJ/kg)** | **Viscosity (mm2/s)** | **Density (kg/l)** | **Cetane Number** | **Flash Point (°C)** |
|---|---|---|---|---|---|
| **Jatropha** | 38.5-42 | 3.7-5.8 | 0.864-0.880 | 46-55 | 163-238 |
| **Canola oil** | 36.55-40.5 | 4.2-4.5 | 0.83-0.886 | 49-52.9 | 94-183 |
| **Corn oil** | 37.5 | 4.17-4.21 | 0.884-0.890 | 60.9 | - |
| **Sunflower** | 39.575 | 37.1 | - | 37.1 | 274 |

| | | | | | |
|---|---|---|---|---|---|
| **Rapeseed oil** | - | 4.439 | 0.882 | - | - |
| **Cotton** | 39.6 | 50 | 0.912 | 41.2-59.5 | 210 |
| **Rubber seed oil** | 36.5 | 5.81 | 0.860 | 37 | 130 |
| **Palm oil** | 39.8 | 4.56 | 0.856 | 61 | 167.3 |
| **Beef tallow** | - | 4.89 | 0.832 | - | 152 |
| **Lard** | 36.5 | 4.84 | 0.877 | - | 143.5 |

### 1.3.2 Natural gas

Natural gas is a flammable mixture of hydrocarbon gases that mostly consists of methane (CH4), other hydrocarbons, ethane, propane, butane, pentane, hexane, and a variety of other minor gas elements, and its composition varies depending on the source of the gas. Natural gas is created over millions of years when layers of decomposing plant and animal waste are exposed to tremendous heat and pressure beneath the Earth's surface. Natural gas composition changes significantly from location to location and throughout time. The specific composition of any given site will fluctuate between regions and over time. Each well has a unique Natural Gas constitution with varying proportions of each hydrocarbon gas constituent, but they always contain a large quantity of methane.

The primary member of the alkane family is methane, which is always the dominant component of natural gas. Natural gas is considered as the cleanest fossil fuel because of its high H/C ratio. Many countries employ natural gas engines in city buses because of the environmental benefits. Due to the overuse of fossil fuels, $CO_2$ levels in the atmosphere, which should be between 180 and 280 ppm, hit 405 ppm in September 2018 [42]. As a result, many governments promote the use of natural gas in vehicles rather than gasoline and diesel. Natural gas is easy to ignite, delivers clean combustion, and produces a lot of heat since it mixes properly with air.

Natural gas is a high-octane (around 110) fuel that allows SI engines to run more efficiently. The flame speed is higher as a result of the high-octane number, and the engine can run at a higher compression ratio, resulting in more powerful performance in SI engines.

Natural gas-powered internal combustion engines, unlike gasoline and diesel engines, do not require fuel enrichment during cold starts, and their exhaust emissions are unaffected by cold

temperatures. According to vehicles that use petroleum-derived fuel, natural gas vehicles produce emission values that are lower than the EURO 6 standard [43].

### 1.3.3 Methanol

Methanol, as the most common alcohol, is a cost-effective alternative transportation fuel due because of its efficient burning, ease of transportation, and global availability. Methanol is one of the most promising fuels being investigated as a substitute for gasoline, and it has undergone extensive study and development. Because of the high-octane number and rapid flame speed, methanol engines have a higher thermal efficiency than gasoline engines. Methanol is manufactured from natural gas in plants that have a total energy efficiency of 60%. Methanol can be produced from any carbon-rich renewable resource, including seaweed, scrap wood, or rubbish, after it has been converted into synthesis gas. Syn gas can be made from biomass, agricultural waste, lumber waste, and municipal solid waste using a gasification and thermo-chemical process [44]. Steam reforming and the water gas shift process are used to produce syngas, which is then used to produce methanol.

Reaction of steam reforming:

$$CH_4 + H_2O \xrightarrow[800-1000℃,20-30\ atm]{Zinc\ based\ catalyst} CO + H_2 \quad (1.1)$$

Water-gas shift reaction:

$$CO + H_2O \rightarrow CO_2 + H_2 \quad (1.2)$$

Reaction of methanol synthesis:

$$2H_2 + CO \xrightarrow[800-1000℃,20-30\ atm]{Zinc\ based\ catalyst} CH_3OH \quad (1.3)$$

Despite its low cetane rating, methanol can be used as a diesel fuel alternative in CI engines. For trucks, buses, and off-road vehicles, dual-fuel heavy-duty engines that run on both diesel and methanol can enhance efficiency and drastically reduce pollution.

Methanol is a light, volatile, colorless, flammable, liquid with a distinct odor, also known as methyl alcohol, wood alcohol, wood naphtha, or wood spirits. For many years, pure methanol and varying mixes of methanol and gasoline have been widely tested in engines and automobiles. M85 (a

mixture of 85 percent methanol and 15 percent gasoline) and M10 (a mixture of 10 percent methanol and 90 percent gasoline) are the most popular mixtures that can be used as an alternative fuel in flexible fuel vehicles.

**Table. 1.2** Physical properties of fuels [25, 45, 46, 47]

| **Properties** | **Methanol** | **Ethanol** | **Natural Gas** | **Diesel** | **Gasoline** |
|---|---|---|---|---|---|
| **Chemical Formula** | $CH_3OH$ | $C_2H_5OH$ | $CH_4$ | $C_{12}H_{26}$ | $C_8H_{18}$ |
| **Specific gravity** | 0.791 | 0.785 | 0.79 | 0.84-0.88 | 0.72-0.78 |
| **Auto ignition temperature (℃)** | 463 | 423 | 650 | 250 | 257 |
| **Stoichiometric ratio** | 6.5 | 9 | 17.2 | 14.5 | 14.7 |
| **Motor octane number** | 88.6 | 89.7 | 120 | - | 80-90 |
| **Cetane Number** | 3.8 | 5-8 | - | 40-55 | >15 |
| **Molecular weight** | 32.4 | 46 | ~18 | ~170 | ~114 |
| **Boiling point (℃) at 1 bar** | 65 | 78.3 | -160 | 190-280 | 30-225 |
| **Adiabatic flame temperature (K)** | - | 2193 | 2320 | 2200 | 2300 |
| **Oxygen content** | 49.93 | 34.73 | 0 | 0 | 0 |
| **Maximum flame speed (m/s)** | - | 0.61 | 0.42 | 0.3 | 0.5 |
| **Lower heating value (MJ/kg)** | 20.1 | 26.9 | 50 | 42.5 | 43 |

## 1.3.4 Ethanol

Ethanol is now commonly utilized as an engine fuel in a number of nations, including Brazil, the United States, and Sweden [48, 49]. Ethanol can be used in a variety of ways as an engine fuel.

For example, in ethanol fuel E85, which meets the requirements of ASTM 5798 and EN 15376:2014-CEN, ethanol is blended with gasoline and additives to provide smooth engine ignition at cold temperatures (below +5℃), corrosion resistance in engine subsystems, and fuel storage. While a little amount of ethanol added to gasoline has the potential to enhance combustion and emissions, the thermal efficiency is not greatly improved.

Many studies have attempted to enhance the thermal efficiency of ethanol-fueled engines to diesel-like levels by adding next-generation combustion modes.

The usage of ethanol in the transport sector can help reduce fossil fuel consumption and greenhouse gas emissions. IC engines can run on bio-ethanol produced through biochemical processes from biomass or waste. Use of ethanol as an alternative fuel for IC engines to reduce pollutant emissions, greenhouse effect by lowering CO, $CO_2$, NOx, Sox is the focus of this research. Ethanol can be utilized as a fuel in an internal combustion engine in two ways: straight and mixed. Engine modification is not required for low ethanol mixtures. As a result, the use of ethanol lends a helping hand in lowering dependence on foreign fuel.

Because of its various renewable sources, ethanol is a possible alternative fuel in IC engines and has been identified as a gasoline substitute. Table 1.2 shows the physical and chemical characteristics of ethanol and other fuels that can be utilized in SI and CI engines without requiring structural changes.

The production of ethanol for use as a fuel involves both biological and physical processes. The fermentation of sugars by yeast is the primary manufacturing process. Corn, wheat, sugar beet, molasses, sugar cane or starch, cereals, shale oil, cellulosic biomass, and other crops can be used to make the raw materials.

First, the raw ingredient is fermented, followed by distillation to achieve the needed purity. Eqs. (1.4) and (1.5) describe the chemical reaction of ethanol production. Apart from the basic ethanol production process, numerous additional procedures have been created over time. Ethanol, or more accurately bioethanol, is commonly produced from biomass waste using fermentation techniques, as shown in Fig. 1.7. Ethanol has a high- octane number than gasoline, which needs a higher burning temperature for autoignition. An SI engine with a higher compression ratio can use ethanol as fuel because of its high-octane number. [50] An increase in volumetric efficiency can be

achieved by using latent vaporization heat from ethanol, which increases the cooling effect of the cylinder [51]. Ethanol is a cleaner burning fuel than gasoline and diesel, producing less CO, $CO_2$, and NOx. Alcohols, which have comparable properties to gasoline but have a higher oxygen concentration, can minimize exhaust gas emissions [52,53].

This fuel may blend and ignite properly with a high rate of combustion efficiency due to the presence of oxygen. When employed in traditional gasoline and diesel engines, this feature is expected to reduce exhaust pollutants such as CO, NOx, and UHCs.

$$\left(\overset{Starch}{C_6H_{10}O_5}\right)_n + n\left(\overset{Water}{H_2O}\right) \rightarrow n\left(\overset{Glucose}{C_6H_{12}O_6}\right) \tag{1.4}$$

$$\overset{Glucose}{C_6H_{12}O_6} \overset{Yeast}{\Longrightarrow} 2\left(\overset{Ethanol}{C_2H_5OH}\right) + 2CO_2 \tag{1.5}$$

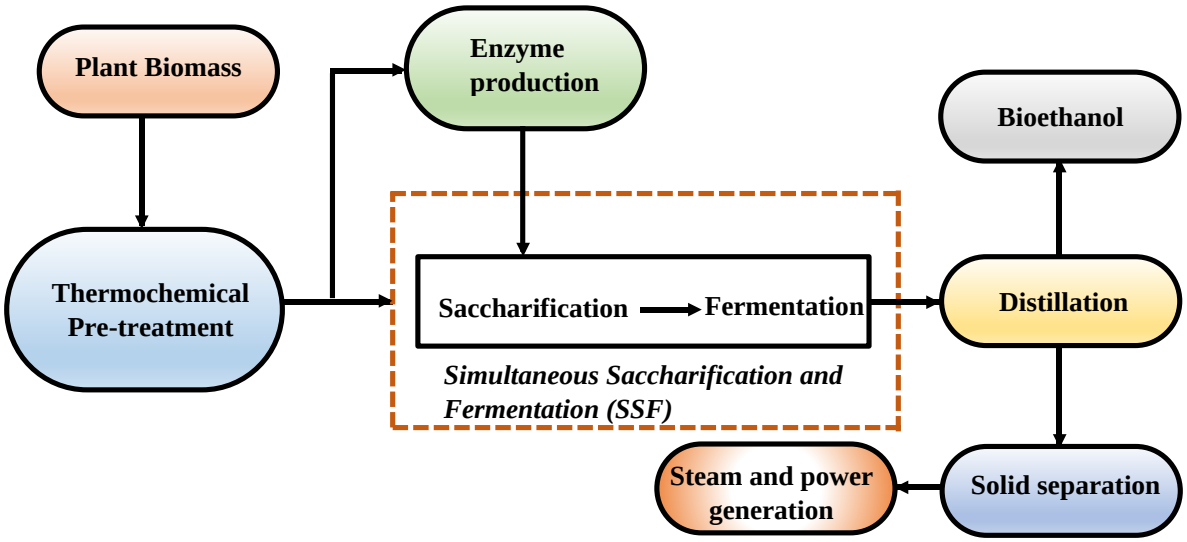


**Fig. 1.7.** Production of bioethanol from biomass [54]

The advantages and disadvantages of using ethanol in IC engines are shown in Fig. 1.8.

**For use as a fuel in SI engines, ethanol offers certain unique characteristics: [55]**

- A high-octane number results in a high level of knock resistance and, as a result, the capability to enhance the engine performance

- Because of the high oxygen concentration, the air/fuel mixture will be more homogenous and will ignite properly, resulting in a reduction in unburned hydrocarbon emissions such as UHC and CO.
- A density similar to that of gasoline.
- A high latent heat of vaporization allows for a “cooling effect” of air, which allows for a denser fuel–air charge, as a result, improves filling efficiency.

**On the other hand, there are some drawbacks to consider:**

- The presence of oxygen (30% wt) in the molecule causes an increase in the volumetric consumption of fuel.
- In cold situations, particularly cold start, the high latent heat of vaporization might cause running problems.
- Ethanol produces azeotropes containing light hydrocarbon fractions, which might cause volatility problems.
- Because of its high oxygen concentration and its potential to oxidize into acetic acid, some components utilized in the engine, including metals or polymers, are incompatible with ethanol.
- Because of its miscibility with water, it can produce demixing problems when mixed with hydrocarbons.
- Engines that burn ethanol emit aldehydes, which can have a harmful effect on health.

**IC engines can run on pure ethanol, although there are certain drawbacks [56]. These drawbacks are as follows;**

- Because of the corrosive nature of the fuel, the materials and surfaces of combustion chamber parts, as well as any polymers in contact with the fuel and the fuel injection system, must be improved.

- No passenger vehicle has been developed to run completely on ethanol. Pure ethanol can cause engine damage. Even Ethanol concentrations can reach up to 85 % in engines that can operate on gasoline-ethanol blends.
- It has a poor cold-starting performance due to its lower flame speed. In the winter, it is difficult to use as fuel.
- Because of its low energy density and cetane number, it is difficult to use in traditional CI engines.

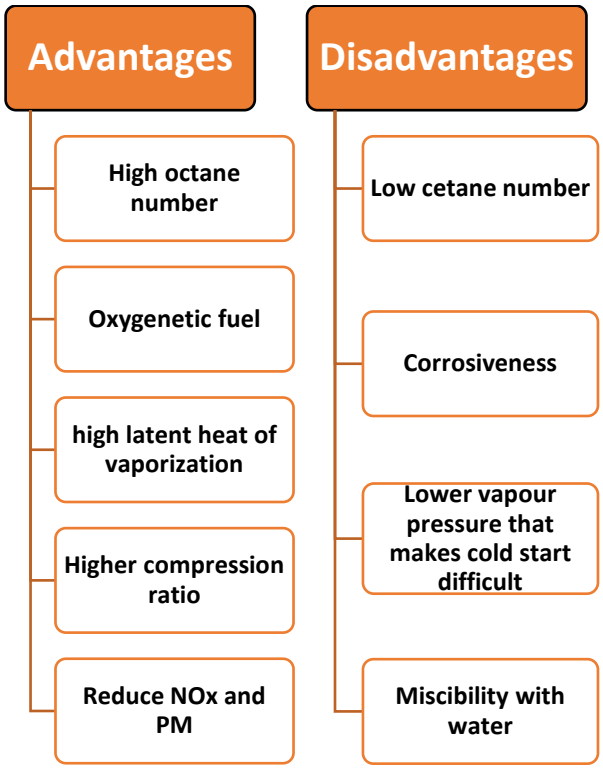


**Fig. 1.8** The advantages and disadvantages of using ethanol in IC engines

**Key benefits of Ethanol blending with Gasoline in lines on comparison of ethanol with gasoline are shown below:**

- Octane number of Ethanol is usually 108 compare to gasoline 90 which allows the engine to operate higher compression ratio resulting higher thermal efficiency and reduces the knock formation.
- Flame speed of Ethanol is 61 cm/s compare to gasoline 50 cm/s and this support the burning of maximum amount of fuel and hence reduces the emissions of unburned hydrocarbon and hence makes the engine little environment friendly.

- Ethanol contains a significant amount of oxygen being an oxygenated fuel compare to gasoline which has no oxygen. This makes the air/fuel mixture more homogenous which help in ignition, resulting in the reduction of unburned hydrocarbon and CO emissions.
- Latent heat of vaporization of ethanol is considerably higher than gasoline which allows for a "cooling effect" of air, which allows for a denser fuel–air charge, as a result, improves filling efficiency

### 1.3.5 Wet-ethanol

A detailed study [57, 58] on the production and use of ethanol from corn found a slight energy benefit with a net energy gain of 21%, including a 15 % energy gain in co-product and a 6 % energy gain in ethanol. As seen in Fig. 1.9, transportation, distribution, production, mashing and cooking, dehydration and distillation consume a significant amount of energy. The net energy gain is the energy that remains after all of the energy consumption has been taken into account, and its made up of two parts: net energy in the ethanol and net energy in the co-products [59].

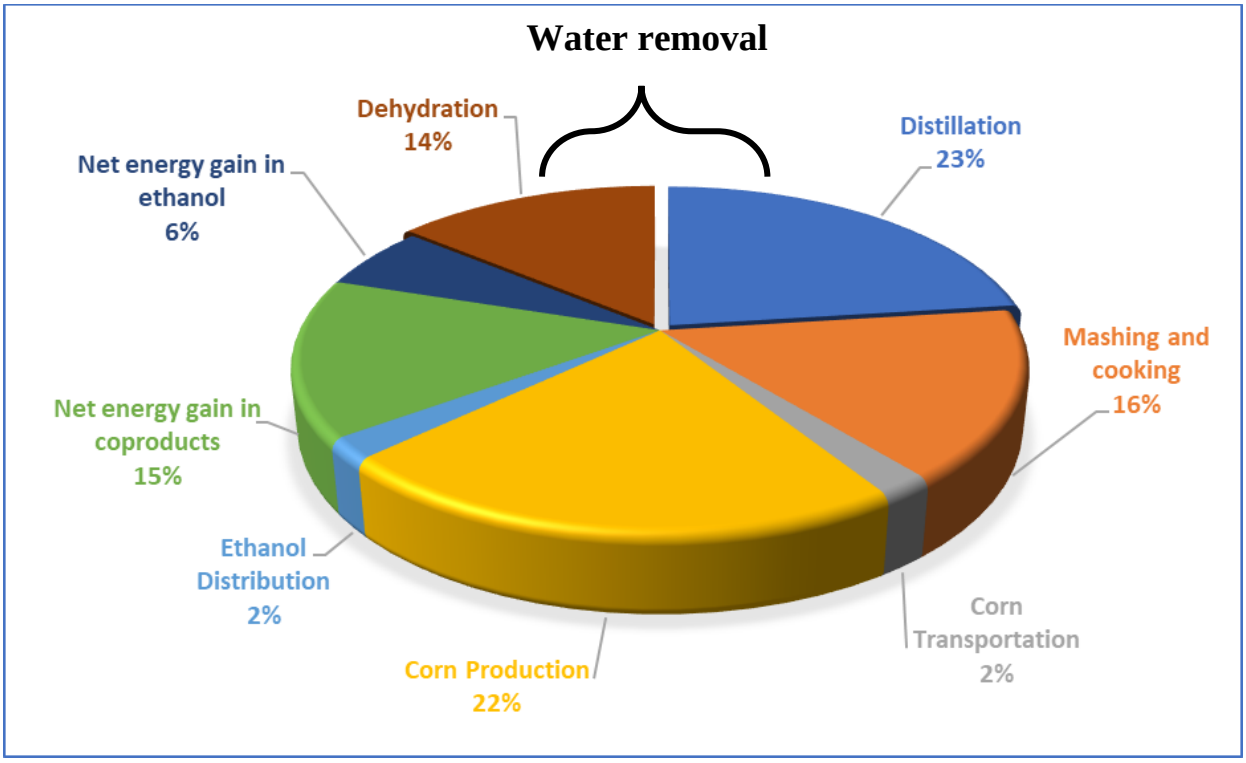


**Fig. 1.9.** Net energy balance for ethanol produced from corn

The development of novel utilization technologies is required in order to increase net energy gains and, therefore, minimize the energy consumption of converting ethanol into a useable form. Fig. 1.9 indicates that water removal (distillation and dehydration) consumes 37% of the energy required to produce ethanol. The use of direct wet-ethanol (ethanol-water mixture) reduces the energy consumed in water removal, the energy consumption of making pure ethanol and its coproducts is reduced from 37 % to only 3% percent, resulting in a net energy gain that improves from 21% to 55 % as illustrated in Fig. 1.10 [60].

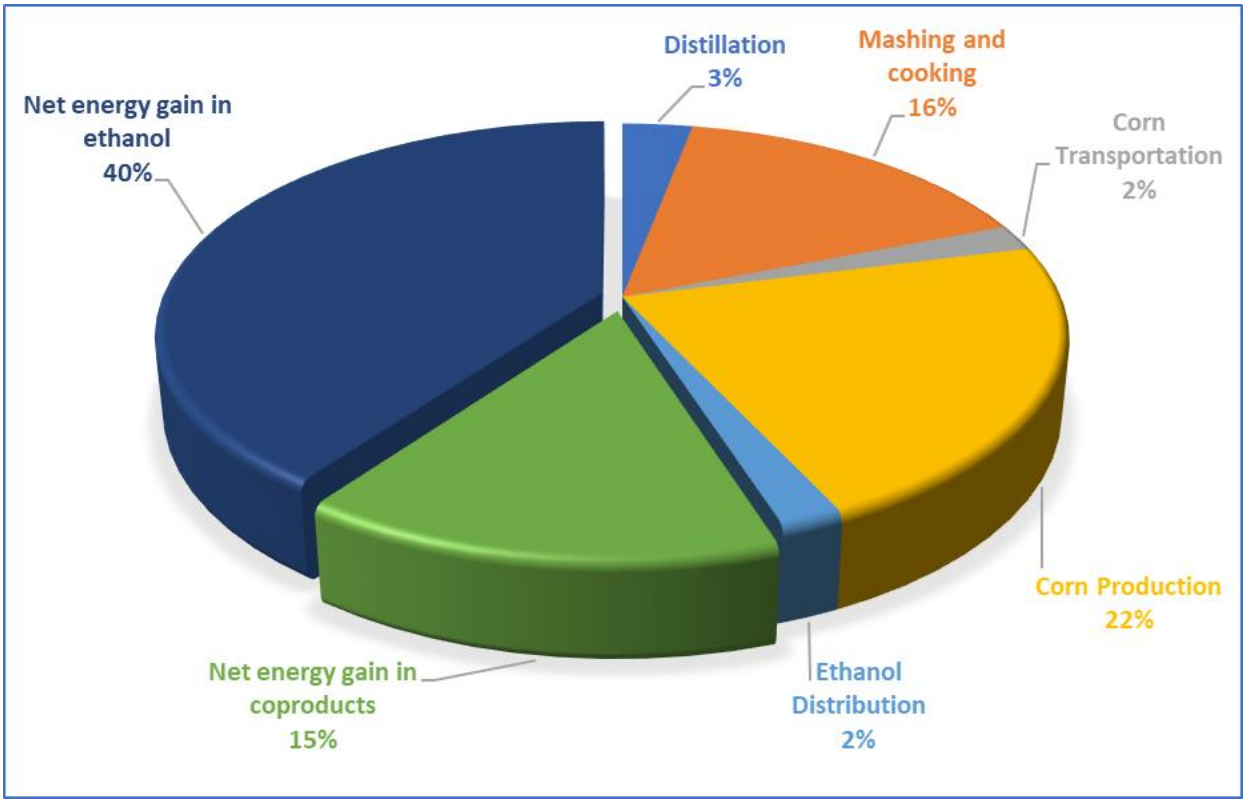


**Fig. 1.10.** Net energy balance for direct utilization of wet-ethanol produced from corn

SI and CI are the conventional modes of combustion for IC engines used in surface transportation and distributed power generation, but they do not operate well with wet-ethanol. Flame propagation starts combustion in SI engines at the spark plug and continues through the combustion chamber. As a result of highly water concentrations in the fuel, the fuel-air mixture is diluted significantly. Misfires are caused by excessive dilution, which delays flame propagation. Additional requirements for knock-free operation of SI engines include low intake temperature (less than ~60°C) and low compression ratio (less than ~11). The engine's efficiency is limited by

its low compression ratio, and the intake temperature controls the humidity of the intake gases, as condensation in the intake could damage engine components or contaminate the oil, reducing lubricity. Wet-ethanol also presents challenges for CI engines. Due to its high autoignition resistance, pure ethanol is not a good fuel for CI engines (high octane number and low cetane number). Because water slows chemical reactions by cooling the air inside the combustion chamber as it evaporates, using wet ethanol enhances resistance to autoignition. In a CI engine, it is therefore difficult to achieve satisfactory combustion of wet ethanol in the short period allowed for combustion.

The homogeneous charge compression ignition (HCCI) engine is a modified engine combustion technology that includes the fundamental benefits of both SI and CI combustion (HCCI). Wet ethanol combustion in engines for sustainable transportation has been proven to be more promising with this technology.

## 1.4 Advance combustion mode

Because of the large number of automobiles manufactured around the world, there is a rapid depletion of fossil fuels and pollutant emissions from their combustion products, resulting in environmental degradation and a rise in energy consumption. As a result, in light of the energy demand, greenhouse gas emission caused by CO, $CO_2$, PM, toxic hydrocarbon emissions, acid rain, haze, and NOx [61,62], engine researchers and developers are focusing much on advanced combustion modes based on traditional SI and CI engine.

The homogeneous charge compression ignition (HCCI) engine is a next-generation engine technology that provides an alternative combustion mode to traditional SI and CI engines. HCCI engines incorporate the best features of both SI and CI engines without the drawbacks. HCCI engines use a homogenous mixture of fuel-air in the intake charge, similar to SI engines, but the fuel-air mixture is compression ignited, similar to CI engines. Due to stringent limits for NOx emissions from IC engines, and the aim to minimize fuel consumption and greenhouse gas emissions like $CO_2$, interest in this innovative combustion technique has increased in recent years. This technology has the advantage of allowing cleaner combustion (low NOx, soot, and PM) as SI engines and high-efficiency compression-ignited combustion as CI engines.

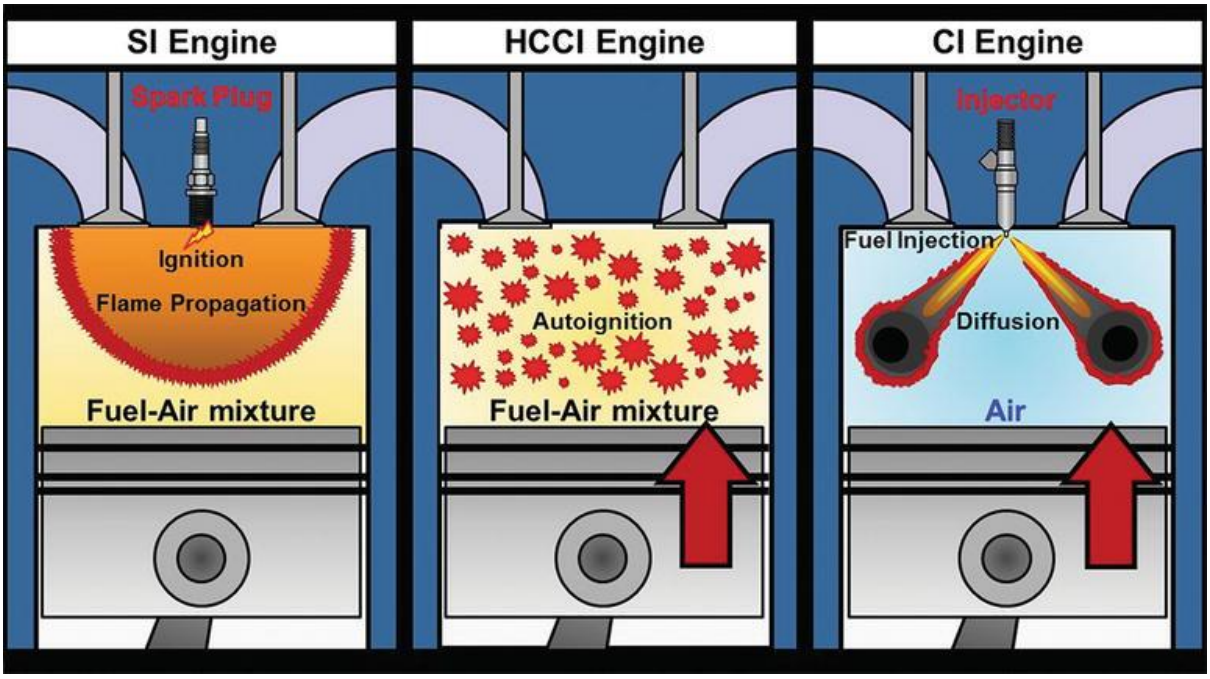


**Fig. 1.11.** A schematic representation of SI, CI and HCCI combustion modes [63]

Unlike traditional SI and CI engines, which use a spark or injected fuel to start ignition, HCCI engines do not require an external ignition source as shown in Fig. 1.11. The HCCI engine is dependent on the thermochemical behavior of the compressed mixture. As a result, ignition is affected by the gas mixture's temperature and pressure history. To enhance efficiency and minimize emissions, engines are run in the lower equivalence ratio range. The lean combustion technique is mostly used in IC engines due to the massive increase in vehicle population. The only way to reduce NOx emissions is to lower the combustion flame temperature.

Low temperatures are produced by lean-burn engines, which is a key element in reducing the generation of thermal nitrogen oxide. Lean burning uses more air, which allows for more efficient combustion of the fuel, reducing both UHC and CO emissions. It is important to note that only by maintaining combustion temperatures as low as possible can heat transfer losses be minimized in an IC engine. Low temperature combustion (LTC) is employed in the HCCI combustion to minimize heat transfer losses, and the heat of the fuel is fully discharged in a few crank angles at the top dead center (TDC). A premixed fuel-air mixture, and, occasionally, internal residuals are compressed to the point of autoignition in the HCCI engine. In an ideal case, combustion would begin a few degrees before or after Top Dead Center (TDC). The ignition is fully regulated by chemical kinetics and is driven by species concentration and mixture temperatures [64]. As a

result, HCCI combustion releases energy at a much faster rate than traditional SI or CI combustion, which depends on the air-fuel mixing or flame propagation for their respective burning rates. Processes of expansion and emission are similar to those of the SI and CI engine. The HCCI cycle is a version of the traditional engine cycles that exhibits elements of both the Otto and Diesel cycles from the perspective of gas power cycles. The ideal HCCI cycle, like both of these cycles, starts with adiabatic and reversible compression during stroke one, as indicated in Fig. 1.12 by the isentropic from state 1' to state 2'. In comparison to SI engines, HCCI engines operate on a thermodynamic process that is much more similar to the ideal Otto cycle (shown in Fig. 1.12).

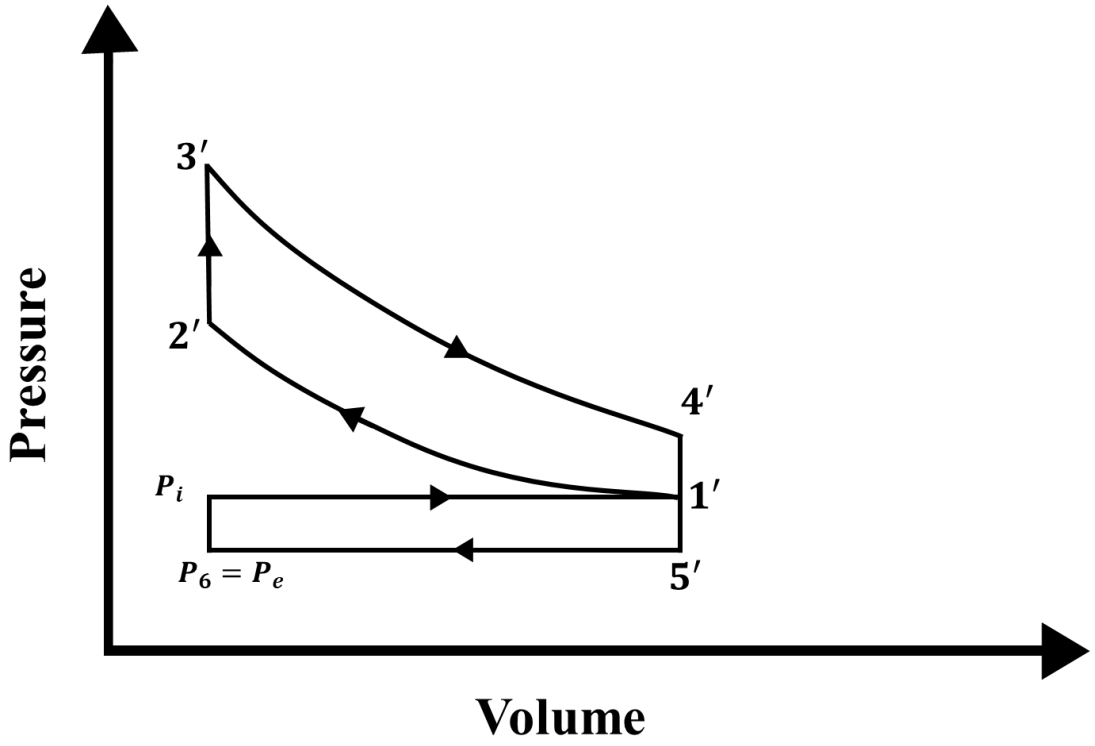


**Fig. 1.12** PV diagram of the ideal HCCI cycle

High compression ratios, comparable to those found in traditional CI engines, are used in HCCI engines, as is constant volume heat addition, which is often associated with SI combustion. The range of HCCI compression ratios can be from 14:1 [65-67] to 22:1 [68, 69] depending on the intake conditions and type of fuel; however, in spark-assisted HCCI implementations, lower compression ratios could be used. In HCCI, the range of fuel-air equivalence ratios from 0.20 to

0.55 for implementations without exhaust gas recirculation [68], but can reach 1.0 (stoichiometric) for systems that use significant dilution with exhaust gas recirculation [65].

One factor for HCCI engines' ability to produce higher thermal efficiency (similar to CI engines) is their higher compression ratios when compared to SI engines. The inlet air is not throttled for output power regulation, which is another aspect contributing to the higher efficiency of the HCCI engine. As a consequence, HCCI engines do not suffer from the throttling losses that influence part-load working circumstances in SI engines. Table 1.3 shows comparative parameters related to the combustion processes of the SI, CI and HCCI engine.

**Table 1.3** Comparison of SI, CI and HCCI combustion engines [70]

| **Engine type** | **SI** | **CI** | **HCCI** |
|---|---|---|---|
| **Fuel** | Gasoline-like fuel | Diesel-like fuel | Flexible fuel |
| **Ignition method** | Spark ignition | Compression ignition | Auto-ignition |
| **Charge** | Premixed homogeneous before ignition | Heterogeneous | Premixed homogeneous before ignition |
| **Ignition point** | Single | Single | Multiple |
| **Throttle loss** | Yes | - | No |
| **Compression ratio** | Low | - | High |
| **Combustion flame** | Flame propagation | Diffusive flame | Multi-point autoignition |
| **Speed** | High | | Low |
| **Flame front** | Yes | Yes | Without |
| **Fuel economy** | Good | Better | Comparable to CI |
| **Max. efficiency** | 30% | 40% | >40% |
| **Injection type** | Port injection | Direct injection | Both port and direct injection |
| **Major emissions** | UHC, CO and NOx | NOx, PM and UHC | UHC and CO |
| **Equivalence ratio** | 1 | | <1 |

| | | | |
|---|---|---|---|
| **Combustion temperature** | High | Partially high | Relatively low |
| **Combustion timing** | Spark discharge | Fuel injection | indirect: temperature pressure history |

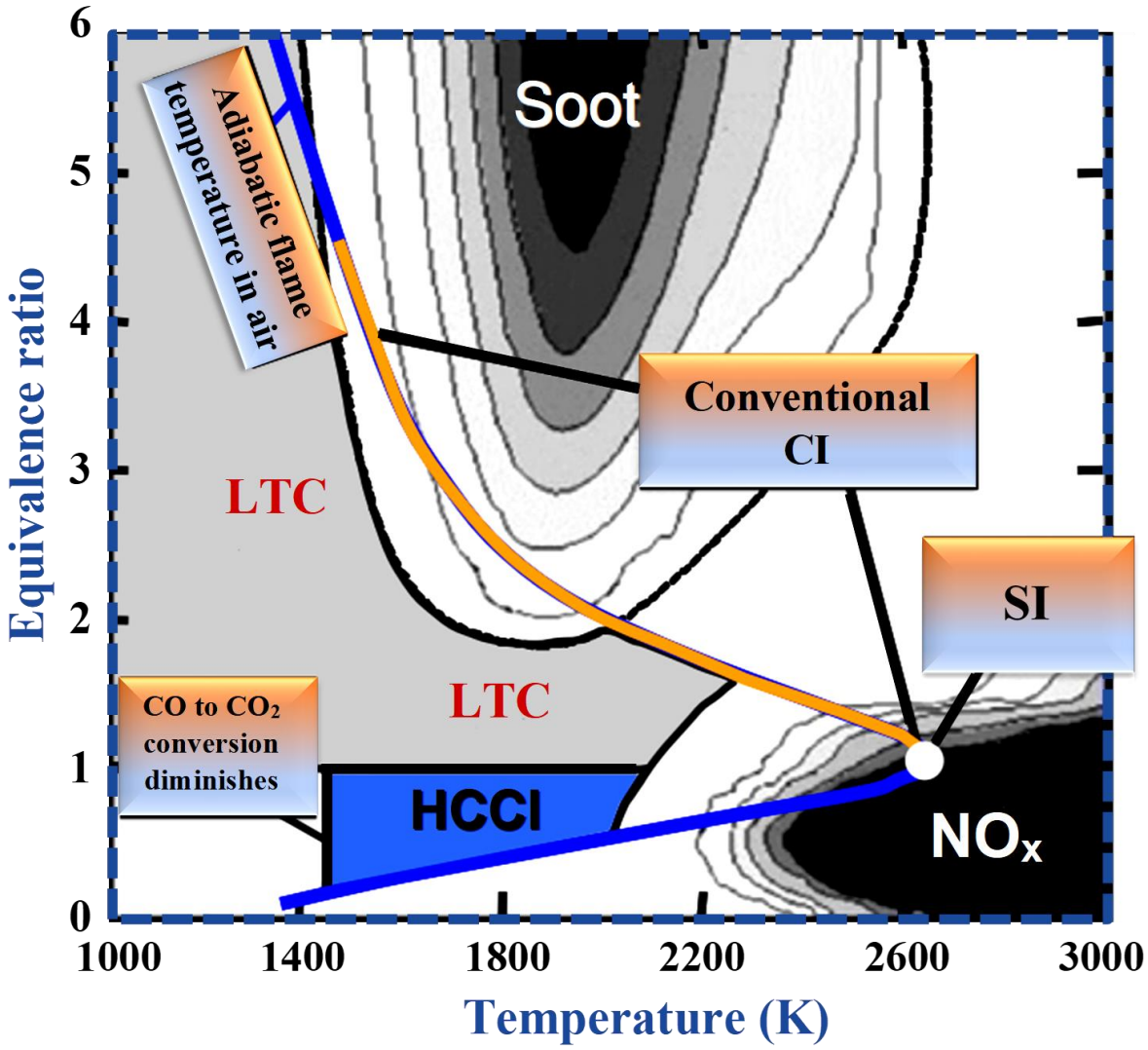


**Fig. 1.13.** The NOx or soot formation in the zones of different combustion modes [90]

There is no NOx or soot formation in the zone of HCCI combustion above the UHC/CO oxidation limit, as shown in Fig. 1.13. Because it provides a wide range of fuel flexibility [60,71,72], improved thermal efficiency, and reduced air pollution, HCCI combustion is believed to be one of the best combustion technologies to be used more widely in the automotive sector in the upcoming years. Fuel flexibility is also mentioned as a key advantage [73]. To reduce NOx and soot

emissions from the engine, HCCI technology employs the lean premixed homogenous mixture and low combustion temperature [74]. Before the start of ignition in HCCI engines, a lean homogenous flammable mixture (fuel-air equivalence ratio <1) is formed and auto ignited as a result of temperature increase during the compression stroke.

HCCI combustion modes are suitable for a wide range of fuels with various octane values because these combustion modes offer high fuel flexibility. In recent years, the variety of fuels used in HCCI engines has increased considerably. Biofuels, hydrocarbon fuels, and reformed fuels are all examples of HCCI fuels. These engines are capable of scaling up to nearly any size of transportation engine, including from motorcycles to large ship engines, and they might be employed in many applications, including stationary applications like oil and gas production, electricity generating, and pipeline pumping.

## 1.5 History Perspective or HCCI background

Onishi et al. [75] at Nippon Clean Engine Research Institute Co. reported the first research findings of employing compression ignition of a homogeneous mixture, which they called Active Thermo Atmosphere Combustion (ATAC). The fundamental idea was to improve fuel consumption and exhaust pollutants by running a 2-stroke gasoline engine with lean mixtures during part-load operation. During the scavenging phase of throttled operation, a large amount of burnt gas was retained inside the cylinder. The average charge temperature was raised to the degree where auto-ignition happened, which is self-ignition. It was able to employ an oxidizing catalyst and generate clean exhaust emissions because lean mixtures were utilized.

Onishi also offered an ideal model (Fig. 1.14) of the ATAC concept, that became highly popular and was studied in several later HCCI and ATAC publications. It describes the fundamental difference between an ATAC and a SI engine in an easy-to-understand manner. The fuel is burned in a reaction zone – the flame front – in a SI engine, and the flame front propagates across the combustion chamber, consuming the fuel. This indicates that the burned and unburned zones are completely separated. All of the fuel is burned simultaneously in the ATAC case but at a slower rate. During the oxidation process, the fuel is divided into intermediate species, which ends until there are no combustible species left. Onishi further demonstrated that, as compared to conventional spark ignition, cycle-to-cycle changes were extremely small, resulting in increased

overall engine efficiency. Small generators ("NiCE," with an electrical power of 1 kW) were the first commercial products to use ATAC technology. Honda Motorcycle Company later developed a similar technology in which a valve in the exhaust system controlled the burned gas fraction. This technology was applied in small motorbikes, and the approach was given the title Active Radical Combustion [76, 77].

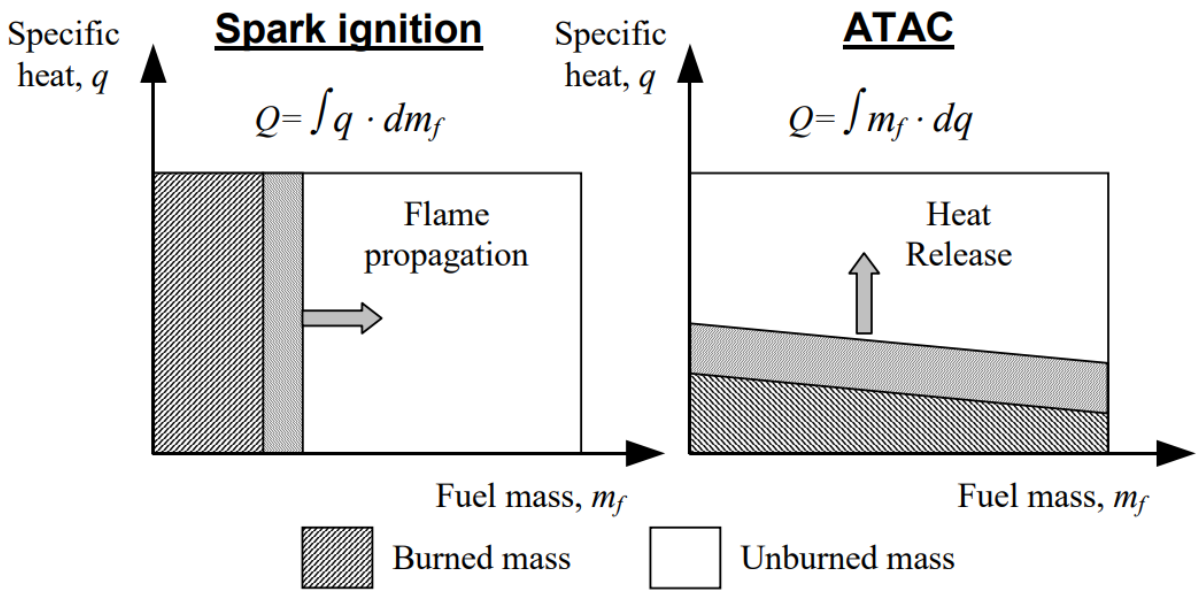


**Fig. 1.14.** The ideal model of spark ignition and ATAC proposed by Onishi.

The same technology was developed and called “TS (Toyota-Soken) combustion” by Noguchi et al. [78] at the Toyota Motor Co. Ltd. during the same time period. ATAC and TS (Toyota-Soken) combustion were the names given by Onishi and Noguchi for their research; although, they were describing the same concept. It was discovered that considerable fuel savings were achieved in both cases, along with a reduction in the cycle-to-cycle unpredictability commonly found in 2 stroke SI engines.

In a four-stroke gasoline engine, Najt and Foster [64] successfully achieved compression ignition homogeneous charge (CIHC) combustion in 1983. Because of the increasing ability to modify the parameters of the gas exchange process, most of the present study has shifted from its early roots in two-stroke research to four-stroke research.

First, in 1989, Thring [79] coined the term HCCI to describe his study (which investigates the effects of exhaust gas recirculation (EGR), intake temperature, and compression ratio) and to

summarize prior studies by Onishi et al. [75], Noguchi et al. [78], and Najt and Foster [64]. HCCI has been given an additional ten different names in the 10 years before Thring's work [79] and the 20 years since, such as ATAC (Active Thermo-Atmospheric Combustion), TS (Toyota-Soken), ARC (Active Radical Combustion) in traditional 2-stroke engines, CIHC (Compression-Ignited Homogeneous Charge) [64], CAI (Controlled Auto-Ignition) [80–83], PREDIC (PREmixed lean Diesel Combustion) [84], MK (Modulated Kinetics) [85], UNIBUS (Uniform Bulky Combustion System) [86], OKP (Optimized Kinetic Process) [87], PCCI (Premixed Charge Compression Ignition) [88], and so on. Zhao [89] summarized the many names and abbreviations in the following observations: "When you look at these names and the reasoning behind them, you'll notice that they all describe two key aspects of the new combustion process: 1) premixed air-fuel mixtures, and 2) auto-ignited combustion." For all HCCI activities until the time of publishing, Zhao [89] proposed two names: The first name, HCCI, refers to work done in conditions more related to CI combustion, such as higher compression ratios and significantly low octane/high cetane fuels. The second name, CAI (controlled auto-ignition), refers to methods that are more similar to SI combustion, such as high octane/low cetane fuels and significantly lower compression ratios. This difference was introduced to show that compression alone is insufficient for igniting high octane/low cetane fuels; The charge must be sufficiently heated and can be misleading to refer to the complete process as simply compression ignition [89]. The name HCCI will be used to describe the method throughout the work presented here.

## 1.6 Advantages and disadvantages of HCCI technology

### 1.6.1 Advantages

The following are some of the benefits of HCCI technology:

1. HCCI engines have a higher thermal efficiency, and because the majority of the combustion energy is discharged during thecombustion and expansion stroke, they produce lower waste exhaust heat than traditional SI and CI engines.
2. A cleaner burning, lower emissions, and particularly negligible NOx emissions are possible with this technology.
3. HCCI engines consume less fuel because it runs on a very lean mixture (highly diluted).

4. Low flame temperatures result in much lower emissions of NOx and PM due to the extreme lean fueling rates.
5. Because the pre-mixed air-fuel in the HCCI engine prevents diffusion flame burning (as in CI engines), which reduces PM emissions, and It also does not generate soot.
6. It also runs at very high compression ratios, which improves its efficiency (high than traditional SI engines) and fuel efficiency by a considerable amount.
7. Another attractive feature of HCCI engines is their fuel flexibility. It is capable of running on a number of different types of fuel, including gasoline, diesel fuel, and most alternative and renewable fuels.

### 1.6.2 Disadvantages

On the other hand, the following are some of the disadvantages of HCCI technology:

1. HCCI engines have a limited power range, with lean flammability constraints at low loads and in-cylinder pressure restrictions at high loads. The increased pressure makes it difficult for this type of engine to operate at a high load.
2. Damage to the engine can be caused by high in-cylinder peak pressures.
3. Due to its temperature and pressure history, the auto-ignition event is difficult to manage compared with conventional engines that use spark plugs and fuel injectors.
4. Incomplete oxidation (due to the fast combustion event and low combustion temperatures) and trapped crevice gases lead UHC and CO emissions to be higher in HCCI than in a conventional SI engine.
5. Cold start is the main drawback with HCCI engines.

## 1.7 Challenges to HCCI and proposed solution

Before applying the advantages of HCCI combustion engines for engine performance and exhaust emissions, some of the challenges of commercial production must be overcome. Fig. 1.15 depicts the main operational challenges of HCCI combustion.

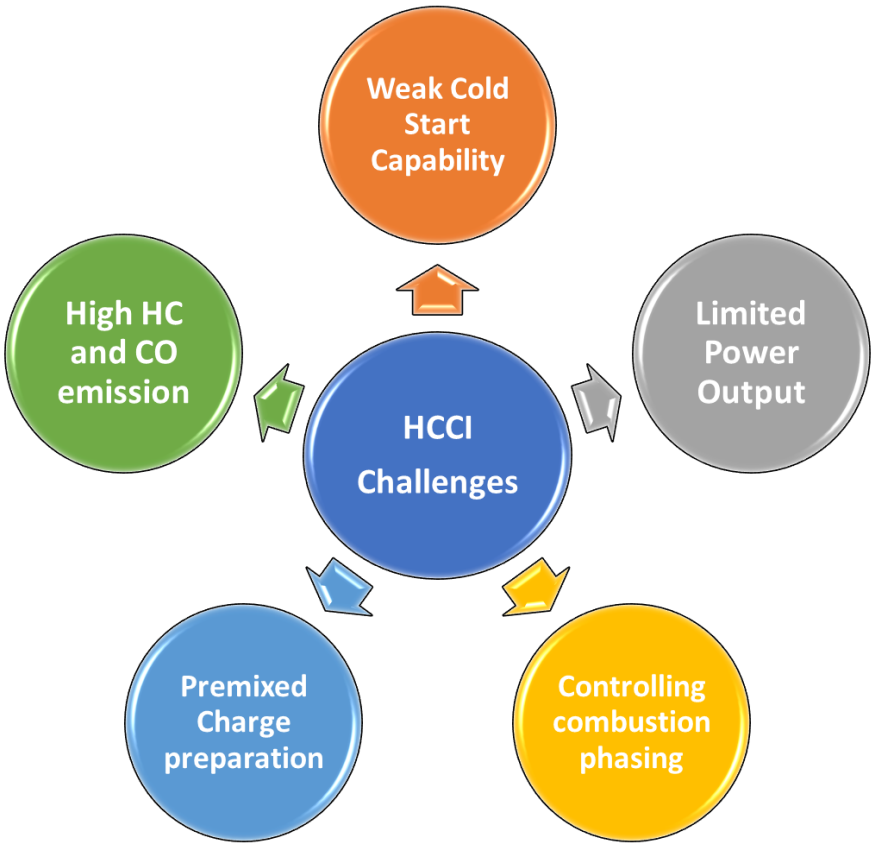


**Fig. 1.15**. Challenges with HCCI engines.

### 1.7.1 High unburned Hydrocarbon (UHC) and carbon monoxide (CO) emissions

The possible rise in noise, UHC (unburned hydrocarbon), and CO emissions is the main barrier for HCCI operation. In comparison to CI engines, UHC and CO emissions from HCCI engines are considerably higher [91]. At lower engine loads, HCCI combustion releases low NOx and PM emissions, but comparatively high UHC and CO emissions at low to medium loads, and also high NOx emissions at high loads. The burning of either rich or extremely lean stoichiometric mixtures produces UHC and CO emissions in an IC engine. Temperature limits inflammability in lean mixtures, while a shortage of oxidants in the combustion chamber in rich mixtures [25]. UHC and CO are produced in large amounts by the lean operation of the HCCI combustion. In HCCI engines, unburned hydrocarbon emissions are mostly caused by incomplete fuel oxidation resulting from an excess oxidant that is ready for ignition. The top ring land crevice of the combustion chamber is the primary source of UHC production. Along the midline, bowl/central

clearance volume, and squish volume, unburned UHC regions can be seen [92]. To overcome the problem of high UHC and CO emissions, especially at low loads, emission control systems and control strategies must be developed. Where fuel optimization was not applied, exhaust emission control devices are required in most conditions to control UHC and CO emissions from HCCI engines. CO is not entirely oxidized to carbon dioxide ($CO_2$) due to the lower combustion temperatures, and for complete oxidation, it needs above 1177 ℃ temperatures. CO emissions drop as the premixing ratio, fuel-air ratio, and load increase [93]. Increasing the inlet air temperature [94] and compression ratio [95] can simultaneously reduce UHC and CO emissions. Catalyst technology has been used in automobiles for many years to reduce HC and CO emissions. It is therefore anticipated that to fulfill future UHC and CO environmental regulations, oxidation catalysts will be needed to regulate tailpipe emissions from HCCI engines with low-temperature steam exhaust [93]. In comparison to NOx and PM emission control devices, UHC and CO emission control devices are easier, more reliable, and less dependent on scarce, costly precious metals [96]. As a result, In an HCCI engine, oxidation of UHC and CO simultaneously is significantly simpler than simultaneous NOx and PM reduction in a CI engine.

### 1.7.2 Weak cold-start capability

For most geographically cold places, the cold start problem in HCCI engines is another challenge. Much more research and development are required in the HCCI engine for cold starts. Inlet charge temperature affects HCCI ignition, making a cold start problematic [97], and the combustion process is difficult without thermal inertia, and small changes modify combustion phasing dramatically. Additionally, the initial temperature necessary for self-ignition changes depending on the fuel characteristics and operating parameters. When starting an HCCI engine from a cold start, the compressed-gas temperature will be decreased due to a lack of preheating from the inlet manifold and fast cooling via transfer of heat to the walls of the cold combustion chamber. Low compressed charge temperatures, in the absence of a compensation technique, may prohibit an HCCI engine from burning. Take full advantage of HCCI engines, achieving cold start operation at both low and high loads is essential.

Researchers have used several successful strategies to overcome the weak cold start performance of HCCI engines. A frequently proposed solution is to use a dual-mode (SI-HCCI / CI-HCCI) technology, in which the engine initiates in the SI / CI mode at quite higher and lower load

conditions due to dilution restrictions, and after a short warm-up period then switches to the HCCI mode. Increasing the compression ratio with variable compression ratio (VCR), or variable valve timing (VVT), switching to a different fuel or fuel additive, and installing glow plugs are some of the other proposed solutions. Using Spark Assisted Compression Ignition (SACI) technology as a bridge between SI and HCCI engines could be a practical solution [98]. It is just as crucial to have a strong HCCI combustion at very low loads with complete HCCI advantages in fuel performance and emissions as it is to extend HCCI operation to high load conditions. To enhance these technologies and prepare them for manufacturing engines, significant research and development will be needed [99].

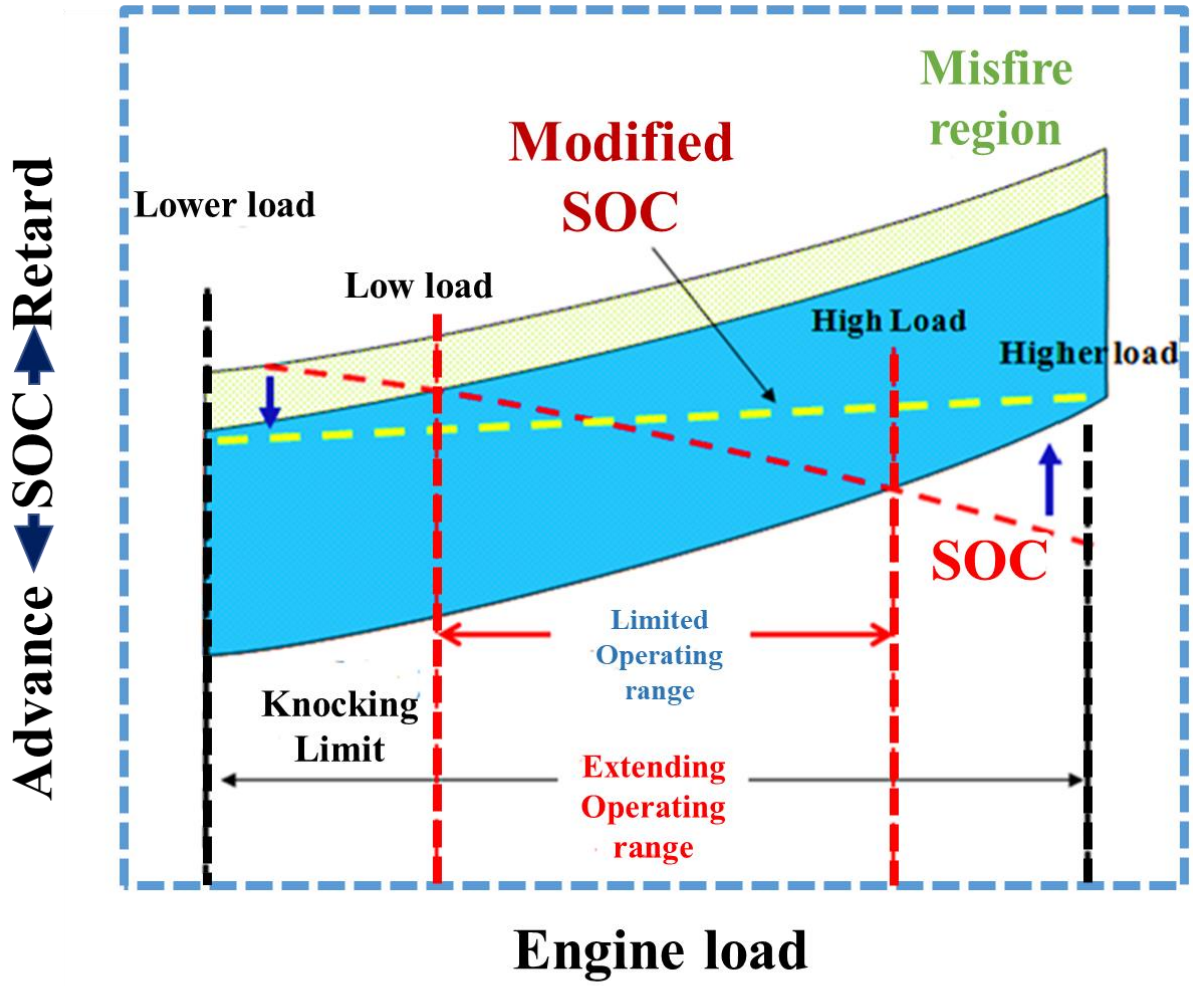


**Fig. 1.16.** Limited and Extended operating range of HCCI engine [100]

### 1.7.3 Limited power output

The limited power output in HCCI engines is another big challenge. In comparison to conventional engines, the HCCI engine has a limited operating range (as shown in Fig. 1.16), which represents a significant commercialization challenge. The auto-ignition characteristics of fuel and engine geometry have a major impact on the operating range. At intermediate loads, HCCI combustion has been shown to work effectively, however, at low and high loads, problems have arisen. Because of the low energy emitted per combustion cycle, auto-ignition of the charge is challenging at low load conditions, making it challenging to keep the combustion chamber at a high temperature. During extremely lean HCCI operation, flammability limits the fuel-air mixture. The combustion process becomes quite fast and powerful when the engine is at a higher load, causing a rapid rise in temperatures and pressures in the combustion chamber, resulting in undesirable noise, potential engine failure, and finally intolerable NOx emissions [101]. Hence, its thermal efficiency declined dramatically, while UHC and CO emissions increased [102]. To avoid excessive noise or engine damage, more study is needed to develop solutions that decrease the rate of heat release during higher-load operation. At the speed of 1000–1500 rpm, the knock limitation BMEP (Brake Mean Effective Pressure) of naturally aspirated HCCI engines is around 5 bars [65,103,104,105]. Due to the risk of severe knocking, HCCI engines cannot be operated at higher loads when the BMEP exceeds 5 bars.

Numerous efforts have been attempted to increase the operating range of HCCI engines in both the low and high-load regions. The intake air pressure must be increased when the high load region is extended. Both, Turbochargers [106] and superchargers [107] can be used to increase the intake air pressure. In this regard, Hyvönen et al. [108] found that when compared to superchargers, turbochargers indicated a 32–97% rise in BMEP. On the other hand, Olsson et al. [109] observed that the inlet air pressure was increased from 1 to 3 bar when the supercharger was used. Therefore, the BMEP penalty for HCCI engines could be more significant than the actual pressure increment caused by parasitic losses. A residual gas trapping approach with cooled EGR [110] and 2-stroke operation in 2-stroke/4-stroke switching engines [111] are two further solutions that have been proposed. It is also possible to extend the low-load region by using a spark [111-114], a dual-mode engine, or by decreasing coolant temperature [115].

### 1.7.4 The difficulty in combustion phasing control

The control of combustion phasing is one of the most challenging aspects of HCCI combustion. In comparison with traditional combustion, there is no direct technique for controlling the start of combustion, including a fuel injector in CI engines or spark plug in SI engines. Rather, a homogeneous air-fuel mixture is prepared, and the auto-ignition chemistry of the fuel-air mixture determines when combustion starts. Chemical kinetics drive HCCI combustion, which is regulated by fuel physicochemical characteristics and also the temperature history of the air-fuel mixture, as is widely recognized. In order to determine combustion phasing in HCCI engines, it is necessary to consider the following factors [66, 116]: fuel auto-ignition properties, fuel composition, compression ratio, intake temperature, combustion period and rate of residual, as well as reactivity and amount of EGR, fuel's latent heat of vaporization, homogeneity of the mixture, and wall temperatures, engine temperature, and transfer of heat to the engine, and speed of the engine and other engine related variables. Hence, the most difficult challenge is to control HCCI combustion across a wide operating range and loads. Engine efficiency and power output are affected by combustion control, which is the most significant factor to be considered. Chemical kinetics governs HCCI combustion, according to the majority of researchers [117-119]. It should also be highlighted that poor combustion control has a significant impact on engine behavior [120]. If the auto-ignition occurs too early before TDC, rapid reactions will occur, resulting in high peak combustion and an increased pressure rate. As a consequence, there is a decrease in power efficiency, as well as an increase in NOx emissions and severe engine damage. If the auto-ignition happens too late after TDC, the combustion duration will be prolonged, and there will be substantial cycle-to-cycle changes in the combustion, which will cause the misfiring of the engine, and causing the engine to stall. Very late HCCI combustion helps in increasing fuel usage while increasing UHC and CO emissions exponentially.

Many solutions for regulating HCCI combustion timing and helping to extend the load range have been examined, with varying degrees of success. The majority of these solutions fall into the following classes: mixture dilution, fuel property modification, in-cylinder direct fuel injection, and quick thermal management. Because of the intricate and highly interrelated nature of the HCCI combustion challenge, numerous researches addressing HCCI control use multiple methods [121]. In HCCI engines, there are many methods of controlling the combustion phase, including modifying two or more fuels [122-124], fuel additives and reforming [125-127], fuel stratification [105, 128, 129], variable valve timing (VVT) method or residual/exhaust gas trapping [130-132],

variable compression ratio (VCR) method [133-135], variable EGR method [136,137], modifying inlet temperature [138,139] variable coolant temperature [140], water injection [141], In-cylinder injection timing [142-144].

### 1.7.5 Homogeneous mixture preparation

The main key element of an HCCI engine is the homogenous charge preparation. The achievement of a good homogeneous mixture determines the performance and emission parameters. For getting maximum fuel efficiency, lowering UHC, NOx, and PM emissions, and eliminating oil dilution, impactful homogenous mixture preparation, eliminating wall impingement, and increasing fuel vaporization and air mixing are important. This is especially crucial for HCCI combustion with low volatility diesel fuel. In internal combustion, preparing a homogeneous mixture is a challenging task. Because of the short duration of the thermodynamic cycle [90], the period required to prepare a homogenous mixture for combustion is substantially shorter. In-cylinder injection and external mixture are the two methods for preparing homogeneous mixtures. Oil dilution is the fundamental drawback of in-cylinder mixtures, while volumetric efficiency is low with external mixtures. The homogeneity of a mixture cannot be determined directly [145]. In order to overcome the homogeneous charge preparation challenge, investigators have used a number of popular methods. There may be solutions to the homogenous mixture challenge with early in-cylinder injection with highly developed fuel injectors for diesel fuels [146,147] or fuel injection in a very turbulent port flow for gaseous and extremely volatile fuels [148,149]. The ignition delay period and fuel injection timing are the two most important factors in determining the homogeneity of the mixture in fuel injection. As a way of illustrating this challenge, authors have introduced the term degree of homogeneity (β). The ratio of the extent to conventional homogeneity can be used to define the degree of homogeneity. The homogeneity of the mixture decreases when fuel is injected closer to the TDC region, as seen in Fig. 1.17. An effectively homogeneous mixture is produced by HCCI with port fuel injection (PFI), but late fuel injection produces a more heterogeneous mixture than traditional CI injection. Only by raising the duration for mixture preparation can the degree of homogeneity of the air-fuel mixture be significantly enhanced.

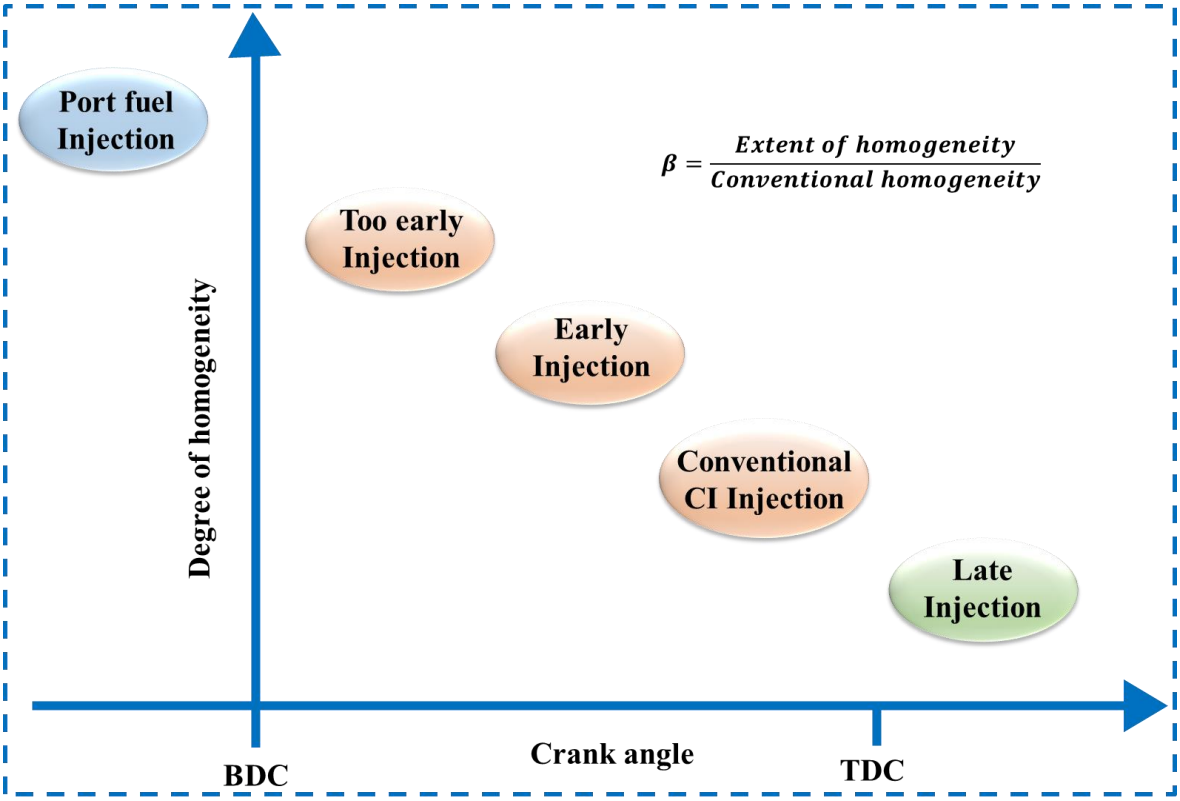


**Fig 1.17.** Variation of homogeneity with different injection strategies.

## 1.8 The Significance of Exergy Analysis

The science of thermodynamics has developed with the objective of understanding the interrelations between thermal, mechanical, and chemical phenomena. The study of process effectiveness of energy systems is one of the main applications of engineering thermodynamics. Traditional techniques to investigate the effectiveness (or efficiency) of an energy system are based on the first law of thermodynamics; i.e., the energy balance equation. Energy balance techniques do not differentiate between the different grades of energy crossing the system boundary and treat all forms of energy equivalently [150]. For example, from a first law perspective, in a power plant working based on the Rankine cycle, the work output from the turbine is treated equivalently to the heat transfer to the environment from the condenser. In other words, the low grade thermal energy rejected in a condenser of a power plant and the high grade work output of the turbine have the same quality based on the first law of thermodynamics. Moreover, the energy balance does not provide any information about internal losses. Considering only the energy balance in thermodynamic analyses could be potentially misleading in the sense that an adiabatic system such as a heat exchanger (with only internal heat exchange), a throttling valve, or a combustion chamber

may be interpreted as free from losses. The first law of thermodynamics has been used for a long time for investigation of different energy systems [151-153]. By neglecting the kinetic and potential energies inside a system, the first law of thermodynamics for an open system can be written as [154]:

$$\frac{dU}{dt} = \dot{Q}_0 + \dot{Q}_{ht} - P\frac{dV}{dt} + \sum \dot{m}_{in} h_{in} - \sum \dot{m}_{out} h_{out} \quad (1.6)$$

where, U is the internal energy, V is the volume and h is the specific enthalpy of the flow entering (subscript in) and exiting (subscript out) the system, $\dot{Q}_0$ is the heat transfer interaction of the system and environment (a suitably idealized system), and $\dot{Q}_{ht}$ shows the rest of the heat transfer interactions of the system with other systems. In the present work, the environment is defined as temperature of 25°C ($T_0$), pressure of 1 bar ($P_0$) and is assumed to be composed of $O_2$, $N_2$, $CO_2$, $H_2O$ with the mole fractions of $x_{0,O_2} = 0.2035$, $x_{0,N_2}$ = 0.7567, $x_{0,CO_2}$= 0.0003, $x_{0,H_2O}$ = 0.0303, $x_{0,other}$ = 0.0092 [155]. The second law of thermodynamics, on the other hand, provides a strong foundation to quantify the "quality" of energy transfers and thermodynamic irreversibilities in an energy system or process. For example, the isentropic efficiency is a metric based on the second law of thermodynamics than can address the irreversibilities associated with (adiabatic) turbines, compressors, pumps or nozzles. It compares the actual performance of a device with what would be achieved under idealized circumstances for the same inlet conditions [156]. For instance, the isentropic efficiency of a turbine can be defined as the ratio of the actual work output of the turbine and the maximum work output for reversible adiabatic (i.e., isentropic) expansion of its working fluid. The second law of thermodynamics can also explain why some processes occur spontaneously while others do not do so. One implication of the second law is that the total entropy of a system and its surroundings after any process either remains the same (at best) or increases. For ideal (reversible) processes, the total entropy of the system and its surroundings remains the same [157]. For decades, the second law has been used for comparison of irreversibilities in different energy systems [158-160]. The second law of thermodynamics for an open system can be written as [154]:

$$\frac{dS}{dt} = \frac{\dot{Q}_0}{T_0} + \frac{\dot{Q}_{ht}}{T_b} + \sum \dot{m}_{in} s_{in} - \sum \dot{m}_{out} s_{out} + \dot{S}_{gen} \quad (1.7)$$

where, s is the specific entropy of the flow entering or exiting the control volume, S is the total instantaneous entropy inventory in the control volume, $\dot{S}_{gen}$ is the rate of entropy generation within the control volume, and subscripts "0" and "b" indicate the environment and boundary, respectively. As long as two systems at different thermodynamic states are in contact with each other, the opportunity for extracting work exists. Exergy is defined as the maximum theoretical useful work obtained from a combined system consisting of a system of interest and an exergy reference environment. In other words, exergy is defined as the maximum work obtainable from a system when it interacts reversibly with the environment. Availability is defined as the maximum work that is available in a system or a flow [154]. Therefore, exergy of a system or flow is the difference between the non-flow availability of the system and the environment. Non-flow availability (A) and flow availability (b) can be obtained by combining the first and second laws of thermodynamics. Therefore, $\dot{Q}_0$ can be extracted from Eq. (1.7) and substituted in Eq. (1.6), and arranged to find work output of the system as follows:

$$P\frac{dV}{dt} = \frac{d(U-T_0S)}{dt} + \left(1-\frac{T_0}{T_b}\right)\dot{Q}_{ht} + \sum \dot{m}_{in}(h_{in}-T_0s_{in}) - \sum \dot{m}_{out}(h_{out}-T_0s_{out}) - T_0\dot{S}_{gen} \quad (1.8)$$

To complete the above equation, $P_0\frac{dV}{dt}$ which is the amount of work transferred to the environment should be subtracted from the useful system work:

$$(P-P_0)\frac{dV}{dt} = \frac{d(U+P_0V-T_0S)}{dt} + \left(1-\frac{T_0}{T_b}\right)\dot{Q}_{ht} + \sum \dot{m}_{in}(h_{in}-T_0s_{in}) - \sum \dot{m}_{out}(h_{out}-T_0s_{out}) - T_0\dot{S}_{gen} \quad (1.9)$$

According to Eq. (1.9), $U+P_0V-T_0S$ is non-flow availability and $h-T_0s$ is the flow availability. The difference between availabilities of a system or flow at their given conditions and at environmental conditions provides the exergy of the system or flow. By knowing exergy of different components of a process or whole plant, the exergy balance equation can be developed to find different terms such as exergy destruction (irreversibilities) or exergy lost due to heat transfer. Therefore, exergy analysis of a process or a whole plant can quantify the available work that has been lost by thermodynamic irreversibilities in various parts of the process or the plant. Over the past several decades, exergy analysis has been used for recognizing the source irreversibilities in different energy systems and quantifying the maximum work output of different energy systems [161-164]. Internal combustion engines are among the most ubiquitous prime

movers in the world but there is still significant potential to increase the fuel conversion efficiency (FCE) of IC engines. Exergy analysis can provide a detailed understanding of the maximum potential work output of an IC engine by quantifying the exergy distributions among the various processes occurring during an engine cycle.

## 1.9 Relevance of exergy analysis to IC engines

Increasing the FCE of IC engines continues to be one of the primary challenges faced by engine designers. In particular, the heavy-duty trucking industry is faced with a new paradigm of demonstrating engine technologies to achieve 55% brake thermal efficiency (BTE) for future heavy-duty diesel engine trucks under the aegis of the US Department of Energy's ongoing SuperTruck II program [165]. To achieve the difficult target of 55% brake FCE, it is necessary to exploit as much of the fuel's chemical exergy that is provided to the engine. Exergy analysis is a useful analytical method that can quantify the crank angle resolved exergy flow within a complete engine cycle. This is especially important during the closed portion of the engine cycle from intake valve closure (IVC) to exhaust valve opening (EVO) when most of the thermodynamic irreversibilities occur. On the other hand, engine exhaust flows also contain a significant portion of fuel exergy that has the potential to be exploited via waste heat recovery to increase the overall work output of an engine. Exergy analysis of IC engines can provide unique information about the various sources of irreversibilities. In fact, one of the primary goals of exergy analysis is to devise strategies to minimize exergy destruction during engine operation. This might be achieved by changing the engine operating conditions and the combustion process, once the sources of exergy destruction are known. Beside providing avenues for minimizing exergy destruction, exergy analysis can also help quantify other portions of fuel exergy that are lost with exhaust flow and heat transfer. Reducing engine heat transfer has been considered as an efficiency improvement strategy in IC engines in the past [166-167]. However, exergy analysis can provide quantitative information about the actual fraction of fuel exergy that is lost with the heat transfer process so that engine designers can determine if targeting engine heat transfer reduction is really worthwhile. Exhaust flows account for a significant fraction of the fuel exergy but they can be partially recovered to augment overall engine work output. As part of the portfolio of strategies being considered to enable high FCE operation, various waste energy recovery (WER) systems are significant. Exergy analysis of in-cylinder phenomena can provide a general overview about the

portion of fuel exergy in the exhaust flow. Exhaust WER is an important, practically feasible FCE improvement strategy and a detailed thermodynamic analysis of exhaust exergy flows is needed to inform the design of exhaust WER systems. Understanding different components of exhaust exergy flow can help increase the work output of exhaust WER systems, which in turn, leads to higher overall engine efficiency. By definition, the thermal and mechanical components of exergy are attributed to the temperature and pressure differences, respectively, between the system and the environment [154] and both exergy components may be relevant for the purposes of exhaust WER. A combination of in-cylinder and exhaust exergy analyses can help with potentially increasing the overall FCE of IC engines by changing engine operating conditions to minimize in-cylinder exergy destruction and to increase exhaust exergy, as needed.

## 1.10 Research Objectives and Thesis Overview

The aforementioned exergy analysis approaches have been found as the most relevant techniques for increasing the fuel to energy conversion efficiency of internal combustion (IC) engines. Exergy analysis provides a detailed understanding of the flow of different exergy components inside the cylinder and also reveal how various operative conditions can affect the destruction of exergy, exergy accompanied by the engine exhaust gases and energetic output of an engine. While minimizing in-cylinder irreversibilities can potentially be achieved by changing the operating conditions to alter the combustion process, exhaust exergy analysis and recovery is required to maximize the overall energetic output of the engine. This can be accomplished by understanding how different waste to energy generation systems exploit different portions of exergy accompanied by the exhaust gases. Also, it should be noted that application of waste to energy system in an engine affects the exhaust back pressure which results in different distributions of exhaust exergy and energetic output of the engine.

The present research investigation provides a promising methodology to increase the energetic output and fuel to energy conversion efficiencies of IC engine. The specific objectives of the present thesis are to:

1. Develop and perform a comprehensive exergy analysis of in-cylinder phenomena and other associated components of an IC engine operating on an advanced combustion technology (i.e., homogeneous charge compression ignition engine (HCCI).

2. Introduce and implement a combined, traditional energy analysis, computational exergy analysis methodology of exhaust flows to recover the enthalpy and exergy of engine exhaust gases for additional energy generation (power and cooling, simultaneously).

Fig. 1.18 shows graphically the specific objectives of the present thesis:

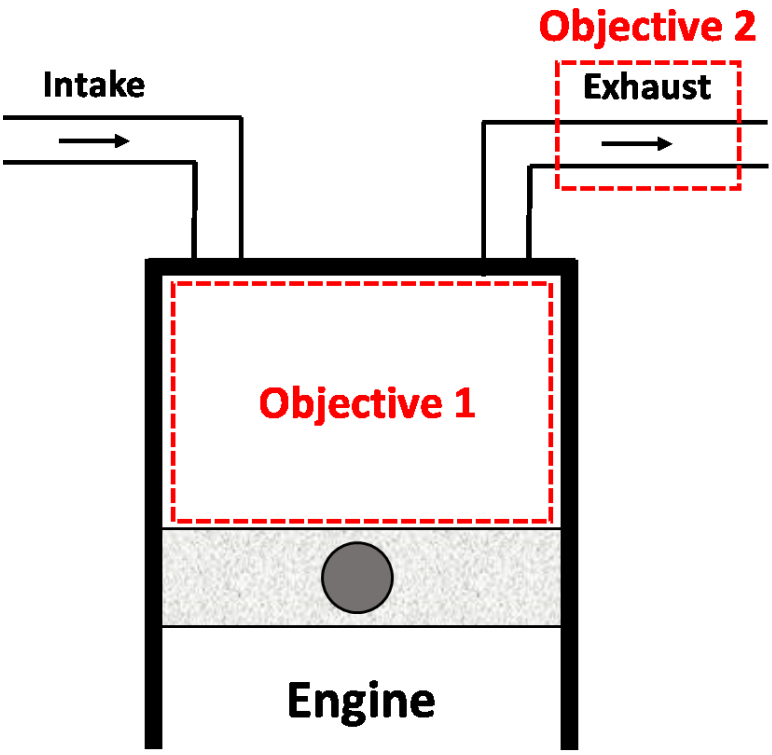


**Fig. 1.18** Specific objectives of the present study

In this regard, the present thesis is organized as follows:

- In Chapter 2, a framework for quantifying in-cylinder exergy transformations in IC engines is developed. The exergy analysis, study of variation of exergy components, and investigation of the effect of operating conditions on in-cylinder exergy distribution and irreversibilities are then carried out using a previously validated thermodynamic model of a wet-ethanol fueled HCCI engine. Finally, the practical application of exergy analysis for an HCCI engine is explained and implemented, with an exhaust waste energy recovery system consisting of an ORC combined with an ERC for converting a significant portion of the exhaust heat of a wet-ethanol fueled engine into useful power and cooling to meet a variety of consumer demands in a sustainable manner. The results of this study have been published in the ***Energy*** Journal of Elsevier Publications [**Mohd. Asjad. Siddiqui,**

Abdul Khaliq**,** Rajesh Kumar (2021) **"**Proposal and analysis of a novel cooling-power cogeneration system driven by the exhaust gas heat of HCCI engine fueled by wet-ethanol" *Energy, Vol. 232, pp. 120954* ***(Impact Factor: 7.14)*****]**

- In Chapter 3, an attempt was made for the proposal and analysis of a novel combined cycle consists of a wet-ethanol fueled and turbocharged HCCI engine coupled to ERC and ARC for the simultaneous generation of two distinct outputs namely power and refrigeration. A newly developed thermodynamic model was applied to investigate the performance of combined cycle and also ERC versus ARC output was compared and assessed after altering operating parameters. The results of this study have been published in the *Journal of ASME Transactions* [**Mohd. Asjad Siddiqui,** Abdul Khaliq**,** Rajesh Kumar **(**2022**)** **"**Thermodynamic and comparative analysis of ERC and ARC integrated wet-ethanol fueled HCCI engine for cogeneration of power and cooling**"** ***Transactions of ASME***: Journal of Thermal Science and Engineering Applications**,** *Vol. 14, pp. 041003-1, USA* ***(Impact Factor 1.47)*****].**
- In Chapter 4, a novel energy recovery technology for effectively utilizing the thermal exhaust of natural gas fueled HCCI engine was developed and assessed. In this technology, a two-phase ejector was combined with the natural gas fueled engine for the simultaneous production refrigeration and air conditioning (for food preservation and cabin cooling). The effect of equivalence ratio, engine speed, condenser temperature, refrigeration evaporator temperature, air conditioning evaporator temperature, and type of refrigerant employed in the ejector cooling cycle on the energetic and exergetic performances of the combined cycle was ascertained. The results of this study have been published in in the *ASME Journal of Energy Resources Technology* **[**Abdul Khaliq, Bandar. A. Almohammadi, Mathkar A. Alharthi, **Mohd. Asjad. Siddiqui**, Rajesh Kumar **(**2021**)** **"**Investigation of a combined refrigeration and air conditioning system based on two-phase ejector driven by exhaust gases of natural gas fueled homogeneous charge compression ignition engine" ***Transactions of ASME*****:** *Journal of Energy Resources Technology, Vol. 143 pp. 120911, USA* ***(Impact Factor: 2.90)*****].**
- Chapter 5 provides a summary of significant findings and conclusions from the present research, and also provides recommendations for future research work.

# Chapter 2

# Proposal and analysis of a novel cooling-power cogeneration system driven by the exhaust gas heat of HCCI engine fuelled by wet-ethanol

## 2.1 Introduction

Rapid consumption of traditional fuels to meet the increasing energy demand and associated environmental problems resulted in the search for alternative fuels. Ethanol as a renewable and oxygenated fuel has been found a promising option as it provides a high rate of combustion efficiency and reduces pollutant emissions. Ethanol is likely to produce from various agricultural products like corn and sugarcane. In the United States, corn has been considered as the most traditional source of ethanol production and it is reported that around 37% of total energy input is spent in driving away water from ethanol via distillation and dehydration processes [168]. Direct use of ethanol-water mixture (wet-ethanol) in combustion engines by eliminating the energy consumed in the removal of water may appreciably increase the net energy gain, from 21% to 55% [60]. Prior studies [169, 170] established that wet-ethanol is not suited to internal combustion engines operated in conventional modes of combustion like spark ignited (SI) and compression ignited (CI) and hence a modified mode of combustion is required for the best use of wet-ethanol in engines. Homogeneous charge compression ignition (HCCI) combustion is an emerging technology where the best characteristics of CI and SI engines are combined and such engines utilized premixed and lean fuel-air mixture at high compression ratio which drastically reduces the emissions of PM and $NO_x$ while providing a higher thermal efficiency [149, 171].

Energy analyses applied to internal combustion engines discovered that only 30-40% of fuel energy input to the engine is transformed into power and the rest is rejected as waste enthalpy to the atmosphere via engine exhaust and cooling system [172-174]. Recovery of high-temperature waste energy for useful energy generation is of great significance. Additional generation of cooling and power through engine exhaust heat as input is expected to provide economic benefits and to increase the energy utilization efficiency.

Among the technologies found suitable and widely applied to utilize the waste heat of moderate temperature, thermal energy sources are the ORC (organic Rankine cycle) which has been receiving considerable attention due to better efficiency, reliability, and flexibility [175-177]. Many investigations concerning the performance analysis of organic Rankine cycles utilized to recover the low-grade waste heat are reported [178-180]. Further, Tchanche et al. [181] analyzed the maturity of ORC for its existing applications in engine heat recovery. Srinivas et al. [182] estimated the waste heat potential accompanied by exhaust gases of combustion engines operated in dual fuel mode using the ORC. They observed an improvement of 7 percentage points in the fuel conversion efficiency for all loads. Vaja and Gambarotta [183] presented the evaluation of extra power achievable by employing the vapor power cycle at the engine exhaust when it is operated at full load. They determined that power produced through waste heat recovery may be reutilized in the engine propulsion which will reduce the fuel consumption and environmental impact.

Following the advantages of exergy analysis over the energy methodology, Khaliq et al. [184] carried out a new investigation based on second-law theory applied to HCCI engine fuelled by wet-ethanol. They observed the effect of turbocharger pressure ratio and ambient temperature on both first and second-law efficiencies of the engine by evaluating the exergy destruction in each

component to determine its real performance. Saxena et al. [185] presented the exergy analysis of homogeneous charge compression ignition (HCCI) engines dealing with a breakdown of mixture exergy and exergy destroyed. Exergy analysis applied to a multi-zone HCCI simulation was validated against engine experiments for ethanol-fuelled operation. Further, Khaliq and Trivedi [186] have studied a wet-ethanol fuelled HCCI engine bottoming with the organic Rankine cycle for exhaust heat recovery and performed the computational analysis based on the first and second laws of thermodynamics.

Comfortable journey with commercial vehicles requires an air conditioning system whose compressor is driven by a pulley connected to the engine shaft which creates a major parasitic load on the engine and it is estimated that, on average, engine shaft driven air conditioning increases the fuel consumption of vehicle by 20% [187]. An important development in the direction of reducing this parasitic load has been the use of vapor absorption refrigeration cycles which are heat-driven and are environment friendly but the obligatory standards concerning the weight of the empty vehicle disregard the use of absorption refrigeration systems as they are bulky, expensive and complex in design. To surmount this limitation, ERC (ejector refrigeration cycle) is found to be a promising option as it eliminates the use of CFCs and shaft-driven compressors. Moreover, ejectors are more compact and easier to maintain than compression and absorption cooling systems [188, 189]. In this context, an organic Rankine cycle combined with the ejector is considered to be the most potential solution for engine waste heat recovery. Very few investigations on exergy analysis of ORC combined with the ejector cooling are reported [190-192]. As mentioned above, many examples exist in the literature concerning the ORC coupled to internal combustion engines for efficient exploitation of the waste heat accompanied by exhaust gases. Some investigators focussed on the use of absorption refrigeration cycle, and the combination of ORC with the ejector

refrigeration system for engine exhaust heat recovery is found [193, 194]. Very little information is available concerning the application of ORC combined with the ERC for converting a major part of the exhaust heat of an alternative fuelled engine into useful power and cooling to meet the diverse consumer's demands sustainably. Therefore, investigation and employment of the new cooling-power cogeneration cycle that conjoin the condenser and generator of ORC and ERC through components integration for the recovery of waste heat carried by the exhaust gases of HCCI engine running on wet-ethanol is novel and worth studying.

The following aspects reflect the novelty of this work:

1- The organic Rankine cycle (ORC) integrated with the ejector refrigeration cycle (ERC) is developed to make efficient use of the exhaust heat of a wet-ethanol fueled HCCI engine through the simultaneous generation of power and cooling energy.
2- A mathematical model is formulated and a thermodynamic assessment is carried out using the Engineering Equation Solver (EES) software to evaluate the best possible design parameters and configuration to achieve the maximum energetic and exergetic performance of the combined thermal system.

In this study, a parametric study has been conducted to examine the role of various design parameters such as; turbocharger pressure ratio, turbocharger compressor efficiency, vapor generator temperature, entrainment ratio of ejector, ERC evaporator pressure, motive flow degree of superheat, and a rise in ambient temperature on the thermal and exergy efficiencies of wet-ethanol fuelled HCCI engine integrated to ORC combined with ERC. The effect of altering these operative parameters was also ascertained on the net power output of the combined system and its cooling capacity as well as on the exergy of refrigeration.

## 2.2. Description of the proposed work

A detailed description of the proposed cogeneration cycle may be illustrated as shown in Fig. 2.1 and can be described as: compressed air at (state 2) enters the fuel-air mixer where wet-ethanol (state 4) is injected and vaporizes to form a homogeneous mixture of ethanol-water-air which enters the HCCI engine (state 5) for combustion. Exhaust gases of the engine are directed to the catalytic converter (state 6) at a high temperature and exiting the converter at a higher temperature with less harmful gases which enter the turbine (state 7) after leaving the convertor and generate power to drive the turbocharger. The turbine exhaust through the regenerator is delivered to the boiler of ORC (state 9) for vaporizing the refrigerant. The vaporized refrigerant enters the ORC turbine (state 19) and generates additional power to compensate for parasitic losses to some extent. The refrigerant turbine exhaust enters the conjoining heat exchanger (HE) (state 20) which simultaneously acts as a condenser for ORC and boiler/generator for ERC. The low-pressure liquid is pumped back to the vapor generator (state 22) to complete the ORC for additional power generation ($\dot{W}_{T2}$). The high-pressure refrigerant after vaporizing in the HE is directed to the ejector as motive stream (state 11) and entrains the superheated vapor of lower pressure from the evaporator (state 16) into the ejector where the two streams mixed where a supersonic stream is formed which passes through a constant area section where normal shock wave occurs, with a significant pressure rise. The velocity of the mixed stream after the shock changes to subsonic and decelerates in the diffuser. The mixed stream from the ejector exit enters the condenser of ERC at (state 12) where the process of heat rejection to the ambient occurs. The saturated liquid leaving the condenser (state 13) is divided into two parts. One part enters the throttling valve (state 14) and then to the evaporator (state 15) to produce the required refrigeration ($\dot{Q}_{ref}$) for cooling

customers. The remaining liquid is back to HE through the pump (P1) (state 18) to complete the ERC.

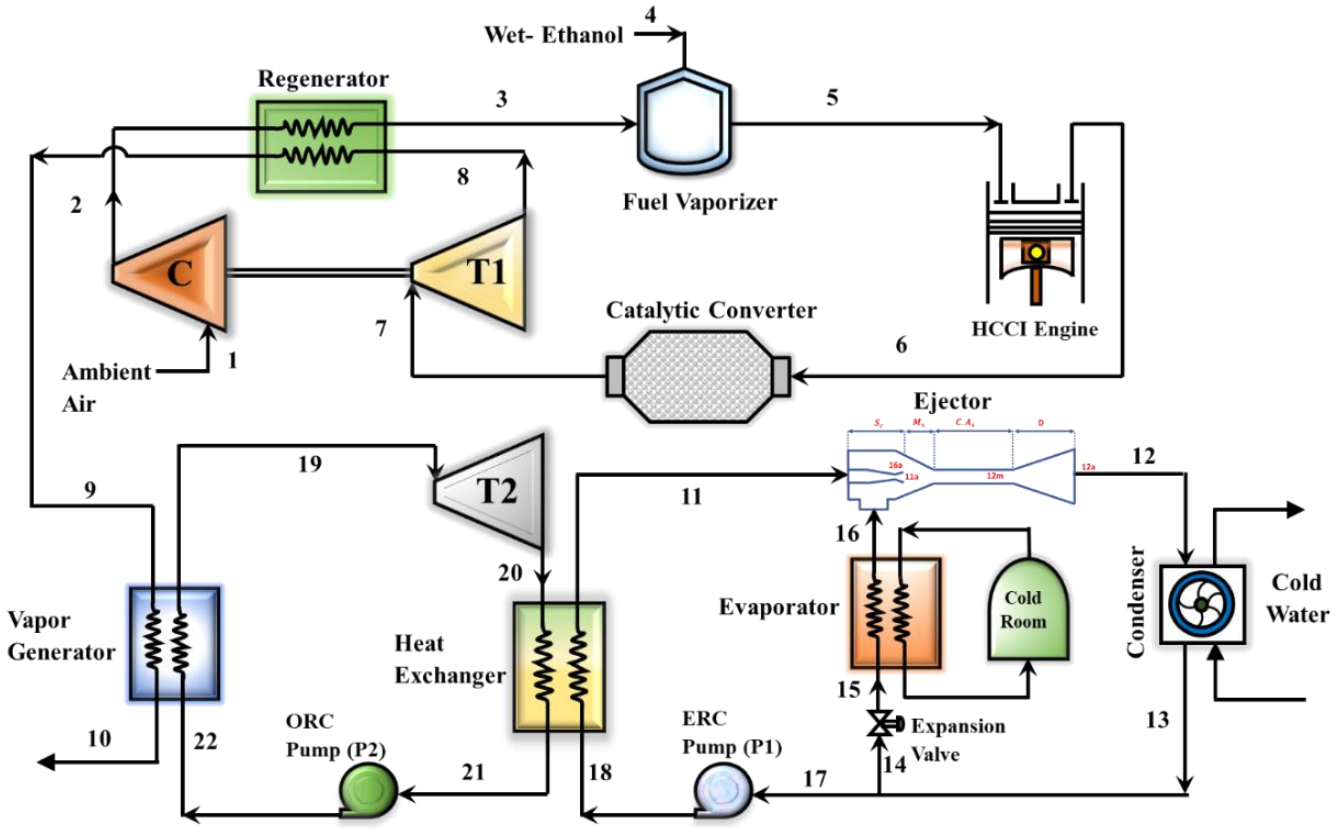


**Fig. 2.1.** System layout of wet ethanol operated HCCI engine based cooling-power cogeneration

## 2.3. Working fluid thermodynamic properties

In the ideal engine cycle, the working fluid for processes that occurs in the cylinder is considered simply as air. However, in actual cycles, the working fluid consists of several gaseous species.

The specific heat of gases varies with temperature in real engine application, and its variation with pressure is negligible. In the present model of molar specific heat $\bar{C}_p(T)$ variation with temperature, the coefficients ($a_1$-$a_5$) for each species, are taken from literature in the range of temperature from 300K to 3000K [195]

$$\bar{C}_p(T) = \bar{R}(a_1 + a_2T + a_3T^2 + a_4T^3 + a_5T^5) \quad (2.1)$$

The enthalpy and entropy of the gaseous species i in terms of specific heat capacity may be expressed as below [196]

$$\bar{h}_{i_{(T)}} = \bar{h}_{i_{(T_0)}} + \int_{T_0}^{T} \bar{C}_{p_i}(T)dT \quad (2.2)$$

$$\bar{s}_{i\ (T,p)} = \bar{s}_{i_{(T_0,p_0)}} + \int_{T_0}^{T} \frac{\bar{C}_{p_i}(T)}{T} dT - \bar{R}ln\left(\frac{y_i p}{p_0}\right) \quad (2.3)$$

The intake air, combustion products, and engine exhaust gases are considered to be a mixture of various species. Below are the equations which can be utilized for the computation of molar specific enthalpy, molar specific entropy, and Molecular mass of the mixture [196].

$$\bar{h}_{mix_{(T)}} = \sum_{i=1}^{n} y_i \bar{h}_{i_{(T)}}; \qquad \bar{s}_{mix_{(T,P)}} = \sum_{i=1}^{n} y_i \bar{s}_{i_{(T,P)}}\ ; \qquad M_{mix} = \sum_{i=1}^{n} y_i M_i \quad (2.4)$$

In the present analysis, the fuel-air mixture is stoichiometric because ethanol containing w ater obtain all the required dilution. The combustion equation for burning wet-ethanol in the HCCI engine can be considered as below [184].

$$C_2H_5OH + 6H_2O + 3(O_2 + 3.77N_2) = 1.8\,CO_2 + 0.1CO + 0.05C_2H_5OH + 8.85H_2O + 0.2O_2 + 11.319N_2 \quad (2.5)$$

Unburned hydrocarbons and carbon monoxide which formed as emissions in the HCCI engine can be further oxidized by using Pd-loaded $SiO_2 - Al_2O_3$ as the oxidizing catalyst. Assuming the complete conversion of unburned fuel and carbon monoxide and the application of mass and energy balances, the composition and temperature of gases at the exit of the catalytic converter can be determined

$$\sum_{Product} n_e\left(\bar{h}_f^{\circ} + \Delta\bar{h}\right)_e = \sum_{Reactant} n_i\left(\bar{h}_f^{\circ} + \Delta\bar{h}\right)_i \quad (2.6)$$

Where i refers to the streams inlet to catalytic convertor and e refers to the exiting stream of products leaving the converter [186]. The equation for the chemical reaction of engine exhaust gases in the catalytic converter is assumed to be as follows:

$$1.8\,CO_2 + 0.1\,CO + 0.05\,C_2H_5OH + 8.85\,H_2O + 0.2\,O_2 + 11.319\,N_2 = 2\,CO_2 + 9\,H_2O + 11.319\,N_2 \quad (2.7)$$

### 2.3.1 Turbocharger compressor

For a given pressure ratio and considered polytropic efficiency, the temperature of the air leaving the compressor can be determined after applying the equation,

$$\mathrm{T}_2 = \mathrm{T}_1 \left(\frac{\mathrm{P}_2}{\mathrm{P}_1}\right)^{\frac{(\gamma-1)}{\gamma\eta_C}} \quad (2.8)$$

### 2.3.2 Regenerator

The performance of the regenerator which preheats the compressed air is determined through its effectiveness and is given by

$$\varepsilon_h = \frac{\left[(\dot{m}.\mathrm{c}_p)_2(\mathrm{T}_3-\mathrm{T}_2)\right]}{\left[(\dot{m}.\mathrm{c}_p)_{min}(\mathrm{T}_8-\mathrm{T}_2)\right]} \quad (2.9)$$

The assumption, $(\dot{m}.\,\mathrm{c}_p)_2 = (\dot{m}.\,\mathrm{c}_p)_{min}$ is taken to estimate the temperature, $\mathrm{T}_3$, the air temperature at the regenerator exit, and with this relation, it is expressed as

$$\mathrm{T}_3 = \mathrm{T}_8\varepsilon_h + \mathrm{T}_2(1-\varepsilon_h) \quad (2.10)$$

The temperature at the regenerator exit is computed by applying the energy balance over it which is reported in Table 2.1.

### 2.3.3 HCCI engine

The premixed ethanol-water mixture leaving the mixer enters the HCCI engine and due to operation at a higher compression ratio, the charge is heating up to the level of ignition and combustion. But auto-ignition process is observed in the HCCI engine for combustion which is controlling through chemical kinetics [184]. The combustion efficiency is considered to be 94%. The temperature of the mixture containing the fresh charge and residual gases at the end of the engine intake process $(i - 1')$ is computed by employing the expression and the ratio of pressure for inlet/exhaust is considered to be 1.4 [186].

$$T_{1'} = \frac{\mathrm{T}_i(1-f)}{1-\frac{1}{(n.\mathrm{r}_c)\left[\frac{\mathrm{p}_e}{\mathrm{p}_i}+(n-1)\right]}} \tag{2.11}$$

Where $1'$ signifies the location before the process of compression of fuel-air-residual gas mixture and $P_{1'} = \mathrm{P}_1$

Polytropic compression stroke $(1' - 2')$

$$P_{2'} = P_{1'}\left(\frac{V_{1'}}{V_{2'}}\right)^n = P_{1'}(\mathrm{r}_c)^n \tag{2.12}$$

$$T_{2'} = T_{1'}(\mathrm{r}_c)^{n-1} \tag{2.13}$$

Assuming the heat addition process $(2' - 3')$ as constant volume gives

$$T_{3'} = T_{2'} + q_{in}(1 - f)/c_v \tag{2.14}$$

$$P_{3'} = P_{2'}\left(\frac{T_{3'}}{T_{2'}}\right) \tag{2.15}$$

Expansion stroke $(3' - 4')$ is polytropic and this gives

$$P_{4'} = P_{3'}\left(\frac{1}{\mathrm{r}_c}\right)^{n} \tag{2.16}$$

$$T_{4'} = T_{3'}\left(\frac{1}{\mathrm{r}_c}\right)^{n-1} \tag{2.17}$$

Polytropic blowdown $(4' - 5')$

$$T_{5'} = T_{4'}\left(\frac{P_{4'}}{P_e}\right)^{\frac{(1-n)}{n}} \tag{2.18}$$

$$P_{5'} = P_e \tag{2.19}$$

The exhaust stroke is assumed to be polytropic and isobaric $(5' - 6')$, it gives

$$T_{5'} = T_e \tag{2.20}$$

$$P_6 = P_{5'} = P_e \tag{2.21}$$

$$f = \frac{1}{\mathrm{r}_c}\left(\frac{P_e}{P_4}\right)^{\frac{1}{n}} \tag{2.22}$$

Residual gas fraction (f=0.03) is found to be lower due to the large compression ratio.

The heat rejection to the environment during the processes of exhaust and blowdown is computed by considering 9% loss of heat accompanied by these processes [186].

The formulation for calculating the HCCI engine's chemical exergy may be seen as below

$$e_{HCCI}^{ch} = -\Delta g + \bar{R}\mathrm{T}_0\left\{x\mathrm{O}_2 ln\frac{P_{\mathrm{O}_2}^{00}}{P^0} + y\mathrm{H}_2 O ln\frac{P_{H_2O}^{00}}{P^0} - \sum_K \mathrm{x}_k ln\frac{P_k^{00}}{P^0}\right\} \tag{2.23}$$

The details of the symbols used in the above equation can be found in Ref. [186].

### 2.3.4 Turbine

Exhaust gases after passing through the convertor are expanded over the turbine and the temperature at the turbine outlet can be determined by [60]

$$T_8 = T_7 \left(\frac{P_8}{P_7}\right)^{\frac{(n-1)\eta_T}{n}} \quad (2.24)$$

## 2.4. Energy and exergy analyses

Based on the layout of the system proposed and described in section 2, theory of analysis emerges after combining the second laws of thermodynamics with the first law approach is employed to carry out the investigations which reveal the insights in the performance of the proposed cooling-power cogeneration applied to wet-ethanol fueled HCCI engine [184, 185].

The traditional law of conservation of energy along with the mass conservation principle applies to the thermodynamic system operating at a steady state while ignoring the change in kinetic and potential energies gives

$$\Sigma \dot{m}_i - \Sigma \dot{m}_o = 0 \quad (2.25)$$

$$\Sigma \dot{Q} - \Sigma \dot{W} + \Sigma \dot{m}_i h_i - \Sigma \dot{m}_o h_o = 0 \quad (2.26)$$

Employment of the detailed thermodynamic theory of wet-ethanol fuelled HCCI engine described by Khaliq and Trivedi [186] and Rostamzadeh et al. [197] along with their assumed operative conditions, and the consideration of equations leading to conservation of mass and energy, the equation of energy balance for each component of the combined cooling-power system was developed which are presented in Table 2.1 as below.

**Table 2.1** Component wise energy balance equations for the combined HCCI engine with ORC and ERC

| **Component** | **Balance Equations** |
|---|---|
| Compressor (C) | $\dot{W}_C = \dot{m}_a(h_2 - h_1)$ |
| Regenerator (Reg) | $\dot{m}_a\,(h_3 - h_2) = \dot{m}_{exh}\,(h_8 - h_9)$ |
| Fuel vaporizer (FV) | $\dot{m}_a\,h_3 + \dot{m}_f h_4 = (\dot{m}_a\, + \dot{m}_f)h_5$ |
| HCCI engine (Compression) process,1´- 2´ | $\left(\dot{m}_a\, + \dot{m}_f + \dot{m}_{rg}\right)(h_{2'} - h_{1'}) = \dot{W}_{comp} - \dot{Q}_{surr}$ |
| Heat addition process, 2´- 3´ | $\left(\dot{m}_a\, + \dot{m}_f + \dot{m}_{rg}\right)(h_{3'} - h_{2'}) = \dot{Q}_H$ |
| Expansion process,3´- 4´ | $\left(\dot{m}_a\, + \dot{m}_f + \dot{m}_{rg}\right)(h_{3'} - h_{4'}) = \dot{W}_{exp} + \dot{Q}_{surr}$ |
| Blowdown Process, 4´-5´ | $\dot{m}_{exh}\,h_{4'} = \dot{m}_{exh}\,h_{5'} + \dot{Q}_{surr}$ |
| Catalytic convertor (CC) | $\sum_{Product} n_e\left(\bar{h}_f^{\circ} + \Delta\bar{h}\right)_e = \sum_{Reactant} n_i\left(\bar{h}_f^{\circ} + \Delta\bar{h}\right)_i$ |
| Power turbine (T1) | $\dot{W}_{T1} = \dot{m}_{exh}\,(h_7 - h_8)$ |
| Vapor generator (VG) | $\dot{Q}_{VG} = \dot{m}_{19}(h_{19} - h_{22}) = \dot{m}_9(h_9 - h_{10})$ |
| ORC pump (P2) | $\dot{W}_{P2} = \dot{m}_{22}\,(h_{22} - h_{21})$ |
| ORC turbine (T2) | $\dot{W}_{T2} = \dot{m}_{19}\,(h_{19} - h_{20})$ |
| Heat exchanger (HE) | $\dot{Q}_{HE} = \dot{m}_{19}(h_{20} - h_{21}) = \dot{m}_{11}(h_{11} - h_{18})$ |

| | |
|---|---|
| Ejector (Eje) | $\dot{m}_{11}h_{11} + \dot{m}_{16}h_{16} = \dot{m}_{12}h_{12}$ |
| Condenser (Cond) | $\dot{Q}_{Cond} = \dot{m}_{12}(h_{12} - h_{13})$ |
| Expansion valve (EV) | $h_{14} = h_{15}$ |
| ERC pump (P1) | $\dot{W}_{P1} = \dot{m}_{18}(h_{18} - h_{17})$ |
| Evaporator (Evap) | $\dot{Q}_{ref} = \dot{m}_{16}(h_{16} - h_{15})$ |

A relatively new thermodynamic property called exergy is used to measure the maximum theoretical work that could be delivered by the system after undergoing the reversible transition from state considered to dead state. In any gaseous species, it is the summation of chemical and physical exergy. Its balance during a process is given by

$$\dot{E}_{x,D} = \sum\left(1 - \frac{T_0}{T_j}\right)\dot{Q}_{CV} - \dot{W}_{CV} + \sum \dot{m}_i e_{x,i} - \sum \dot{m}_e e_{x,e} \quad (2.27)$$

Where, $\dot{m}$ is the rate of mass rate of the flowing stream; First and the second term on the right-hand side of Eq. (2.27) refers to the exergy transfer rates by heat and work. $\dot{E}_{x,D}$ is the rate of exergy destroyed during the process and $e_x$ is the specific flow exergy which is given by the following expression

$$e_x = (h - h_0) - T_0(s - s_0) \quad (2.28)$$

Taking the exergy definition in view of assumptions listed, and balances proposed, the equations for the determination of exergy destruction in the processes refer to main components of the novel configuration of cooling-power cogeneration system are developed and depicted in Table 2.2.

**Table 2.2** Component wise exergy balance equations for the combined HCCI engine with ORC and ERC

| **Component** | **Balance Equations** |
|---|---|
| Compressor (C) | $\dot{\mathrm{E}}_{\mathrm{x,D,C}} = \dot{\mathrm{m}}_1\left(e_{x,1} - e_{x,2}\right) + \dot{W}_C$ |
| Regenerator (Reg) | $\dot{\mathrm{E}}_{\mathrm{x,D,Reg}} = \dot{\mathrm{m}}_2\left(e_{x,2} - e_{x,3}\right) + \dot{\mathrm{m}}_8\left(e_{x,8} - e_{x,9}\right)$ |
| Fuel vaporizer (FV) | $\dot{\mathrm{E}}_{\mathrm{x,D,FV}} = \dot{\mathrm{m}}_3 e_{x,3} + \dot{\mathrm{m}}_4 e_{x,4} - \dot{\mathrm{m}}_5 e_{x,5}$ |
| HCCI engine (Compression) process,1´-2´ | $\dot{\mathrm{E}}_{\mathrm{x,D,comp}} = \dot{\mathrm{m}}_5\left(e_{x,1'} - e_{x,2'}\right) + \dot{W}_{comp} - \dot{Q}_{surr}\left(1 - \frac{T_0}{T}\right)$ |
| Heat addition process, 2´-3´ | $\dot{\mathrm{E}}_{\mathrm{x,D,Heat\,addition}} = \dot{\mathrm{m}}_5\left(e_{x,2'} - e_{x,3'}\right) + \dot{Q}_H\left(1 - \frac{T_0}{T_H}\right)$ |
| Expansion process, 3´- 4´ | $\dot{\mathrm{E}}_{\mathrm{x,D,exp}} = \dot{m}_5\left(e_{x,3'} - e_{x,4'}\right) - \dot{W}_{exp} - \dot{Q}_{surr}\left(1 - \frac{T_0}{T}\right)$ |
| Blowdown Process, 4´-5´ | $\dot{\mathrm{E}}_{\mathrm{x,D},exh\,\&\,blowdown} = \dot{m}_5\left(e_{x,4'} - e_{x,5'}\right) - \dot{Q}_{surr}\left(1 - \frac{T_0}{T}\right)$ |
| Catalytic convertor (CC) | $\dot{\mathrm{E}}_{\mathrm{x,D,CC}} = \dot{\mathrm{m}}_6 e_{x,6} - \dot{\mathrm{m}}_7 e_{x,7} + \dot{\mathrm{m}}_6 e_{ch}$ |
| Power turbine (T1) | $\dot{\mathrm{E}}_{\mathrm{x,D,T1}} = \dot{\mathrm{m}}_7\left(e_{x,7} - e_{x,8}\right) - \dot{W}_{T1}$ |
| Vapor generator (VG) | $\dot{\mathrm{E}}_{\mathrm{x,D,VG}} = \dot{\mathrm{m}}_{19}\left(e_{x,22} - e_{x,19}\right) + \dot{\mathrm{m}}_9\left(e_{x,9} - e_{x,10}\right)$ |
| ORC pump (P2) | $\dot{\mathrm{E}}_{\mathrm{x,D,P2}} = \dot{\mathrm{m}}_{21}\left(\mathrm{e}_{\mathrm{x,21}} - \mathrm{e}_{\mathrm{x,22}}\right) + \dot{W}_{\mathrm{P2}}$ |
| ORC turbine (T2) | $\dot{\mathrm{E}}_{\mathrm{x,D,T2}} = \dot{\mathrm{m}}_{19}\left(e_{x,19} - e_{x,20}\right) - \dot{W}_{T2}$ |
| Heat Exchanger (HE) | $\dot{\mathrm{E}}_{\mathrm{x,D,HE}} = \dot{\mathrm{m}}_{20}\left(e_{x,20} - e_{x,21}\right) + \dot{\mathrm{m}}_{11}\left(e_{x,18} - e_{x,11}\right)$ |
| Ejector (Eje) | $\dot{\mathrm{E}}_{\mathrm{x,D,Eje}} = \dot{\mathrm{m}}_{11} e_{x,11} + \dot{\mathrm{m}}_{16} e_{x,16} - \dot{\mathrm{m}}_{12} e_{x,12}$ |

| | |
|---|---|
| Condenser (Cond) | $\dot{\mathrm{E}}_{\mathrm{x,D,Cond}} = \dot{\mathrm{m}}_{12}(e_{x,12} - e_{x,13}) - \dot{Q}_{Cond}\left(1 - \frac{T_0}{T_{Cond}}\right)$ |
| Expansion valve (EV) | $\dot{\mathrm{E}}_{\mathrm{x,D,EV}} = \dot{\mathrm{m}}_{14}\left(e_{x,14} - e_{x,15}\right)$ |
| ERC Pump (P1) | $\dot{\mathrm{E}}_{\mathrm{x,D,P1}} = \dot{\mathrm{m}}_{17}\left(\mathrm{e}_{\mathrm{x},17} - \mathrm{e}_{\mathrm{x},18}\right) + \dot{W}_{\mathrm{P1}}$ |
| Evaporator (Evap) | $\dot{\mathrm{E}}_{\mathrm{x,D,ref}} = \dot{\mathrm{m}}_{15}\left(e_{x,15} - e_{x,16}\right) - \dot{Q}_{ref}\left(\frac{T_0}{T_{Evap}} - 1\right)$ |

## 2.5. Overall performance evaluation criteria

In general, the performance of a system dealing with energy conversion is evaluated by combining the second law of thermodynamics with the first law analysis. Because of the distinction in the quality of energy accompanied by cooling and power, the conventional equation of thermal efficiency based on the energy balance approach is not suitable for cycles delivering more than one type of energy output. For a thermodynamically correct evaluation, the refrigeration capacity needs to be weighted differently. One alternative for such a valid evaluation is the employment of the COP offered practically by vapor compression refrigeration cycle ($COP_c$) to weigh the energy of refrigeration. In this regard, the most appropriate first law efficiency of the cooling-power cogeneration cycle can be shown as [198]

$$\eta_{th,cogen} = \frac{\dot{W}_{BT} + \dot{W}_{T,ORC} - \dot{W}_{P1,ERC} - \dot{W}_{P2,ORC} + \dot{Q}_{ref}/COP_c}{\dot{m}_f LHV \eta_C} \tag{2.29}$$

where, $\dot{W}_{BT}$ is the brake thermal power, $\dot{W}_{T,ORC}$, $\dot{W}_{P2,ERC}$, and $\dot{W}_{P1,ORC}$ are the power delivered by the ORC turbine and the power required by the pumps of ERC and ORC, respectively. $\dot{m}_f$ is the rate of fuel consumption and LHV is the lower heating value of fuel, $\dot{Q}_{ref}$ is the rate of cooling capacity, and $\eta_C$ is the combustion efficiency.

Efficiency based on exergy provides a more effective measure of the cycle performance and this can be obtained after applying the second law of thermodynamics and can be expressed as

$$\eta_{ex,cogen} = \frac{\dot{W}_{BT}+\dot{W}_{T,ORC}-\dot{W}_{P1,ERC}-W_{P2,ORC}+\dot{E}_{x,ref}}{\dot{m}_f LHV \eta_C \varphi} \quad (2.30)$$

where, $\dot{E}_{x,ref}$is the amount of exergy associated with the cooling capacity $\dot{Q}_{ref}$ and is given by

$$\dot{E}_{x,ref} = \dot{Q}_{ref}\left(\frac{T_0-T_{Evap}}{T_{Evap}}\right) \quad (2.31)$$

Where, $T_{Evap}$ is the evaporator temperature, $T_0$ is ambient, and $\phi$ is the ratio of exergy of the fuel to its energy.

The proposed cooling-power cogeneration cycle's performance was evaluated using the Engineering Equation Solver (EES) which is commercially available and provides built-in mathematical and thermodynamic property functions for solving the equations describing the model developed through balances of exergy, energy, and mass [199]. Every component of the system proposed is assumed to be a steady-state control volume, with the transfer of energy by heat, work, and mass of fluid enters and leaves. The equations derived after applying the balances of mass, energy, and exergy were incorporated to formulate the thermodynamic model. The thermodynamic properties of the refrigerant R134a, R290, and R600a used in the ORC and ERC were computed after employing the REFPROP V 9.1 [200, 201].

For the energetic and exergetic analyses of the cooling-power cogeneration system considered, the thermodynamic model was developed based on the assumptions below [184, 186, 194]:

- The combustion process in HCCI is governed by a time-dependent, variable volume well-mixed reactor.

- The burning rates of HCCI combustion are fast typically and if phasing out correctly in the cycle could approximate the ideal Otto cycle. Fig. 2.2 represents the PV diagram for the HCCI operating under ideal conditions.
- Pressure drop in duct and heat exchanger is ignored.
- Constant speed of engine operation was assumed (1800 RPM) with the invariable load.
- Due to the elevated compression ratio, the residual gas fraction was assumed on the lower side (f = 0.03).
- The minimum volume fraction of ethanol in water necessary for efficient HCCI operation is 35% by liquid volume. As a result, 35% ethanol in water by volume mixture was considered as the fuel input.
- All processes proceed under steady-state conditions.
- Effects of kinetic and potential energies are not considered during the energy conversion.
- The pressure drop in the pipes is not considered.
- Physical exergies of the ORC/ERC fluid are only considered.
- The working fluid is assumed to be a saturated liquid at the condenser exit.

Using mass, momentum, and energy conservation equations, the expression of entrainment ratio of the ejector can be formulated as [190]

$$\mu = \sqrt{\eta_n \eta_m \eta_d (h_{pf,n1} - h_{pf,n2,s'}) / (h_{mf,d,s'} - h_{mf,m})} - 1 \quad (2.32)$$

The efficiencies of different sections of the ejector are presented in Table 2.1.

The ejector comprises three different geometry segments; nozzle, mixing chamber, and diffuser.

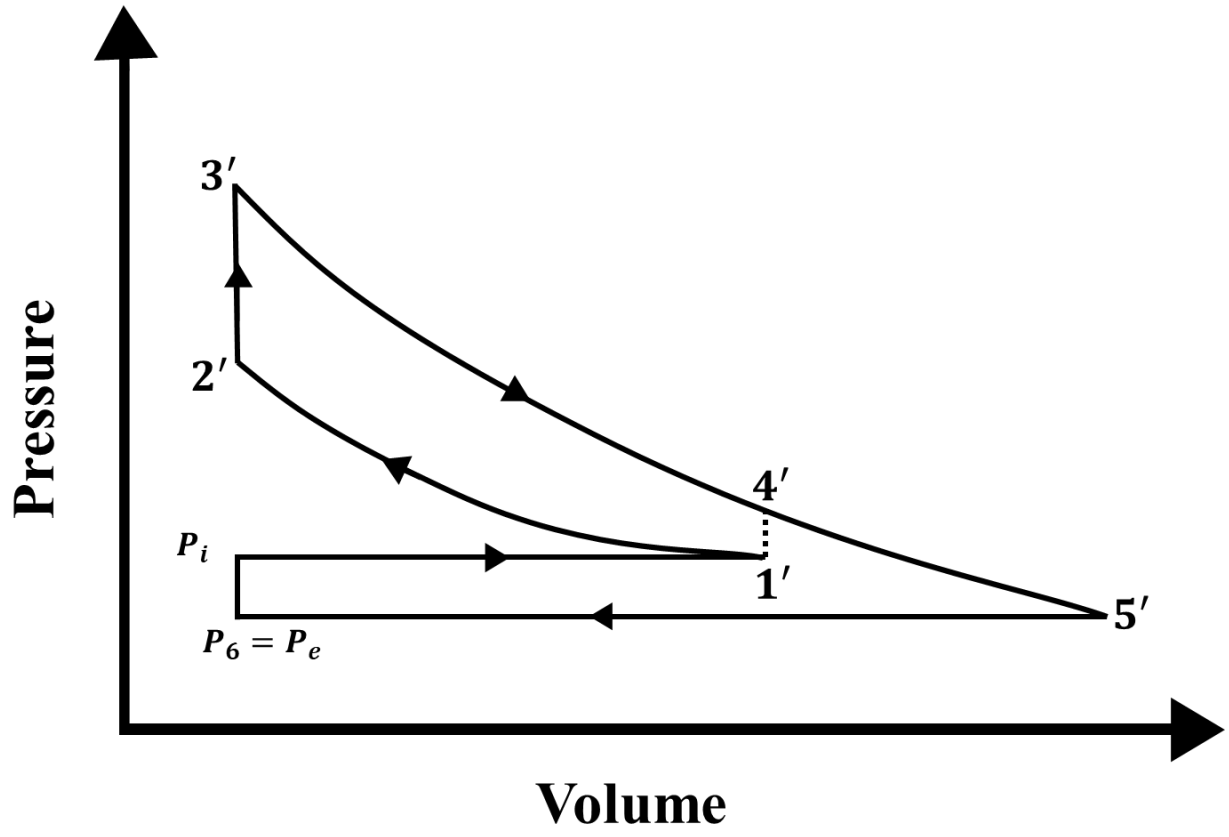


**Fig. 2.2**: PV diagram for the ideal operation of HCCI engine

The energy equation for the adiabatic flow in the nozzle under steady flow condition may be given as:

$$\dot{m}_{pf} h_{pf,n2} + \frac{\dot{m}_{pf} u_{pf,n2}^2}{2} = \dot{m}_{pf} h_{pf,n1} + \frac{\dot{m}_{pf} u_{pf,n1}^2}{2} \tag{2.33}$$

The efficiency of the nozzle may be seen as:

$$\eta_n = \frac{h_{pf,n1} - h_{pf,n2}}{h_{pf,n1} - h_{pf,n2,s'}} \tag{2.34}$$

The momentum conservation equation applied to the mixing section gives:

$$\dot{m}_{pf} u_{pf,n2} + \dot{m}_{sf} u_{sf,n2} = (\dot{m}_{pf} + \dot{m}_{sf}) u_{mf,m,s'} \tag{2.35}$$

The energy equation applied to the diffuser leads to:

$$\frac{1}{2}\left(u_{mf,m}^2 - u_{mf,d,s'}^2\right) = h_{mf,d,s'} - h_{mf,m} \tag{2.36}$$

The efficiency of the diffuser may be shown as:

$$\eta_d = \frac{h_{mf,d,s'} - h_{mf,m}}{h_{mf,d} - h_{mf,m}} \tag{2.37}$$

Details of the equations utilized to model the remaining components of the bottoming cycle such as; vapor generator, ORC pump, turbine, condenser, throttling valve, and the evaporator of ejector can be found from the Ref. [186, 190].

**Table 2.3** Data used for wet ethanol operated HCCI with ORC and ERC configuration

| | |
|---|---|
| Ambient temperature ($T_0$) (K) | 300 |
| Ambient pressure ($P_0$) (kPa) | 101.325 |
| HCCI engine fuel | 35% ethanol in water mixture |
| HCCI engine compression ratio | 16:1 |
| Turbocharger efficiency (%) | 80 |
| Effectiveness of regenerator | 0.78 |
| Catalytic convertor | Oxidizing type catalyst, Pd-loaded $SiO_2$–$Al_2O_3$ |
| Engine speed | 1800 rpm |
| Chemical exergy of ethanol (kJ/kg) | 29604.95 |
| LHV of ethanol (kJ/kg) | 26,900 |
| Volume swept per cylinder ($cm^3$) | 2400 |
| Cylinder diameter (cm) | 13.7 |
| Piston displacement(cm) | 16.5 |

| | |
|---|---|
| Length of connecting rod(cm) | 26.2 |
| Ratio of intake to clearance volume | 16:1 |
| Speed of engine (rpm) | 1800 rpm |
| Engine volumetric efficiency (%) | 100 |
| Ratio of the actual fuel-air mixture to the chemically correct fuel-air mixture | <0.5 |
| Combustion process in HCCI engine | Chemical kinetics applied to control the bulk auto-ignition process |
| Effectiveness of vapor generator | 0.8 |
| ORC turbine inlet pressure (MPa) | 1.8-2.2 |
| ORC turbine isentropic efficiency (%) | 90 |
| ORC pump isentropic efficiency (%) | 90 |
| Effectiveness of heat exchanger | 0.8 |
| ERC pump isentropic efficiency (%) | 90 |
| Evaporator temperature (°C) | 4 |
| $COP_c$ | 2.98 |
| Nozzle efficiency (%) | 90 |
| Mixing chamber efficiency (%) | 85 |
| Diffuser efficiency (%) | 85 |

**Table 2.4** Properties of Refrigerants

| **Refrigerant** | **R134a** | **R290** | **R600a** |
|---|---|---|---|
| **Chemical Formula** | $CH_2FCF_3$ | $C_3H_8$ | $C_4H_{10}$ |
| **Critical temperature (°C)** | 101.1 | 96.7 | 134.7 |
| **Critical pressure (kPa)** | 4059 | 4247 | 3640 |
| **Normal boiling point (°C)** | -26.1 | -42.2 | -12 |

| | | | |
|---|---|---|---|
| **Triple point Temperature (ºC)** | -104.3 | -187.1 | -159.6 |
| **Molecular Weight (kg/kmol)** | 102.03 | 44.1 | 58.12 |
| **Safety class** | A1 | A3 | A3 |
| **ODP** | 0 | 0 | 0 |
| **GWP (100 years)** | <1300 | <3 | <3 |
| **Latent heat of vaporization at boiling point (kJ/kg)** | 216.97 | 426.1 | 366.2 |

## 2.6. Results and discussion

The configuration of the cooling-power cogeneration cycle presented in the current study was investigated after applying the first and second laws of thermodynamics. The performance evaluation of wet-ethanol fuelled HCCI engine bottoming with the ORC combined with the ERC was carried out. Results are computed for the use of R134a, R290, and R600a as the common working fluid for ORC and ERC. Their thermo-physical properties and environment parameters are reported in Table 2.4. In the analysis, the effects of altering the turbocharger pressure ratio, turbocharger compressor efficiency, ambient temperature, vapor generator pressure, motive flow degree of superheat, entrainment ratio, and ejector evaporator pressure are investigated on the efficiencies of cooling-power cogeneration cycle as well as on the energy and exergy accompanied by power and refrigeration. Properties regarding HCCI based cooling-power cogeneration for its baseline operative conditions are described above in Table 2.3 which were taken from literature.

**Model validation**

The model developed for the thermodynamic performance evaluation of HCCI engine running on wet-ethanol is validated with the theoretical data reported in the literature [186]. Some of the preliminary results considering the integration of the organic Rankine cycle (ORC) and the ejector refrigeration cycle (ERC) combined with the wet-ethanol fuelled HCCI engine are validated by comparing with the reported results [186] where an ORC is combined with the wet-ethanol fuelled HCCI engine. Tables 2.5-2.8 list the comparison between the proposed system (HCCI engine combined with the ORC and ERC) and the system presented and investigated in Ref. [186] (HCCI engine combined with ORC). It is observed that the thermal efficiency of the proposed system is much higher than the thermal efficiency of the system exhibited in the reference [186]. The thermal efficiency of the proposed system (R134a is used as working fluid) varies from 47.81% to 50.09% compared to the increase in thermal efficiency in the Ref. [186] (R113 is employed as working fluid) from 35% to 48% when the turbocharger pressure ratio is elevated from 2.5 to 3.5. The comparison of results clearly shows that the proposed system is more efficient to make better use of engine waste heat. The difference in the results of the thermal efficiency of the combined system is found because of the integration of ERC with the ORC and due to the use of different working fluids. Further, a significant difference in the thermal efficiency of the configuration of ORC with ERC and the ORC only is also observed. Such as, the thermal efficiency of the heat recovery sy stem where ORC is combined with ERC and operated on R143a fluid varies from 3.789% to 3.767% while for ORC (reported one) which operated on R113 fluid varies from 2.61% to 2.8% when the turbocharger pressure ratio varies from 2.5 to 3.5. Similar trends are found for the variation in the exergy efficiency of the proposed system and the system reported in Ref. [186]. Effect of ambient temperature on the thermal and exergy efficiencies of the proposed system and the system reported in the Ref. [186] was also observed and a suitable comparison is found. The

type and range of operative conditions of the HCCI engine considered in the present study and the source of literature [186] are the same. They are as follows; turbocharger pressure ratio (2.5-3.5), turbocharger compressor isentropic efficiency (0.7-0.9), ambient temperature (290K-310K). A parametric comparison of computed results of the present study with the literature data is shown below in Tables 2.5-2.8. In sum, the findings of the present study make a solid accept to carry out further research in the area of the exploitation of alternative fuels in HCCI engine to promote sustainability further.

**Table 2.5** Comparison of thermal efficiency of the proposed combined thermal system with the reported data [186] of the system operating under the same condition and same fuel

| **Pressure Ratio** | **Combined thermal efficiency with R134a (Present work)** | **Combined thermal efficiency with R290 (Present work)** | **Combined thermal efficiency with R600a (Present work)** | **Combined thermal efficiency (Reported work)** | **ORC and ERC thermal efficiency with R134a (Present work)** | **ORC and ERC thermal efficiency with R290 (Present work)** | **ORC and ERC thermal efficiency with R600a (Present work)** | **ORC thermal efficiency (Reported work)** |
|---|---|---|---|---|---|---|---|---|
| **2.5** | 47.87 | 47.1 | 48.78 | 35 | 3.789 | 3.014 | 4.699 | 2.61 |
| **2.75** | 48.53 | 47.75 | 49.44 | 38.2 | 3.783 | 3.009 | 4.692 | 2.65 |
| **3** | 49.11 | 48.33 | 50.01 | 41.5 | 3.778 | 3.005 | 4.685 | 2.69 |
| **3.25** | 49.62 | 48.85 | 50.53 | 44.8 | 3.772 | 3.001 | 4.678 | 2.73 |
| **3.5** | 50.09 | 49.32 | 50.99 | 48 | 3.767 | 2.997 | 4.672 | 2.8 |

**Table 2.6** Comparison of exergy efficiency of the proposed combined thermal system with the reported data [186] of the system operating under the same condition and same fuel

| **Pressure Ratio** | **Combined exergy efficiency with R134a (Present work)** | **Combined exergy efficiency with R290 (Present work)** | **Combined exergy efficiency with R600a (Present work)** | **Combined exergy efficiency (Reported work)** | **ORC and ERC exergy efficiency with R134a (Present work)** | **ORC and ERC exergy efficiency with R290 (Present work)** | **ORC and ERC exergy efficiency with R600a (Present work)** | **ORC exergy efficiency (Reported work)** |
|---|---|---|---|---|---|---|---|---|
| **2.5** | 53.87 | 52.5 | 52.31 | 30.02 | 1.474 | 1.518 | 1.158 | 1.48 |

| | | | | | | | | |
|---|---|---|---|---|---|---|---|---|
| **2.75** | 54.6 | 53.23 | 53.04 | 33.3 | 1.47 | 1.514 | 1.155 | 1.476 |
| **3** | 55.25 | 53.88 | 53.69 | 36.9 | 1.467 | 1.511 | 1.153 | 1.473 |
| **3.25** | 55.82 | 54.46 | 54.26 | 40.25 | 1.464 | 1.507 | 1.15 | 1.47 |
| **3.5** | 56.33 | 54.97 | 54.78 | 43.7 | 1.461 | 1.504 | 1.148 | 1.467 |

**Table 2.7** Comparison of thermal efficiency of the proposed combined thermal system with the reported data [186] of the system operating under the same condition and same fuel

| **Ambient temperature** | **Combined thermal efficiency with R134a (Present work)** | **Combined thermal efficiency with R290 (Present work)** | **Combined thermal efficiency with R600a (Present work)** | **Combined thermal efficiency (Reported work)** | **ORC and ERC thermal efficiency with R134a (Present work)** | **ORC and ERC thermal efficiency with R290 (Present work)** | **ORC and ERC thermal efficiency with R600a (Present work)** | **ORC thermal efficiency (Reported work)** |
|---|---|---|---|---|---|---|---|---|
| **290** | 49.2 | 48.43 | 50.11 | 42.02 | 3.773 | 3.001 | 4.679 | 2.4 |
| **295** | 49.15 | 48.38 | 50.06 | 41.65 | 3.775 | 3.003 | 4.682 | 2.545 |
| **300** | 49.11 | 48.33 | 50.01 | 41.5 | 3.778 | 3.005 | 4.685 | 2.69 |
| **305** | 49.06 | 48.28 | 49.97 | 41.105 | 3.78 | 3.007 | 4.688 | 2.895 |
| **310** | 49.01 | 48.24 | 49.92 | 41.01 | 3.782 | 3.009 | 4.691 | 3.008 |

**Table 2.8** Comparison of exergy efficiency of the proposed combined thermal system with the reported data [186] of the system operating under the same condition and same fuel

| **Ambient temperature** | **Combined exergy efficiency with R134a (Present work)** | **Combined exergy efficiency with R290 (Present work)** | **Combined exergy efficiency with R600a (Present work)** | **Combined exergy efficiency (Reported work)** | **ORC and ERC exergy efficiency with R134a (Present work)** | **ORC and ERC exergy efficiency with R290 (Present work)** | **ORC and ERC exergy efficiency with R600a (Present work)** | **ORC exergy efficiency (Reported work)** |
|---|---|---|---|---|---|---|---|---|
| **290** | 55.08 | 53.76 | 53.48 | 37.1 | 1.343 | 1.424 | 0.9752 | 1.4 |
| **295** | 55.17 | 53.82 | 53.58 | 37 | 1.405 | 1.467 | 1.064 | 1.44 |
| **300** | 55.25 | 53.88 | 53.69 | 36.9 | 1.467 | 1.511 | 1.153 | 1.5 |
| **305** | 55.33 | 53.94 | 53.79 | 36.8 | 1.53 | 1.554 | 1.242 | 1.545 |
| **310** | 55.41 | 54 | 53.9 | 36.7 | 1.592 | 1.598 | 1.332 | 1.585 |

Fig. 2.3 represents the change in thermal efficiency of the HCCI engine-based cooling-power cogeneration system after altering the turbocharger pressure ratio. The thermal efficiency evaluated on first law basis is found to be increasing with the rise of pressure ratio across the turbocharger. This is due to the reason higher turbocharger pressure improves the fuel-air mixing along with the increase of charge density which raises the temperature of the mixture and hence the engine power output. Further, for the same turbine and compressor efficiencies and regenerator effectiveness any rise in turbocharger pressure ratio results in the increase of engine exhaust temperature which is an inlet temperature to the ORC combined with ERC and this will increase the heat transfer to refrigerant passes through the vapor generator and this, in turn, improves the ORC power and cooling capacity of the evaporator of ERC. This simultaneous increase in the output of the HCCI engine and the energetic output of bottoming cycle contributes to a rise in the efficiency of the cooling-power cogeneration cycle. Change in working fluid of bottoming cycle considerably influence the energy efficiency of cogeneration because of the considerable difference in their boiling points; (-26.1℃) for R134a and (-42.11$^0$C) for R290, (-12$^0$C) for R600a. Further, lower refrigeration output for the R290 (propane) operated system attributes to the low critical temperature of propane (96.74$^0$C) compared to the higher critical temperature of R134a (101.1$^0$C), and R600a (134.7$^0$C). Relatively a high motive flow temperature is required to produce the decent refrigeration output and hence the lower critical temperature of the refrigerant is a hindrance in obtaining the higher output. It is further noticed that an increase in pressure ratio across the turbocharger from 2.5 to 3.5 raises the efficiency of cooling-power cogeneration from 47.87% to 50.09% when R134a is used as working fluid and from 47.1% to 49.32% when R290 applies, and in case of R600a as bottoming cycle fluid it is increased from 48.78% to 50.99%. The exergy efficiency of HCCI engine based cogeneration is the ratio of power exergy plus exergy of

refrigeration to the fuel exergy, and the exergy of refrigeration is significantly less than the cooling capacity but the exergy of fuel (ethanol) is (29.6 kJ/kg) is considerably greater than the energy of ethanol (26.9 kJ/kg). Since the difference between the energy and exergy of ethanol is dominating over the difference between the energy and exergy of refrigeration, therefore, exergy efficiency of cogeneration is shown to be considerably higher than its corresponding thermal efficiency.

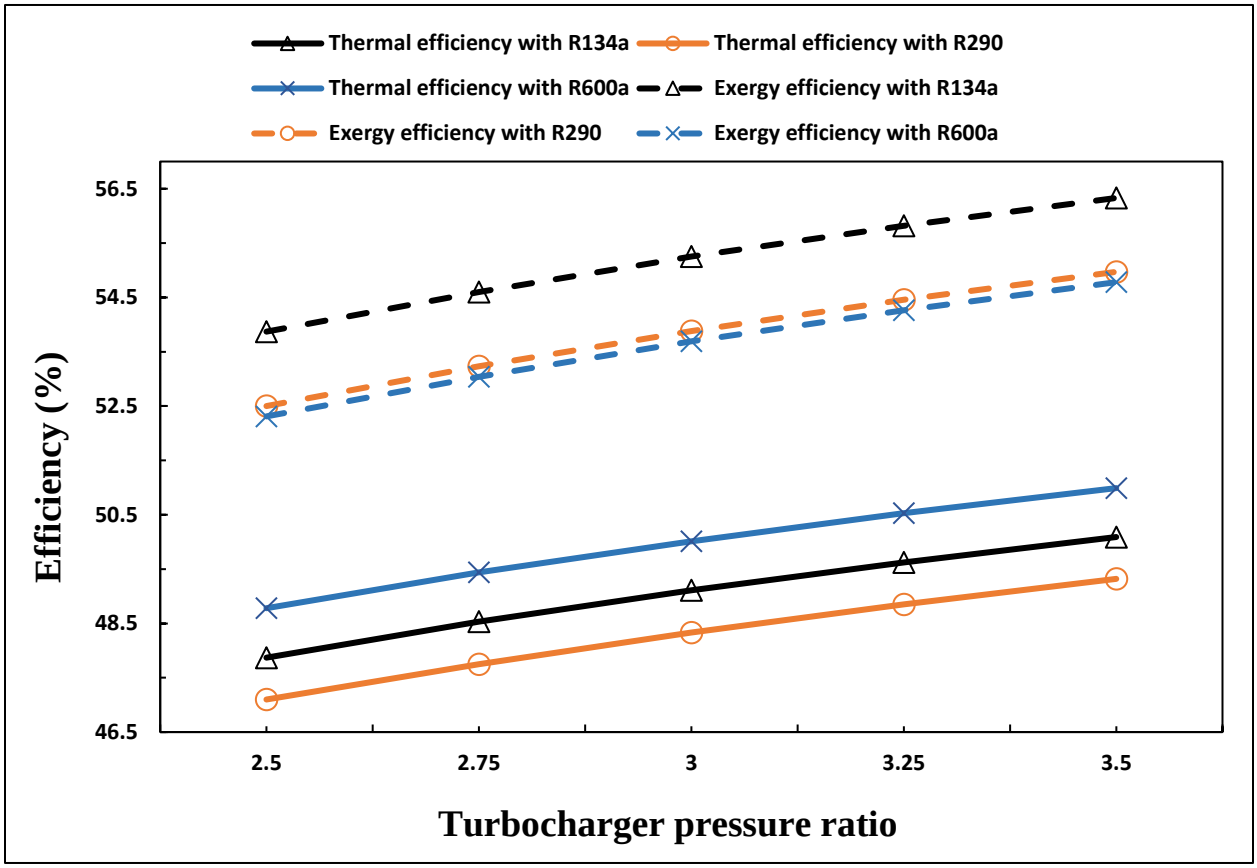


**Fig. 2.3.** Impact of turbocharger pressure ratio on the efficiencies of wet-ethanol fuelled HCCI engine based cooling-power cogeneration system

Fig. 2.4 displays the impact of turbocharger compressor efficiency on the thermal efficiency of the HCCI engine-based cooling-power cogeneration system. The thermal efficiency of the system is found to be increased at the rise of turbocharger compressor efficiency. This is because higher turbocharger efficiency decreases the compressor power input and the turbine power as well which

results in the decrease of engine exhaust temperature and the higher thermal efficiency of the engine. Further, it is to be noted that increase in turbocharger compressor efficiency results in the decrease of energy contents of gases entering the vapor generator which decreases the mass flow rate of the refrigerant that enters the ORC turbine and the evaporator of ERC, and this reduces the power output and refrigeration capacity of the bottoming cycle. Since an increase in HCCI engine power dominates over the decrease of the energetic output of bottoming cycle, therefore, the energy efficiency of the HCCI engine-based cooling-power cogeneration cycle increases when the turbocharger compressor efficiency increases. It is shown that raising of turbocharger efficiency from 0.7 to 0.9 increases the thermal efficiency of cogeneration from 48.29% to 49.7% for the R134a operated bottoming cycle. For R290 operated cogeneration it is increased from 47.52% to 48.93% and for R600a operated cogeneration this increases from 49.2% to 50.61%, respectively. Further, it is observed that raising the turbocharger compressor efficiency also increases the exergy efficiency of cogeneration. This is because at the higher turbocharger compressor efficiency the irreversibility decreases as in the case of the compressor, irreversibility is the difference between the actual power and reversible power input. The exergy efficiency of cogeneration is found to be greater than the thermal efficiency for all three selected working fluids of bottoming cycle because reason exergy of fuel supplied is larger than the energy of fuel. The exergy efficiency of the R134a operated combined system is found to be considerably greater than the exergy efficiency of the R600a operated system. This is because the use of R600a in ORC produces a very high condenser load which is not desired in cycles operated in cogeneration mode.

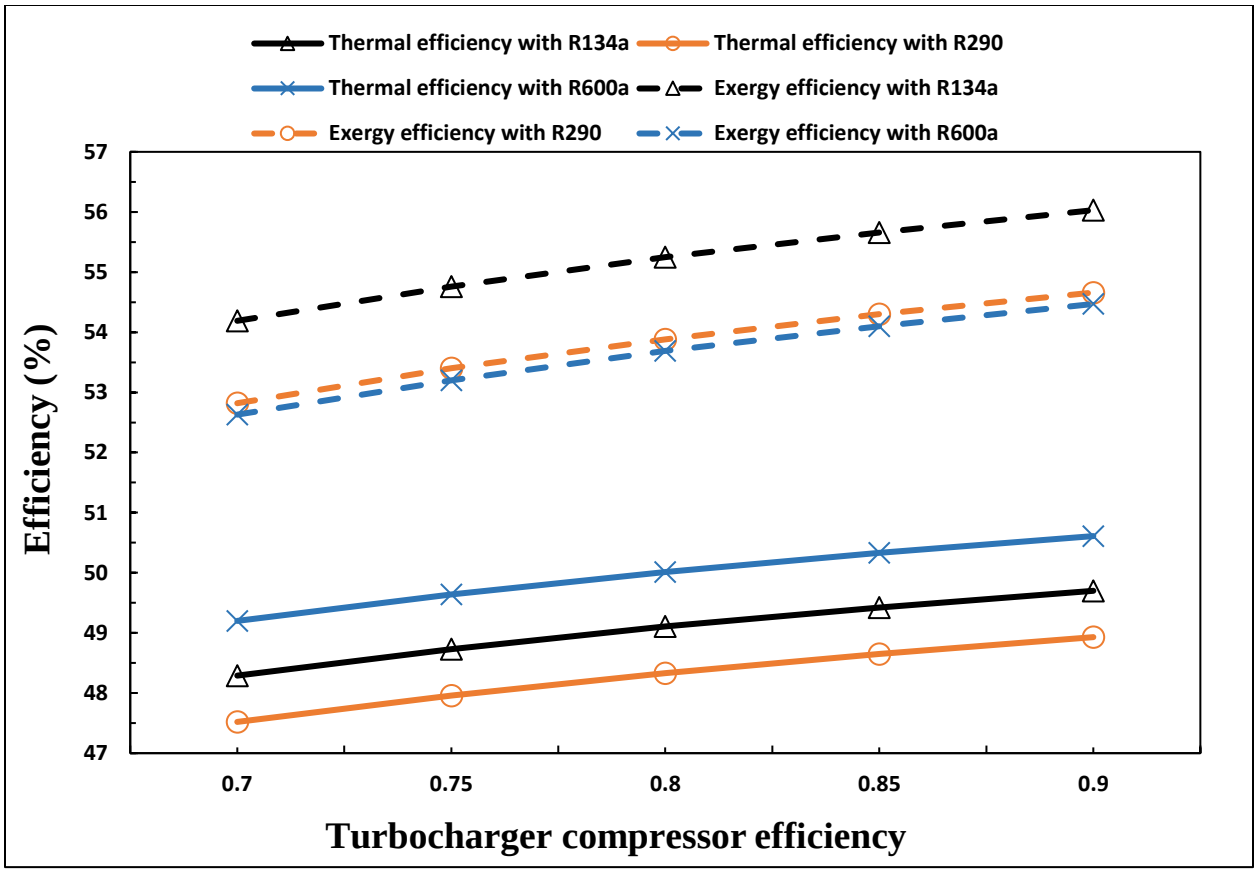


**Fig. 2.4.** Impact of turbocharger compressor efficiency on the efficiencies of wet-ethanol fuelled HCCI engine based cooling-power cogeneration system

Fig. 2.5 shows the effect of changing the ambient temperature on the thermal efficiency of the HCCI engine-based cooling-power cogeneration system. The energy efficiency of the HCCI engine is found to be decreased with the rise of ambient temperature because of the reduction in volumetric efficiency and increase in fuel consumption in the combustion chamber at higher ambient temperature. It is further to be noted that the rate of decrease in thermal efficiency of a cogeneration system is not significant because the refrigeration capacity of ERC start increasing with the increase of ambient temperature due to the reduction of energy losses at the heat exchanger components of ERC but the decrease in the engine output dominates over the increase in capacity of refrigeration. Therefore, the thermal efficiency of cogeneration diminishes gradually when the

ambient temperature rises. Further, it is observed that at a given ambient temperature the exergy destroyed in the condenser and expansion valves of ERC operated on R290 and R600a, separately, is greater than the exergy destroyed in the R134a operated ERC, therefore, the exergy efficiency of R143a operated ERC cogeneration is found to be higher than the efficiency of R290 and R600a operated cogeneration cycles It is further seen that in contrast to thermal efficiency, exergy efficiency of cogeneration cycle starts increasing because of the increase in exergy of refrigeration produced by ERC with the rise of ambient temperature. By definition, the exergy of refrigeration is the ratio of the refrigeration capacity to the Carnot COP operates between the refrigeration temperature and ambient temperature.

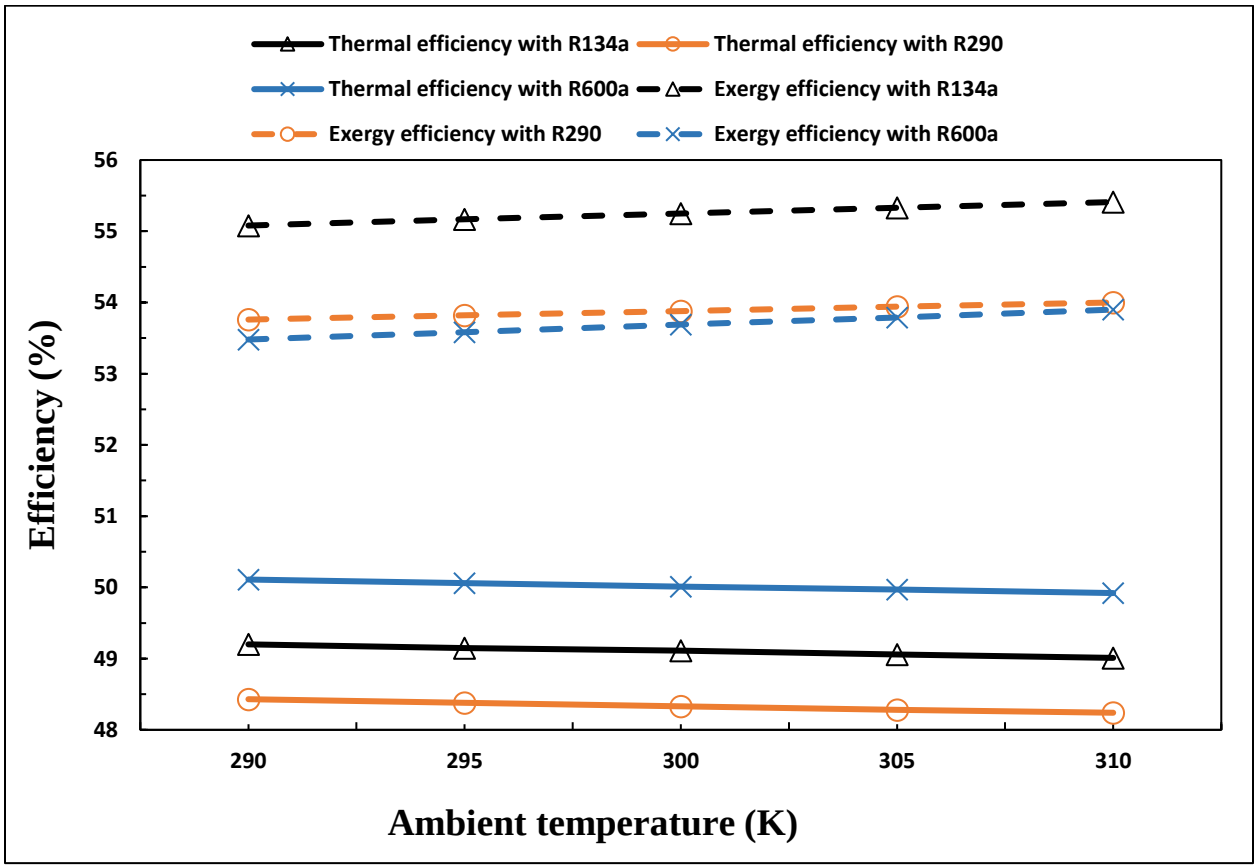


**Fig. 2.5.** Impact of turbocharger compressor efficiency on the efficiencies of wet-ethanol fuelled HCCI engine based cooling-power cogeneration system

Fig. 6 shows the impact of variation in the pressure of the vapor generator ($P_{VG}$) on the net power output and refrigeration capacity of the cogeneration system. The net power output of the cogeneration system increases just by one percent after a large increase in the $P_{VG}$. This is because the energy of stream inlet to turbine increases at elevated pressure and this creates a larger enthalpy drop across the turbine which results in higher ORC turbine power. Meanwhile, the refrigeration capacity of ERC decreases at the increase of $P_{VG}$ because the mass flow rate of the motive stream (primary flow) is decreased by raising the generator pressure which results in the decrease of refrigeration capacity.

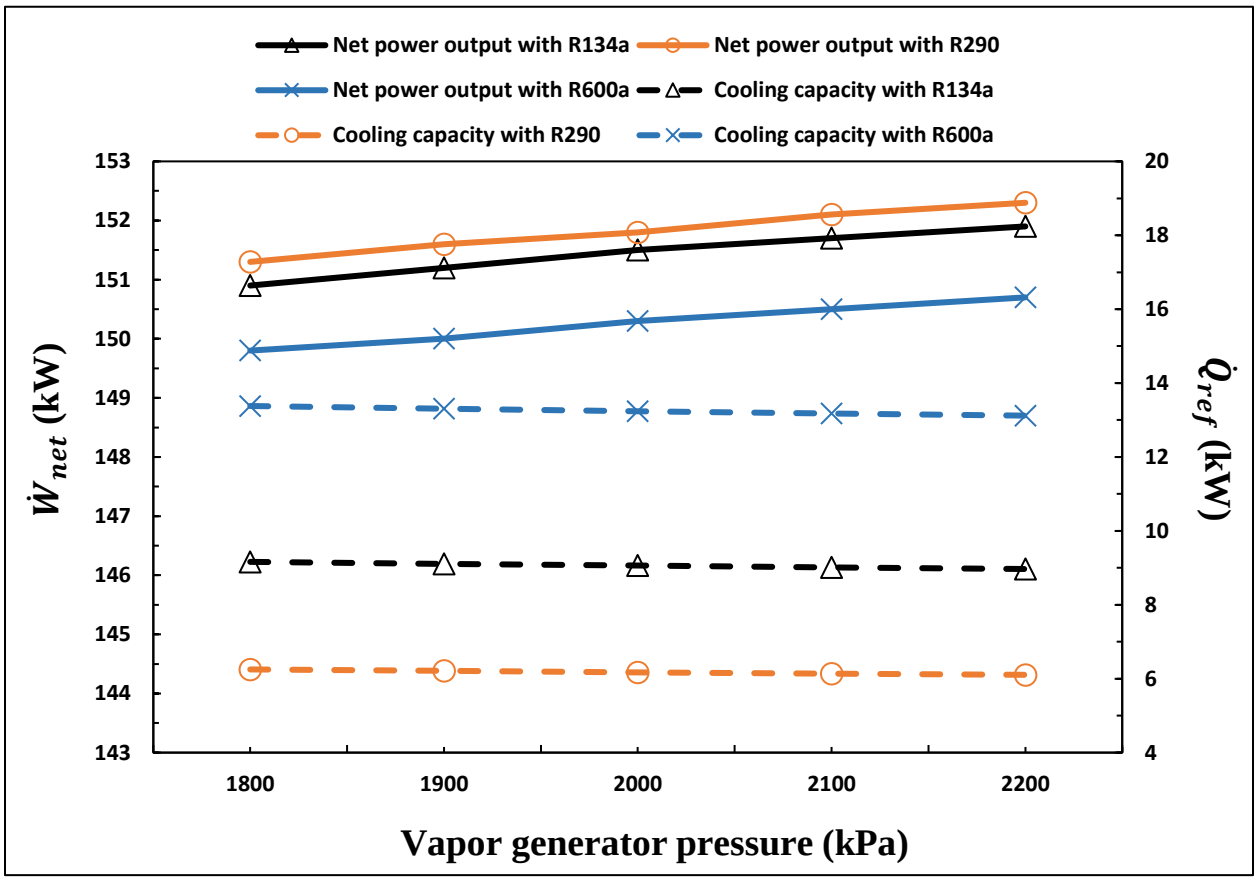


**Fig. 2.6.** Impact of vapor generator pressure on power output and refrigeration capacity of wet-ethanol fueled HCCI engine based cooling-power cogeneration system

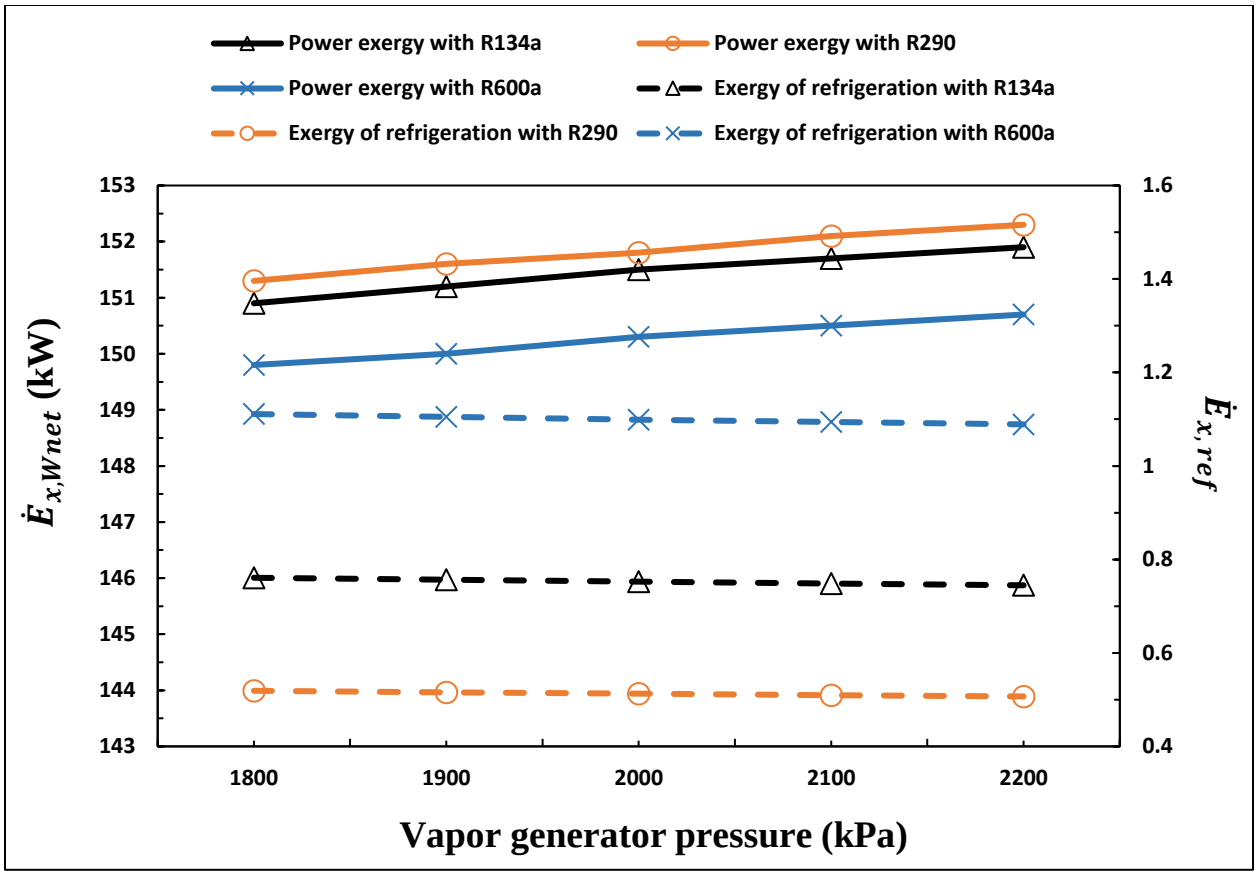


**Fig. 2.7.** Impact of vapor generator pressure on power exergy and exergy of refrigeration of wet-ethanol fueled HCCI engine based cooling-power cogeneration system

Fig. 2.7 shows the impact of change of vapor generator pressure on the power exergy and the exergy of refrigeration. Since the power exergy is the power produced by a turbine which increases at the increase of $P_{VG,}$ therefore, power exergy has also been found to be increased at the elevated pressure. Since the exergy of refrigeration accompanied by cooling capacity is always significantly lower than the capacity of cooling and this shows the trend of decreasing, therefore, the exergy of refrigeration is also found to be reduced at the rise of $P_{VG}$. It is figured out that for R134a operated system, at the pressure of 2000 kPa the exergy of refrigeration is just 0.7523 kW but the corresponding cooling capacity is too high 9.06 kW. Both cooling capacity and the exergy of refrigeration are decreases by greater than 2.0% when the $P_{VG}$ is increased from 1800 kPa to 2200

kPa. But in the case of R600a operated cogeneration this decrease is found to be around 1.9% because R600a despite nature-friendly operation it produces the highest condenser load in ORC, and in the present configuration, the condenser of ORC is the boiler or generator for ERC which support the production of refrigeration and due to this reason, the decrease in both energy and exergy of refrigeration are lower.

Fig. 2.8 shows the impact of variation of $P_{VG}$ on the thermal and exergy efficiencies of the cooling-power cogeneration system. It is determined that increasing the $P_{VG}$ from 1800 kPa to 2200 kPa raises the thermal efficiency of R134a operated cooling-power cogeneration by 0.5% and the exergy efficiency is raised by 0.63%. An increase in exergy efficiency is greater than the thermal efficiency because the exergy efficiency of cogeneration is the ratio of the sum of power exergy and exergy of refrigeration to the exergy input. The exergy of refrigeration which is found to be decreased is significantly less than the energy of refrigeration and hence its contribution towards the exergetic output of bottoming cycle becomes insignificant. Both thermal and exergy efficiencies following the same trend for R290 and R600a operated cogeneration systems.

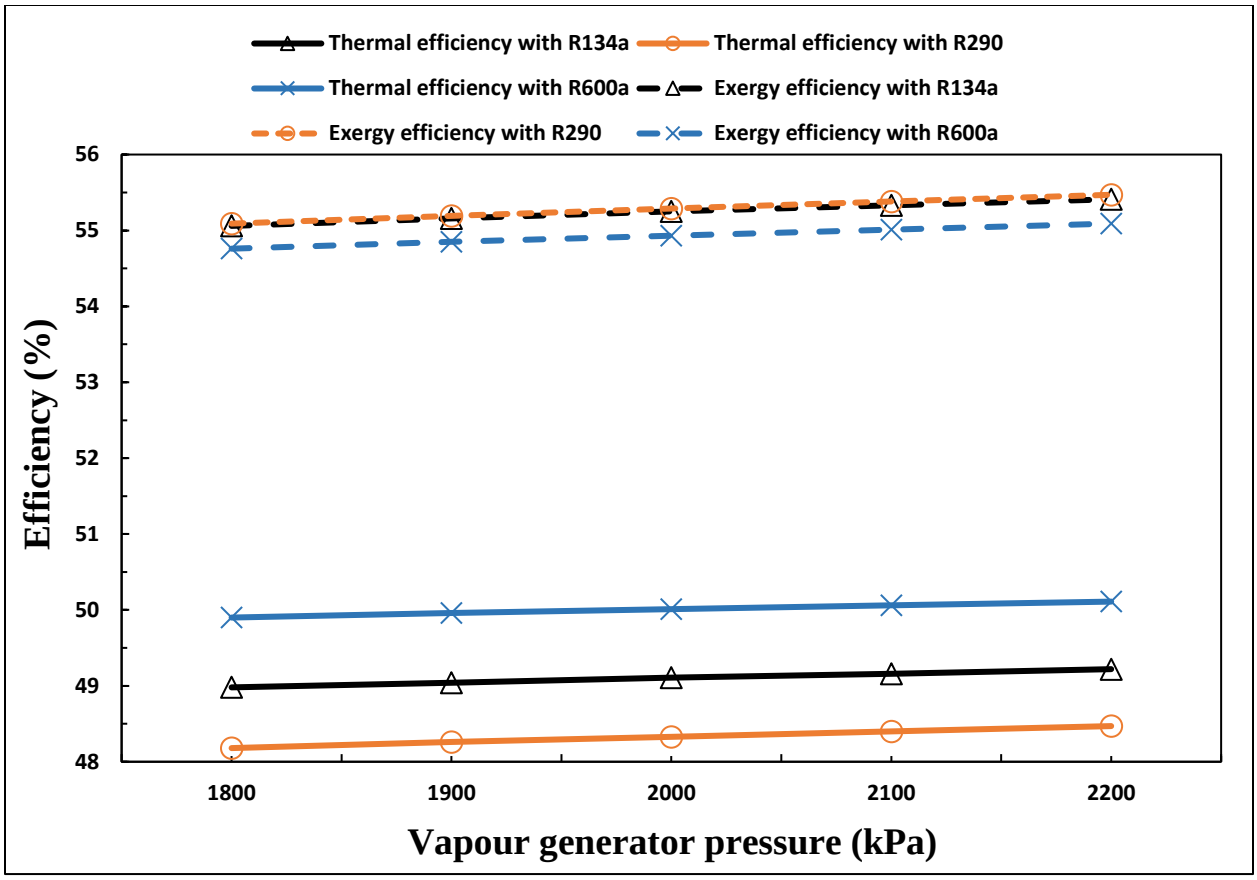


**Fig. 2.8.** Impact of vapor generator pressure on energy and exergy efficiencies of wet-ethanol fueled HCCI engine based cooling-power cogeneration system

The impact of variation of entrainment ratio ($\mu$) on power output and cooling capacity is displayed in Fig. 2.9. It is figured out that the power output of cogeneration is unchanged as inlet and exit states of HCCI engine and ORC turbine are unaffected after altering the $\mu$. The cooling capacity offered by R134a and R290 operated cogeneration system is decreased slightly at the increase of $\mu$ while for R600a operated system an increasing trend of cooling capacity is observed. The reason for obtaining this reverse trend is the higher critical temperature of R600a which supports the motive flow stream temperature. Since the mass flow rate of the motive stream is lower at its higher temperature, therefore, the entrainment ratio increases which results in the increase of cooling capacity.

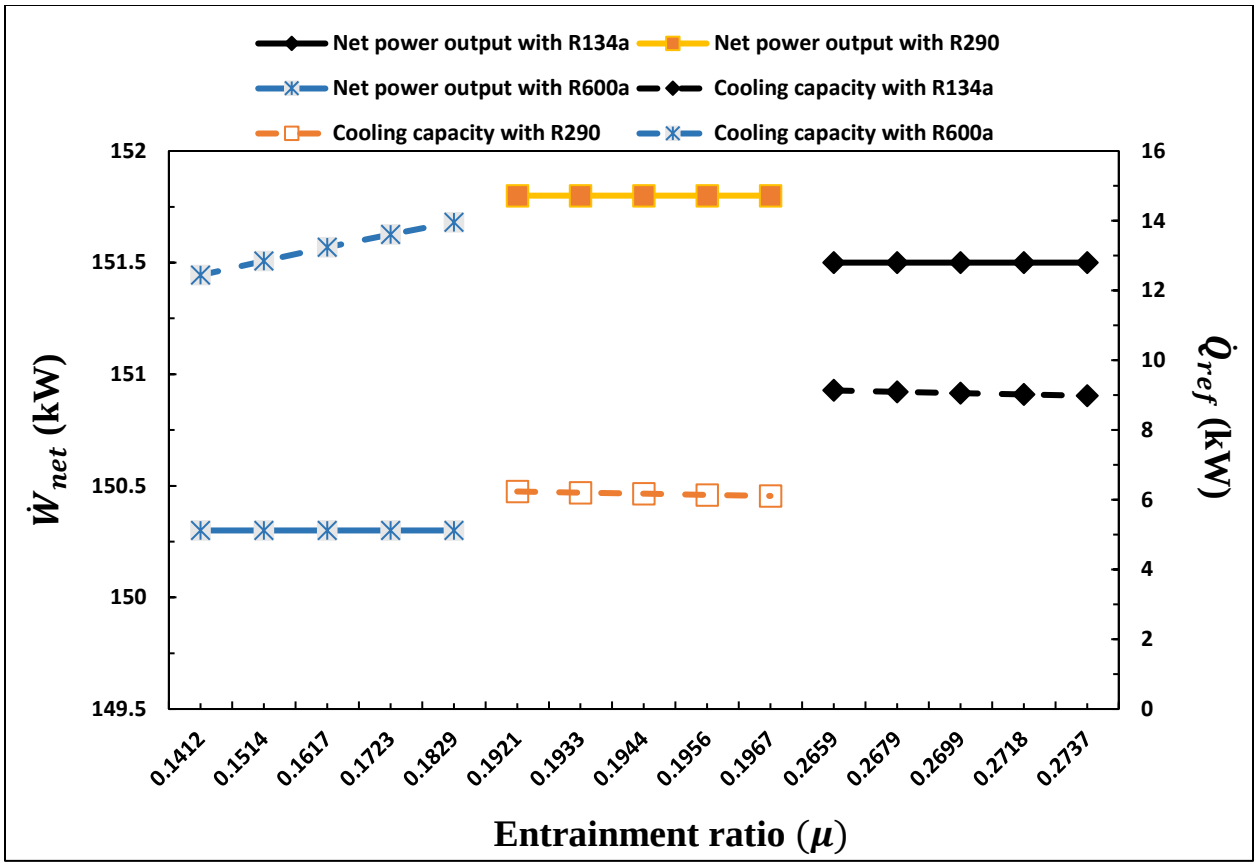


**Fig. 2.9.** Impact of ejector entrainment ratio on power output and refrigeration capacity of wet-ethanol fueled HCCI engine based cooling-power cogeneration system

The impact of entrainment ratio on the power exergy and exergy of refrigeration was also ascertained and depicted in Fig. 2.10. Similar to power output, the power exergy also found to be unchanged because power is free of entropy and hence gives 100% contribution to exergy. The exergy of refrigeration for R134a and R290 operated cogeneration systems is appearing to be decreased while the exergy of refrigeration in the case of the R600a system is increasing considerably when the entrainment ratio is increased. This is because of the concurrent effect of decreasing the mass flow rate of motive stream due to higher critical temperature higher condenser

load of R600a as the working fluid for ORC and ERC. This results in the increased cooling capacity and hence the exergy of refrigeration.

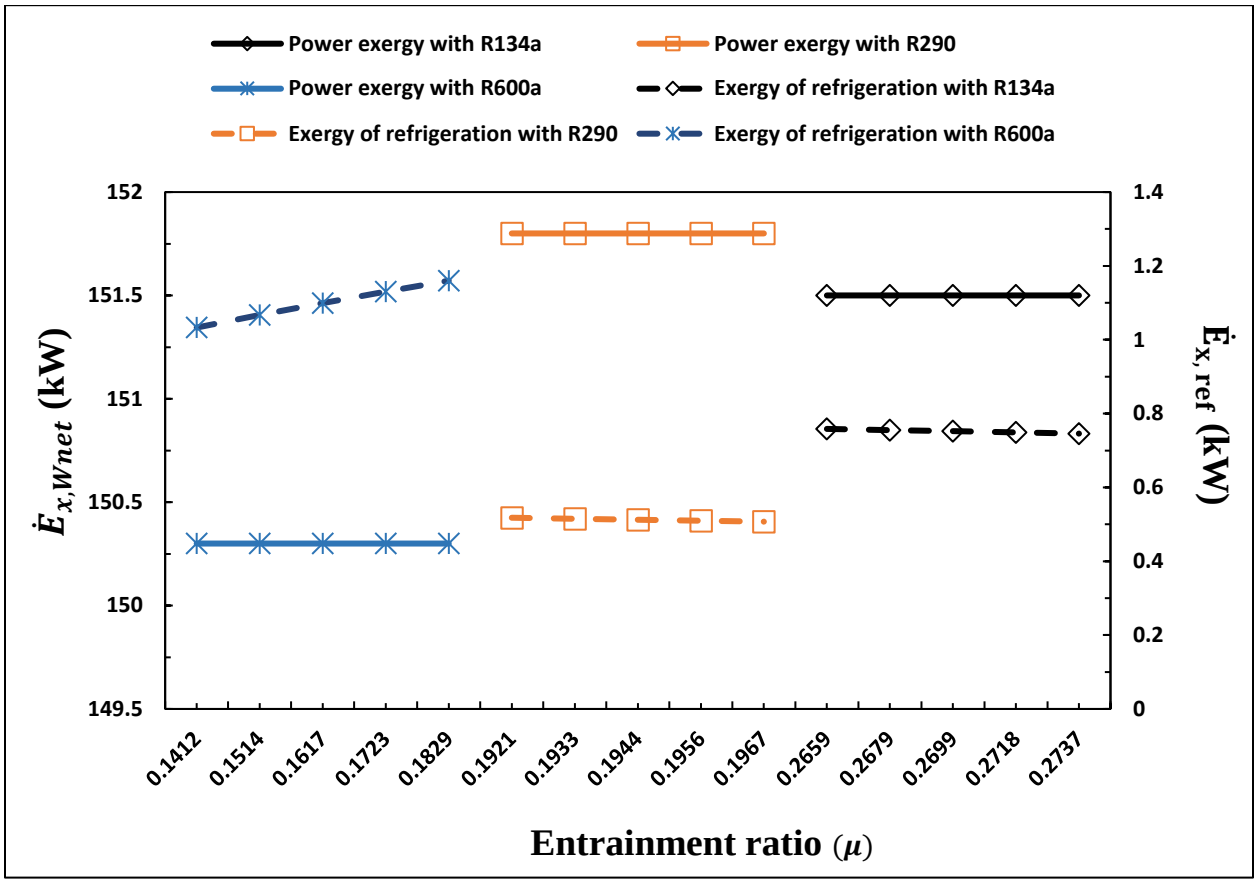


**Fig. 2.10.** Impact of ejector entrainment ratio on power exergy and exergy of refrigeration of wet-ethanol fueled HCCI engine based cooling-power cogeneration system

The impact of ERC evaporator pressure ($P_{Evap}$) on the power output and capacity of refrigeration is depicted in Fig. 2.11. Since the inlet and exit states of the HCCI engine and ORC turbine are unchanged, therefore, the power output is observed to be unaffected. The cooling capacity is found to be increased with the rise of $P_{Evap}$. This is because an increase in evaporator pressure increases the pressure gradient across the nozzle which in turn enhances the mass flow rate of refrigerant of an entrained stream. Considering that the total mass flow rate is constant in ERC, the rate of motive stream decreases and the change in enthalpy of refrigerant across the evaporator increases as $P_{Evap}$

rises. A concurrent increase in the difference of enthalpy and mass flow rate of secondary stream results in the rise of refrigeration capacity of ERC. It is further to be observed that for R134a operated cogeneration system, the cooling capacity is increased by 11.34% when the $P_{Evap}$ rises from 327.4 kPa to 348.7 kPa. In the case of the R600a operated system the cooling capacity is increased by 12.58% at the rise of $P_{Evap}$ from 175.7 kPa to 186.9 kPa.

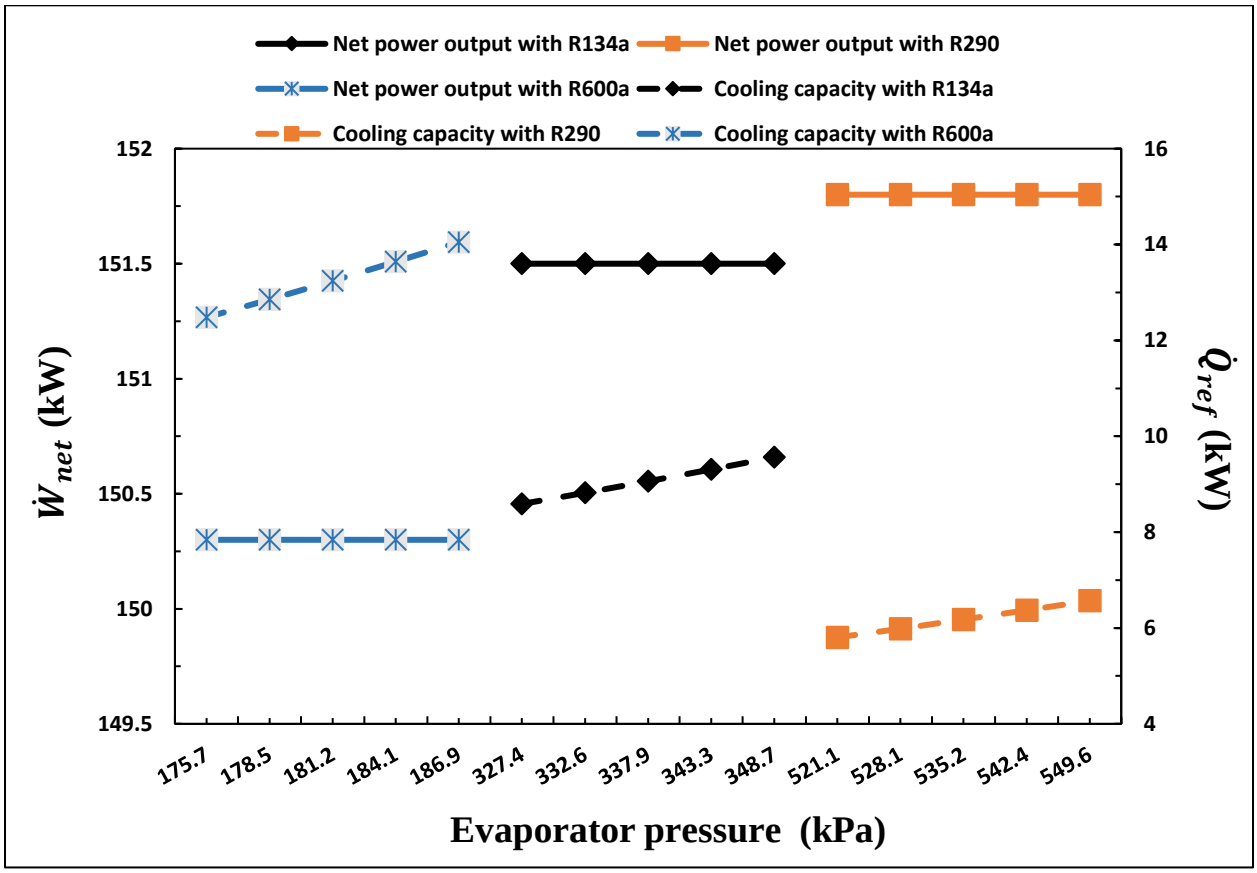


**Fig. 2.11.** Impact of evaporator pressure on power output and refrigeration capacity of wet-ethanol fueled HCCI engine based cooling-power cogeneration system

The impact of ERC evaporator pressure ($P_{Evap}$) was also ascertained on the power exergy and exergy of refrigeration and is shown in Fig. 2.12. Due to the reasons stated above, like the power output, the power exergy is also found to be unaffected. The exergy of refrigeration is found to be increased with the rise of $P_{Evap}$. This is because the increase in evaporator pressure increases the

pressure gradient across the nozzle which in turn enhances the mass flow rate of refrigerant of the entrained stream. Considering that the total mass flow rate is constant in ERC, the rate of motive stream decreases, and the change in enthalpy of refrigerant and hence the physical exergy of refrigerant across the evaporator enhanced as $P_{Evap}$ increases. A simultaneous increase in the difference of physical exergy and mass flow rate of secondary stream results in the increase of the exergy of refrigeration produced by ERC. It is determined that for R134a operated cogeneration system, the exergy of refrigeration is increased by 2.3% when the $P_{Evap}$ rises from 327.4 kPa to 348.7 kPa. In the case of the R600a operated system the exergy of refrigeration is increased by 3.42% at the rise of $P_{Evap}$ from 175.7 kPa to 186.9 kPa. A percentage increase in the exergy of refrigeration delivered by the R600a system is due to its higher critical temperature compared to R134a and R290.

The degree of superheat of motive flow ($\Delta THE$) which is defined as the difference between the temperature of the refrigerant at the HE outlet and the saturation temperature of the refrigerant at the HE pressure. The impact of $\Delta THE$ was also investigated on the power output and refrigeration capacity of the cogeneration system and is shown in Fig. 2.13. Since $\Delta THE$ is related to ERC, therefore, the power output of cogeneration is found to be unaffected. The capacity of refrigeration is found to be slightly declined with the rise of the degree of superheat. This is because as $\Delta THE$ increases there is a concurrent increase in backpressure Ps which means Ps comes closer to evaporator pressure means the difference of pressure ($P_s$- $P_{Evap}$) decreases. This decrease in the difference of pressure poses a drop in the mass flow rate of the entrained stream of the ejector. Since the total flowing mass across the ejector is constant, it means the mass flow rate of motive flowing stream rises with increasing $\Delta THE$ and in turn, the entrainment ratio of ERC reduces owing to which the cooling capacity decreases. In the case of the R134a operated cogeneration

system, the refrigeration capacity is decreased by 1.55% when the $\Delta THE$ rises from 11.31$^0$C to 19.31$^0$C. For R290 operated cogeneration system, the refrigeration capacity is decreased by 2% when $\Delta THE$ is elevated from 20.86$^0$C to 28.86$^0$C. Elevation of $\Delta THE$ from1.7$^0$C to 9.7$^0$C reduces the capacity of refrigeration by 2.32%.

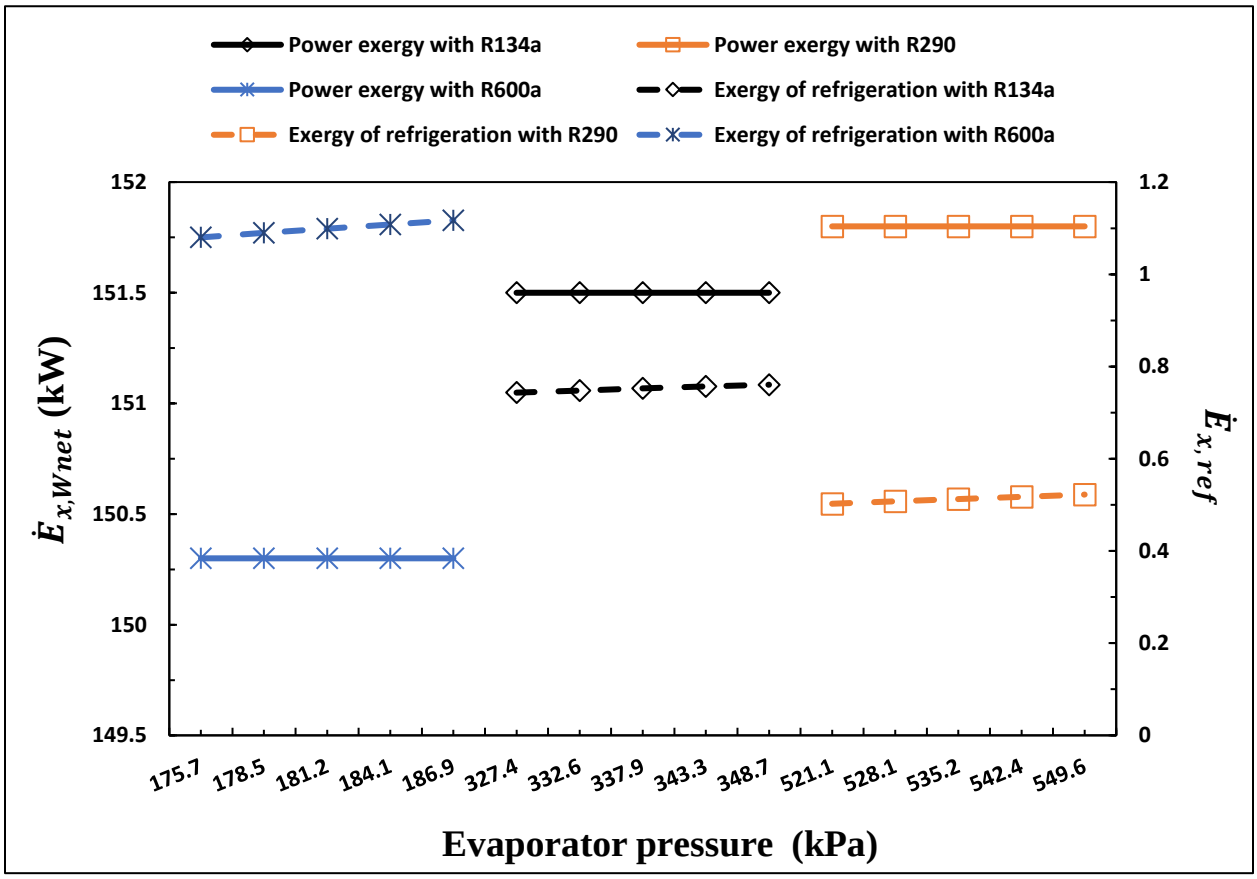


**Fig. 2.12.** Impact of evaporator pressure on power exergy and exergy of refrigeration of wet-ethanol fueled HCCI engine based cooling-power cogeneration system

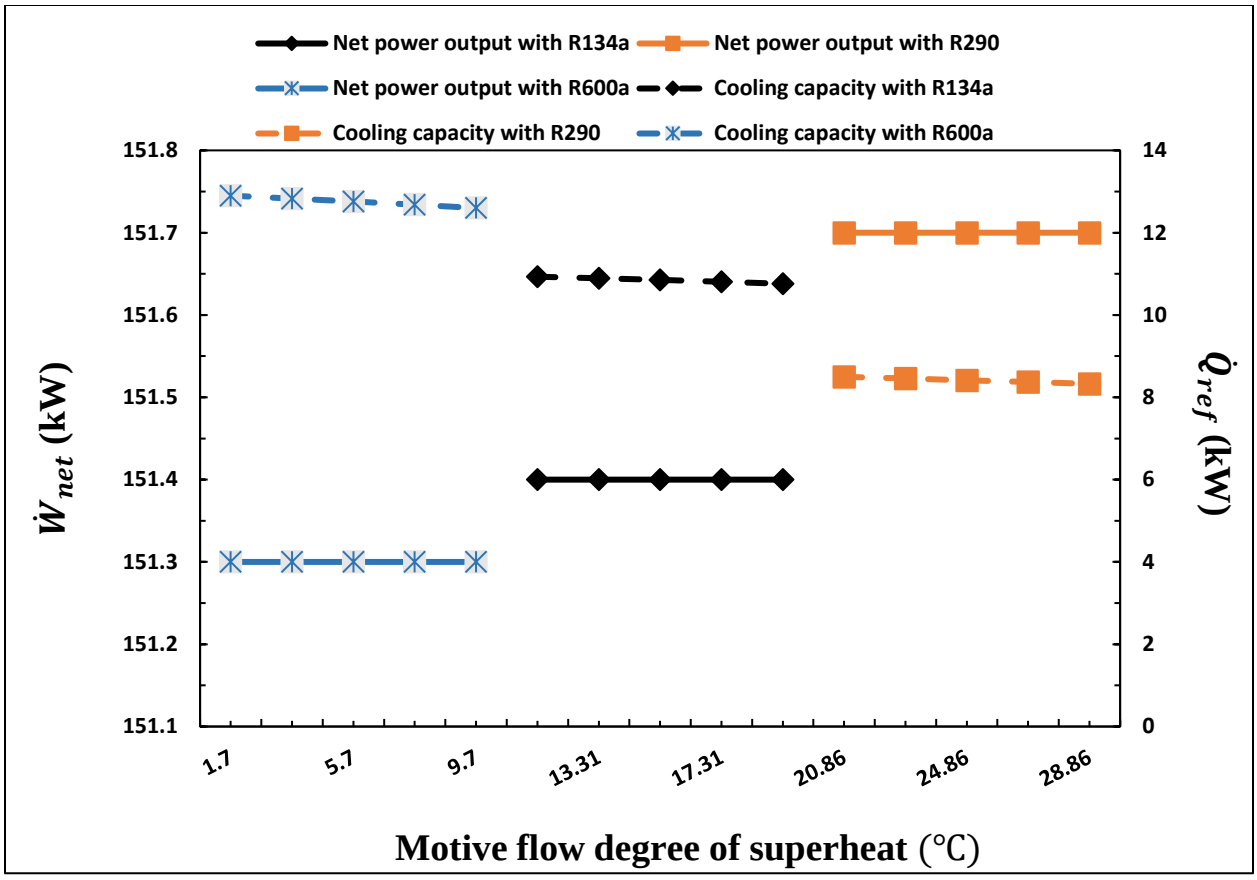


**Fig. 2.13.** Impact of motive flow degree of superheat on power output and refrigeration capacity of wet-ethanol fueled HCCI engine based cooling-power cogeneration system

Fig. 2.14 is presented to ascertain the degree of superheat of motive flow ($\Delta THE$) on the power exergy and exergy of refrigeration. Since $\Delta THE$ is related to ERC, therefore, the power exergy delivered by cogeneration is found to be unaffected. The exergy of refrigeration is found to be slightly declined with the rise of the degree of superheat for all the working fluids of bottoming cycle. The reasons for the decrease in capacity of refrigeration are mentioned and the exergy of refrigeration is defined as the ratio of refrigeration capacity to the COP of Carnot refrigerator operated between the evaporator temperature and ambient. Therefore, for the fixed value of evaporator temperature, the exergy of refrigeration follows the trend of refrigeration capacity, and hence it is also found to be decreased at the increase of the degree of superheat of motive flow.

Since the exergy accompanied by the capacity of refrigeration is significantly less than the cooling capacity, therefore, the rate of decrease of the exergy of refrigeration is shown to be less than the rate of decrease of the capacity of refrigeration for all the working fluids of bottoming cycle.

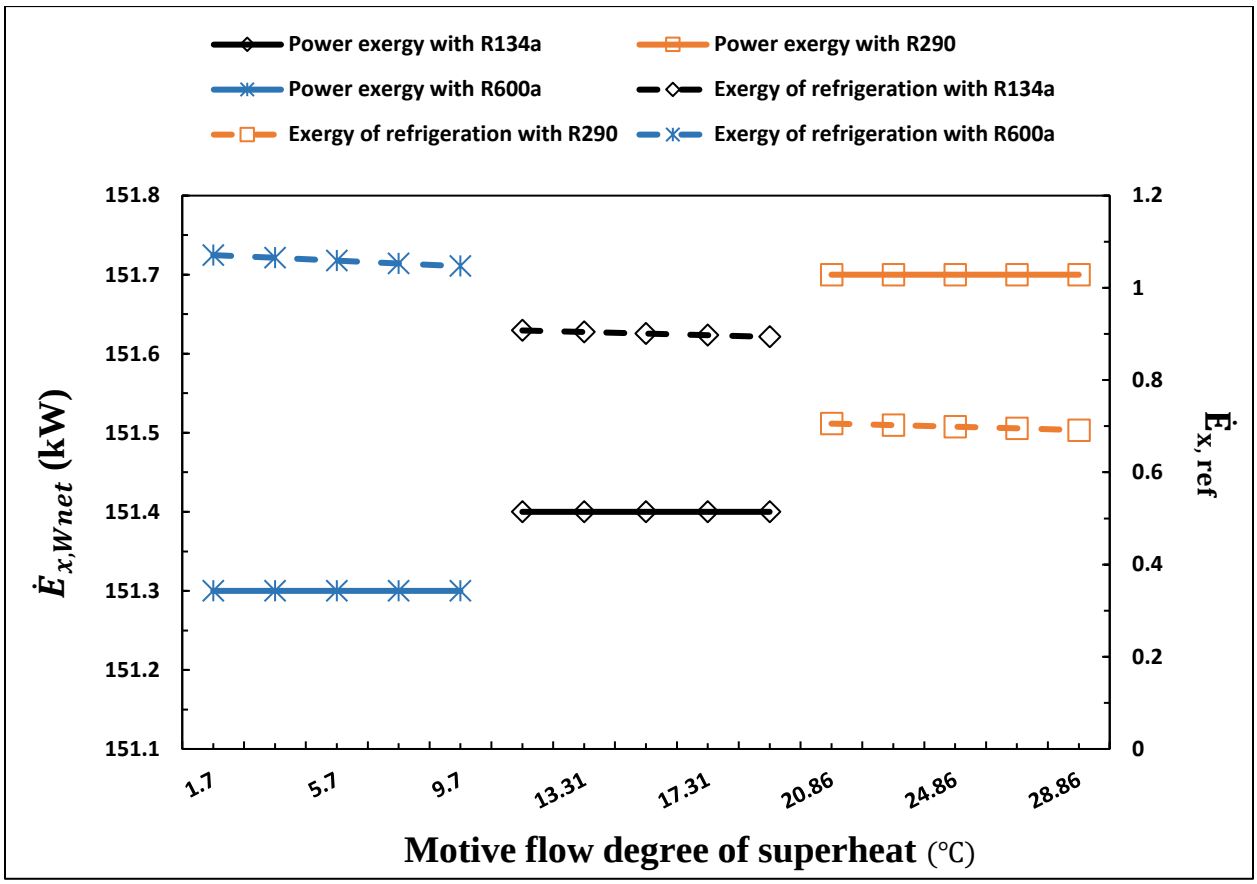


**Fig. 2.14.** Impact of motive flow degree of superheat on power exergy and exergy of refrigeration of wet-ethanol fueled HCCI engine based cooling-power cogeneration system.

# Chapter 3

# Thermodynamic and comparative analysis of ERC and ARC integrated wet-ethanol fueled HCCI engine for cogeneration of power and cooling

## 3.1. Introduction

Establishment of an environmentally benign sustainable society demands the improvement in thermal efficiency of land transportation vehicles. On average two-thirds of the primary energy supplied to internal combustion engines is lost via heat rejection to atmosphere [182, 202, 203]. This significant loss of energy to environment asking for the recovery of this rejected heat that would decrease the fuel consumption and reduce the environmental degradation caused because of the fossil fuels consumption. In view of conserving the fossil fuels and to protect the living environment, many investigators attempted the problems related to the design and development of renewable fueled engines [204, 205]. Among the renewable fuels, ethanol has been found as one of the promising options as it has higher flame speed, higher octane number, and it is oxygenated fuel due to which it provides high rate of combustion efficiency and also reduced level of the pollutant emissions and greenhouse gases. Therefore, ethanol fueled engines can be considered as an alternative to meet the aim of achieving higher engine efficiency at lower emissions [206]. Ethanol can be produced from various agricultural products like corn and sugarcane, and studies carried out in regard of the production of ethanol from corn through energy balance reports that significant amount of energy is required to produce ethanol for water removal processes

(dehydration and distillation) which consumes 37% of the energy which ethanol contains [207]. Therefore, efforts to utilize wet-ethanol directly as fuel in combustion engines was considered as an integral part of research and from some of the investigations it is revealed that this may lead to considerable increase in net gain of energy from 21% to 55% [60, 168]. Utilization of wet ethanol had its challenges in traditional modes of combustion (SI and CI) and hence requires a unique combustion process which combine the characteristics of both SI (spark ignited) and CI (compression ignited) engines [169]. In this regard, homogeneous charge compression ignition (HCCI) engines have been discovered as an option to burn low grade fuels for land transportation purpose because these engines have the distinction of combining the advantages of both SI and CI combustion processes. HCCI engines utilizes premixed and lean fuel-air mixture at high intake temperature and the mixture is thermally auto-ignited following the higher compression ratio. This results in the drastic reduction of the most harmful emissions of $NO_x$ and PM while providing a higher thermal efficiency [149, 171, 208]. Because of the characteristics of utilizing low grade fuels which can be auto-ignited through the process of compression, HCCI engines are expected to exploit wet-ethanol more effectively than the traditional engines and hence can be considered as a suitable mode of combustion for the direct utilization of wet-ethanol as a primary fuel. Analysis joining quality with quantity of energy by combining the first law of thermodynamics with the second law can be used to estimate the quality of energy resource which transform into useful work. This thermodynamic modeling assist in evaluating the exergetic losses and the cycle efficiencies based on energy and exergy [209, 210]. Simultaneous applications of the first and second law applied to investigate the performance of wet-ethanol fueled HCCI engines [174, 184, 186, 211] discovered that significant amount of exergy accompanied by engine exhaust heat is expelled which goes unutilized and leads to inefficient and environmentally harmful engine

performance. This waste heat can be considered as the potential energy source for driving the heat operated refrigeration and air conditioning systems with a view to reduce the environmental impact and improve the system efficiency. Analysis of these systems from exergy point of views can provide a tool for their true theoretical performance assessment. Ejector refrigeration cycle (ERC) and absorption refrigeration cycle (ARC) are heat operated non-traditional cooling systems which can be employed for converting the engine exhaust heat into the refrigeration effect. ERC's have been in use since many decades for air conditioning of residential buildings. The schematic and details of ERC applied for cold production can be seen in [212, 213]. In the field of land transportation, implementation of ejector technology for refrigerating the thermal load of air conditioner or cabin cooling is scarce and hence only few of the investigations are reported in this regard. Jaruwongwittaya and Chen [214] investigated the feasibility of employing a two-stage ejector refrigeration system in a bus and their results discovered that replacement of conventional vapor compression system with the ejector cooling system can be suitably employed as an alternative. Zengenhagen and Ziegler [215] presented the assessment of an engine exhaust heat driven jet-ejector cooling system integrated to turbocharged gasoline engines. They determined the energy efficiency and charge air temperature for the use of R134a as the refrigerant for ejector cooling. Unal [216] worked on the application of the exhaust heat driven two-phase ejector cooling system for reducing the load and fuel consumption of the engine of passenger bus. The author states that application of two-phase ejector as an expansion valve can enhance the performance of bus air conditioning system. Zhang et al. [217] developed an exhaust heat recovery unit for the automobile integrating to ejector refrigeration cycle. They analyzed the performance of ejector cooling system and recommended a suitable range of operating parameters for the efficient operation of combined system. Another suitable option to recover the engine exhaust heat is the

absorption refrigeration system in which the fluid pairs LiBr-$H_2O$ and $NH_3$-$H_2O$ are normally used to produce cooling through these systems. Since a significant portion of energy supplied to internal combustion engines appear as exhaust waste heat and the use of air conditioners in vehicles arrives at the status of essential commodity for modern transportation. In this context, some theoretical and experimental studies are reported in the literature regarding the use of absorption refrigeration cycle to produce cooling through the recovery of engine exhaust heat. Koehler et al. [218] developed a prototype of ARC for truck refrigeration utilizing the exhaust gas. Based on the description of simulated results they reported that system performance could be improved nearly by double after employing the ARC. Manzela et al. [193] presented the experimental investigations of an ammonia-water absorption refrigeration system driven by engine exhaust gases. They evaluated the effect of exhaust gas enthalpy and the employment of ARC on engine performance and exhaust emissions and discovered that application of ARC results in the decrease of specific fuel consumption and reduction in carbon monoxide emission.

No comparative study on the use of exhaust gas waste heat operated cooling systems bottoming with the HCCI engine fueled by wet-ethanol has been found in the literature. Therefore, it is necessary and meaningful to develop and analyze the systems that can be powered by engine exhaust gases and produce cooling for air conditioning of renewable fueled vehicles. In this study, engine operating in HCCI mode and fueled by wet-ethanol was proposed to be bottomed with the ERC and ARC, separately, to recover the exhaust heat for refrigerating the thermal load of vehicle air conditioning. A comparative thermodynamic analysis of proposed cooling-power cogeneration was conducted by considering the quality and quantity of energy transfers during the energy conversion processes of the cycle. Energetic and exergetic performances of cogeneration cycle was assessed by altering the following parameters; turbocharger pressure ratio, turbocharger

compression efficiency, and ambient temperature. In addition, the distribution of fuel energy supplied in terms of energy produced and energy lost as well as the breaking down of exergy of fuel supplied into the exergy produced, exergy destruction in the major components of cogeneration cycle, and the loss of exergy due to thermal exhaust to ambient is also computed, graphed, and discussed. The contribution of exergy destruction is scrutinized and debated in regard of cycle performance improvement. Results are derived for the employment of R134a as the refrigerant of ERC and LiBr-$H_2O$ mixture as the working fluid pair for the ARC. Further, the COP of both ERC and ARC were computed with the variation in the entrainment ratio and generator temperature, respectively.

## 3.2. System description

In this paper, investigation on wet-ethanol fuelled and turbocharged HCCI engine coupled to ejector refrigeration cycle (ERC)/absorption refrigeration cycle (ARC) is performed. Figure 3.1 describes the working of HCCI engine fueled by wet-ethanol and combined with ejector refrigeration cycle. The engine is turbocharged and ethanol fired whose main specifications are reported in Table 3.1. Ambient air (1) enters the compressor (Comp1) which increases its pressure and temperature. The compressed air is heated (2-3) in regenerator (Reg1) and mixed with Wet-ethanol (4) injected into a fuel vaporizer (FV1) where it vaporizes and forms a homogeneous mixture of ethanol-water-air (5) and enters the HCCI engine. The ethanol water air mixture inducted into the cylinder and mixes with hot residual gases within the cylinder and compressed by the piston (1'-2') as shown in Figure 3.3. Charge gets heat through compression and this leads to ignition and combustion (2'-3') and generate power ($W_{Power}$). After combustion engine exhaust gases (6) enter the catalytic converter (CC1) and leave the convertor (7) at a higher temperature due to releasing of heat during combustion of carbon monoxide and unburned hydrocarbon which

were not burned in the combustion chamber. Less harmful gases from catalytic converter (CC1) at higher temperature enter the turbine (T1) and generate power ($W_T$) to drive the turbocharger. The exhaust gases leave the turbine (8) and after having exchanged heat (8-9) with compressed air (2-3) in the regenerator (Reg1) is delivered to the boiler (Boi) for vaporizing (18-11) the refrigerant in ejector refrigeration cycle. The vaporized refrigerant (11) at high pressure and temperature (primary vapor) enters the converging-diverging nozzle of ejector (Eje). The high velocity vapor at the nozzle exit (11a) creates a high vacuum at the entry of mixing chamber where it entrains secondary vapor from the evaporator (16) and mixes with the primary stream. In the mixing chamber both primary (11a) and secondary vapors (16a) mixed together and there it becomes a homogeneous mixture stream. On entering the constant area section, a normal shock wave occurs which results in the rise of pressure. After the shock, the mixed stream (12m) decelerates in the diffuser. The mixed stream (12a) from the ejector enters the condenser (Cond1) where it changes to saturated liquid refrigerant (12-13). One part of this stream as a working fluid goes to the evaporator (Evap1) to produce the desired cooling effect (15-16) through the expansion valve (EV1) (14-15), and the other part of this stream (17) is pumped back (P1) to the boiler. In Figure 3.2, the turbine (T2) exhaust (8) through the regenerator deliver to the generator (Gen) (9-10) for vaporizing (25-19) the solution of LiBr-$H_2O$. The water vapor absorbed in the absorber (Abs) by the solution is driven off and flows to the condenser (Cond2) (19) while the LiBr-$H_2O$ solution returns to the absorber (28) through heat exchanger (HE) (26-27) and an expansion valve (EV2b) (27-28). The vaporized refrigerant is condensed in the condenser (19-20) and then flows through an expansion valve (EV2a) (20-21) to receive heat load at the evaporator (Evap2) (21-22). A LiBr-$H_2O$ solution leaves the generator (26) and enters the absorber (28) to absorb low-pressure water vapor from the evaporator. The pump (P2) receives (23) a LiBr-$H_2O$ solution from the absorber,

raises the pressure of the strong solution (24) and pumped back to the generator (25) after passing

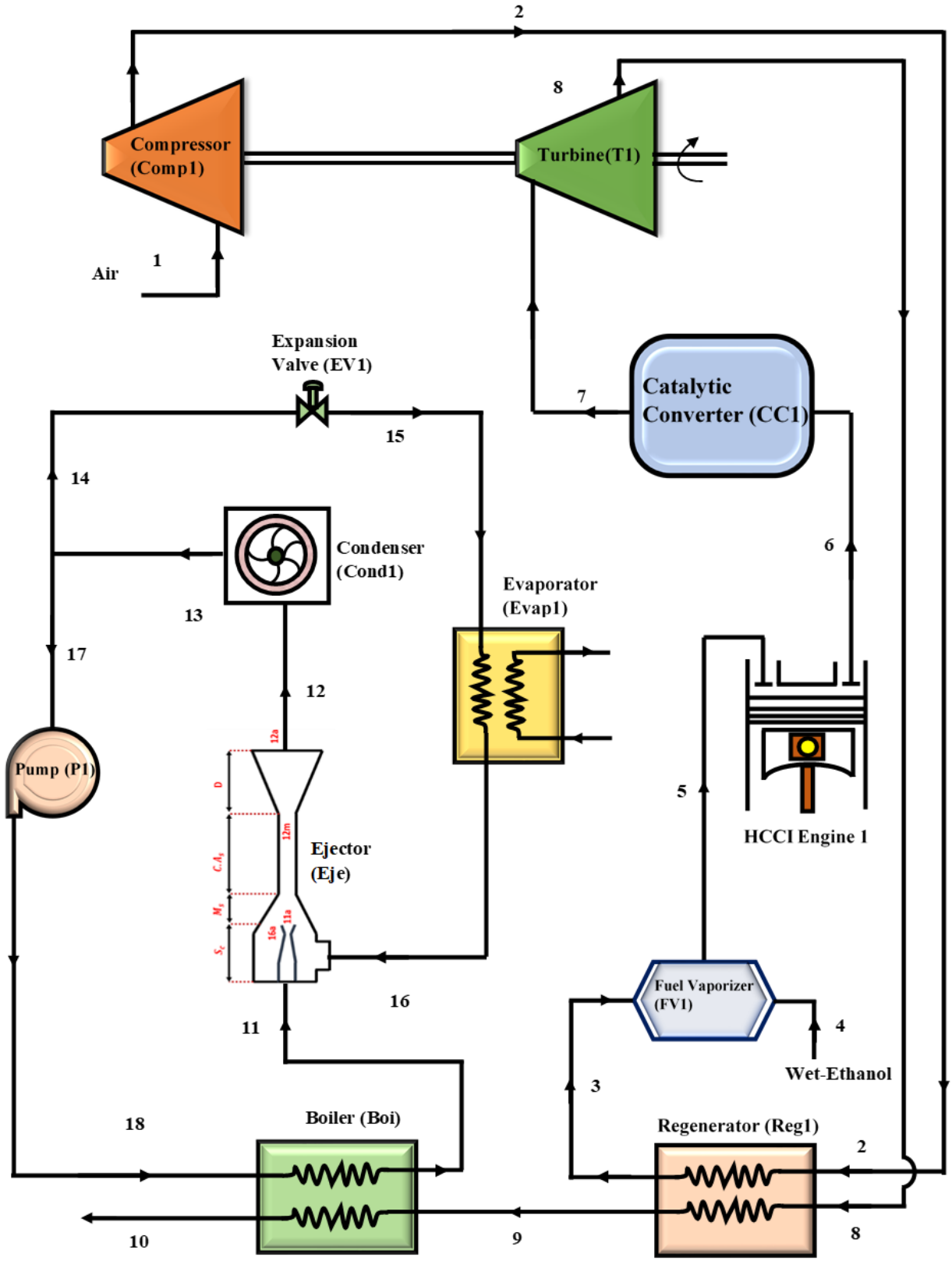

**Fig. 3.1.** System layout of wet ethanol operated HCCI engine integrated ejector refrigeration cycle

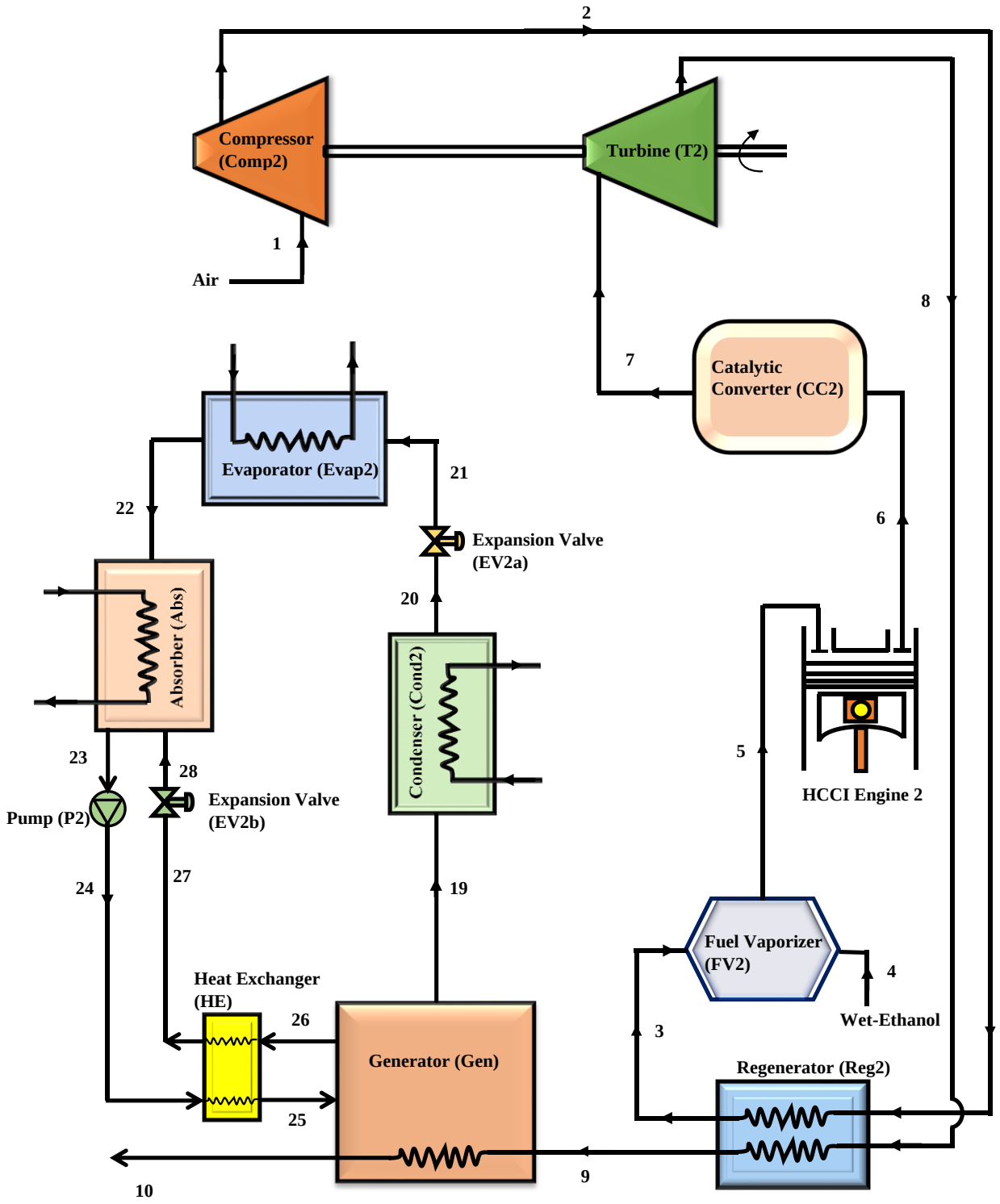

**Fig. 3.2.** System layout of wet ethanol operated HCCI engine integrated to absorption refrigeration cycle

through the heat exchanger (HE).

**Table 3.1** Engine specifications [60]

| | |
|---|---|
| Volume swept per cylinder | 2400 $cm^3$ |
| Cylinder diameter | 13.7 cm |
| Piston displacement | 16.5 cm |
| Length of connecting rod | 26.2 cm |
| Ratio of intake to clearance volume | 16:1 |
| Speed of engine | 30 rps |
| Engine volumetric efficiency | 100% |
| Ratio of actual fuel-air mixture to chemically correct fuel-air mixture | <0.5 |
| Combustion process in HCCI engine | Chemical kinetics applied to control the bulk auto ignition process |

## 3.3. Working fluid thermodynamic properties

In the analysis and design of alternative fueled internal combustion engine, thermodynamic properties of working fluids are necessary to investigate its energetic and exergetic performances. In the ideal engine cycle, the working fluid for processes occurs in the cylinder is considered simply as air. However, in actual cycles, the working fluid consists of several gaseous species.

The specific heat of gases varies with temperature in real engine application, and its variation with pressure is negligible. In the present model of molar specific heat $\bar{C}_p(T)$ variation with

temperature, the coefficients ($a_1$-$a_5$) for each species, are taken from literature in the range of temperature from 300K to 3000K [219]

$$\bar{C}_p(T) = \bar{R}(a_1 + a_2T + a_3T^2 + a_4T^3 + a_5T^5) \quad (3.1)$$

The enthalpy and entropy of the gaseous species i in terms of specific heat capacity may be expressed as [220]

$$\bar{h}_{i_{(T)}} = \bar{h}_{i_{(T_0)}} + \int_{T_0}^{T} \bar{C}_{p_i}(T)dT \quad (3.2)$$

$$\bar{s}_{i\ (T,p)} = \bar{s}_{i_{(T_0,p_0)}} + \int_{T_0}^{T} \frac{\bar{C}_{p_i}(T)}{T} dT - \bar{R}ln\left(\frac{y_i p}{p_0}\right) \quad (3.3)$$

The intake air, combustion products, and engine exhaust gases are considered to be a mixture of various species. Below are the equations which can be utilized for the computation of molar specific enthalpy, molar specific entropy, and Molecular mass of the mixture [220].

$$\bar{h}_{mix_{(T)}} = \sum_{i=1}^{n} y_i \bar{h}_{i_{(T)}}; \qquad \bar{s}_{mix_{(T,P)}} = \sum_{i=1}^{n} y_i \bar{s}_{i_{(T,P)}}\ ; \qquad M_{mix} = \sum_{i=1}^{n} y_i M_i \quad (3.4)$$

In the present analysis, fuel-air mixture is stoichiometric because ethanol containing water obtain all the required dilution. The combustion equation for burning of wet-ethanol in the HCCI engine can be considered as follows [184].

$$C_2H_5OH + 6H_2O + 3(O_2 + 3.77N_2) = 1.8\,CO_2 + 0.1CO + 0.05C_2H_5OH + 8.85H_2O + 0.2O_2 + 11.319N_2 \quad (3.5)$$

The procedure for obtaining the balanced reaction equation of an actual reaction where combustion is incomplete is not always straight forward. Actually combustion is the result of a series of very complicated and rapid chemical reactions and the product formed depend on many factors. When fuel is burned in the cylinder of an engine, the product of reaction varies with the temperature and pressure in the cylinder. The appearance of some carbon monoxide and unburned oxygen and fuel

is due to incomplete mixing, insufficient time for complete combustion, and other factors. The combustion of wet-ethanol in HCCI engine was taking place by assuming a chemical reaction with 90% combustion efficiency.

Unburned hydrocarbons and carbon monoxide which formed as emissions in HCCI engine can be further oxidized by using Pd-loaded $SiO_2 - Al_2O_3$ as the oxidizing catalyst. Because of having the stoichiometric combustion of fuel-air mixture and its operation at higher compression ratio, the temperature of HCCI engine exhaust gases that enters the catalytic convertor is considered to be enough for oxidizing the carbon monoxide and unburned fuel. Assuming the complete conversion of unburned fuel and carbon monoxide and the application of mass and energy balances, the composition and temperature of gases at the exit of catalytic convertor can be determined

$$\sum_{Product} n_e\left(\bar{h}_f^{\circ} + \Delta\bar{h}\right)_e = \sum_{Reactant} n_i\left(\bar{h}_f^{\circ} + \Delta\bar{h}\right)_i \quad (3.6)$$

Where, i refers the incoming streams entering the catalytic convertor and e refers the exiting stream of products leaving the convertor [186]. The equation for chemical reaction of engine exhaust gases in the catalytic convertor is assumed to be as follows:

$$1.8\ CO_2 + 0.1\ CO + 0.05\ C_2H_5OH + 8.85\ H_2O + 0.2\ O_2 + 11.319\ N_2 = 2\ CO_2 + 9\ H_2O + 11.319\ N_2 \quad (3.7)$$

### 3.3.1 Turbocharger compressor

The air inducted is first flows through the compressor to increase its pressure and also the temperature. For a given pressure ratio and considered polytropic efficiency of the compressor, the turbocharger compressor outlet temperature can be determined after applying the equation,

$$T_2 = T_1 \left(\frac{P_2}{P_1}\right)^{\frac{(\gamma-1)}{\gamma \eta_C}} \quad (3.8)$$

### 3.3.2 Regenerator

Air leaving the compressor is delivered to regenerator (an intake air to exhaust gases heat exchanger) where the intake is preheated through exhaust gases. This preheating of air is required to evaporate the wet-ethanol in the fuel vaporizer. The regenerator performance is determined by through its effectiveness which is given by

$$\varepsilon_h = \frac{\left[(\dot{m}.c_p)_2 (T_3 - T_2)\right]}{\left[(\dot{m}.c_p)_{min} (T_8 - T_2)\right]} \quad (3.9)$$

The assumption, $(\dot{m}.\, c_p)_2 = (\dot{m}.\, c_p)_{min}$ is taken to estimate the temperature, $T_3$, the air temperature at the regenerator exit and with this relation, it is expressed as

$$T_3 = T_8 \varepsilon_h + T_2(1 - \varepsilon_h) \quad (3.10)$$

The temperature at the regenerator exit is computed by applying the energy balance over it which is reported in Table 3.2.

### 3.3.3 HCCI engine

The premixed ethanol-water mixture leaving the mixer enters the HCCI engine. The charge enters the engine and before compression it is mixed with hot residual gases. Due to operation of engine at higher compression ratio, the charge is heating up to the level of ignition and combustion. But auto-ignition process is observed in HCCI engine for combustion which is controlled by chemical kinetics [60]. The efficiency of combustion process is considered to be 90%. External exhaust gas recirculation is absent in this model of engine [25]. The temperature of the mixture containing the

fresh charge and residual gases at the end of engine intake process (i-1') is computed by employing the expression and the ratio of pressure for inlet/exhaust is considered to be 1.4 [221].

$$T_{1'} = \frac{\mathrm{T}_i(1-f)}{1-\frac{1}{(n.\mathrm{r}_c)\left[\frac{\mathrm{p}_e}{\mathrm{p}_i}+(n-1)\right]}} \tag{3.11}$$

Where 1' signifies the location before the process of compression of fuel-air-residual gas mixture and $P_{1'} = P_1$.

Polytropic compression stroke (1'-2')

$$P_{2'} = P_{1'}\left(\frac{V_{1'}}{V_{2'}}\right)^n = P_{1'}(\mathrm{r}_c)^n \tag{3.12}$$

$$T_{2'} = T_{1'}(\mathrm{r}_c)^{n-1} \tag{3.13}$$

Assuming the heat addition process (2'-3') as constant volume gives

$$T_{3'} = T_{2'} + q_{in}(1-f)/c_v \tag{3.14}$$

$$P_{3'} = P_{2'}\left(\frac{T_{3'}}{T_{2'}}\right) \tag{3.15}$$

Expansion stroke (3'-4') is polytropic and this gives

$$P_{4'} = P_{3'}\left(\frac{1}{\mathrm{r}_c}\right)^n \tag{3.16}$$

$$T_{4'} = T_{3'}\left(\frac{1}{\mathrm{r}_c}\right)^{n-1} \tag{3.17}$$

Polytropic blowdown (4'-5')

$$T_{5'} = T_{4'}\left(\frac{P_{4'}}{P_e}\right)^{\frac{(1-n)}{n}} \tag{3.18}$$

$$P_{5'} = P_e \tag{3.19}$$

The constant pressure polytropic exhaust stroke (5'-6')

$$T_{5'} = T_e \tag{3.20}$$

$$P_6 = P_{5'} = P_e \tag{3.21}$$

$$f = \frac{1}{\mathrm{r}_c}\left(\frac{P_e}{P_4}\right)^{\frac{1}{n}} \tag{3.22}$$

Residual gas fraction (f=0.03) is found to be lower due to large compression ratio.

The heat lost to the ambient during the processes of exhaust and blowdown is computed by assuming 9% loss of heat during these processes [25].

The formulation for calculating the chemical exergy in HCCI engine may be seen as below

$$e_{HCCI}^{ch} = -\Delta g + \bar{R}\mathrm{T}_0 \left\{ x\mathrm{O}_2 ln \frac{P_{\mathrm{O}_2}^{00}}{P^0} + y\mathrm{H}_2 O ln \frac{P_{H_2O}^{00}}{P^0} - \sum_K \mathrm{x}_k ln \frac{P_k^{00}}{P^0} \right\} \quad (3.23)$$

The details of the symbols used in above equation can be found in the Ref. [18].

### 3.3.4 Turbine

Exhaust from the engine is expanded in the turbine to produce power for driving the compressor.

The temperature at turbine outlet can be determined by [60]

$$\mathrm{T}_8 = \mathrm{T}_7 \left(\frac{\mathrm{P}_8}{\mathrm{P}_7}\right)^{\frac{(n-1)\eta_T}{n}} \quad (3.24)$$

## 3.4. Evaluation criteria and system modeling

The proposed combined cooling-power cycle is analyzed using Engineering Equation Solver (EES) which is commercially available and provides a built in mathematical and thermodynamic property functions for solving the equations describing the model developed through balances of mass, energy, and exergy [199]. Each component of the system proposed is considered as a steady state control volume, with transfer of energy by heat, work, and mass of fluid enters and leaves. The equations derived after applying the balances of mass, energy, and exergy were employed to formulate the thermodynamic model. The thermodynamic properties of the refrigerant R134a used in ERC was computed after employing the REFPROP V 9.1 and the properties of LiBr-$H_2O$ fluid pair for ARC were taken from the Ref. [200, 226].

Application of second law of thermodynamics along with the traditional first law approach leads to analysis that joins the quality with quantity of energy during the process of energy conversion and it quantifies the destruction and loss of exergy appears at various locations of the system.

For the energetic and exergetic analyses of the cooling-power cogeneration system considered, the thermodynamic model was developed based on the assumptions below [184, 217, 218]:

1- All processes proceed under steady state condition.

2- Effects of kinetic and potential energies is not considered during the energy conversion.

3- Thermodynamic equilibrium is maintained between the inlet and exit of cycle key components.

4- The exchange of heat between the components and environment is ignored.

5- Expansion valves of both ERC and ARC are isenthalpic and pressure reduction devices.

6- The pressure drops in the pipes are not considered.

7- Physical exergies of the ERC fluid and LiBr-$H_2O$ fluid pair for ARC are only considered.
8- State of the working fluid at condenser outlet is saturated liquid.
9- The atmospheric pressure $P_0$ and temperature $T_0$ considered for the reference-environment were assumed as (25°C and 101.325 kPa), respectively.

The traditional first law of thermodynamics along with law of conservation of mass applied to any control volume operates at steady state and disregards the change in kinetic and potential energies gives

$$\Sigma \dot{m}_i - \Sigma \dot{m}_o = 0 \tag{3.25}$$

$$\Sigma \dot{Q} - \Sigma \dot{W} + \Sigma \dot{m}_i h_i - \Sigma \dot{m}_o h_o = 0 \tag{3.26}$$

After applying the Eqs. (3.25) and (3.26), the energy balance equations are formulated for the wet-ethanol fuelled HCCI engine corresponding to its P-V diagram shown in Figure 3.3, and also for the ERC and ARC which are employed for engine exhaust heat recovery. The formulated equations are displayed in Table 3.2 &3.3.

**Table 3.2** Component wise energy balance equations for the combined HCCI engine-ERC [184, 223]

| **Component** | **Balance Equations** |
|---|---|
| Compressor (Comp1) | $\dot{W}_{Comp1} = \dot{m}_a(h_2 - h_1)$ |
| Regenerator (Reg1) | $\dot{m}_a\,(h_3 - h_2) = \dot{m}_{exh}\,(h_8 - h_9)$ |
| Fuel vaporizer (FV1) | $\dot{m}_a\,h_3 + \dot{m}_f h_4 = (\dot{m}_a\, + \dot{m}_f)h_5$ |
| HCCI engine (Compression) process,1′- 2′ | $(\dot{m}_a\, + \dot{m}_f + \dot{m}_{rg})(h_{2'} - h_{1'}) = \dot{W}_{comp} - \dot{Q}_{surr}$ |
| Heat addition process, 2′- 3′ | $(\dot{m}_a\, + \dot{m}_f + \dot{m}_{rg})(h_{3'} - h_{2'}) = \dot{Q}_H$ |
| Expansion process,3′- 4′ | $(\dot{m}_a\, + \dot{m}_f + \dot{m}_{rg})(h_{3'} - h_{4'}) = \dot{W}_{exp} + \dot{Q}_{surr}$ |
| Blowdown Process, 4′-5′ | $\dot{m}_{exh}\,h_{4'} = \dot{m}_{exh}\,h_{5'} + \dot{Q}_{surr}$ |
| Catalytic convertor (CC1) | $\sum_{Product} n_e\left(\bar{h}_f^{\circ} + \Delta\bar{h}\right)_e = \sum_{Reactant} n_i\left(\bar{h}_f^{\circ} + \Delta\bar{h}\right)_i$ |
| Turbine (T1) | $\dot{W}_{T1} = \dot{m}_{exh}\,(h_7 - h_8)$ |
| Boiler (Boi) | $\dot{Q}_{boil} = \dot{m}_{11}(h_{11} - h_{18})$ |

| | |
|---|---|
| Pump (P1) | $\dot{W}_{P1} = \dot{m}_{18}\,(h_{18} - h_{17})$ |
| Ejector (Eje) | $\dot{m}_{11}h_{11} + \dot{m}_{16}h_{16} = \dot{m}_{12}h_{12}$ |
| Condenser (Cond1) | $\dot{m}_{12}(\,h_{12} - \,h_{13}) = \dot{m}_{Cond1}(\,h_{Cond1,o} - \,h_{Cond1,i})$ |
| Expansion valve (EV1) | $h_{14} = \,h_{15}$ |
| Evaporator (Evap1) | $\dot{Q}_{Evap1} = \dot{m}_{16}\,(h_{16} - h_{15})$ |

**Table 3.3** Equations of energy balance for the components of ARC [225]

| **Component** | **Balance Equations** |
|---|---|
| Generator (Gen) | $\dot{m}_9h_9 + \,\dot{m}_{25}h_{25} = \,\dot{m}_{10}h_{10} + \,\dot{m}_{ref}h_{19} + (\dot{m}_{sol} - \dot{m}_{ref})\,h_{26}$ |
| Condenser (Cond2) | $\dot{m}_{ref}(h_{19} - \,h_{20}) = \,\dot{m}_{Cond2}(h_{Cond2,o} - \,h_{Cond2,i})$ |
| Expansion Valve (EV2a) | $h_{20} = \,h_{21}$ |
| Evaporator (Evap2) | $\dot{Q}_{Evap2} = \,\dot{m}_{ref}(h_{22} - h_{21})$ |
| Expansion Valve (EV2b) | $h_{28} = h_{27}$ |
| Absorber (Abs) | $(\dot{m}_{sol} - \dot{m}_{ref})h_{28} + \,\dot{m}_{Abs}h_{Abs,i} + \dot{m}_{ref}h_{22} + \,= \,\dot{m}_{sol}h_{23} + \,\dot{m}_{Abs}h_{Abs,o}$ |
| Pump (P2) | $\dot{W}_{P2} = \,\dot{m}_{sol}(h_{24} - h_{23})$ |
| Heat Exchanger (HE) | $\dot{m}_{sol}h_{24} + (\dot{m}_{sol} - \dot{m}_{ref})h_{26} = \,(\dot{m}_{sol} - \dot{m}_{ref})h_{27} + \,\dot{m}_{sol}h_{25}$ |

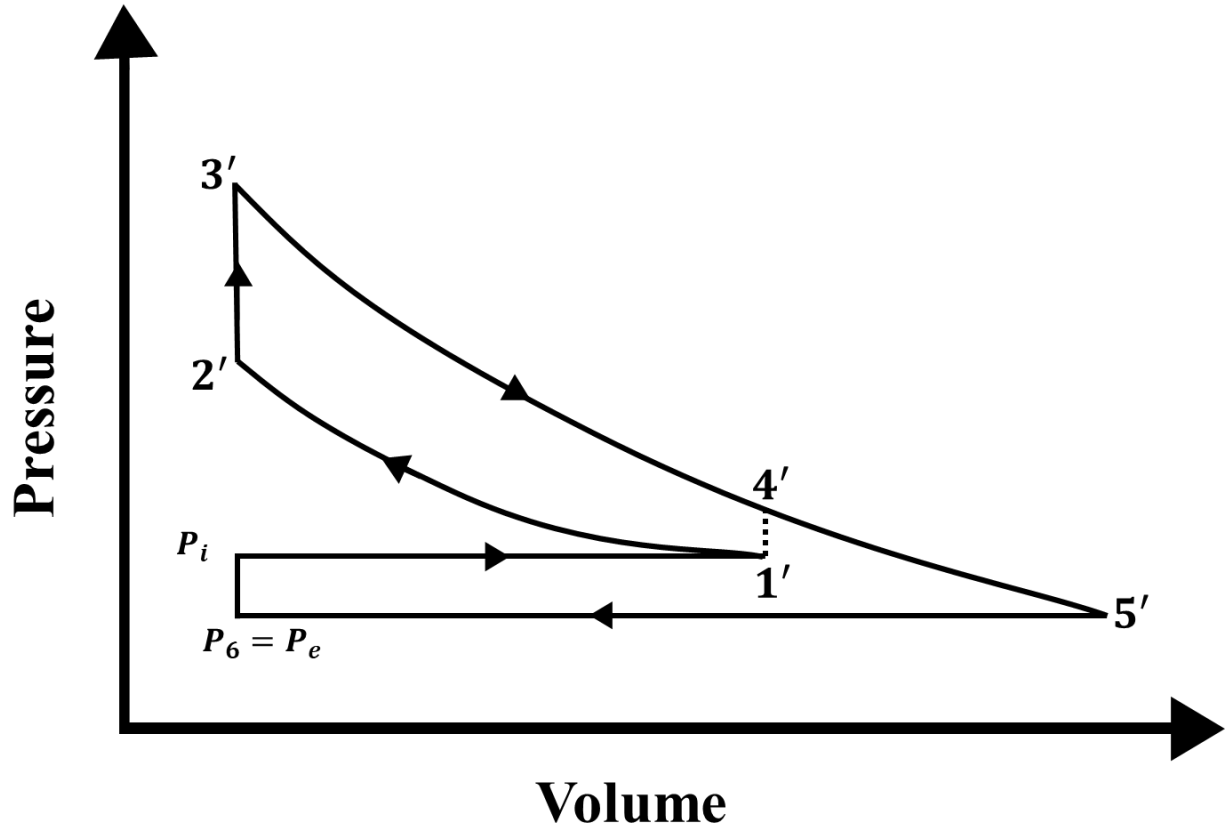


**Fig. 3.3.** P-V diagram for the HCCI engine whose thermodynamic cycle is modelled by a turbocharged Otto cycle

Exergy can be defined as the maximum useful work that can be obtained through a process which brings the system into equilibrium with a thermal reservoir, usually the environment.

The exergy rate balance equation that can be applied to any control volume under steady state operating condition can be presented as

$$\Sigma\left(1-\frac{T_0}{T}\right)\dot{Q}_j - \Sigma\dot{W} + \Sigma\dot{m}_i e_{x_i} - \Sigma\dot{m}_o e_{x_o} - \dot{E}_{x,D} = 0 \tag{3.27}$$

Where, $\dot{m}$ is the mass flow rate of a substance. First two terms on the left-hand side of Eq. (3.27) indicates the exergy transfer via heat, and work during a process.

$\dot{E}_{x,D}$ is the exergy destruction rate during the process. $e_x$ is the flow exergy per unit mass of a substance which can be break down into the chemical and physical exergy and is given by;

$$e_x = e_x^{ph} + e_x^{ch} \tag{3.28}$$

Physical specific exergy ($e_x^{ph}$) accounts for change in enthalpy of a gaseous species and loss in entropy during its transition from a specified state to restricted dead state. It is given by the following expression

$$e_x^{ph} = (h - h_0) - T_0(s - s_0) \tag{3.29}$$

The chemical exergy ($e_x^{ch}$) takes into account the deviations in composition of the substance from the substances occupied the reference environment. It may be expressed as [19]

$$e_x^{ch} = \sum x_i(\mu_i^* - \mu_0) = -\Delta g_i^0 + \sum \bar{R}\, T_0 x_i ln\left(\frac{p}{p_{ref}}\right) \tag{3.30}$$

Where $\mu_i$ is the chemical potential and $g_i$ is the Gibbs function of species "i", and they can be evaluated at a specified temperature T and pressure p. $T_0$ and $p_{ref}$ are the temperature and pressure at the reference environment, respectively. For engine applications, the reference environment temperature and pressure are taken to be as $T_0 = 298\,K$ and $p_{ref} = 1.013\,bar$. For chemical exergy computation in engine applications, the molar composition of the environment is to be taken as: 20.35% $O_2$, 75.67% $N_2$, 0.03% $CO_2$, 3.03% $H_2O$, and 0.92% other substances [185].

Considering the definition of exergy under the assumptions listed, and proposed balances, the equations for the calculation of exergy destroyed during the process occurring in the main components of the proposed configuration of combined energy system are developed and shown in Table 3.4&3.5.

**Table 3.4** Component wise exergy balance equations for the combined HCCI engine-ERC [184, 222]

| **Component** | **Balance Equations** |
|---|---|
| Compressor (Comp1) | $\dot{E}_{x,D,Comp1} = \dot{m}_1(e_{x,1} - e_{x,2}) + \dot{W}_{Comp1}$ |
| Regenerator (Reg1) | $\dot{E}_{x,D,Reg1} = \dot{m}_2(e_{x,2} - e_{x,3}) + \dot{m}_8(e_{x,8} - e_{x,9})$ |
| Fuel vaporizer (FV1) | $\dot{E}_{x,D,FV1} = \dot{m}_3 e_{x,3} + \dot{m}_4 e_{x,4} - \dot{m}_5 e_{x,5}$ |
| HCCI engine<br>(Compression) process,1′-2′ | $\dot{E}_{x,D,Comp} = \dot{m}_5(e_{x,1'} - e_{x,2'}) + \dot{W}_{comp} - \dot{Q}_{surr}\left(1 - \frac{T_0}{T}\right)$ |
| Heat addition process, 2′-3′ | $\dot{E}_{x,D,Heat\ addition} = \dot{m}_5(e_{x,2'} - e_{x,3'}) + \dot{Q}_H\left(1 - \frac{T_0}{T_H}\right)$ |
| Expansion process, 3′- 4′ | $\dot{E}_{x,D,exp} = \dot{m}_5(e_{x,3'} - e_{x,4'}) - \dot{W}_{exp} - \dot{Q}_{surr}\left(1 - \frac{T_0}{T}\right)$ |
| Blowdown Process, 4′-5′ | $\dot{E}_{x,D,exh\ \&\ blowdown} = \dot{m}_5(e_{x,4'} - e_{x,5'}) - \dot{Q}_{surr}\left(1 - \frac{T_0}{T}\right)$ |
| Catalytic convertor (CC1) | $\dot{E}_{x,D,CC1} = \dot{m}_6 e_{x,6} - \dot{m}_7 e_{x,7} + \dot{m}_6 e_{ch}$ |
| Turbine (T1) | $\dot{E}_{x,D,T1} = \dot{m}_7(e_{x,7} - e_{x,8}) - w_{T1}$ |
| Boiler (Boi) | $\dot{m}_{18} ex_{18} + \dot{Q}_{boi}\left(1 - \frac{T_0}{T_{ave,boi}}\right) = \dot{m}_{11} ex_{11} + \dot{m}_{boi} ex_{d,boi}$ |
| Pump (P1) | $\dot{E}_{x,D,P1} = \dot{m}_{17}(e_{x,17} - e_{x,18}) + \dot{W}_{P1}$ |
| Ejector (Eje) | $\dot{E}_{x,D,Eje} = \dot{m}_{11} e_{x,11} + \dot{m}_{16} e_{x,16} - \dot{m}_{12} e_{x,12}$ |
| Condenser (Cond1) | $\dot{E}_{x,D,Cond1} = \dot{m}_{12} e_{x,12} + \dot{m}_{Cond1}(e_{x,Cond1,i} - e_{x,Cond1,o}) - \dot{m}_{13} e_{x,13}$ |
| Expansion valve (EV1) | $\dot{E}_{x,D,EV1} = \dot{m}_{14}(e_{x,14} - e_{x,15})$ |

| | |
|---|---|
| Evaporator (Evap1) | $\dot{E}_{x,D,Evap1} = \dot{m}_{15}(e_{x,15} - e_{x,16}) + \dot{m}_{Evap1}(e_{x,Evap1,i} - e_{x,Evap1,o})$ |

**Table 3.5:** Equations of exergy balance for the components of ARC cooling cycle [224]

| Component | Balance Equations |
|---|---|
| Generator (Gen) | $\dot{E}_{x,D,Gen} = \dot{m}_{9}(e_{x,9} - e_{x,10}) + \dot{m}_{sol}e_{x,25} - (\dot{m}_{sol} - \dot{m}_{ref})e_{x,26} - \dot{m}_{ref}e_{x,19}$ |
| Condenser (Cond2) | $\dot{E}_{x,D,Cond2} = \dot{m}_{ref}(e_{x,19} - e_{x,20}) + \dot{m}_{Cond2}(e_{x,Cond2,i} - e_{x,Cond2,o})$ |
| Expansion Valve (EV2a) | $\dot{E}_{x,D,EV,abs} = \dot{m}_{ref}(e_{x,20} - e_{x,21})$ |
| Evaporator (Evap2) | $\dot{E}_{x,D,Evap2} = \dot{m}_{ref}e_{x,21} + \dot{m}_{Evap2}e_{x,Evap2,i} - \dot{m}_{r}e_{x,22} - \dot{m}_{Evap2}e_{x,Evap2,o}$ |
| Expansion Valve (EV2b) | $\dot{E}_{x,D,EV2b} = (\dot{m}_{sol} - \dot{m}_{r})(e_{x,27} - e_{x,28})$ |
| Absorber (Abs) | $\dot{E}_{x,D,ab} = (\dot{m}_{sol} - \dot{m}_{ref})e_{x,28} + \dot{m}_{ref}e_{x,22} + \dot{m}_{Abs}e_{x,Abs,i} - \dot{m}_{sol}e_{x,23} - \dot{m}_{Abs}e_{x,Abs,o}$ |
| Pump (P2) | $\dot{E}_{x,D,P2} = \dot{m}_{sol}(e_{x,23} - e_{x,24}) + \dot{W}_{P2}$ |
| Heat Exchanger (HE) | $\dot{E}_{x,D,HE} = (\dot{m}_{sol} - \dot{m}_{ref})(e_{x,26} - e_{x,27}) + \dot{m}_{sol}(e_{x,24} - e_{x,25})$ |

## 3.5 Evaluation criteria

Habitually, the performance of energy conversion system is determined based on first law efficiency which is a measure of the percentage of the energy input that is transformed to useful energy output. The energy efficiency of the proposed cooling power-cogeneration system which can be evaluated by applying first law, may be presented as:

$$\eta_{en,comb} = \frac{\dot{W}_{BT-} \dot{W}_{Eje,P} + \dot{Q}_{ref}}{\dot{m}_f LHV \eta_{cc}} \quad (3.31)$$

where, $\dot{W}_{BT}$ is the brake thermal power, and $\dot{W}_{Eje,P}$ is the power consumed by the refrigerant pump, respectively. $\dot{m}_f$ is the rate of fuel consumption, and LHV is the lower heating value of fuel, $\dot{Q}_{ref}$ is the rate of cooling capacity, and $\eta_{cc}$ is the combustion efficiency.

The network produced in the HCCI engine which will be available as a useful work may be obtained after using the expression [30]

$$WD = \left[\left(\frac{P_3'V_3' - P_4'V_4'}{n-1}\right) - \left(\frac{P_2'V_2' - P_1'V_1'}{n-1}\right)\right] \quad (3.32)$$

$$W_{BT} = Actual\ WD = 0.8 * WD \quad (3.33)$$

Where $W_{BT}$ is the actual work done which is used to calculate brake thermal efficiency of HCCI engine

Since the two energy outputs of the proposed cycle; power generation and rate of cooling produced are different from quality point of view because power is free from entropy and cooling is associated with entropy, therefore, thermal efficiency based on traditional first law approach is not suitable for systems which produce two different outputs of energy. In this context, a relatively new term called exergy efficiency was introduced which provides a more accurate measure of thermodynamic performance of the cycle and it is given by

$$\eta_{ex,comb} = \frac{\dot{W}_{BT} - \dot{W}_{Eje,P} + \dot{E}_{ref}}{\dot{m}_f LHV \eta_{cc} \varphi} \quad (3.34)$$

where, $\dot{E}_{ref}$ is the amount of exergy associated with the cooling capacity $\dot{Q}_{ref}$ and is given by

$$\dot{E}_{ref} = \dot{Q}_{ref}\left(\frac{T_0 - T_{Evap}}{T_{Evap}}\right) \quad (3.35)$$

Where, $T_{Evap}$ is the evaporator temperature, $T_0$ is the ambient temperature, and $\phi$ is the ratio of exergy of the fuel to its energy [186].

## 3.6. Results and discussion

Below are the computational results revealed after conducting the energetic and exergetic performances of the HCCI engine fueled by wet-ethanol and bottoming with the ERC/ARC for cooling-power cogeneration. Results are computed for the use of R134a and R290 as the refrigerants of ERC, and LiBr-$H_2O$ as working fluid pair for ARC. In the analysis, the effects of altering the turbocharger pressure ratio, turbocharger compression ratio, ambient temperature is investigated on the efficiencies of combined cycle. The effect of entrainment ratio and generator temperature variation was also examined on the COPs of ERC and ARC, respectively.

Fig. 3.4 represents the change in energy efficiency of HCCI engine based combined system after altering the turbocharger pressure ratio. The HCCI engine efficiency evaluated on first law basis is found to be increasing with the rise of pressure ratio across the turbocharger. This is due to the reason higher turbocharger pressure improves the fuel-air mixing along with the increase of charge density which raises the temperature of mixture and hence the engine power output. Further, for the same turbine and compressor efficiencies and regenerator effectiveness any rise in turbocharger pressure ratio results in the increase of engine exhaust temperature which is an inlet temperature to the boiler and this will increase the heat transfer to refrigerant passes through the boiler of ERC or the generator of ARC and this in turn improves the cooling capacity of the evaporator of cycle concerned. This simultaneous increase in the output of HCCI engine and the cooling capacity of refrigeration cycle contributes to rise in the efficiency of cooling-power cogeneration cycle. Change of refrigerant in the ERC from R134a to R290 reduces the energy

efficiency of cogeneration cycle because of the considerable difference in boiling point of (-26.1℃) for R134a and (-42.11$^0$C) for R290. Further, lower refrigeration output for R290 (propane) operated system attributes to the low critical temperature of propane (96.74$^0$C) compared to higher critical temperature of R134a (101.1$^0$C). Relatively a high motive flow temperature is required to produce the decent refrigeration output and hence the lower critical temperature of refrigerant is a hinderance in obtaining the higher output. It is further noticed that an increase in pressure ratio across the turbocharger from 2.5 to 3.5 raises the HCCI engine first law efficiency from 44.09% to 46.32%, and for cogeneration it is increased from 47% to 49.21% when R134a is used as ERC refrigerant and from 46.06% to 48.29% when R290 is the ERC refrigerant, and in case of ARC bottoming it is increased from 55.08% to 57.25%.

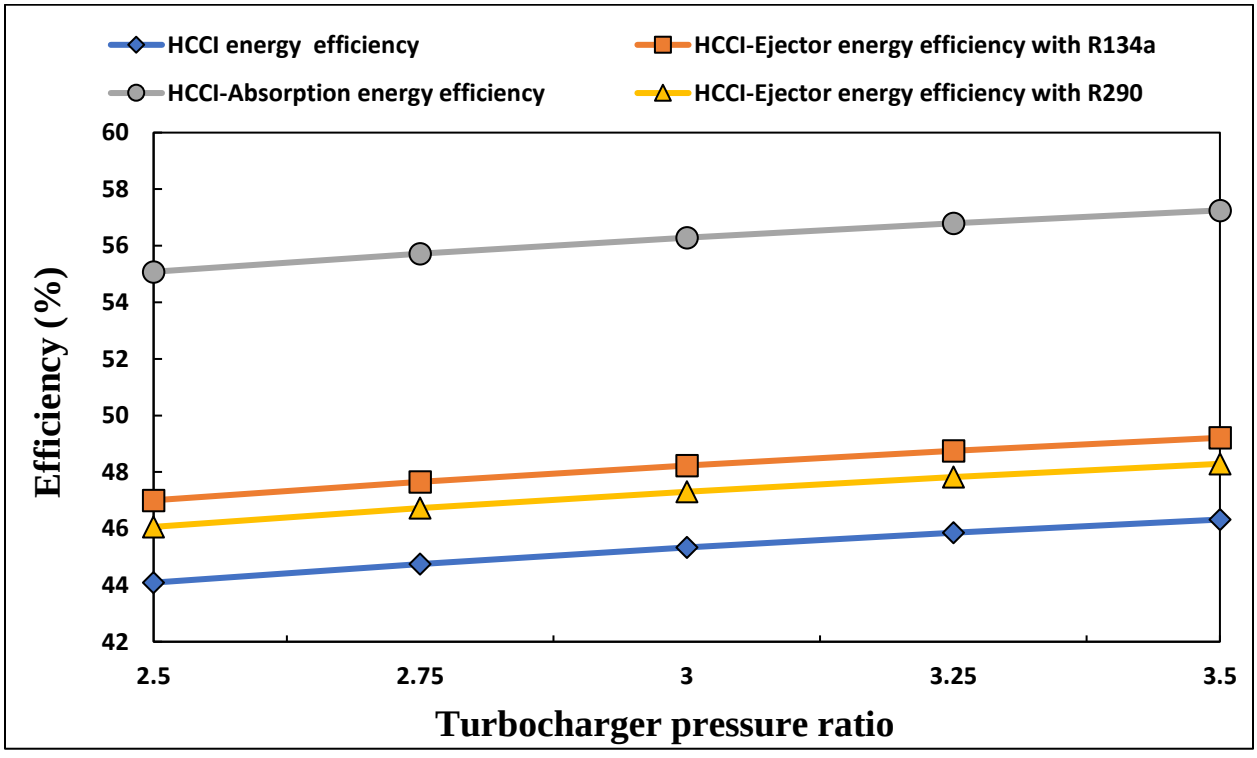


**Fig. 3.4.** Variation of energy efficiency of HCCI, HCCI-Ejector system, HCCI-Absorption system with turbocharger pressure ratio

Fig. 3.5 displays the influence of turbocharger pressure ratio on the exergy efficiency of HCCI engine and the cogeneration system for both ERC and ARC, respectively. The exergy efficiency of HCCI engine is shown to be distinct than its energy efficiency and this difference is found because of the considerable difference between the exergy and energy of fuel supplied. Since exergy efficiency of HCCI engine is the ratio of power exergy to the fuel exergy, therefore, exergy efficiency is higher than the corresponding energy efficiency of HCCI engine. The exergy efficiency of combined cycle (power and cooling) is found to be lower than its energy efficiency. The exergy of refrigeration is thermodynamically lower than the refrigeration capacity and since this difference dominates over the difference between the exergy and energy of ethanol, therefore, exergy efficiency of cogeneration which is the exergetic output to the exergy of fuel input is appeared to be lower than the energy efficiency of cogeneration. Similar to the trend of energy efficiency of cogeneration, the exergy efficiency of cogeneration cycle where cooling is produced by the bottoming of ARC is found to be larger than the exergy efficiency of cogeneration bottoming with ERC.

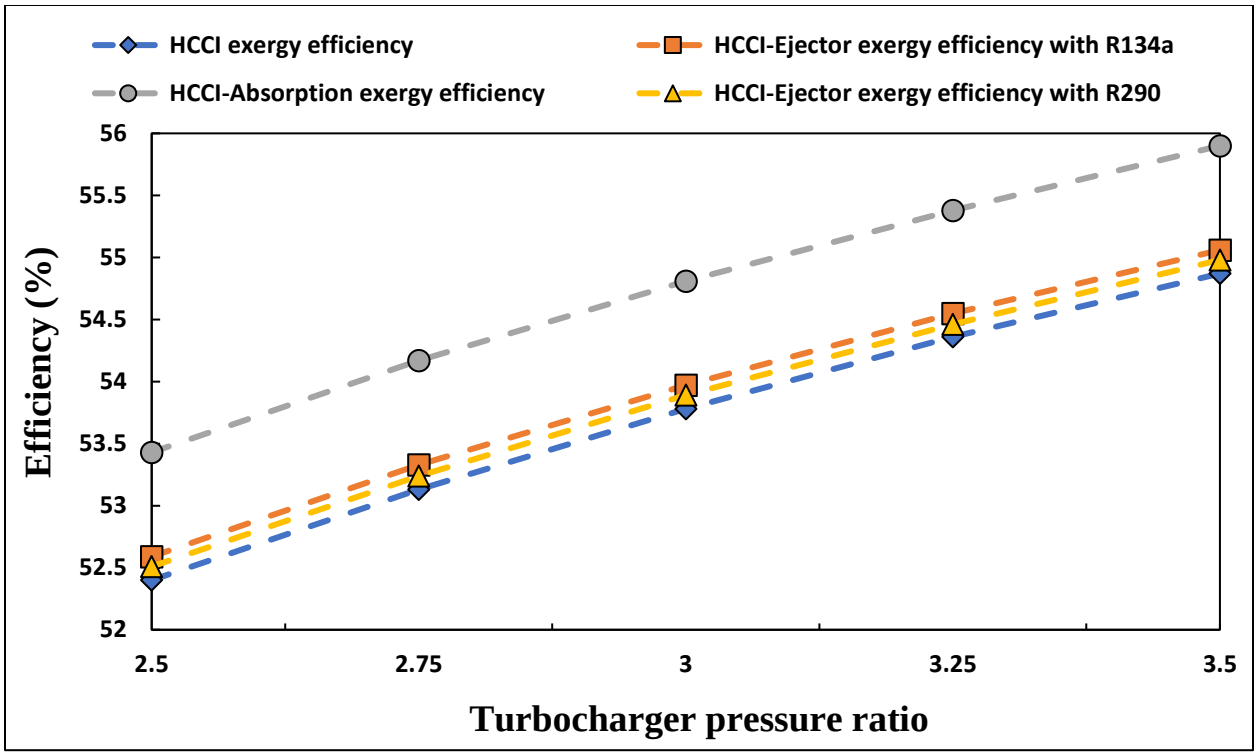


**Fig. 3.5.** Variation of exergy efficiency of HCCI, HCCI-Ejector system, HCCI-Absorption system with turbocharger pressure ratio

Fig. 3.6 displays the impact of turbocharger compressor efficiency on the energy efficiency of HCCI engine and cogeneration with both ERC and ARC. The energy efficiency of HCCI engine is found to be increased at the rise of turbocharger compressor efficiency. This is because higher turbocharger efficiency decreases the compressor power input and the turbine power as well which results in the decrease of engine exhaust temperature and the higher energy efficiency of the engine. Further, it is to be noted that increase in turbocharger compressor efficiency results in the decrease of energy contents of gases enters the boiler/generator of ERC/ARC which decreases the mass flow rate of the refrigerant and hence the refrigeration capacity of the bottoming cycle. Since increase in HCCI engine power dominates over the decrease of cooling capacity of ERC/ARC, therefore, the energy efficiency of cooling-power cogeneration cycle is also increased when the turbocharger compressor efficiency increases. At a given turbocharger compressor efficiency, the

energy efficiency of cogeneration cycle ARC is employed as the bottoming cycle is considerably higher than ERC employed cycle for cooling. It is shown that raising of turbocharger efficiency from 0.7 to 0.9 increases the HCCI engine efficiency from 44.51% to 45.93%, and the energy efficiency of R134a operated ERC cogeneration increases from 47.41% to 48.83% and of the ARC cogeneration increases from 46.48% to 47.9%, respectively.

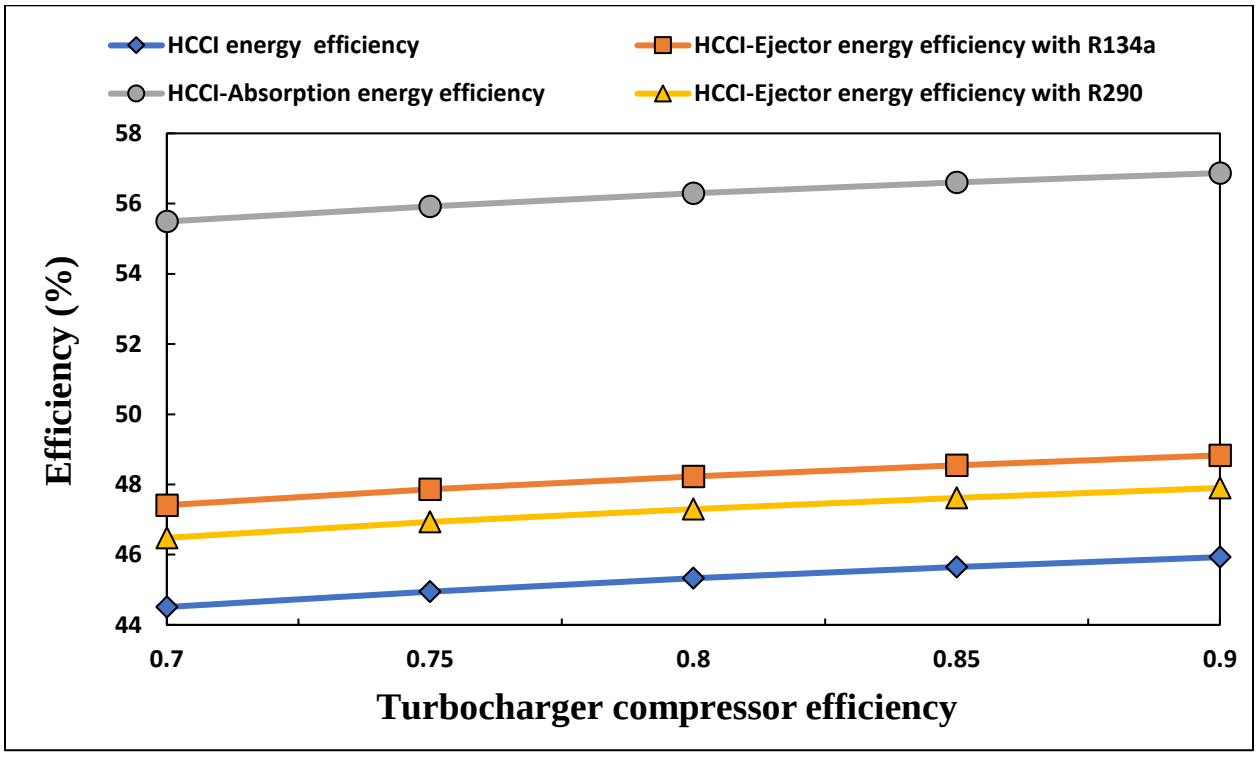


**Fig. 3.6.** Variation of energy efficiency of HCCI, HCCI-Ejector system, HCCI-Absorption system with turbocharger compressor efficiency

The variation of the exergy efficiency of HCCI engine and the cogeneration cycle for ERC and ARC with the turbocharger compressor efficiency is depicted in Fig. 3.7. It is observed that as the turbocharger compressor efficiency increases the exergy efficiency of HCCI engine increases. This is because at the higher turbocharger compressor efficiency the irreversibility decreases as in case of compressor, irreversibility is the difference between the actual power and reversible power input. Since the exergy of refrigeration is significantly less than the refrigeration effect, therefore,

the exergy efficiency of cogeneration cycle is little higher than the exergy efficiency of HCCI engine. It is recorded that increase in turbocharger compressor efficiency from 0.7 to 0.9 raises the exergy efficiency of HCCI engine from 52.72% to 54.56%, and for the ARC cogeneration cycle it is increased from 53.75% to 55.58%, respectively.

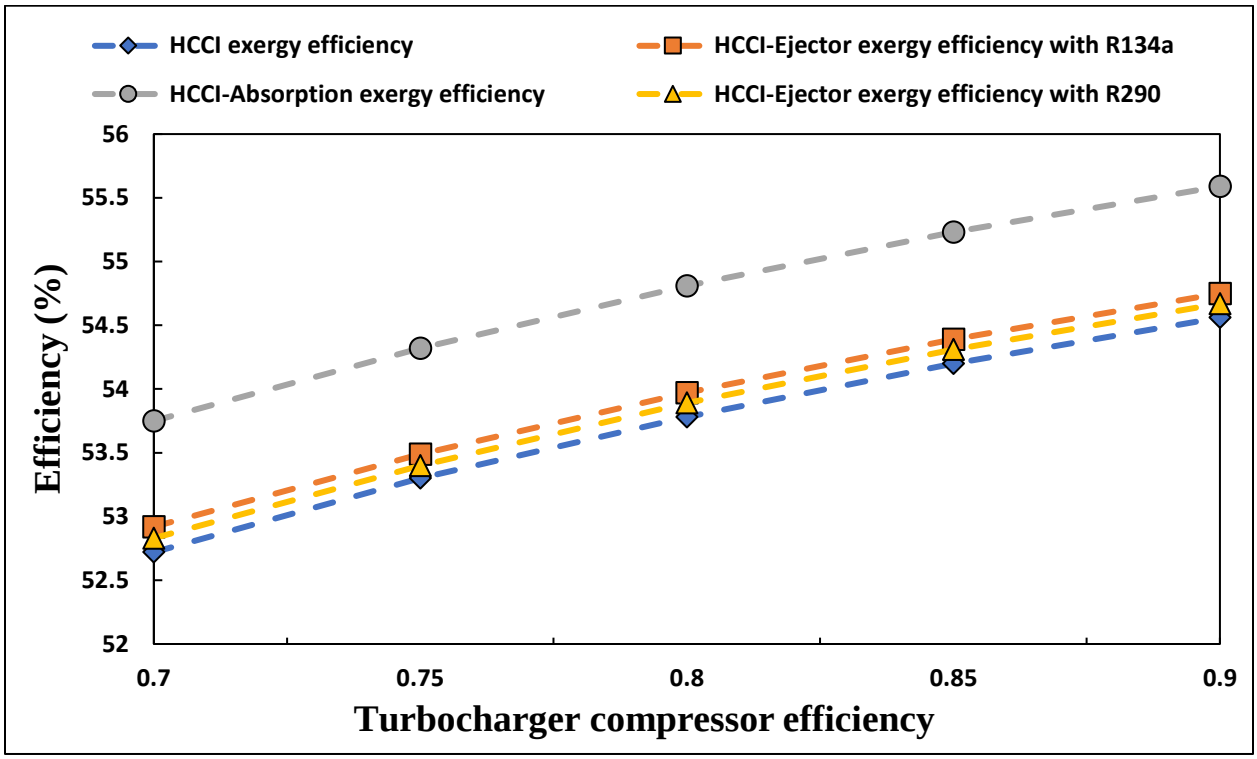


**Fig. 3.7.** Variation of exergy efficiency of HCCI, HCCI-Ejector system, HCCI-Absorption system with turbocharger compressor efficiency

Fig. 3.8 shows the effect of changing the ambient temperature on the energy efficiency of HCCI engine and cooling-power cogeneration cycle. The energy efficiency of HCCI engine is found to be decreased with the rise of ambient temperature because of the reduction in volumetric efficiency and increase in fuel consumption in the combustion chamber at higher ambient temperature. It is further to be noted that the rate of decrease in energy efficiency of cogeneration cycle is less than the rate of decrease in the energy efficiency of HCCI engine. This is because the refrigeration capacity of ERC/ARC start increasing with the increase of ambient temperature due to the

reduction of energy losses at the heat exchanger components of ERC and ARC but the decrease in the engine output dominates over the increase in capacity of refrigeration. Therefore, the efficiency of cogeneration diminishes gradually when the ambient temperature rises. Since the refrigeration capacity of ARC at a given temperature is greater than the refrigeration capacity of ERC, therefore, the efficiency of HCCI engine combined with the ARC is considerably greater than the case of ERC bottoming. Further, it is observed that at a given ambient temperature the exergy destroyed in the R290 operated ERC at the condenser and expansion valves is greater than the exergy destroyed in the R134a operated ERC, therefore, the efficiency of R143a operated ERC cogeneration is found to be higher than the efficiency of R290 operated cogeneration cycle.

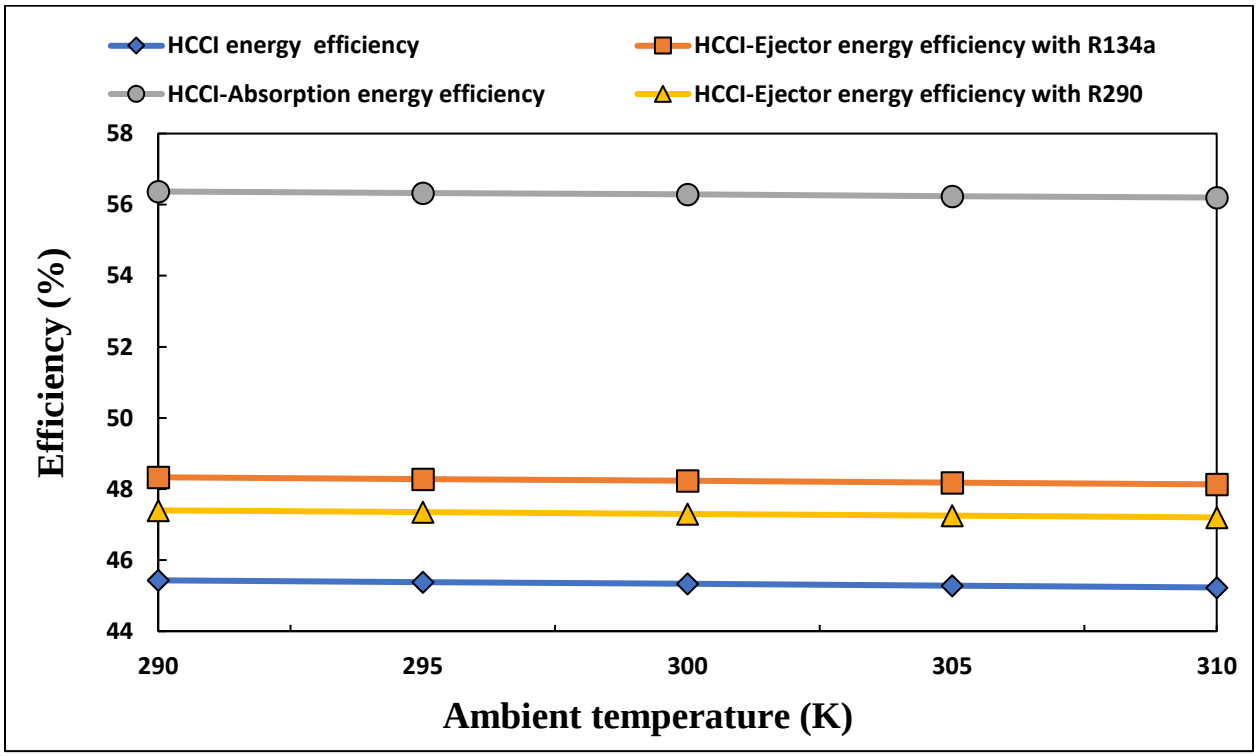


**Fig. 3.8.** Variation of energy efficiency of HCCI, HCCI-Ejector system, HCCI-Absorption system with ambient temperature

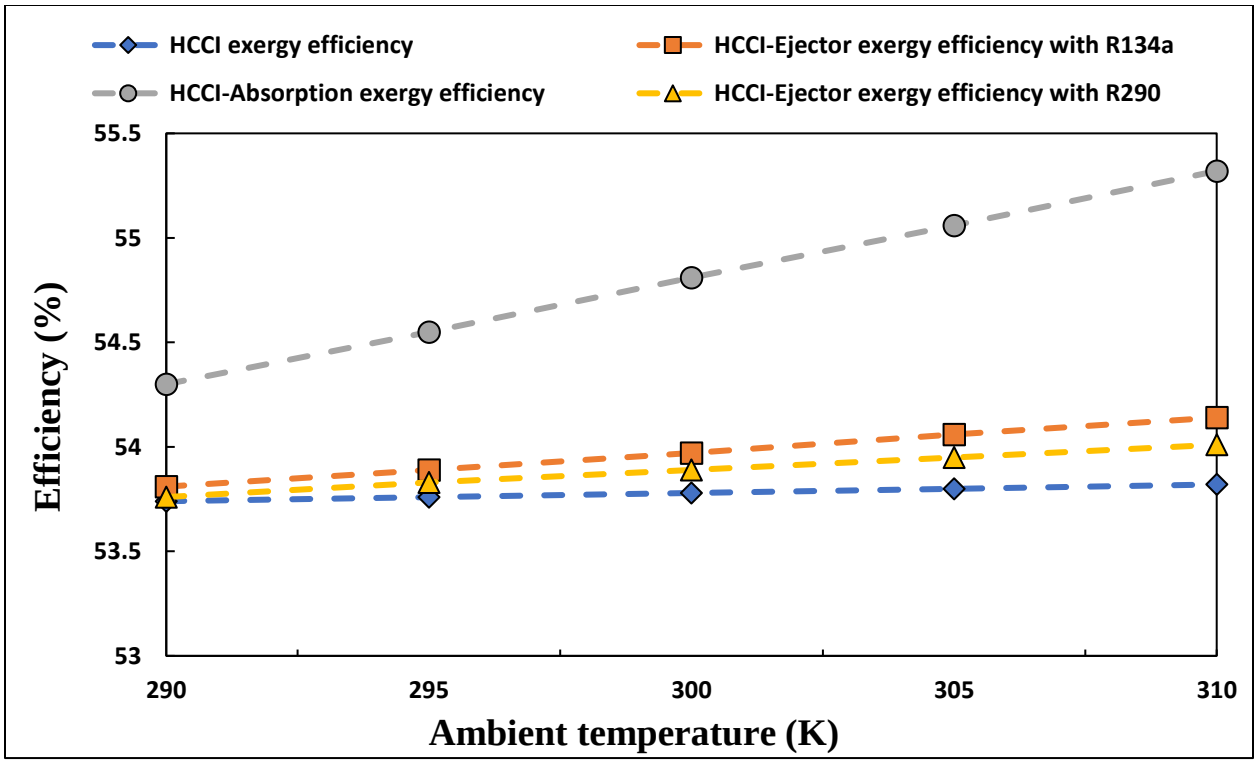


**Fig. 3.9.** Variation of exergy efficiency of HCCI, HCCI-Ejector system, HCCI-Absorption system with ambient temperature

The influence of ambient temperature on the exergy efficiency of HCCI engine and the cogeneration cycle was also computed and depicted in Fig. 3.9. The exergy efficiency of HCCI engine behave similar to its energy efficiency but diminishes more gradually because of decrease in physical exergy of fuel at higher ambient temperature. On the other hand, the exergy efficiency of cogeneration cycle combined with ARC/ERC start increasing because of the increase of exergy of refrigeration with the rise of ambient temperature. By definition, exergy of refrigeration is the ratio of the refrigeration capacity to the Carnot COP operates between the refrigeration temperature and ambient temperature. Since cooling capacity of ARC for the same heat input is greater than the cooling capacity of ERC, therefore, the rate of increase in the exergy efficiency of cogeneration (HCCI engine combined with ARC) is significantly higher than the rate of increase in the exergy

efficiency of cogeneration (HCCI engine combined with ERC) for the same increase of ambient temperature.

The effect of change in the entrainment ratio and refrigerant type on the energetic and exergetic COPs of ERC was also examined and is shown below in Fig. 3.10. Both energetic and exergetic COPs are found to be decreased gradually when the entrainment ratio is increased. This is because entrainment ratio (refrigerant mass flow rate via evaporator to the flowing mass entering the ejector) increases with the increase of boiler temperature and for the constant heat load of the boiler this leads to the reduced mass flow of refrigerant entering the ejector and hence a lower entrained mass flow rate from the evaporator. Since the decrease in entrained mass flow rate of refrigerant is less than the decrease of its motive mass flow rate, therefore, amount of cooling produced which diminishes gradually which shows a slight decrement in the COP of ERC. The magnitude of the exergy of refrigeration is always less than the refrigeration effect but both depend strongly on mass of refrigerant flowing through the evaporator to generate cooling, therefore, the exergetic COP of ERC is also decreases gradually with the rise of entrainment ratio.

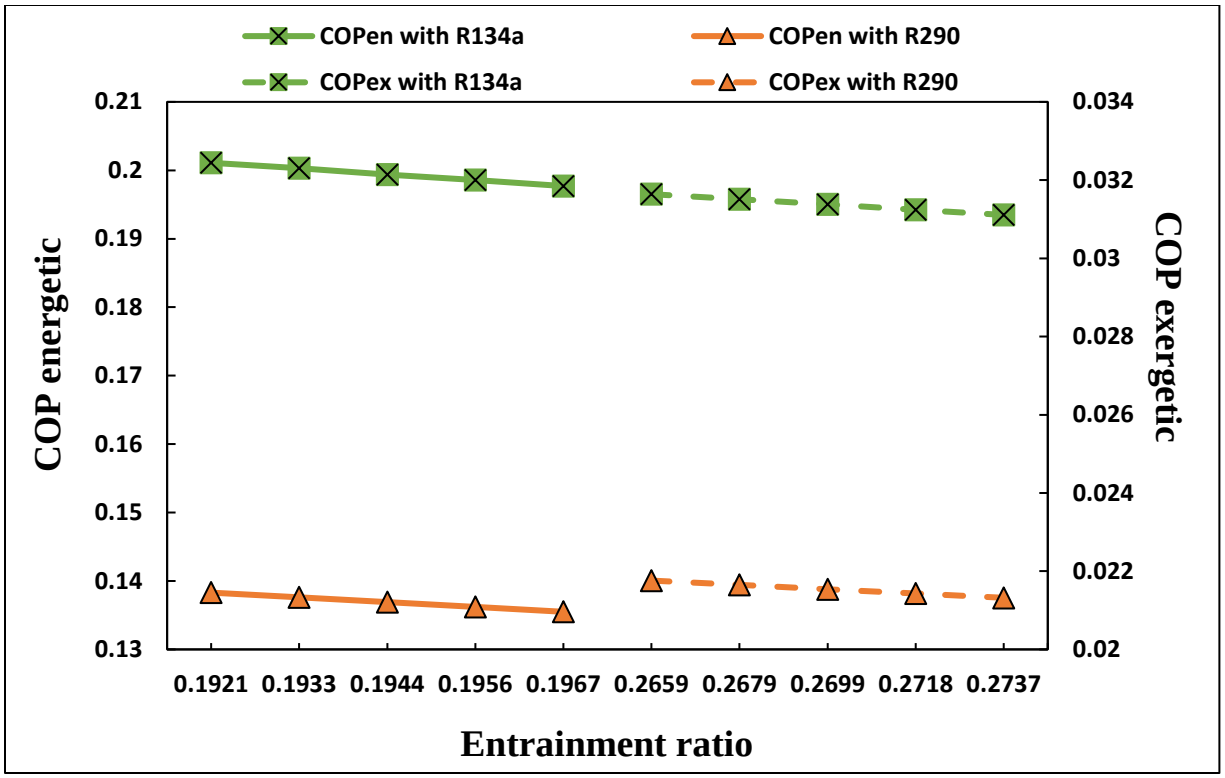


**Fig. 3.10.** Variation of energetic and exergetic COPs with entrainment ratio

Fig. 3.11 shows the variation in COP of the absorption refrigeration cycle (ARC) with the rise in generator temperature. At a constant evaporative cooling, temperature of heat transfer fluid has been increased which results in the increase of generator temperature. This rise in temperature also increases the pressure. This in turn decrease the pressure at the outlet of expansion valve, which determines the evaporator temperature and refrigeration capacity. Therefore, the heat input to generator is increased, while keeping the cooling output as constant in the ARC. Since the energy and exergy supplied to the generator plays an important role in the determination of COP, therefore, the energetic and exergetic COP of ARC are decreased at the rise of generator temperature. A rise in generator temperature from 359K to 367K, declines the energetic COP of ARC from 0.7333 to 0.7299 and its exergetic COP from 0.1100 to 0.1094, respectively.

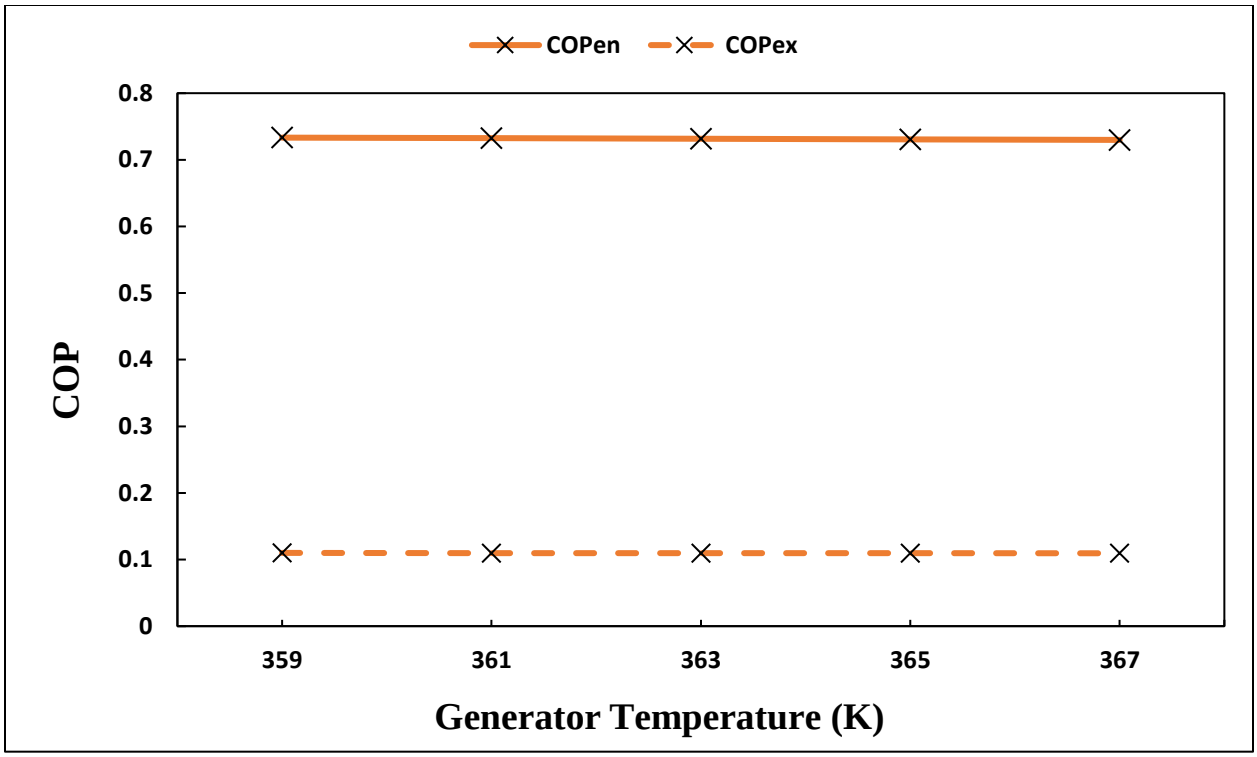


**Fig. 3.11.** Variation of energetic and exergetic COPs with generator temperature

The breaking down of fuel energy supplies to combined cycle (HCCI engine-ERC) at its base line operation is illustrated in Fig. 3.12. From the ERC employed combined cycle where R134a is the refrigerant, it is determined that out of 333.36 kW of fuel energy supplied, 130.1 kW is the produced power and 9.767 kW is the refrigeration of thermal load. About 101.34 kW of energy is lost via engine heat transfer and 45.72 kW is the energy lost via thermal exhaust to atmosphere, and 59.07 kW is the energy losses at the refrigerant condenser. In case of R290 operated ERC, because of the lower boiling point, refrigeration effect produced by R290 refrigerant is considerably less than R134a and found as 6.706 kW and energy losses at the refrigerant condenser also reduces from 59.07 kW to 56.04 kW.

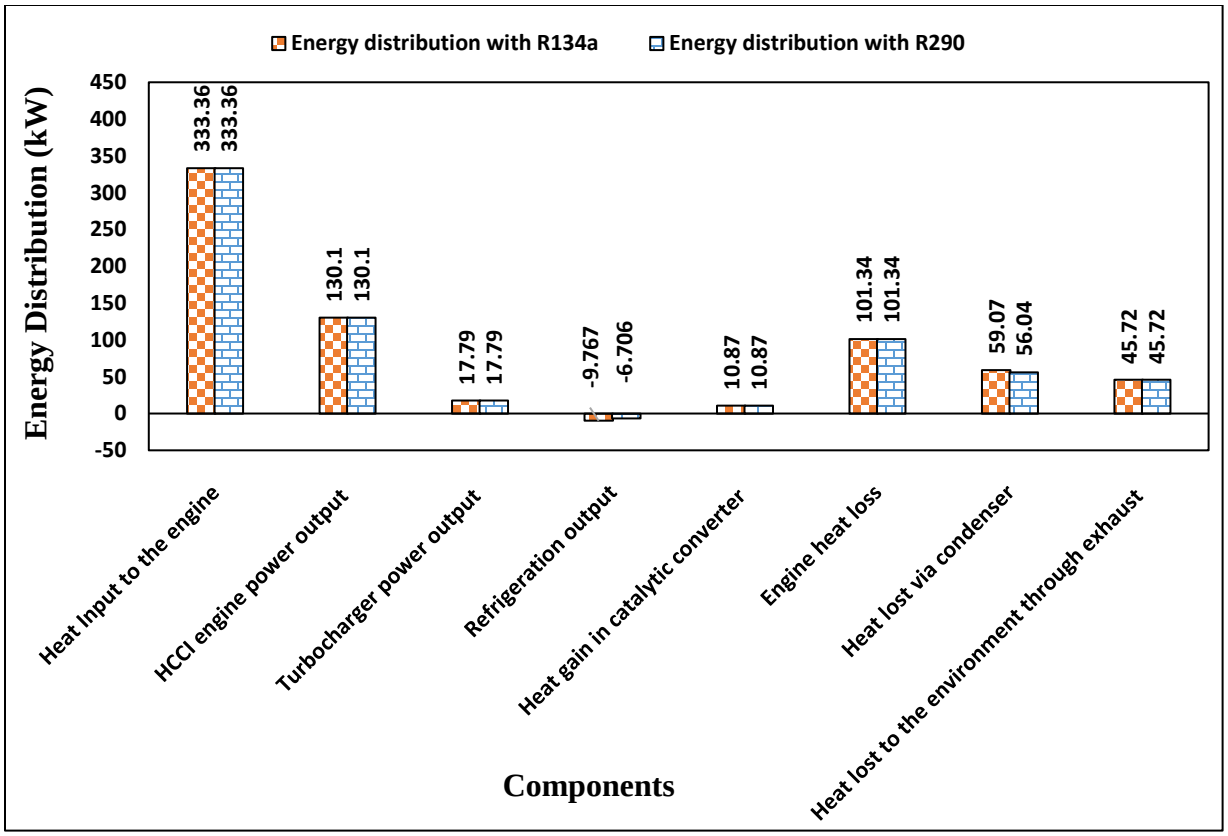


**Fig. 3.12.** Distribution of fuel energy in the HCCI engine-ERC combined cycle of cogeneration

The breaking down of fuel energy supplies to combined cycle (HCCI engine-ARC) at its base line operation is illustrated in Fig. 3.13. The distribution of fuel energy supplied to HCCI engine-ARC is showing quite different figure for the refrigeration effect and the energy losses at the refrigerant condenser. The refrigeration produced by ARC is significantly larger than ERC because of the higher boiling point of water which act as refrigerant in the LiBr-$H_2O$ mixture and it is found as 35.62 kW. The energy losses at the condenser and absorber of ARC are 38.3 kW and 46.29 kW, respectively. The distribution of fuel energy in the components of HCCI engine is unaltered by changing the type of bottoming cycle from ERC to ARC.

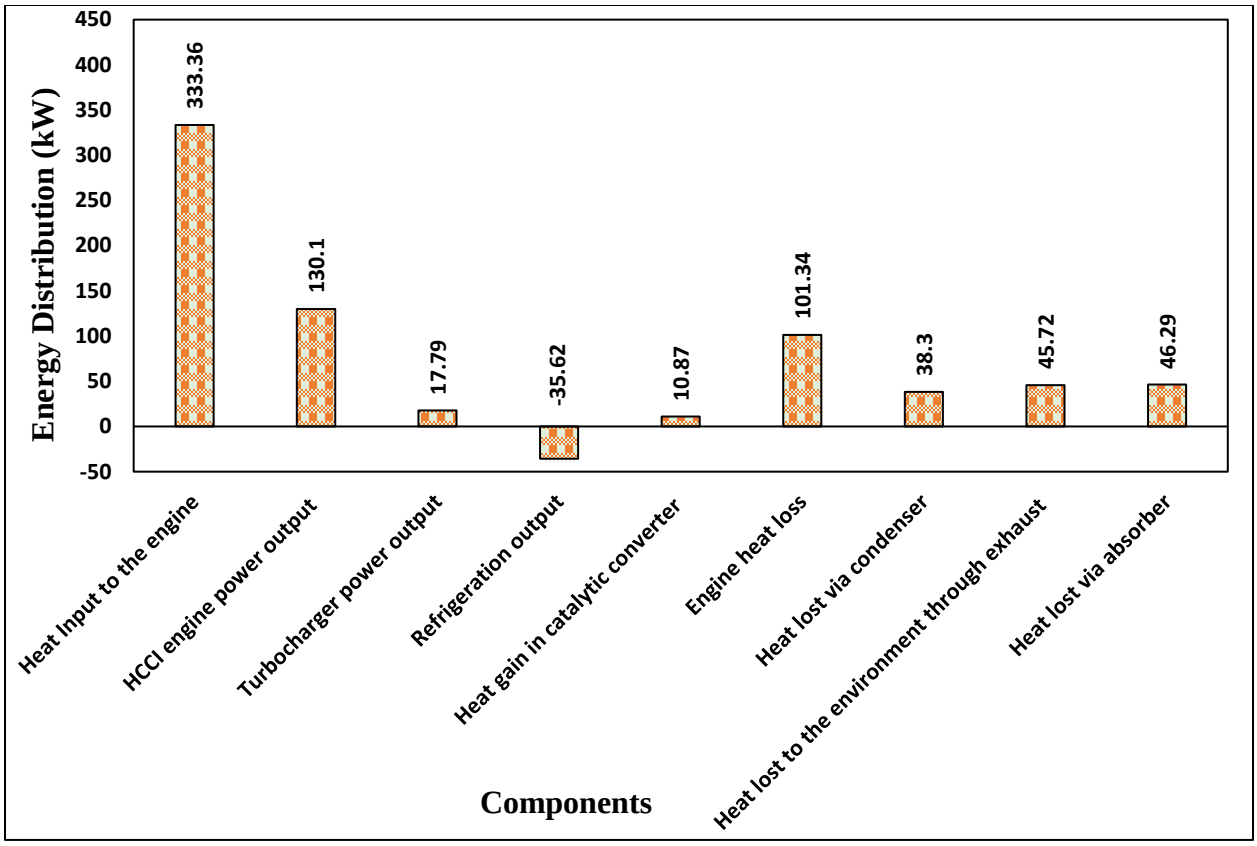


**Fig. 3.13.** Distribution of fuel energy in the HCCI engine-ARC combined cycle of cogeneration

Employment of the principle of the decrease of exergy enunciated from the combined application of the first and second laws of thermodynamics to the developed wet-ethanol fuelled combined power and cooling cycle provides a breakdown of the amount of fuel exergy supplied and is converted into engine power exergy and the refrigeration exergy, and loss of exergy as well as the exergy degraded due to generation of entropy during energy transformation in the cycle components. To this effect, the breaking down of input exergy into the exergy destroyed, loss of exergy, and the exergy produced was computed and is depicted in Fig. 3.14.

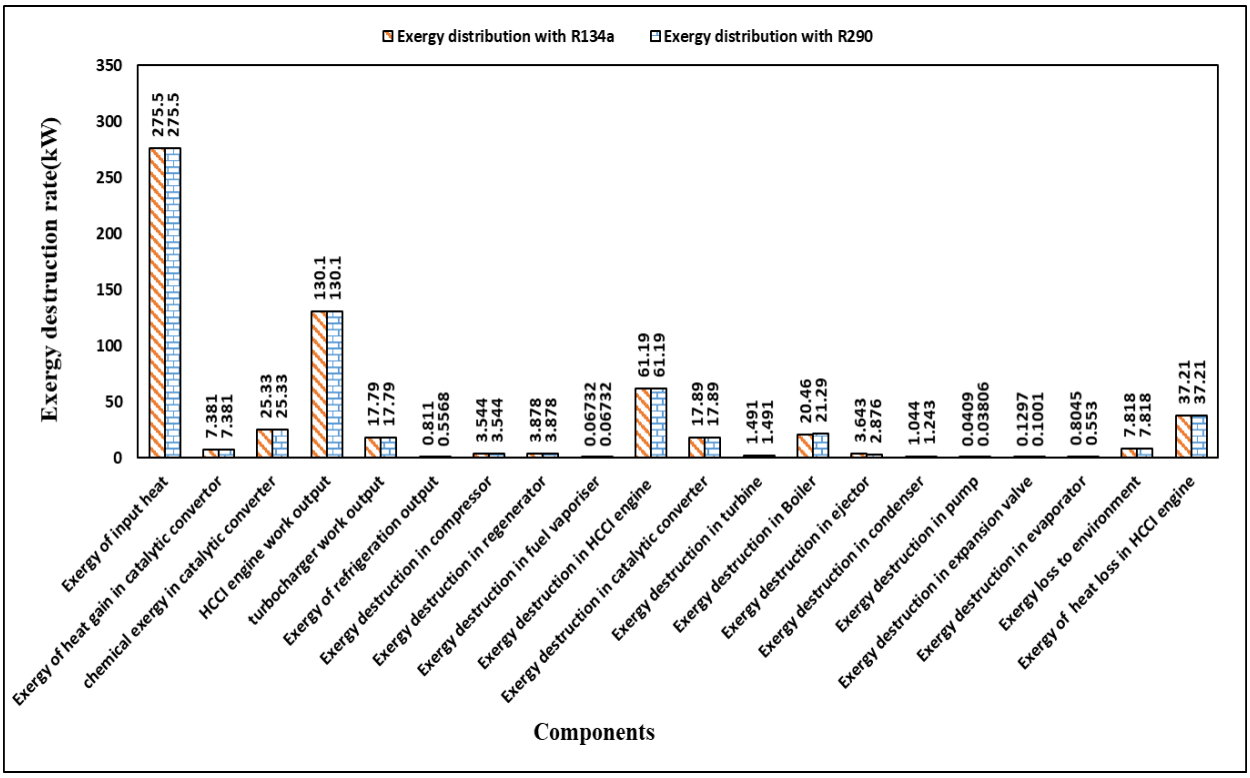


**Fig. 3.14.** Distribution of fuel exergy in the combined cycle (HCCI engine-ERC) configuration

In case of ERC employed bottoming cycle for cold production, from the 275.5 kW of exergy supplied to combined cycle, 130.1 kW is the power exergy and 0.811 kW is the exergy of refrigeration (R134a refrigerant). Following are seen as the components of high exergy destruction; HCCI engine (61.19 kW), boiler (20.46 kW), catalytic convertor (17.89 kW), and the exergy destruction in rest of the components of combined cycle is significantly less compared to above figures and hence not mentioned by shown clearly in Fig. 3.14. The losses of exergy via engine heat transfer and thermal exhaust are found to be as 37.21 kW and 7.818 kW, respectively. Replacement of R134a with R290 as the ERC refrigerant changes the exergy of refrigeration from 0.811 kW to 0.5568 kW, exergy destruction in the boiler from 20.46 kW to 21.29 kW, exergy destruction in the ejector from 3.643 kW to 2.876 kW, exergy losses at the condenser from 1.044 kW to 1.243 kW, respectively. These differences of refrigeration exergy and exergy destruction in

the boiler, ejector, and condenser arises due to the considerable difference of boiling point of two refrigerants.

The breaking of fuel exergy into the exergy destroyed, exergy produced, and losses of exergy via exhaust to environment for the combined cycle of HCCI engine-ARC configuration is displayed in Fig. 3.15. A significantly high exergy of refrigeration is found 2.819 kW compared to less than 1 found in case of ERC. Exergy destruction in the generator is 18.69 kW and in the condenser is 1.18 kW. These figures are different from ERC because of having a considerable difference of boiling points of R134a, R290, and water which are utilized as refrigerants in cycles considered for analysis. The exergy destruction in the evaporator of ARC is 0.105 kW compared to 0.805 Kw in case of R134a ERC. This distinction arises because of the difference of the LiBr-$H_2O$ ARC evaporator temperature above than $0^0$C and can be much less than $0^0$C in case of ERC evaporator. The exergy destruction in the absorber is also found to be considerable 2.115 kW because of the mixing (source of entropy generation) of absorbent and refrigerant in the absorber. Similar to energy distribution, exergy distribution of fuel in the HCCI engine components is also found unaltered after changing the bottoming cycle from ERC to ARC.

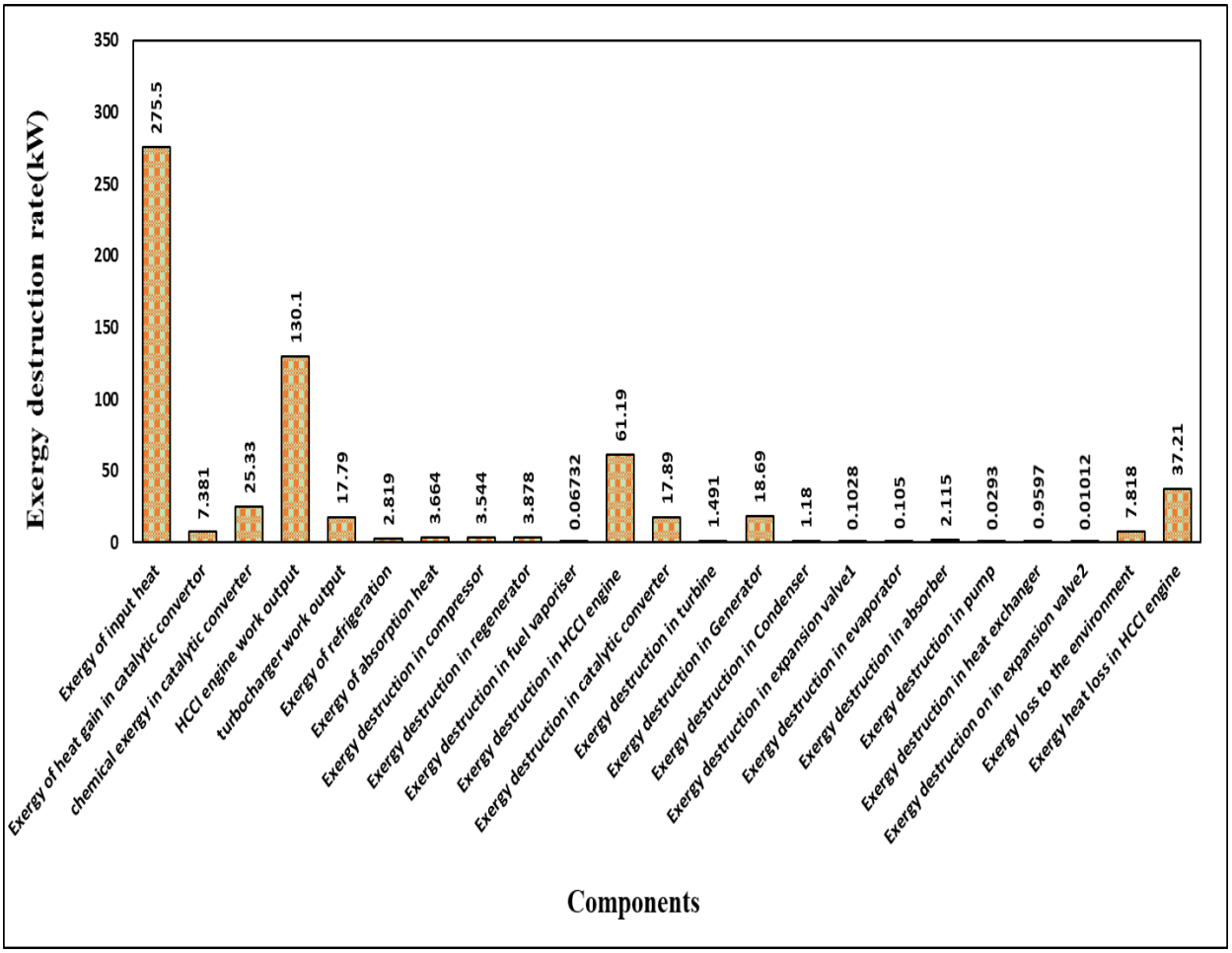


**Fig. 3.15.** Distribution of fuel exergy in the combined cycle (HCCI engine-ARC) configuration

# Chapter 4

# Investigation of a combined refrigeration and air conditioning system based on two-phase ejector driven by exhaust gases of natural gas fueled homogeneous charge compression ignition engine

## 4.1. Introduction

The increasing rate of the global energy consumption for refrigeration and air conditioning is a basic issue that our society has to manage due to the consequent problems, as the greater increase of greenhouse gas emissions and fast depletion of fossil fuel reserves [202]. Commitment to meet out the refrigeration and air conditioning needs in a sustainable manner is a climate change challenge. In this regard, waste energy recovery from prime movers such as; gas turbine, internal combustion engines, and steam power plants creates an appealing opportunity of energy saving and mitigation of carbon footprint [227]. Moreover, development of cooling-power cogeneration system provides an assistance in resolving the concern related to energy crisis and climate change. Producing the refrigeration is more expensive than heating and power generation in majority of applications as it requires refrigeration machine and electricity. Therefore, recovery of waste heat from the engines for the additional generation of power and cooling energy is capable to provide economic benefits [187, 193]

Maintenance of quality through preservation of food products which are transported through road vehicles with comfortable journey requires cooling for refrigeration and air conditioning. In the land transportation vehicles such as diesel engine aboard trucks, approximately two-thirds of the

total energy input is lost as heat rejection to the environment because of the high exhaust gas temperature which usually varies between $400^0$C and $600^0$C [172, 228]. Therefore, development of systems that can convert the engine waste heat directly into cooling in various range of temperatures provide a promising means of effectively meeting the cooling demand of land transportation vehicles. Cooling systems powered by waste heat of internal combustion engines have been widely investigated by many researchers in the recent past. Cooling systems which are often used as bottoming cycles in the internal combustion engine are based on absorption refrigeration which is considered as a cooling technology where the working fluid pair (strong solution) at the expense of thermal energy of the heat source get separated into the absorbent and refrigerant. Finally, the refrigerant takes heat to refrigerate the required thermal load at the evaporator. Most commonly chosen working fluid pairs for absorption refrigeration systems (ARS) are LiBr-$H_2O$ and $NH_3$-$H_2O$ that can provide cooling in different range of temperatures. In the LiBr-$H_2O$ operated ARS, use of water as the refrigerant makes the system un-functional when the evaporator temperature is lower than $0^o$C. For producing the refrigeration below $0^o$C, $NH_3$-$H_2O$ operated ARS is commonly used, and this in general, is the case of industrial refrigeration [229]. However, in the power cycles or internal combustion engines combined with $NH_3$-$H_2O$ operated ARS, a rectifying column is required which results in the reduction of system performance. Moreover, when the high temperature engine exhaust gas is used to drive the absorption refrigeration cycles directly, the serious temperature mismatch between the heat source and the working fluid results in huge exergy destruction [198]. Further, ARS are largely used for exhaust heat recovery applications in industrial and marine applications. It is scarce to have a waste heat recovery from automobile engines using ARS.

The limitations accompanied by absorption refrigeration systems created a need for the search of alternative energy-efficient and sustainable cooling solutions. In this regard, ejector refrigeration cycle (ERC) has recently been emerges as one of the very attractive cooling technology options because it offers better energy efficiency and low cost of installation. Moreover, its operation requires no mechanical power and shows a flexibility in operation with various kind of refrigerants [230. In addition to this, ejectors have been found as compact and easier in maintenance compared to traditional cooling systems [231-235]. In the literature, many studies are reported regarding the application of ejector cooling technology for achieving the processes of sustainable refrigeration. The investigations devoted to the study of ERC driven by the exhaust gases of internal combustion engine are relatively rare. Yilmaz and Aktas [236] investigated the performance of an ejector refrigeration (ER) system driven by the exhaust waste heat of a heavy vehicle engine. In their configuration, refrigerants R134a and R245fa were used for the comparative simulation and their results show that, the performance of the system would be higher if R245fa is preferred rather than R134a with the given operating conditions. Jaruwongwittaya and Chen [214] investigated the feasibility of implementing a two stage ejector cooling system in a bus using water as a working fluid. Their results indicated that the application of two-stage ejector cooling system to replace the vapor compression system for engine waste heat recovery is a suitable alternative and its applications leads to the reduction of fuel consumption, green-house gas reduction as well as resolve the problem of a high condensing temperature of the cooling system in a bus engine. Xia et al. [194] developed a combined power and cooling system for engine waste heat recovery which comprises an organic Rankine cycle (ORC) and an ejector refrigeration cycle (ERC). The system overall performance was evaluated and an optimization was carried out to search the optimal system performance from exergy point of view. Two-phase ejector refrigeration systems have been

largely investigated theoretically and experimentally, and in this regard, following studies are found. Kornhauser [237] presented a study conducted on different working fluids in vapor compression refrigeration system using two-phase ejector. Chaiwongsa and Wongwises [238] investigated the performance of ejector refrigeration cycle which consists of a single evaporator and a refrigerant separator. The effects of exit diameter of nozzle and the throat section of the ejector was ascertained. Pottker et al. [239] performed an experimental investigation on ejector cooling system and carried out the analysis without considering the ejector dimensions. Their analysis reveals that application of R410A refrigerant in the system provide great thermodynamic benefits. A two-phase ejector refrigeration cycle operated on low pressure refrigerants was investigated theoretically and experimentally by Lawrence [240]. A theoretical comparative study on the use of R143a and R1234yf as refrigerants in ejector cooling system was conducted by Lawrence and Elbel [241]. An increase in the COP of 5% and 6%, respectively, was found. Wang and Yu [242] examined the effect of component efficiencies on the performance of two-phase ejector. In their investigation, a new method of calculation for the component efficiencies of ejector was proposed by combining ejector model with the reported data. Zengenhagen and Ziegler [215] presented the assessment of an engine exhaust heat driven jet-ejector cooling system integrated to turbocharged gasoline engines. They determined the energy efficiency and charge air temperature for the use of R134a as the refrigerant in ejector cooling. Unal [216] developed the exhaust heat driven two-phase ejector cooling system for reducing the load and fuel consumption of the engine of passenger bus. The author stated that application of two-phase ejector as an expansion valve can enhance the performance of bus air conditioning system. Zhang et al. [217] developed an exhaust heat recovery unit for the automobile integrating to ERC. They analyzed the performance of ejector cooling system and recommended a suitable range of operating parameters for the

efficient operation of combined system. Above reported investigations proved that two-phase ejector cooling systems has a great potential for the recovery of engine exhaust heat. Siddiqui et al. [243] proposed a novel combined power and cooling system consisting of the ejector refrigeration cycle (ERC) and organic Rankine cycle (ORC) to enhance the overall efficiency of wet-ethanol fueled homogeneous charge compression ignition (HCCI) engine. Their results show that increase in evaporator pressure of ERC is of the great benefit of thermodynamic performance of cogeneration system because its elevation significantly increases the cooling capacity. Yu et al. [244] presented a novel cooling-power cogeneration system consisting of the ORC and ERC for the efficient utilization of low grade waste heat. They optimized the system performance and working selection for the fixed cooling outputs. Their investigations found perfluoropropane as the most suitable working fluid for the proposed system.

Studies carried out on the recovery of thermal exhaust of alternative fueled internal combustion engine reveals that integration of two-phase ejector with the natural gas fueled engine for the simultaneous production refrigeration and air conditioning (for food preservation and cabin cooling) has not to date been reported in the literature. Moreover, proposal and analysis of a two-phase ejector cooling system applied for exhaust heat recovery from the relatively new combustion technology engine that runs on lean air-fuel mixture and produces least harmful emissions while maintaining the higher engine efficiency is very much missing in the literature. Therefore, employment of a shaft power driven two-phase ejector which consists of a hermetic reciprocating compressor, an air cooled condenser, a separator, and two evaporators for combined production of refrigeration and air conditioning and integrated to HCCI engine operated on natural gas has been found worth and novel for current investigation. The development of such a cooling-power cogeneration system satisfy the diverse consumer's demands and is having three fold benefits;

cooling produced by low temperature evaporator will refrigerate a thermal load for food and vaccine preservations and the cooling produced by high temperature evaporator will provide cabin cooling or air conditioning of vehicle, and decrease in exhaust temperature due to waste heat recovery will reduce the thermal pollution. Proposed system is investigated parametrically to study the role of key operating variables such as; equivalence ratio, engine speed, refrigerant condenser temperature, efficiency of ejector nozzle, temperature of refrigeration evaporator, and air conditioning evaporator on the thermal and exergetic efficiencies of combined cycle as well as on the efficiencies of natural gas fueled HCCI engine.

## 4.2. Proposed combined cycle description

Schematic diagram of the combined cycle proposed in this study is displayed in Fig. 4.1. The proposed system comprised of a natural gas-fueled HCCI engine and a two-phase ejector system and the combined cycle generates power and cooling for air-conditioning and refrigeration, simultaneously. The main components of the proposed system are as follows: two compressors, regenerator, fuel vaporizer, HCCI engine, catalytic convertor, turbine, heat exchanger, an air-cooled condenser, an air-conditioner, an ejector, a refrigerator, a separator, and two expansion valves.

Ambient air (1) enters the compressor (C1) where it is compressed to higher pressure (2) and the passes through regenerator (Reg) which increases its temperature (3) and then mixed with natural gas (4) injected into the fuel mixer (FM). In the fuel mixer, compressed air and natural gas mixture forms a homogeneous air-gas mixture (5) and enters to the HCCI engine. This homogeneous mixture and residual gases mixed in the cylinder and engine exhaust gases enter (6) to the catalytic convertor (CC). The unburned hydrocarbon (UHC) and carbon monoxide (CO) combust in the

convertor (CC) which were not burned in the combustion chamber and increases exhaust gas temperature due to heat release. The less harmful gases from the catalytic convertor (CC) enter (7) to the turbine (T) and generates power to drive the compressors (C1 & C2). The exhaust gases from the turbine (T) enter (8) the regenerator (Reg) and exchange heat with the compressed air coming from the compressor (C1) and leaves the system (9).

The compressed air from the compressor (C2) enters the condenser (Cond) (10) where heat is rejected out to the environment. The refrigerant leaves the condenser as saturated liquid at (11) and goes to the air- conditioner (AC), where it evaporates completely to vapor for air-conditioning (13) through the heat exchanger (HX) (11-12) and expansion valve (EV1) (12-13). A heat exchanger (HX) between the expansion valve (EV1) and the condenser (Cond) transfers heat from the saturated liquid leaving the condenser (Cond) to the saturated vapor going into the compressor (C2). The two-phase fluid at the air-conditioner (AC) exit (14) flow into the ejector (Eje) motive nozzle. The high-velocity vapor (14a) entrains secondary fluid from the refrigerator (ref) (18) and mixes with the primary fluid. Stream (14a) and (18a) mixed together in the mixing chamber, resulting in a homogeneous mixture. Pressure increases due to normal shock when mixed fluid enters the constant area section. The mixed fluid (15m) decelerates in the diffuser after the shock. The mixed two-phase fluid from the ejector (Eje) (15) enters the separator (Sep). The saturated liquid fluid at the bottom of the separator (Sep) (16) flows into the refrigerator (ref) to produce desired refrigeration effect (17) through the expansion valve (EV2) and the saturated vapor fluid (19) is heated when it goes through the heat exchanger (HX) and then enters to the compressor (C2) (20).

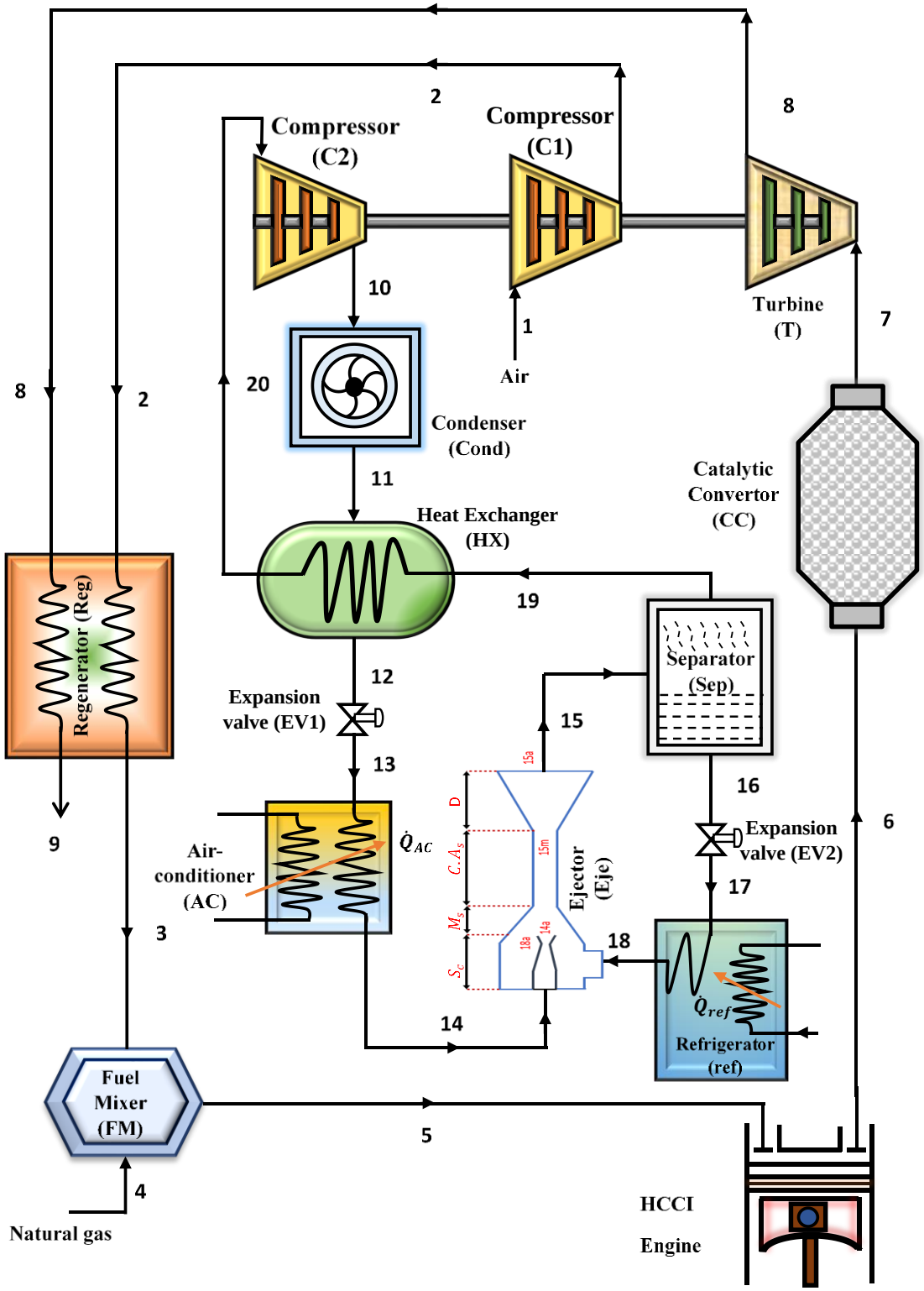


**Fig. 4.1. N**atural gas operated power and cooling combined cycle

## 4.3. Thermodynamic properties evaluation

In the internal combustion engines operated on ideal cycle, air is considered as working fluid for the processes occurring in the engine cylinder. However, the working fluid appears to be a mixture of many gaseous species in the actual engine cycle operation.

Variation of specific heat of gases with temperature is quite considered in the actual cycle operation by ignoring its variation with pressure. The molar specific heat model considered in the current study consisting of the variation of $\bar{C}_p(T)$ with temperature in the range 300K to 3000K are available in the Ref. [195]

$$\bar{C}_p(T) = \bar{R}(a_1 + a_2T + a_3T^2 + a_4T^3 + a_5T^5) \tag{4.1}$$

The relation of specific heat with two most prominent thermodynamic properties such as enthalpy and entropy can be found as [196]

$$\bar{h}_{i\,(T)} = \bar{h}_{\iota(T_0)} + \int_{T_0}^{T} \bar{C}_{p_i}(T)dT \tag{4.2}$$

$$\bar{s}_{i\,(T,p)} = \bar{s}_{i(T_0,p_0)} + \int_{T_0}^{T} \frac{\bar{C}_{p_i}(T)}{T} dT - \bar{R}ln\left(\frac{y_i p}{p_0}\right) \tag{4.3}$$

In the current investigation, flow streams such as exhaust gases, products of combustion, and the air inducted are assumed as gaseous species mixture. Commonly used thermodynamic properties of the mixture can be expressed as [196].

$$\bar{h}_{mix(T)} = \sum_{i=1}^{n} y_i \bar{h}_{i\,(T)}\,; \qquad \bar{s}_{mix(T,P)} = \sum_{i=1}^{n} y_i \bar{s}_{i\,(T,P)}\,; \qquad M_{mix} = \sum_{i=1}^{n} y_i M_i \tag{4.4}$$

The combustion species produce under ideal condition are; water ($H_2O$), carbon di oxide ($CO_2$), and nitrogen ($N_2$) from the air. But for the actual combustion process, engine exhaust gases contain several other compounds along with $H_2O$, $CO_2$ and $N_2$. The combustion of natural gas in the HCCI

engine is assumed to produce the following combustion products as: CO, $H_2O$, $CO_2$, $O_2$, $H_2$, and $N_2$. After considering methane as the main component of natural gas, its combustion with air results in the formulation of the equation which can be expressed as [245]

$$CH_4 + \left(\frac{2}{\emptyset}\right)(O_2 + 3.76N_2) \rightarrow n_1CO_2 + n_2H_2O + n_3N_2 + n_4O_2 + n_5CO + n_6H_2 \quad (4.5)$$

The mole fractions, $n_i$, combustion product species have been computed under the conditions of equilibrium.

Emissions from the HCCI engines such as carbon monoxide and unburned hydrocarbons can undergo the process of further oxidation by using Pd-loaded $SiO_2 - Al_2O_3$ as the oxidizing catalyst. By employing the equations, the composition and temperature of outlet gases can be calculated as [186]

$$\sum_{Product} n_e\left(\bar{h}_f^{\circ} + \Delta\bar{h}\right)_e = \sum_{Reactant} n_i\left(\bar{h}_f^{\circ} + \Delta\bar{h}\right)_i \quad (4.6)$$

### 4.3.1 Turbocharger compressor

After considering the fixed value of polytropic efficiency at a given pressure, the air temperature at the outlet of compressor can be calculated after employing the equation [60],

$$\mathrm{T_2} = \mathrm{T_1}\left(\frac{\mathrm{P_2}}{\mathrm{P_1}}\right)^{\frac{(\gamma-1)}{\gamma\eta_C}} \quad (4.7)$$

Energy balance applies to compressor gives

$$\mathrm{w}_c = \mathrm{h_2} - \mathrm{h_1} \quad (4.8)$$

### 4.3.2 Regenerator

The compressed air is preheated in the regenerator whose performance is evaluated using its effectiveness and it can be shown as

$$\varepsilon_h = \frac{\left[(\dot{m}.c_p)_2(T_3 - T_2)\right]}{\left[(\dot{m}.c_p)_{min}(T_8 - T_2)\right]} \tag{4.9}$$

The assumption, $(\dot{m}.c_p)_2 = (\dot{m}.c_p)_{min}$ is considered to calculate the temperature, $T_3$, the temperature of air at the outlet of regenerator is determined after applying the equations given below

$$T_3 = T_8\varepsilon_h + T_2(1 - \varepsilon_h) \tag{4.10}$$

$$H_3 - H_2 = H_8 - H_9 \rightarrow H_9 = H_8 - H_3 + H_2 \tag{4.11}$$

### 4.3.3 Fuel-air mixer (FM)

The temperature at the outlet of fuel-air is determined after applying

$$H_5 = H_3 + H_4 \tag{4.12}$$

### 4.3.4 HCCI engine

The gaseous mixture from fuel-air mixer is delivered to HCCI engine and its thermodynamic cycle is given in Fig. 4.2. The relation applied to compute the temperature of the mixture for intake process $(i - 1')$ can be expressed as [245].

$$T_{1'} = \frac{T_i(1-f)}{1 - \frac{1}{(n.r_c)\left[\frac{p_e}{p_i} + (n-1)\right]}} \tag{4.13}$$

Where n is the average specific heat capacity ratio which was taken as 1.35 for lean combustion, f was assumed as 0.03 and $p_i/p_e$ = 1.4 [246].

The pressure remains unchanged:

$$P_{1'} = \mathrm{P}_i \tag{4.14}$$

The mixture following the process of compression $(1' - 2')$ and combustion, and properties at 2' can be determined.

Properties after completing the process of heat addition (2'-3') are computed by

$$\dot{Q}_{in} = \dot{Q}_{fuel} - \dot{Q}_l \tag{4.15}$$

Where $\dot{Q}_{fuel}$ is given as

$$\dot{Q}_{fuel} = \eta_{comb} \dot{m}_{fuel} Q_{LHV} \tag{4.16}$$

The losses inside the combustion chamber are evaluated by considering the combustion efficiency [247]

$$\eta_{cc} = 100 - \mathrm{V}_{\%} - (1.26 + 0.25\mathrm{C}_{e2} + 0.4\mathrm{C}_{e2}^2) + (\emptyset - 0.2486)8.1 \tag{4.17}$$

Where $\mathrm{C}_{e2} = Ln(\mathrm{V}_{\%})/Ln(2)$

$\dot{Q}_l$ (heat losses from cylinder walls) is determined using:

$$\dot{Q}_l = h_c * 10^{-3}(A_{ch} + A_{cyl})(T_{avr} - T_w)/(2 * \dot{m}_a) \tag{4.18}$$

Where, $h_c$ is the heat transfer coefficient and given as [248].

$$h_c = (3.26L^{-0.2} p^{0.8} \mathrm{T}_{avr}^{-0.73} \omega^{0.8}) \tag{4.19}$$

Where,$\omega = 2.28\bar{s}_p + (3.24 * 10^{-3}/6)(V_d T_{ref}(p - p_{mot})/(p_{ref} V_{ref}))$ (4.20)

Where $p_{mot}$ is the pressure at motored conditions [25]:

$$p_{mot} = p_{ref}(V_{ref}/V)^n \quad (4.21)$$

The parameters from exit of expansion process (3'-4') are determined similar to the method adopted for the compression stroke (1'-2').

The parameters at the outlet of blowdown process are computed using:

$$p_{5'} = p_e \quad (4.22)$$

$$T_{5'} = T_{4'}(p_{4'}/p_e)^{(1-n)/n} \quad (4.23)$$

$$v_{5'} = \frac{\bar{R}}{M_{mix}} * \frac{T_{5'}}{p_{5'}} \quad (4.24)$$

Finally, temperature and pressure of gases leaving the exhaust process (5'-6') are given by:

$$T_e = T_{5'} \quad (4.25)$$

$$p_6 = p_{5'} = p_e \quad (4.26)$$

The heat released by friction is computed by employing the relation [249]

$$\dot{Q}_f = \dot{m}_t \left(183 + 2.3\left(\left(\frac{N}{60}\right) - N_o\right)V_D\right) \quad (4.27)$$

Where $N_o = 30\sqrt{3/(1000V_d)}$

The heat accompanied by exhaust gases can be calculated after using:

$$\dot{Q}_{out} = \dot{m}_t[(h_4 - r.T_4) - (h_5 - r.T_5)] \quad (4.28)$$

The net power produced by HCCI engine:

$$\dot{W}_{net} = \dot{Q}_{in} - \dot{Q}_{out} - \dot{Q}_f \quad (4.29)$$

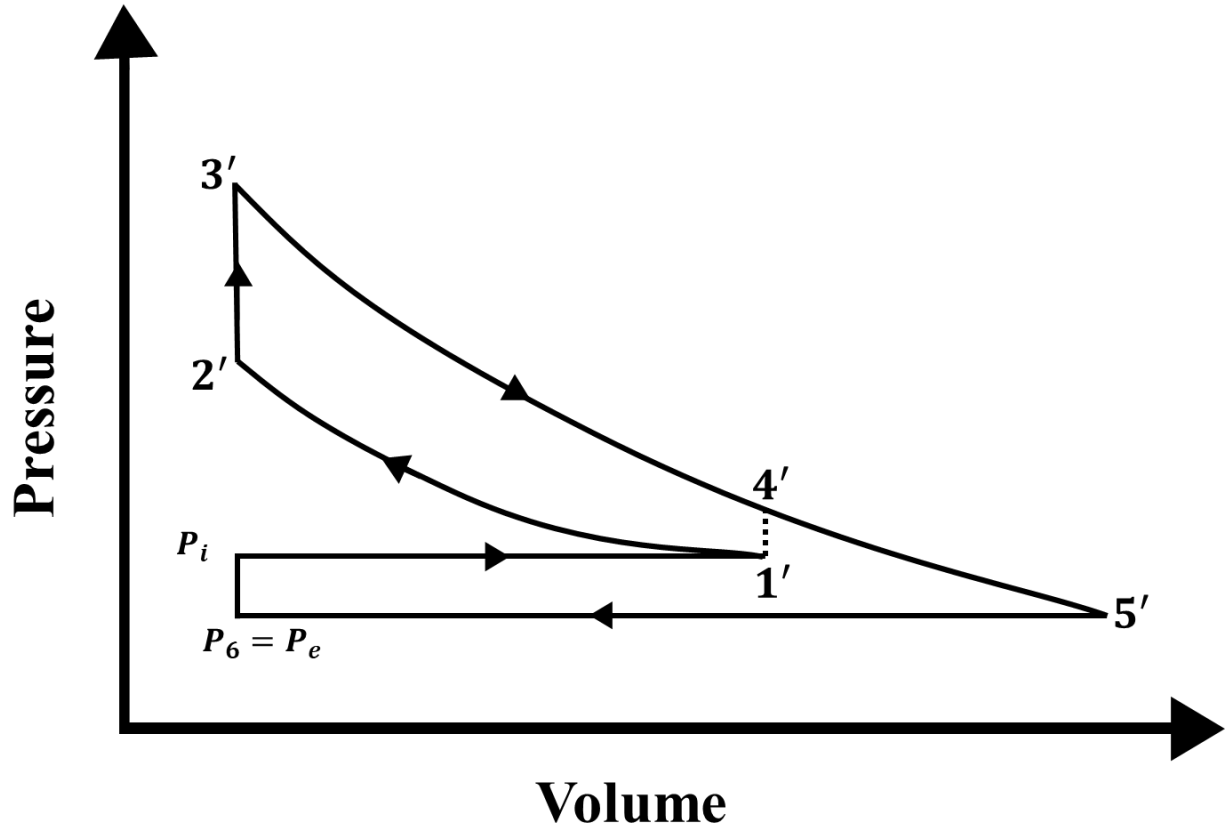


**Fig. 4.2**. PV diagram

## 4.4. Energy and exergy analyses

Based on the specifications of the proposed system described above, theory leading to simultaneous applications of first and second laws of thermodynamics is employed to carry out the analysis which reveals the insights in performance of the proposed combined cycle that simultaneously generate power and cooling energy for refrigeration and air conditioning [198, 245].

The law of conservation of mass and the principle of energy balance applied to thermodynamic system operating under steady state conditions entails the following equations.

$$\Sigma \dot{m}_i - \Sigma \dot{m}_o = 0 \tag{4.30}$$

$$\Sigma\dot{Q} - \Sigma\dot{W} + \Sigma\dot{m}_i h_i - \Sigma\dot{m}_o h_o = 0 \quad (4.31)$$

Application of thermodynamic theory related to analysis of natural gas fueled HCCI engine [245] and the two-phase ejector cycle described by Wang and Yu [242], the equations leading to energy balance in the components of the natural gas fueled HCCI engine based refrigeration and air-conditioning system were derived and are reported in Table 4.1.

**Table 4.1** Component wise energy balance equations for natural gas operated HCCI engine based refrigeration and air-conditioning system [60, 241, 245]

| **Component** | **Balance Equations** |
|---|---|
| Compressor (C1) | $\dot{W}_{C1} = \dot{m}_a(h_2 - h_1)$ |
| Regenerator (Reg) | $\dot{m}_a\,(h_3 - h_2) = \dot{m}_{exh}\,(h_8 - h_9)$ |
| Fuel mixer (FM) | $\dot{m}_a\,h_3 + \dot{m}_f h_4 = (\dot{m}_a\, + \dot{m}_f)h_5$ |
| HCCI engine (Compression) process,1´- 2´ | $\left(\dot{m}_a\, + \dot{m}_f + \dot{m}_{rg}\right)(h_{2'} - h_{1'}) = \dot{W}_{comp} - \dot{Q}_{surr}$ |
| Heat addition process, 2´- 3´ | $\left(\dot{m}_a\, + \dot{m}_f + \dot{m}_{rg}\right)(h_{3'} - h_{2'}) = \dot{Q}_H$ |
| Expansion process,3´- 4´ | $\left(\dot{m}_a\, + \dot{m}_f + \dot{m}_{rg}\right)(h_{3'} - h_{4'}) = \dot{W}_{exp} + \dot{Q}_{surr}$ |
| Blowdown Process, 4´-5´ | $\dot{m}_{exh}\,h_{4'} = \dot{m}_{exh}\,h_{5'} + \dot{Q}_{surr}$ |
| Catalytic convertor (CC) | $\sum_{Product} n_e\left(\bar{h}_f^{\circ} + \Delta\bar{h}\right)_e = \sum_{Reactant} n_i\left(\bar{h}_f^{\circ} + \Delta\bar{h}\right)_i$ |
| Turbine (T) | $\dot{W}_{T1} = \dot{m}_{exh}\,(h_7 - h_8)$ |
| Compressor (C2) | $\dot{W}_{C2} = \dot{m}_{10}(h_{10} - h_{20})$ |
| Condenser (Cond) | $\dot{Q}_{Cond} = \dot{m}_{10}(\,h_{10} - \,h_{11})$ |

| | |
|---|---|
| Heat exchanger (HX) | $\dot{Q}_{HX} = \dot{m}_{11}(h_{11} - h_{12}) = \dot{m}_{20}(h_{20} - h_{19})$ |
| Expansion valve (EV1) | $h_{12} = h_{13}$ |
| Air-conditioner (AC) | $\dot{Q}_{AC} = \dot{m}_{14}(h_{14} - h_{13})$ |
| Ejector (Eje) | $\dot{m}_{14}h_{14} + \dot{m}_{18}h_{18} = \dot{m}_{15}h_{15}$ |
| Separator (Sep) | $\dot{m}_{16}h_{16} + \dot{m}_{19}h_{19} = \dot{m}_{15}h_{15}$ |
| Expansion valve (EV2) | $h_{16} = h_{17}$ |
| Refrigerator (ref) | $\dot{Q}_{ref} = \dot{m}_{18}(h_{18} - h_{17})$ |

Inefficiencies in the system can be evaluated through the incorporation of exergy into the analysis. Further, inclusion of exergy leads to the determination of quality and quantity of energy transformation during the change of thermodynamic state. The general expression for the exergy of flowing stream operates under the condition of steady-state and ignoring the changes in kinetic and potential energies can be presented as

$$\dot{E}_{x,D} = \sum\left(1 - \frac{T_0}{T_j}\right)\dot{Q}_{CV} - \dot{W}_{CV} + \sum \dot{m}_i e_{x,i} - \sum \dot{m}_e e_{x,e} \quad (4.32)$$

$\dot{E}_{x,D}$ is the exergy destruction rate and $e_x$ is the flow exergy of the stream per unit mass and consist of: physical, chemical, potential and kinetic and is given by the following expression

$$ex = ex^k + ex^p + ex^{ph} + ex^{ch} \quad (4.33)$$

The physical exergy is given by

$$ex^{ph} = (h - h_o) - T_o(s - s_o) \quad (4.34)$$

Chemical exergy appears due to the deviations in chemical composition of the substance from the species present in the environment [245]:

$$ex^{ch} = \sum x_i(\mu_i^* - \mu_{i,o}) = -\Delta g_i^o + \sum \bar{R} T_o x_i ln\left(\frac{p}{p_{ref}}\right) \quad (4.35)$$

The equation which can estimate the destruction of exergy in the components of the proposed combined cycle are formulated in Table 4.2.

**Table 4.2** Component wise exergy balance equations for natural gas operated HCCI engine based refrigeration and air-conditioning system [186, 241, 242, 245]

| **Component** | **Balance Equations** |
|---|---|
| Compressor (C1) | $\dot{E}_{x,D,C1} = \dot{m}_1(e_{x,1} - e_{x,2}) + \dot{W}_{C1}$ |
| Regenerator (Reg) | $\dot{E}_{x,D,Reg} = \dot{m}_2(e_{x,2} - e_{x,3}) + \dot{m}_8(e_{x,8} - e_{x,9})$ |
| Fuel mixer (FM) | $\dot{E}_{x,D,FM} = \dot{m}_3 e_{x,3} + \dot{m}_4 e_{x,4} - \dot{m}_5 e_{x,5}$ |
| HCCI engine (Compression) process,1´-2´ | $\dot{E}_{x,D,comp} = \dot{m}_5(e_{x,1'} - e_{x,2'}) + \dot{W}_{comp} - \dot{Q}_{surr}\left(1 - \frac{T_0}{T}\right)$ |
| Heat addition process, 2´-3´ | $\dot{E}_{x,D,Heat\ addition} = \dot{m}_5(e_{x,2'} - e_{x,3'}) + \dot{Q}_H\left(1 - \frac{T_0}{T_H}\right)$ |
| Expansion process, 3´- 4´ | $\dot{E}_{x,D,exp} = \dot{m}_5(e_{x,3'} - e_{x,4'}) - \dot{W}_{exp} - \dot{Q}_{surr}\left(1 - \frac{T_0}{T}\right)$ |
| Blowdown Process, 4´-5´ | $\dot{E}_{x,D,exh\ \&\ blowdown} = \dot{m}_5(e_{x,4'} - e_{x,5'}) - \dot{Q}_{surr}\left(1 - \frac{T_0}{T}\right)$ |
| Catalytic convertor (CC) | $\dot{E}_{x,D,CC} = \dot{m}_6(e_{x,6}^{ph} - e_{x,7}^{ph} + e_{x,cat}^{ch})$ |
| Turbine (T) | $\dot{E}_{x,D,T} = \dot{m}_7(e_{x,7} - e_{x,8}) - \dot{W}_T$ |
| Compressor (C2) | $\dot{E}_{x,D,C1} = \dot{m}_1(e_{x,20} - e_{x,10}) + \dot{W}_{C2}$ |

| | |
|---|---|
| Condenser (Cond) | $\dot{E}_{x,D,Cond} = \dot{m}_{10}(e_{x,10} - e_{x,11}) - \dot{Q}_{Cond}\left(1 - \frac{T_0}{T_{Cond}}\right)$ |
| Heat Exchanger (HX) | $\dot{E}_{x,D,HX} = \dot{m}_{11}(e_{x,11} - e_{x,12}) + \dot{m}_{20}(e_{x,19} - e_{x,20})$ |
| Expansion valve (EV1) | $\dot{E}_{x,D,EV1} = \dot{m}_{12}(e_{x,12} - e_{x,13})$ |
| Air-conditioner (AC) | $\dot{E}_{x,D,AC} = \dot{m}_{13}(e_{x,13} - e_{x,14}) - \dot{Q}_{AC}\left(\frac{T_0}{T_{AC}} - 1\right)$ |
| Ejector (Eje) | $\dot{E}_{x,D,Eje} = \dot{m}_{14}e_{x,14} + \dot{m}_{18}e_{x,18} - \dot{m}_{15}e_{x,15}$ |
| Separator (Sep) | $\dot{E}_{x,D,Sep} = \dot{m}_{15}e_{x,15} - \dot{m}_{16}e_{x,16} - \dot{m}_{19}e_{x,19}$ |
| Expansion valve (EV2) | $\dot{E}_{x,D,EV2} = \dot{m}_{16}(e_{x,16} - e_{x,17})$ |
| Refrigerator (ref) | $\dot{E}_{x,D,ref} = \dot{m}_{17}(e_{x,17} - e_{x,18}) - \dot{Q}_{ref}\left(\frac{T_0}{T_{ref}} - 1\right)$ |

## 4.5. Criteria for the overall performance evaluation of the cycle

The thermal efficiency of the proposed system may be determined by applying first law and it can be presented as:

$$\eta_{th,comb} = \frac{\dot{W}_{net+}\ \dot{Q}_{AC} + \dot{Q}_{ref}}{\dot{m}_{f\,\mathrm{QLHV}}\eta_{cc}} \tag{4.36}$$

where, $\dot{W}_{net}$ is the net power produced by HCCI engine, $\dot{m}_f$ is fuel flow rate, $Q_{LHV}$ is the fuel heating value of fuel (natural gas), and $\eta_{cc}$ is the combustion efficiency. $\dot{Q}_{ref}$ and $\dot{Q}_{AC}$ are the cooling capacities of the refrigeration evaporator and air-conditioning evaporator, respectively, and the expression for their evaluation are presented in Table 4.2.

Efficiency based on exergy can be presented as

$$\eta_{ex,com} = \frac{\dot{W}_{net} + \dot{E}_{x,AC} + \dot{E}_{x,ref}}{\dot{m}_f\, ex^{ch}\, \eta_{cc}} \tag{4.37}$$

where, $\dot{E}_{x,AC}$ and $\dot{E}_{x,ref}$ are exergy accompanied $\dot{Q}_{AC}$ and $\dot{Q}_{ref}$ respectively, and are given by

$$\dot{E}_{x,AC} = \dot{Q}_{AC}\left(\frac{T_0 - T_{AC}}{T_{AC}}\right) \tag{4.38}$$

$$\dot{E}_{x,ref} = \dot{Q}_{ref}\left(\frac{T_0 - T_{ref}}{T_{ref}}\right) \tag{4.39}$$

Where, $T_{ref}, T_{AC}, T_0$ are the refrigeration evaporator temperature, air-conditioning evaporator temperature, and ambient temperature, respectively, and $ex^{ch}$ is the chemical exergy of fuel.

Engineering Equation Solver (EES) and REFPROP V 9.1 was employed to evaluate the combined cycle performance [199, 200].

Combined cycle consisting of an HCCI engine and the refrigeration, and air -conditioning evaporators, following assumptions were taken to develop the thermodynamic model [241, 242, 245]:

- In the duct and heat exchanger, pressure losses are neglected.
- Engine speed was assumed to vary from 1400-2200 rpm.
- The residual gas fraction was considered to be lower because of the elevated compression ratio (f = 0.03).
- All processes are assumed to be of steady state conditions.
- No consideration of pressure drop in the pipes.
- For the components of two-phase ejector cooling cycle, only physical exergy of the working fluid is considered in the analysis.

The chemical exergy of fuel can be expressed as

$$e_{fuel}^{ch} = -\Delta g + \bar{R}\mathrm{T}_0\left\{x\mathrm{O}_2 ln\frac{P_{\mathrm{O}_2}^{00}}{P^0} + y\mathrm{H}_2 O ln\frac{P_{H_2O}^{00}}{P^0} - \sum_K \mathrm{x}_k ln\frac{P_k^{00}}{P^0}\right\} \tag{4.40}$$

The symbols appeared in above equation are defined in detail in the Ref. [243].

Description of the equations employed to model the components of the two-phase ejector which is considered in the proposed configuration is formulated in Ref. [242].

**Table 4.3** Characteristics of Refrigerants

| **Refrigerant** | **R717** | **R290** | **R600a** |
|---|---|---|---|
| **Chemical Formula** | $NH_3$ | $C_3H_8$ | $C_4H_{10}$ |
| **Normal boiling point (ºC)** | -33.35 | -42.2 | -12 |
| **Critical pressure (kPa)** | 11277 | 4247 | 3640 |
| **Critical temperature (ºC)** | 132.4 | 96.7 | 134.7 |
| **Triple point Temperature (ºC)** | -77.5 | -187.1 | -159.6 |
| **Molecular Weight (kg/kmol)** | 17.03 | 44.1 | 58.12 |
| **Safety class** | B2 | A3 | A3 |
| **GWP (100 years)** | 0 | <3 | <3 |
| **ODP** | 0 | 0 | 0 |

## 4.6. Results and discussion

The natural gas fueled HCCI engine integrated with the two-phase ejector cooling cycle is investigated and explored parametrically. R717, R290, and R600a were employed as refrigerant in the two-phase ejector. Properties of these refrigerants are presented in Table 4.3. The effects of changing the equivalence ratio, engine speed, refrigerant condenser temperature, efficiency of ejector nozzle, refrigeration evaporator temperature, and air conditioning evaporator temperature is investigated on the performance of proposed system. Properties utilized in the study of HCCI

engine based combined cycle for its base line operation are shown in Table 4.4 and they are in line with the reported values of the literature.

**Table 4.4** Input data used for the computation of results of the natural gas operated HCCI engine based refrigeration and air-conditioning system

| | |
|---|---|
| Environmental temperature ($T_0$) (℃) | 30 |
| Environmental pressure ($P_0$) (kPa) | 101.325 |
| Effectiveness of regenerator | 0.78 |
| Turbocharger efficiency (%) | 80 |
| Compression ratio of engine | 16:1 |
| Catalytic converter | Oxidizing type catalyst, Pd-loaded $SiO_2$–$Al_2O_3$ |
| Volume of displacement per cylinder | 2400 $cm^3$ |
| Diameter of cylinder | 13.7 cm |
| Stroke | 16.5 cm |
| Connecting rod length | 26.2 cm |
| Fraction of residual gases | 0.03 |
| Speed of engine | 1400 - 2200 rpm |
| Engine volumetric efficiency (%) | 100 |
| Combustion process in HCCI engine | Controlling the bulk auto ignition mechanism using chemical kinetics |
| Equivalence ratio | 0.3-0.9 |
| Condenser Temperature (℃) | 30-40 |
| Effectiveness of heat exchanger | 0.8 |
| AC evaporator Temperature (℃) | 15-25 |
| Refrigeration evaporator Temperature(℃) | (-15) - (-25) |
| Nozzle efficiency (%) | 85-95 |
| Mixing chamber efficiency (%) | 90 |
| Diffuser efficiency (%) | 85 |

In Fig. 4.3, impact of varying the equivalence ratio on the thermal efficiency of combined cycle is observed for the use of three different refrigerants in the two-phase ejector. The energy supplied to the engine is determined by the equivalence ratio. Increase in equivalence ratio results in the greater release of energy which elevates the in-cylinder pressure and temperature and this in turn increase the power generated by the engine from 129 kW to 135.8 kW when an equivalence ratio is promoted from 0.3 to 0.9. Further, any increment in equivalence ratio leads to the elevation of temperature of catalytic convertor exhaust which expanded in the turbine to generate power in order to drive the compressors employed in the combined cycle. The power supplied to drive the compressor of bottoming cooling cycle ($W_{C2}$) is raised from 15.69 kW to 16.57 kW when the equivalence ratio is increased from 0.3 to 0.9. This in turn increases the refrigeration capacity $Q_{ref}$ from 37.43 kW to 39.52 kW and the cooling capacity of air conditioner $Q_{AC}$ from 9.91 kW to 10.47 kW. Enhancement in the performance of HCCI engine along with the simultaneous increase in the output of two-phase ejector cooling cycle results in the significant increase of the efficiency of combined cycle. Variation of equivalence ratio from 0.3 to 0.9 causes an increase of thermal efficiency of combined cycle from 60.05% to 63.26% when R600a is the refrigerant and from 57.87% to 60.89% when R717 is employed as the refrigerant, and for the application of R290 as the refrigerant the efficiency rises from 57.67% to 60.73%. This deviation is observed due to the fact that the mass flow rate of refrigerant enters the evaporator is found highest in the R600a and lowest in R717 and hence the rate of refrigeration produced by R600a operated bottoming cycle is significantly higher due to which the thermal of the cycle is also higher. In case of ammonia (R717), the mass flow rate of refrigerant is less but the enthalpy of vaporization is found to be greater. On the other hand, in case of propane (R290), the mass flow rate is little higher but enthalpy of vaporization is less. Since the enthalpy of vaporization dominates over the mass flow

rate, therefore, the thermal efficiency of R717 operated combined cycle is slightly higher than R290 operated cycle.

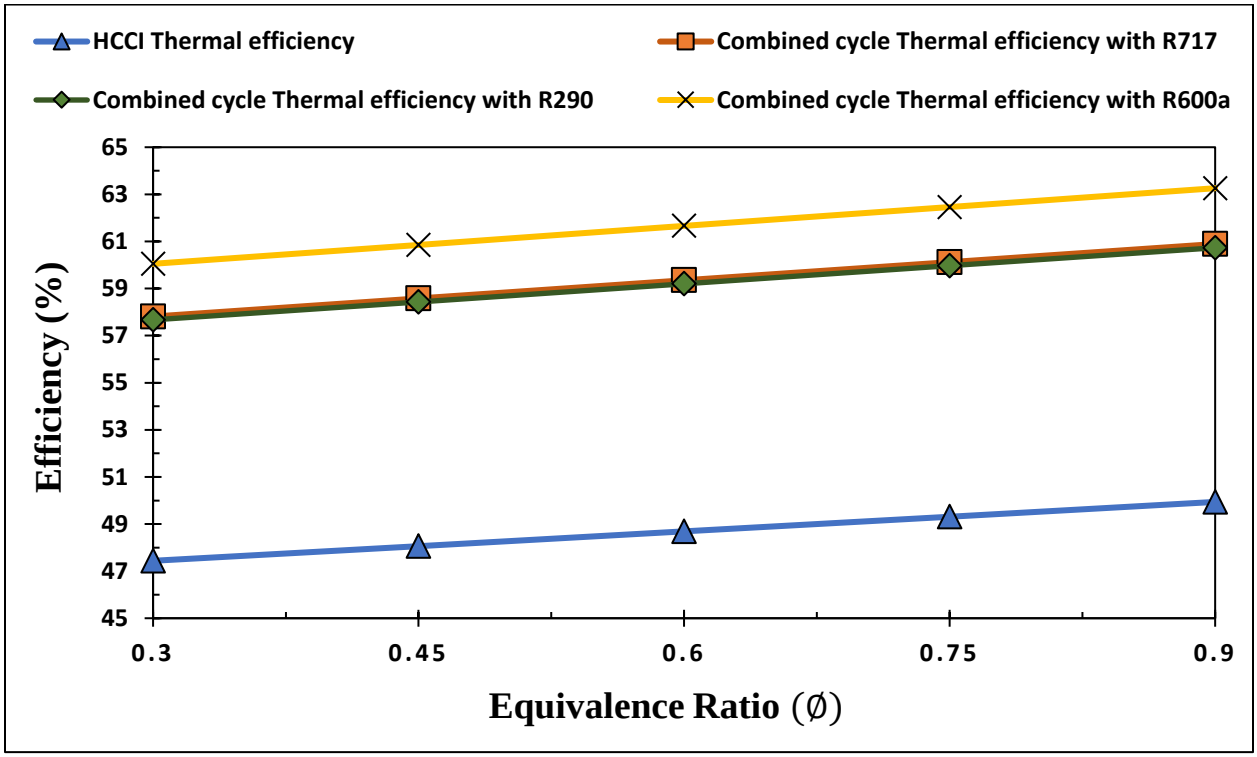


**Fig. 4.3.** Effect of equivalence ratio on the thermal efficiency of HCCI engine and combined cycle

Since exergy efficiency pertaining to HCCI engine is defined as the ratio of power exergy to exergy of fuel supplied, therefore, exergy efficiency is lower than the corresponding thermal efficiency of HCCI engine because fuel exergy is found larger than the fuel energy. Change in equivalence ratio from 0.3 to 0.9 entails an increase in the exergy efficiency of HCCI engine from 40.15% to 42.12% while its thermal efficiency increased from 47.44% to 49.94% as shown in Fig. 4.4. It is interesting to see the exergy efficiency of combined cycle (power and cooling) is lower than the exergy efficiency of HCCI engine. This is because in the proposed configuration the net power output of HCCI engine alone is the HCCI power plus the net power output of the turbocharger ($W_T$-$W_{C1}$). In the absence of the bottoming cooling cycle, the net power of

turbocharger will be added to engine power and hence the net power output of HCCI will increase. In case of the employment of bottoming cooling cycle, the net power of turbocharger will be utilized to drive the cooling cycle whose evaporators are producing the exergy of refrigeration and exergy of air conditioning but these exergies are considerably less than turbocharger net output.

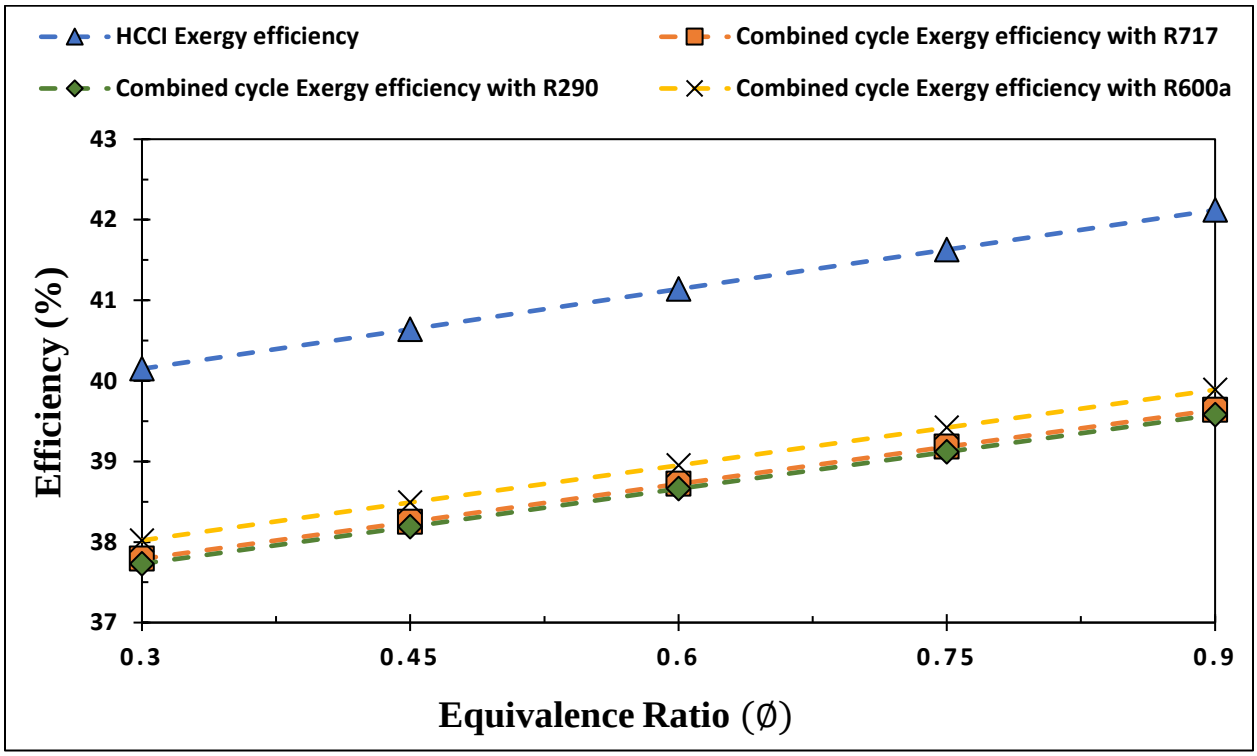


**Fig. 4.4.** Effect of equivalence ratio on the exergy efficiency of HCCI engine and combined cycle

Figs. 4.5 and 4.6 shows the impact of change in engine speed on the performance of HCCI engine and combined cycle, and both are found to be largely dependent on engine speed. This is because at higher engine speed fuel-air mixing is improved and the charge-flow intensity is increased. Moreover, the increase in engine speed decreases the loss of heat to cylinder wall and loss in exhaust gases. Due to these factors, the thermal efficiency of HCCI engine increase as engine speed increases (Fig. 4.5). Since the exergy accompanied by the loss of heat to cylinder wall and the engine exhaust gases are also reduced with the engine speed, therefore, its exergy efficiency

also increases. The thermal efficiency of combined cycle is higher than the exergy efficiency of HCCI engine because of the reasons explained for the trends obtained in Fig. 4.3. In addition, Fig. 4.5 shows that thermal efficiency of combined cycle increases because heat supplied to the combined cycle decreases due to reduced heat losses at higher engine speed. Since the exergy associated with heat input also decrease as the engine speed increases which results in increase in the exergy efficiency of the combined cycle as depicted in Fig. 4.6.

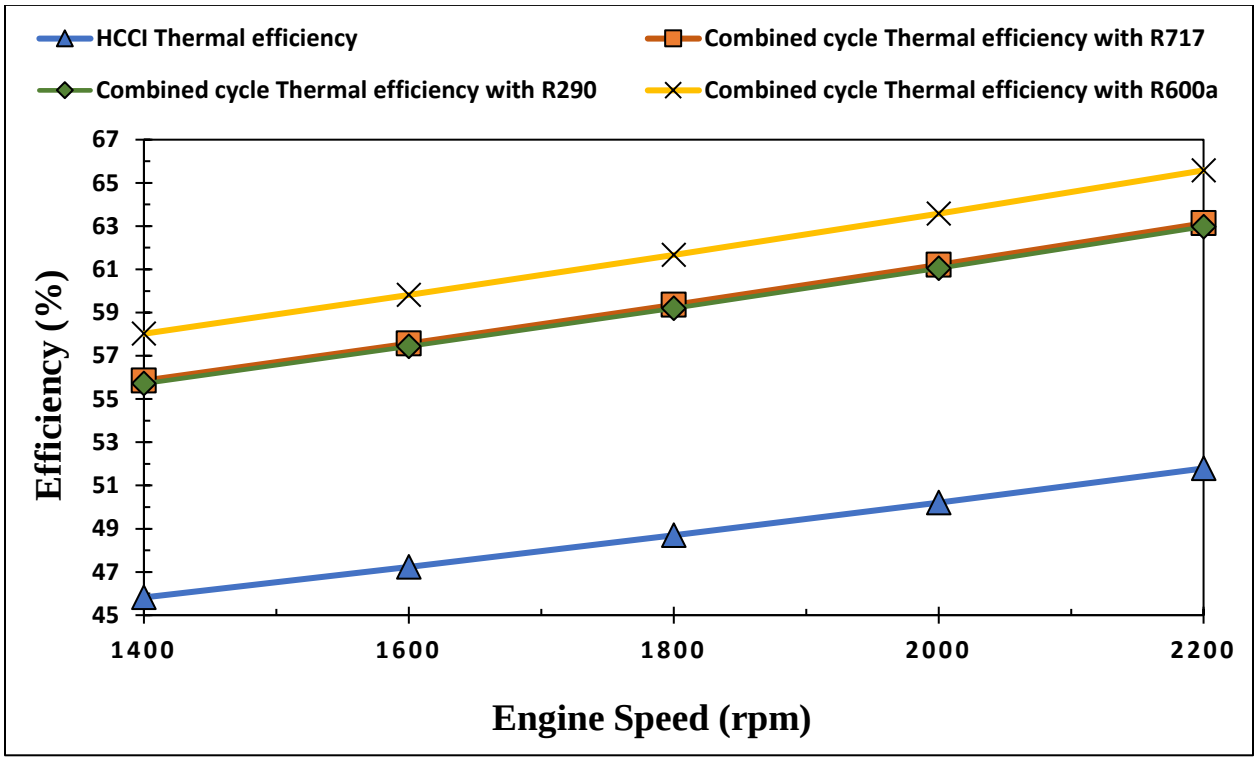


**Fig. 4.5** Effect of engine speed on the thermal efficiency of HCCI engine and the combined cycle

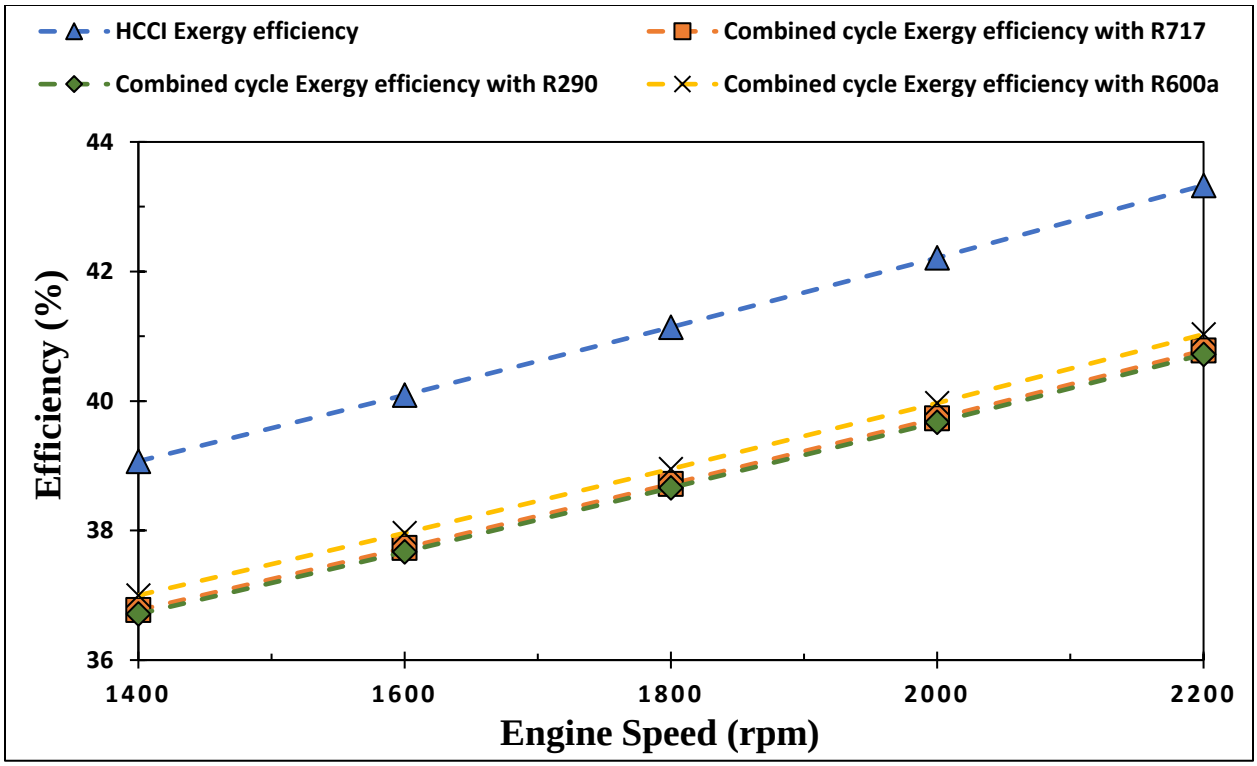


**Fig. 4.6.** Effect of engine speed on the exergy efficiency of HCCI engine and the combined cycle

Fig. 4.7 shows the effect of change in the AC evaporator temperature ($T_{AC}$) on the thermal and exergy efficiencies. The temperature of AC evaporator is irrelevant to net power output of HCCI engine but it has an impact on the cooling capacity of AC evaporator ($Q_{AC}$) and also on the cooling capacity of the refrigeration evaporator ($Q_{ref}$) of the bottoming cycle. As $T_{AC}$ increases, the thermal efficiency of the combined cycle goes up in case of the use of R600a and R717 and in case of R290 applications as working fluid, and it shows a downward trend. This is because in case of all three refrigerants, $Q_{AC}$ increases with the increase of $T_{AC}$. Further, increase in $T_{AC}$ raises the enthalpy of refrigerant enter the ejector which result in the increase of its velocity at the nozzle exit, causing to extract more fluid from the refrigerant evaporator which results in the rise of $Q_{ref}$ in case of R717 and R600a fluids while in case of R290 applications, a little decrement in $Q_{ref}$ is observed. Since the contribution of $Q_{AC}$ and $Q_{ref}$ towards the total energetic performance of the combined

cycle is quite small compared to net power output of the HCCI engine, therefore, a considerable increase in $T_{AC}$ is resulting in the insignificant variation of the thermal efficiency of combined cycle. The exergy efficiency of the combined cycle is lower than its thermal efficiency, because exergy associated with $Q_{AC}$ and $Q_{ref}$ is significantly less than the magnitudes of $Q_{AC}$ and $Q_{ref.}$ The variation is quite insignificant because in case of R717 and R600a fluids $Q_{AC}$ decreases while $Q_{ref}$ increases and in case of R290 applications both $Q_{AC}$ and $Q_{ref}$ are found to be decreasing with the increase of $T_{AC}$.

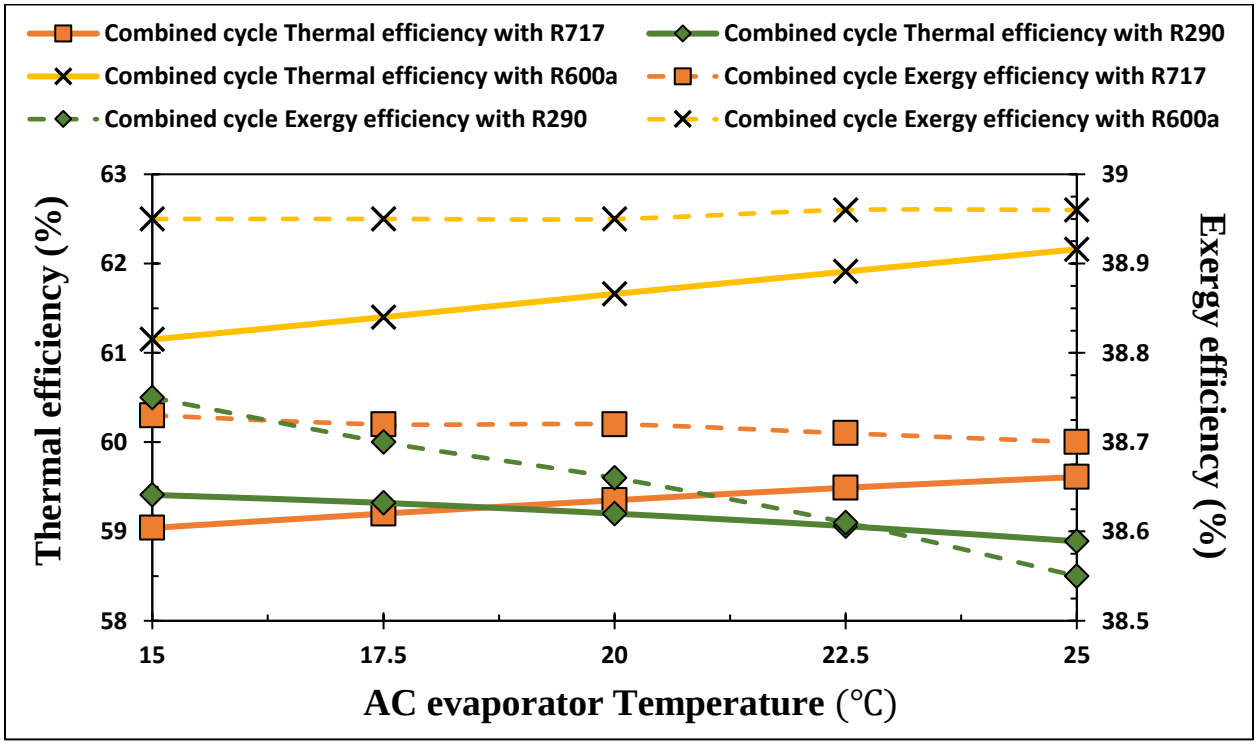


**Fig. 4.7.** Effect of AC evaporator temperature on the thermal and exergy efficiencies of combined cycle

Fig. 4.8 illustrates the effect of change of refrigeration evaporator temperature ($T_{ref}$) on the thermal and exergy efficiencies of the combined cycle. The $T_{ref}$ is unrelated to HCCI engine power output. Thus, the engine power output and the power exergy are remained unchanged. An increase in $T_{ref}$

increases the refrigeration capacity $Q_{ref}$ due to which the energetic outcome of the combined cycle increased and hence its thermal efficiency increases. The decrement in the exergy efficiency of the cycle is so small because the rate of decrease in the exergy of refrigeration reduces with the rise of refrigeration temperature. It is seen as $T_{ref}$ increases the thermal efficiency increases from 60.04% to 63.52% for R600a operated cycle and it is increased from 57.58% to 61.07% for R717 operated cycle when $T_{ref}$ rises from $-25^0$C to $-15^0$C.

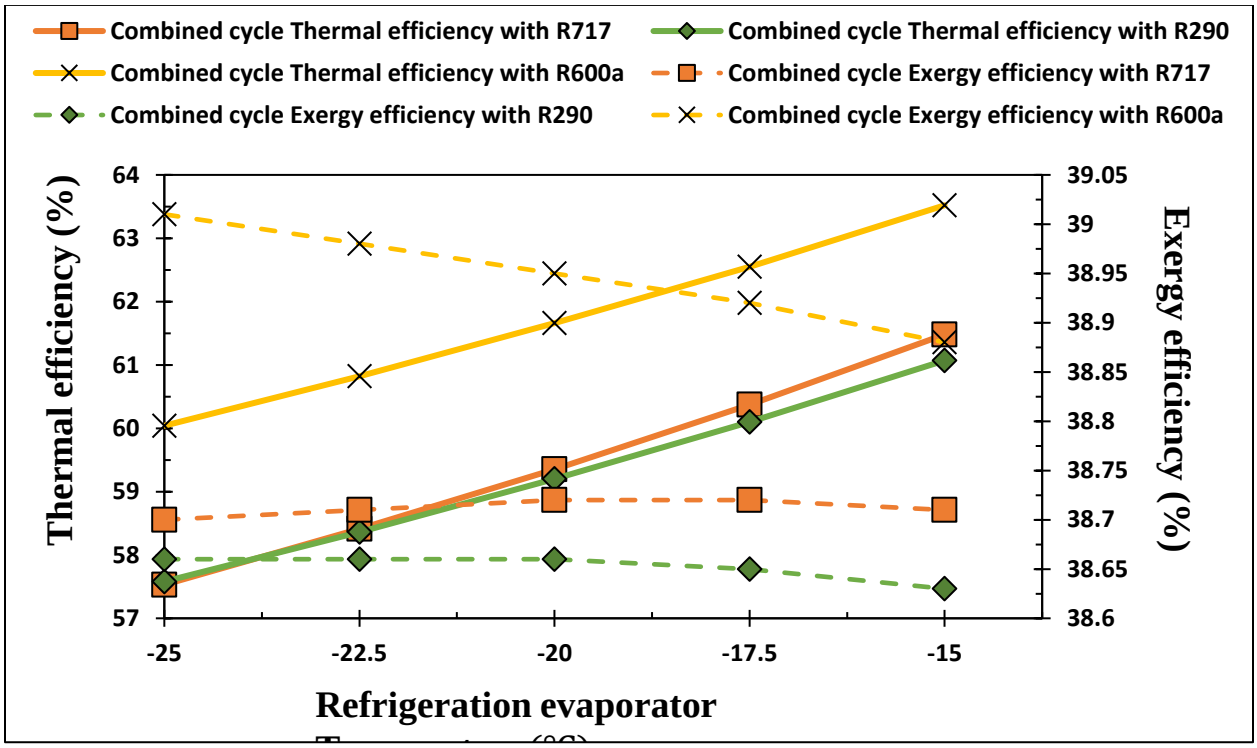


**Fig. 4.8.** Effect of refrigeration evaporator temperature on the thermal and exergy efficiencies of combined cycle

As depicted in Fig. 4.9, thermal efficiency of combined cycle declines markedly with growing $T_{cond.}$ The condenser temperature is irrelevant to net power output of the engine, so the turbine and compressors power remain unchanged. For greater values of $T_{cond}$, large enthalpy difference across the compressor is determined. For the fixed compressor power, lower mass flow rate of refrigerant enters the AC evaporator at state (13) which reduces the cooling capacity. Reduced mass flow rate

of primary stream at state (14) causes the corresponding lowering of secondary fluid flow rate and consequent drop in cooling capacity of refrigeration evaporator. Simultaneous reduction in the cooling capacity of AC evaporator and refrigeration evaporator causes combined cycle efficiency to decrease considerably with the rise of condenser temperature. Since combined cycle thermal efficiency is weakly prevailed by $Q_{AC}$ and $Q_{ref,}$ therefore, thermal efficiency exhibits a small reduction with increasing $T_{cond}$ for all of the refrigerants. It is further seen in Fig. 4.9 that exergy efficiency of the combined cycle shares a common characteristic: decreasing as $T_{cond}$ increases. It is determined that as $T_{cond}$ rises, a very slight decline in the exergy efficiency for all of the refrigerants is observed. This is because the exergy accompanied by cooling water increases with the increase of condenser temperature which in turn reduces the exergy accompanied by $Q_{AC}$ and $Q_{ref}$. Computation of results reveal that $Q_{ref.}$ decreases from 44 kW to 33 kW and the $Q_{AC}$ decreases from 11 kw to 9 kW while the exergy accompanied by $Q_{ref}$ decreases 8.1 to 6.2 kw and the exergy associated with $Q_{AC}$ decreases from 0.28 kw to 0.21 kW when $T_{cond}$ increases from $30^0$C to $40^0$C. Since the exergy associated with $Q_{AC}$ and $Q_{ref}$ are quite small compared to $Q_{AC}$ and $Q_{ref,}$ therefore, the exergy efficiency despite of showing a similar trend appears to change insignificantly contrary to a significant change in thermal efficiency of the cycle. For R717 fluid, the thermal efficiency of the cycle decreases from 61.69% to 57.41% and exergy efficiency also decreases marginally from 39.01% to 38.57% consequent to the rise $T_{cond}$ from $30^0$C to $40^0$C.

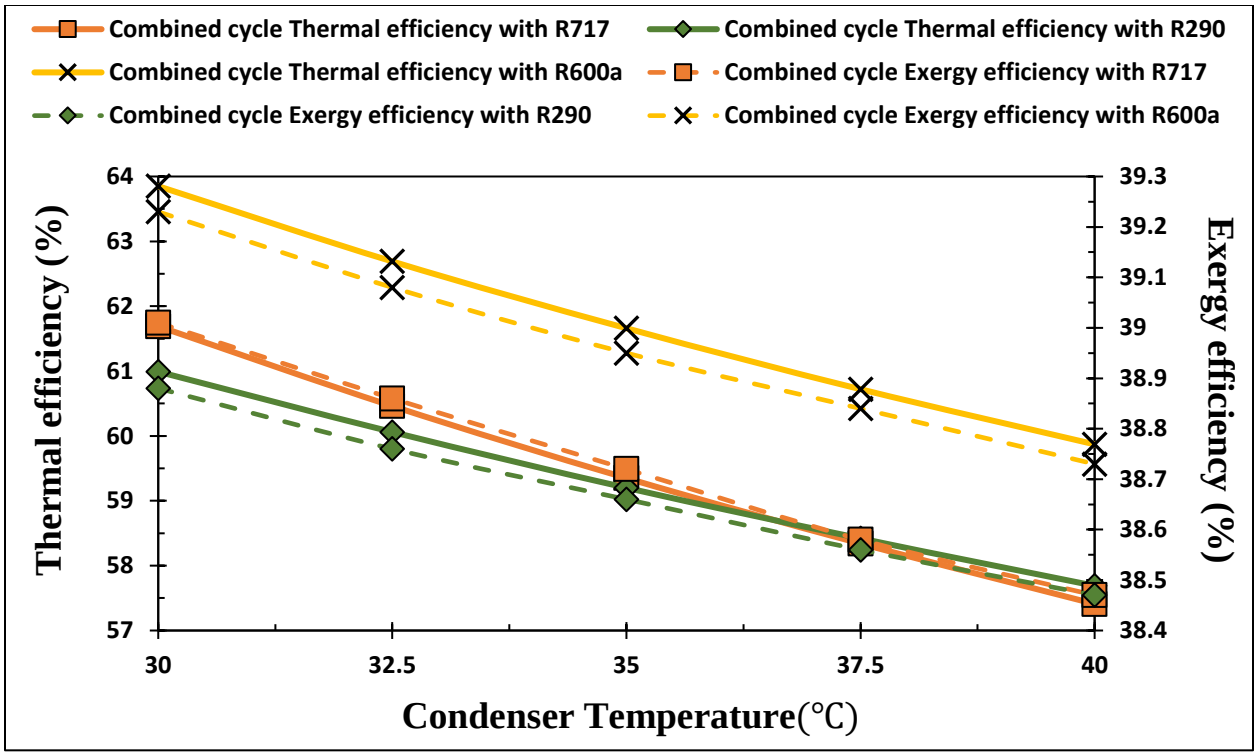


**Fig. 4.9.** Variation of thermal and exergy efficiencies of combined cycle with condenser temperature

The influence of the nozzle efficiency on performance of the combined cycle is shown in Fig. 4.10. Both thermal and exergy efficiencies of the combined cycle are found to be increasing with the rise of nozzle efficiency. Enhancement in nozzle efficiency of the ejector, enhances the velocity of the motive flow stream at the exit of nozzle which results in the simultaneous increase of the mass flow rate of primary fluid and the entrained secondary fluid from the refrigeration evaporator. This leads to the increase of cooling capacities of the AC evaporator and refrigeration evaporator of the system. Due to this reason, increase in nozzle efficiency, thermal efficiency of the combined cycle increases slightly. As the exergy associated by the cooling capacities of both the evaporator also increases, therefore, the exergy efficiency of the combined cycle also shares the same trend of increasing with the increase of nozzle efficiency. The same trend is observed for all the three

refrigerants. An increasing trend is found for the application of all three refrigerants but the change in refrigerant does not exhibit a significant variation in the thermal and exergy efficiencies of the combined cycle.

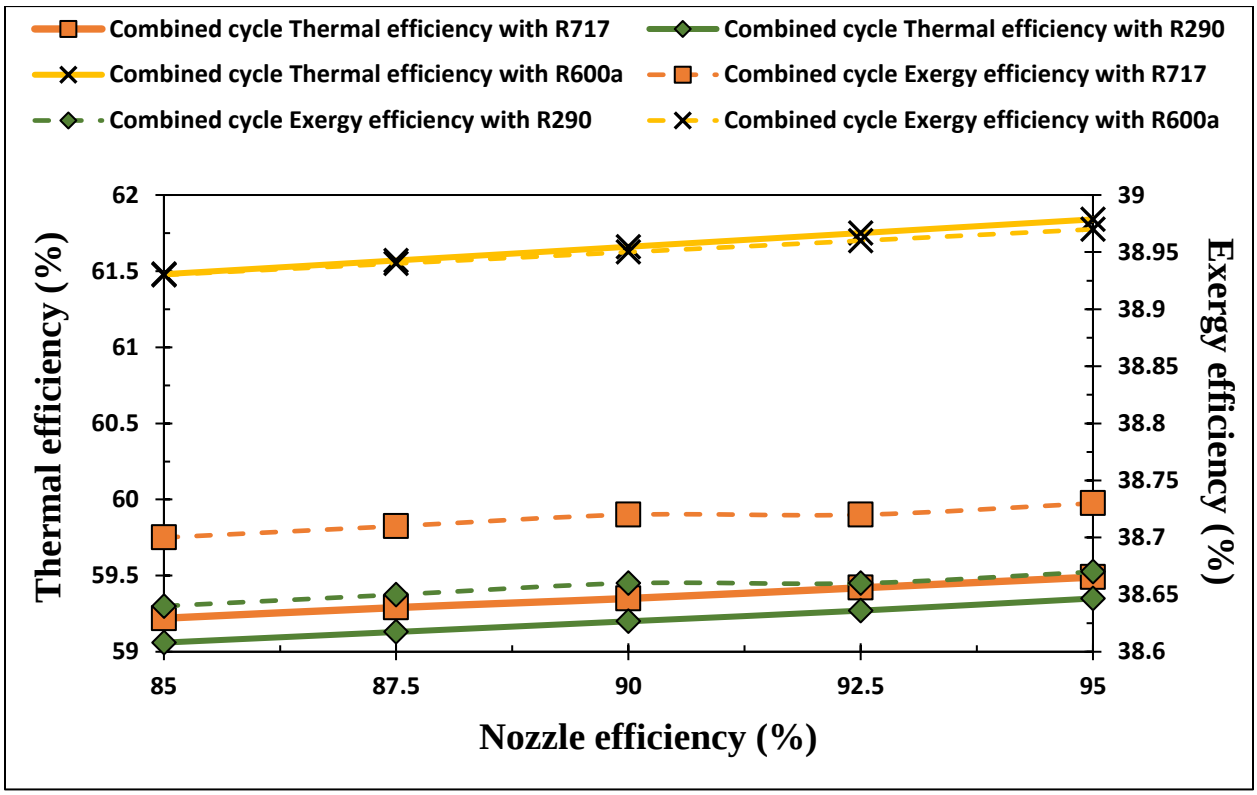


**Fig. 4.10.** Variation of thermal and exergy efficiencies of combined cycle with nozzle efficiency

After carrying out the energetic performance study, the distribution of energy possessed by natural gas which is supplied to the cycle is computed in terms of energy output and energy loss at the base case and is illustrated in Fig. 4.11. The results show that for R600a refrigerant, from 305 kW of energy input the energetic output of the cycle appears as; net power produced by HCCI engine is 132.4 kW, cooling capacity of refrigeration evaporator is 42.75 kW, cooling capacity of AC evaporator is 12.93 kW. Engine heat loss is 108.94 kW, heat loss via condenser is 66.78 kW, and heat loss via thermal exhaust to ambient is 52.56 kW. Employment of a different refrigerant in the bottoming cycle does not alter the engine power output and energy losses but it has an impact on

the cooling capacities and condenser heat loss. It is found that in case of R717 refrigerant, $Q_{ref}$ becomes 38.48 kW, $Q_{AC}$ becomes 10.19 kW, and condenser heat loss becomes 59.77 kW. For R290 refrigerant, $Q_{ref}$ appears as 37.22 kW, $Q_{AC}$ is 12.93 kW, and condenser heat loss becomes 59.30 kW.

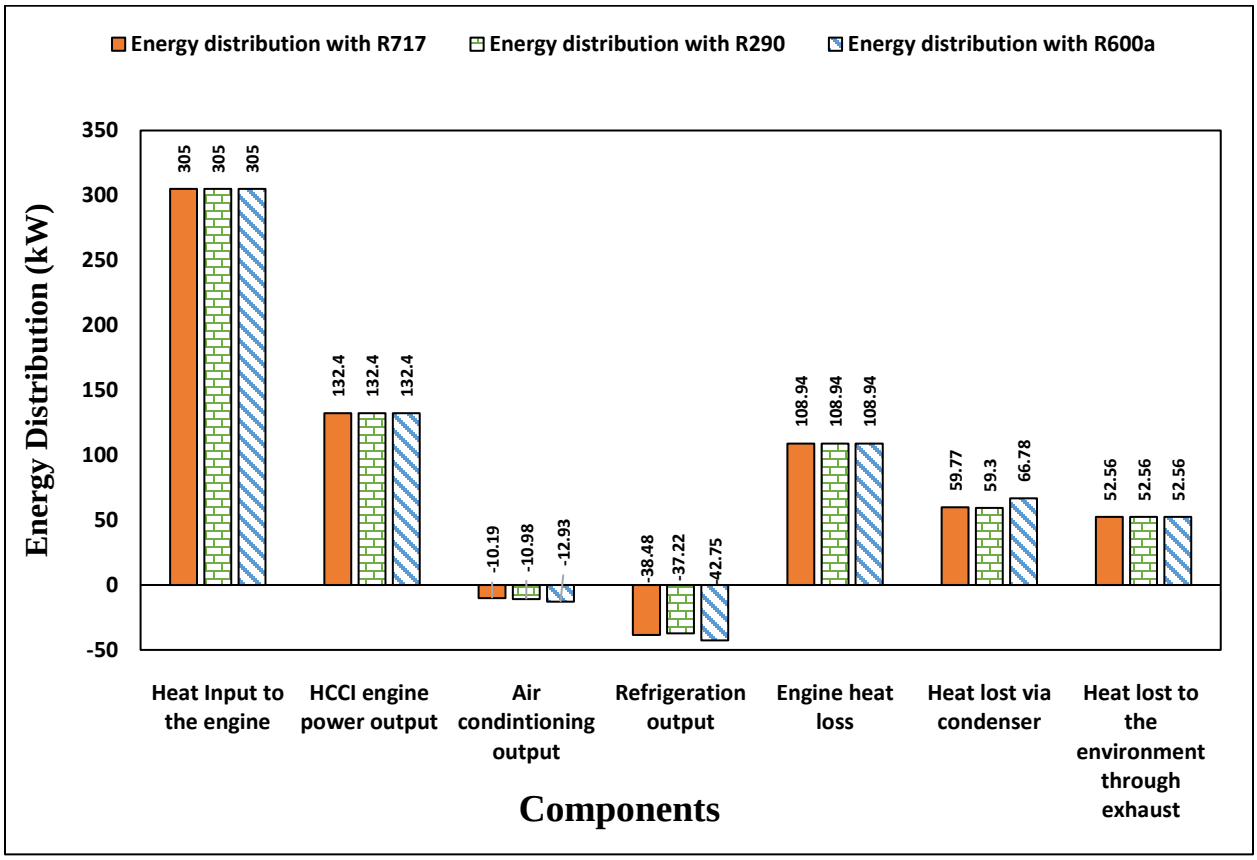


**Fig. 4.11.** Distribution of fuel energy in natural gas operated HCCI engine based combined cycle

Fig. 4.12 presents the breaking down of exergy of natural gas in the combined cycle at the base case. The total input exergy to the combined cycle is 361 kW (100%). It is evident that out of 100% exergy input, in case of R717 operated combined cycle, 139.79 kW (38.72%) is the total exergy output. Exergy destruction and losses are found as 164.21 kW (45.49%) and 57 kW (15.79%), respectively. For R290 refrigerant, exergy output is 139.58 kW (38.67%), exergy destruction is 163.98 kW (45.42%), and exergy loss is 57.44 kW (15.91%). For R600a, exergy

produced is 140.65 kW (38.96%), exergy destruction is 163.75 kW (45.36%), and exergy loss is 56.6 kW (15.67%). This data clearly show that change in refrigerant from R717 to R600a, and to R290, minorly influence the percentages of exergy produced, exergy destroyed, and exergy loss.

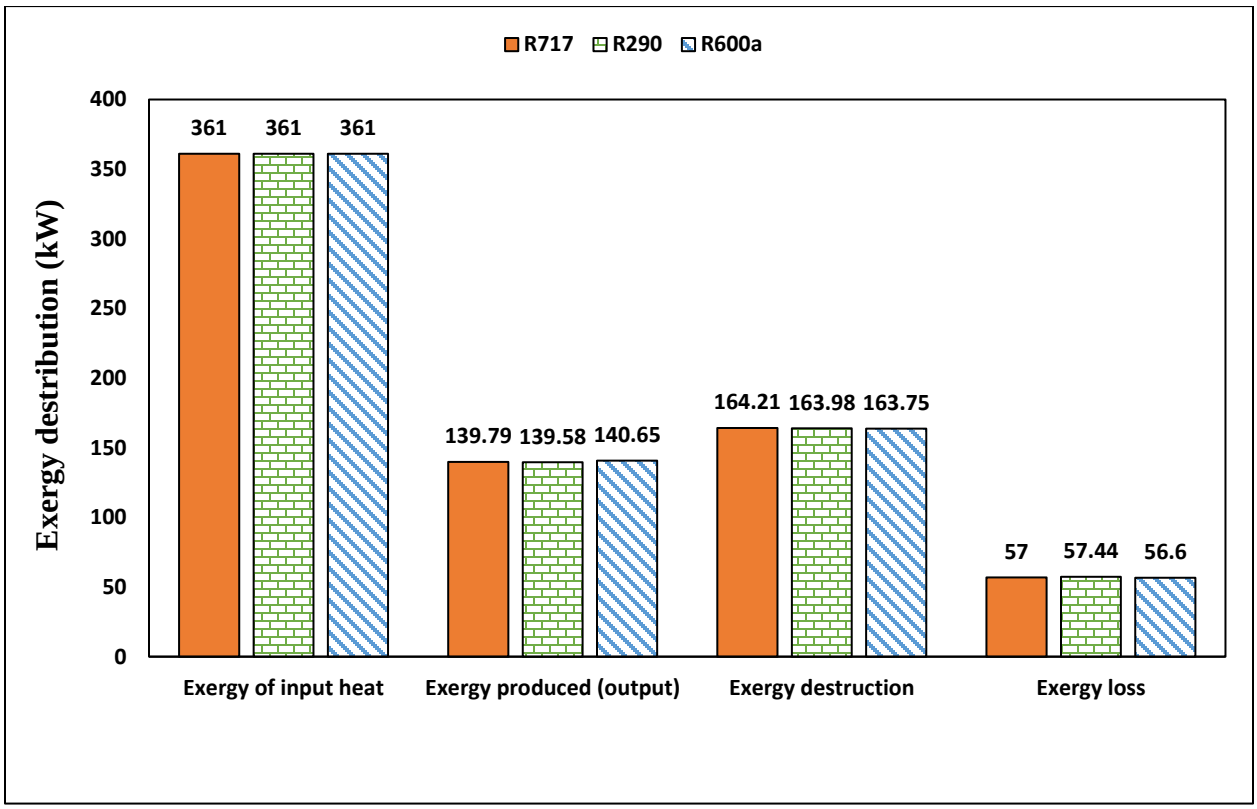


**Fig. 4.12.** Distribution of fuel exergy input in the produced, exergy destroyed and exergy loss in the proposed combined cycle

A detailed distribution of exergy destruction and exergy loss in each component of the combined cycle is illustrated in Fig. 4.13 as an appropriate exergy analysis provide a better understanding of the irriversibility of the proposed combined cycle. Detailed analysis reveals HCCI engine as the major exergy destructive component where 113.3 kW (31.38%) of the exergy is destroyed. Moreover, 36.84 kW (10.21%) of exergy loss in detected in HCCI engine that is the exergy of heat losses from cylinder walls to the ambient. Exergy destruction and exergy losses in HCCI engine are significantly high because of the irrevesible nature of the combustion process. Next highest destruction of exergy of 31.47 kW (8.71%) is found in the catalytic convertor. This is

because during this process, the combustion gases react with the material of convertor that leads to a chemical reaction which is the main source of entropy generation. Exergy destruction in the other components of the system does not exhibit significantly because these components does not directly utilize fuel exergy but instead heat exchanging process between the two fluid streams are involved that contribute to entropy generation. It is indicating that that there is no potential for improvement under the operating parameters considered. Further, loss of exergy from the fluid stream of the combined cycle to the ambient is also computed which found to be varies with the change of refrigerant in the two-phase ejector cooling cycle. It is shown that for the application of R600a, R717, and R290 the losses of exergy are found as 19.76 kW (5.47%), 20.16 kW (5.58%), and 20.6 kW (5.70%), respectively. This shows that exergy flow loss does not change appreciably with the change of refrigerant assumed in the analysis of the proposed combined cycle.

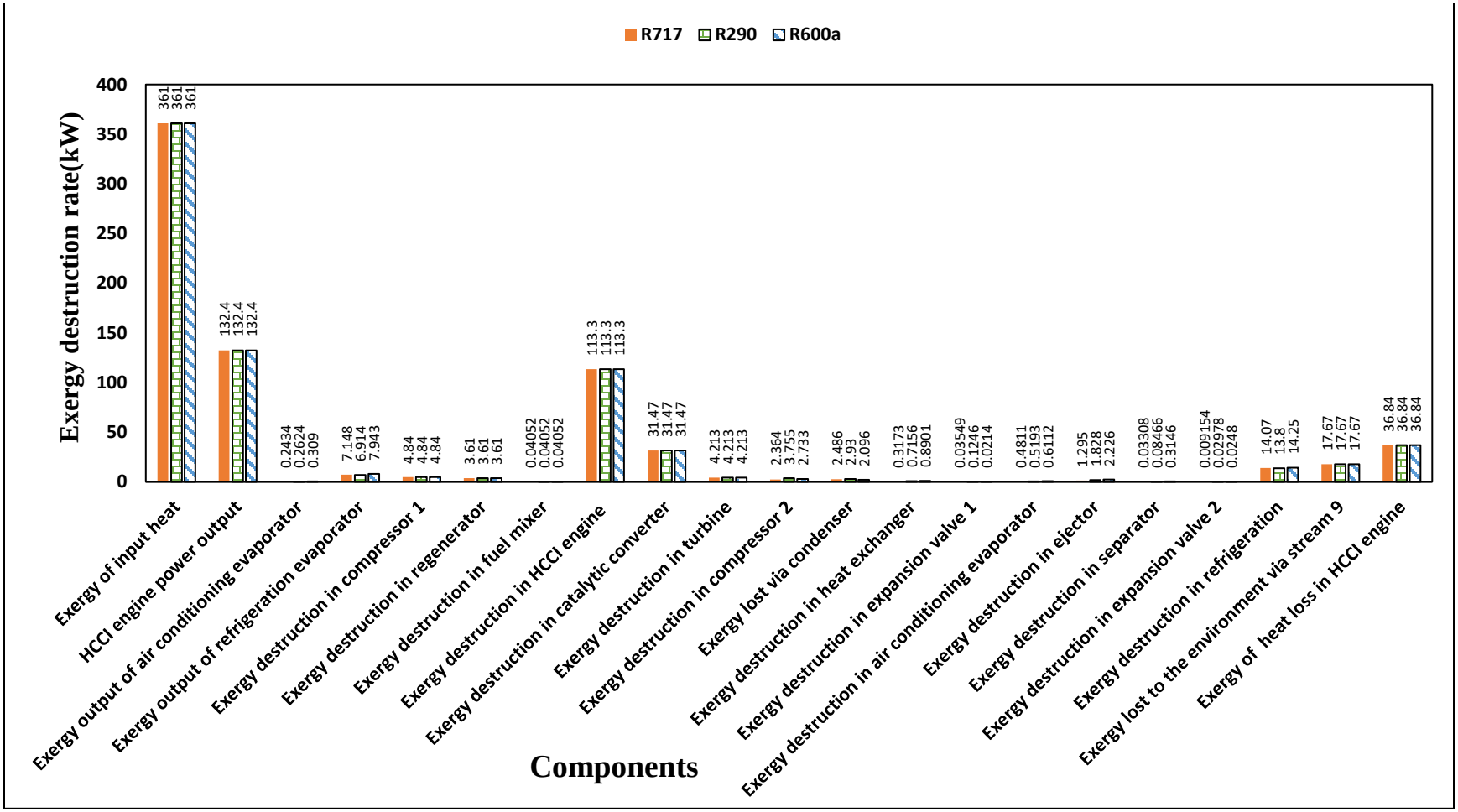


**Fig. 4.13.** Breaking down of the fuel exergy input in the components of the proposed combined cycle

# Chapter 5

# Conclusion & Further Recommendation

## 5.1 Conclusion

In the present thesis, efforts have been made to reduce the level of pollutant emissions and the consumption of fossil fuels in internal combustions engines. A modified mode of combustion called HCCI is investigated for the effective exploitation of wet-ethanol with the aim to achieve the goal of sustainable transportation. The effect of change of fuel from wet-ethanol to natural gas is also determined and the computed results are graphed and commented upon. The impact of the variation of key operating parameters of the engine such as turbocharger pressure ratio, isentropic efficiency of compressor of turbocharger, engine speed, fuel-air equivalence ratio is observed on the output power of HCCI engine and its thermodynamic efficiencies. Thermodynamic analysis carried out to investigate the performance of wet-ethanol fueled as well as the natural gas operated HCCI engines revealed that significant amount of exergy accompanied by engine exhaust heat is expelled which goes unutilized and leads to inefficient and environmentally harmful engine performance. This waste heat has been utilized as the potential energy source for driving the heat operated refrigeration and air conditioning systems in view of reducing the environmental impact and to improve the system efficiency. Exergy analysis which systematically combines the First and Second Law of Thermodynamics and enables the work generation capacity of energy losses by taking into account the quality of energy into consideration has been applied to evaluate the theoretical performance of HCCI

engine combined with waste heat operated cooling systems. This method of analysis revealed the processes where energy is conserved but the capacity to do work is not. The following important conclusions were drawn from the computational results of the present thesis:

- It is determined that an increase in pressure ratio across the turbocharger from 2.5 to 3.5 raises the thermal efficiency of cooling-power cogeneration from 47.87% to 50.09% when R134a is used as working fluid. Change in refrigerant alters both thermal and exergy efficiencies system.
- As the ambient temperature increases from 290K to 310K, the thermal efficiency of the combined system of cogeneration is lowering down but the exergy efficiency of the system is raised by a little percentage.
- Both cooling capacity and the exergy of refrigeration are decreased by greater than 2.0% in the case of the R134a operated system when the vapor generator pressure ($P_{VG}$) is elevated from 1800 kPa to 2200 kPa. But in the case of R600a operated cogeneration this decrease is found to be around 1.9%.
- The cooling capacity offered by R134a and R290 operated cogeneration system is decreased slightly at the increase of entrainment ratio of ERC ($\mu$) while for R600a operated system the cooling capacity is found to be increased.
- It is demonstrated that for R134a operated cogeneration system, the cooling capacity is increased by 11.34% when the evaporator pressure of ERC ($P_{Evap}$) rises from 327.4 kPa to 348.7 kPa. In the case of the R600a operated system the cooling capacity is increased by 12.58% at the rise of $P_{Evap}$ from 175.7 kPa to 186.9 kPa.
- The change of the degree of superheat of motive flow ($\Delta THE$) shows; in the case of the R134a operated cogeneration system, the refrigeration capacity is reduced by 1.55% when the $\Delta THE$ rises from $11.31^0$C to $19.31^0$C. For R290 operated cogeneration system, the refrigeration capacity is decreased by 2% when $\Delta THE$ is elevated from

$20.86^0$C to $28.86^0$C. Elevation of $\Delta THE$ from$1.7^0$C to $9.7^0$C in the case of R600a reduces the capacity of refrigeration by 2.32%.

- Both energetic and exergetic efficiencies of HCCI engine as well as of cogeneration cycle are found slightly increasing when the turbocharger compressor efficiency is increased.
- Elevation of turbocharger pressure resulting in the simultaneous increase of HCCI engine power and refrigeration of thermal load.
- The increase of ambient temperature involves the decline of energy and exergy efficiencies of HCCI engine and also the energy efficiency of cogeneration while the exergy efficiency of cogeneration is found increasing.
- Variation of entrainment ratio and type of refrigerant employed shows a marginal decline in the energetic and exergetic COPs of ERC.
- Bottoming of cooling cycles reveals that at the system base line operation, the refrigeration performed by ARC, R134a ERC, and R290 ERC were to be as 35.62 kW, 9.767 kW, and 6.706 kW, respectively.
- HCCI engine (61.19 kW), boiler of ERC (20.46 kW), generator of ARC (18.69 kW), catalytic convertor (17.89 kW) are discovered as the components of significant exergy destruction.
- Replacement of R134a with R290 as the ERC refrigerant changes the exergy of refrigeration from 0.811 kW to 0.5568 kW, exergy destroyed in the boiler from 20.46 kW to 21.29 kW, exergy destroyed in the ejector from 3.643 kW to 2.876 kW, exergy losses at the condenser from 1.044 kW to 1.243 kW, respectively.
- The exergy destruction in the evaporator of ARC is 0.105 kW compared to 0.805 kW in case of R134a ERC.

- As the equivalence ratio increases (0.3-0.9), the thermal efficiency of the HCCI engine is increased from 47.44% to 49.94%. Thermal efficiency of the combined cycle display a similar trend of increasing and rises from 60.05% to 63.26% in case of R600a operated cooling cycle and this increasing trend is observed for all the considered refrigerants.

- Increase in equivalence ratio from 0.3 to 0.9 causes an increase in HCCI engine exergy efficiency from 42.15% to 42.12% and the combined cycle exergy efficiency for R600a application is found to be increased from 38.02% to 39.89%, respectively. Variation of exergy efficiency display a similar charactreistic for other two refrigerants R290 and R717.

- Increasing of engine speed in the range of 1400-2200 r.p.m. leads to an increasing trend in both the efficiencies of HCCI engine and the combined cycle. For R600a refrigerant, $\eta_{th,cc}$ increases from 58.02% to 65.58% and the $\eta_{ex,cc}$ increases from 37% to 41%, respectively.

- The influence of increase in condenser temperarture ($T_{cond}$) leads to a decreasing trend for the thermal efficiency of combined cycle. It is found that for R717 $\eta_{th,cc}$ decreases from 61.69% $to$ 57.41%, for R290 decreased from 60.99% to 57.69%, and for R600a it is decreased from 63.85% to 59.87%, respectively, when $T_{cond}$ rises from $30^0$C to $40^0$C.

- Energetic analysis of the cycle carried out show that employment of a different refrigerant in the bottoming cycle does not alter the engine power output and energy losses but it has an impact on the cooling capacities and condenser heat loss.

- Distribution of fuel exergy results show that out of 100% exergy input, in case of R717 operated combined cycle, 139.79 kw (38.72%) is the total exergy output and 164.21 kW (45.49%) and 57 kW (15.79%), are the values for exergy destruction and exergy

losses. Further, it is determined that change in refrigerant from R717 to R600a, and to R290, minorly influence the percentages of exergy produced, destroyed, and loss.

- Among all the components of the combined cycle HCCI engine had the main contribution in exergy destruction (31.38%) and exegy loss (10.21%) for all the refrigerants considered.

Findings of present study clearly reveals the benefits of exergy analysis over the traditional energy analysis. The comparison between the destruction of exergy at the individual component determined that HCCI engine carries a potential of major improvement in view of improving the overall efficiency of proposed cogeneration cycle. Estimation of the fuel's energy and exergy distribution in the proposed configuration of power-cooling cogeneration behaves distinctly. Moreover, the change in type of refrigerant in the cooling system considerably influenced the system's energetic and exergetic output parameters.

## 5.2 Recommendations for Future Research Work

Ethanol production from corn and the use of wet-ethanol in HCCI engines along with the exhaust heat recovery for generation of cooling has been found as one of the most effective technologies for realizing the dream of sustainable transportation. Application of the exergy analysis methodology in this research helped demonstrate the powerful advantage of this method in the analysis of HCCI engine processes and also in the processes of waste heat operated cooling cycles. Fuel exergy transformation was investigated using a thermodynamic simulation of HCCI combustion operated on wet-ethanol and natural gas. Distribution of fuel exergy into the exergy produced, destroyed, and lost from the proposed combined power and cooling system computed. There are different aspects of the current study that can be extended as follows:

- Extending the model to hydrogen enriched natural gas fueled HCCI engine simulation can provide additional information of more sustainable exergy transformation during the combustion processes. Blending of hydrogen enhance the flame speed of fuel and reducing the carbon emissions.
- Hydrogen enrichment of wet-ethanol and natural gas can provide the opportunity to investigate the effect of blending on the reduction of engine irreversibilities, especially on in-cylinder exergy destruction.
- Model of waste heat recovery can be extended to investigate the performance of HCCI engine integrated with the new kind of ejector-absorption chiller called $NH_3$-$LiNO_3$ operated ARC to produce cooling below freezing for food preservations.
- The EES thermodynamic simulation was developed specifically for cooling production using the exhaust heat of HCCI engine through the employment of absorption refrigeration cycle and ejector refrigeration cycle. This simulation can be extended to simulate other modes of waste heat recovery with a variety of cooling options for refrigeration needed in the deep freezing range (e.g., transcritical $CO_2$ operated cycle, $N_2O$ operated cascaded cycle, etc.) to compare the efficiency of engine exhaust energy recovery for cold production required at various levels of temperature.

## 5.3 Limitations of proposed model

The thermodynamic model employed in the present investigation possess some limitations and they can be stated as below:

- The model developed is applicable to steady state condition of HCCI engine which is assumed to be operated as an ideal Otto cycle. Real HCCI engine operation deviates considerably from Otto cycle behavior.
- The model is applicable to quantify and identify only the Thermodynamic irreversibilities (exergy destruction and losses) occurs during the four basic processes of the engine; compression, combustion, expansion, and exhaust. Though in real operation of HCCI engine significant amount of thermodynamic irreversibility occurs

during the closed portion of the engine cycle from intake valve closure to exhaust valve opening. Therefore, to address the real challenges in HCCI engine the model based on the theory called “crank angle resoved exergy flow within a complete engine cycle” is to be developed and applied to compute the actual fuel exergy distribution in HCCI engine cycle.

- Combustion efficiency is assumed in this model and not been computed by incorporating the heat transfer losses during combustion. Though, in real HCCI combustion a significant amount of exergy is transferred or loss via heat transfer from in-cylinder gas to the surrounding walls which affects the fuel exergy distribution.
- Present model is limited to apply to the situation of 9% heat lost to the surroundings during exhaust and blowdown processes. Though in real operation of HCCI engine heat lost during exhaust and blowdown varies and requires to be computed.

Therefore, for future applications to address the real challenges of HCCI engine a generalized model can be developed after eliminating the assumptions taken in the present model.

## References


[1] “World Population Prospects 2019” United Nations, Dept of Economic and Social Affairs. 2019.

[2] U. S. Energy Information Administration, 2019, “International Energy Outlook 2019,”

[3] IEA., 2021, “Global Energy Review 2021,” IEA, Paris https://www.iea.org/reports/global-energy-review-2021.

[4] U. S. Energy Information Administration, “Annual Energy Outlook 2021,” 2021.

[5] McKinsey & Company, 2021, “Global Energy Perspective”

[6] International Energy Outlook 2014: World Petroleum and Other Liquid Fuels, U.S. Energy Information Administration (EIA), Washington, DC 20585, 2014.

[7] ExxonMobil, Explore the Outlook for Energy: A View to 2040, 2016.

[8] Li, T., Moriwaki, R., Ogawa, H., Kakizaki, R., Murase, M., 2011, “Dependence of premixed low-temperature diesel combustion on fuel ignitability and volatility,” International Journal of Engine Research, 13 pp. 14-27.

[9] World Energy Outlook 2014, International Energy Agency 2014.

[10] Xu, C.L., Bell, L., 2014, “Global reserves, oil production show increases for 2014,” Oil Gas J., 112 pp. 30-31.

[11] Sabri, M., Danapalasingam, K., Rahmat, M., 2016, “A review on hybrid electric vehicles architecture and energy management strategies,” Renew Sustain Energy Rev, 53 pp. 1433–42.

[12] Hannan, M., Azidin, F., Mohamed, A., 2014, “Hybrid electric vehicles and their challenges: a review,” Renew Sustain Energy Rev, 29 pp. 135–50.

[13]Kester, J., Noel, L., de Rubens, G.Z., Sovacool, B.K., 2018, “Policy mechanisms to accelerate electric vehicle adoption: a qualitative review from the Nordic region,” Renew Sustain Energy Rev, 94, pp. 719–31.

[14]Tang, Q., Duan, X., Liu, Y., Li, S., Zhao, Z., Ren, K., 2020, “Experimental study the effects of acetone–butanol–ethanol (ABE), spark timing and lambda on the performance and emissions characteristics of a high-speed SI engine,” Fuel, 279 pp. 118499.

[15]Xie, Y., Li, Y., Zhao, Z., Dong, H., Wang, S., Liu, J., 2020, “Microsimulation of electric vehicle energy consumption and driving range,” Appl Energy, 267 pp. 115081.

[16]Das, H.S., Tan, C.W., Yatim, A., 2017, “Fuel cell hybrid electric vehicles: a review on power conditioning units and topologies,” Renew Sustain Energy Rev., 76 pp. 268–91.

[17]Hwang, J.J., 2013, “Sustainability study of hydrogen pathways for fuel cell vehicle applications,” Renew Sustain Energy Rev., 19 pp. 220–9.

[18]Dudley, B., 2018, “BP statistical review of world energy,” BP Statistical Review, London, UK.

[19]Liu, J., Dumitrescu, C.E., 2018, “Flame development analysis in a diesel optical engine converted to spark ignition natural gas operation,” Appl Energy, 230 pp. 1205–17.

[20]Liu, J., Dumitrescu, C.E., 2018, “3D CFD simulation of a CI engine converted to SI natural gas operation using the G-equation,” Fuel 232 pp. 833–44.

[21]Liu, J., Dumitrescu, C.E., 2019, “Methodology to separate the two burn stages of natural-gas lean premixed-combustion inside a diesel geometry,” Energy Convers Manage., 195 pp. 21–31.

[22]Liu, J., Dumitrescu, C.E., 2019, “Analysis of two-stage natural-gas lean combustion inside a diesel geometry,” Appl Therm Eng., 160 pp. 114116.

[23]Liu, J., Dumitrescu, C.E., 2019, “Numerical investigation of methane number and wobbe index effects in lean-burn natural gas spark-ignition combustion,” Energy Fuels, 33 pp. 4564–74.

[24]Wu, H.W., Wang, R.H., Ou, D.J., Chen, Y.C., Chen, T.Y., 2011, “Reduction of smoke and nitrogen oxides of a partial HCCI engine using premixed gasoline and ethanol with air,” Appl Energy, 88 pp. 3882–90. doi:10.1016/j.apenergy.2011.03.027.

[25]Heywood, J.B., 1988, “Internal Combustion Engine Fundamentals,” McGraw Hill Book Company, New York.

[26]Turkish Petroleum. 2017 Crude Oil and Gas Sector Report. 2018.50 h

[27]Xingcai, Lu., Han, D., Huang, Z., 2011, “Fuel design and management for the control of advanced compression-ignition combustion modes,” Progress in Energy and Combustion Science, 37 pp. 741–83.

[28]Rajasekar, E., Murugesan, A., Subramanian, R., and Nedunchezhian, N., 2010, “Review of NOx reduction technologies in CI engines fuelled with oxygenated biomass fuels,” Renewable and Sustainable Energy Reviews, 14(7) pp. 2113-2121

[29]Monyem, A., Gerpen, j.V., Canakci, M., 2001, “The effect of timing and oxidation on emissions from biodiesel-fueled engines,” Transactions of the ASAE, 44(1) pp. 35.

[30]Agarwal, A.K., 2007, “Biofuels (alcohols and biodiesel) applications as fuels for internal combustion engines,” Prog Energy Combust Sci., 33 pp. 233–71. doi:10.1016/j.pecs.2006.08.003

[31]Bae, C., and Kim, J., 2017, “Alternative fuels for internal combustion engines,” Proceedings of the Combustion Institute, 36(3) pp. 3389-3413.

[32]Geng, P., Cao, E., Tan, Q., and Wei, L., 2017, “Effects of alternative fuels on the combustion characteristics and emission products from diesel engines: A review,” Renewable and Sustainable Energy Reviews, 71 pp. 523-534.

[33]Rajasekar, E., Murugesan, A., Subramanian, R., Nedunchezhian, N., 2010, “Review of NOx reduction technologies in CI engines fuelled with oxygenated biomass fuels,” Renewable and Sustainable Energy Reviews, 14(7) pp. 2113-2121.

[34]Ghazali, W.N.M.W., Mamat, R., Masjuki, H., Najafi, G., 2015, “Effects of biodiesel from different feedstocks on engine performance and emissions: A review,” Renewable and Sustainable Energy Reviews, 51 pp. 585-602.

[35]Banković-Ilić, I.B., Stojković, I.J., Stamenković, O.S., Veljkovic, V.B., Hung, Y.T., 2014, “Waste animal fats as feedstocks for biodiesel production,” Renewable and Sustainable Energy Reviews, 32 pp. 238-254.

[36]Azad, A.K., Rasul, M., Khan, M.M.K., Sharma, S.C., Hazrat, M., 2015, “Prospect of biofuels as an alternative transport fuel in Australia,” Renewable and Sustainable Energy Reviews, 43 pp. 331-351.

[37]Chakraborty, R., Gupta, A.K., Chowdhury, R., 2014, “Conversion of slaughterhouse and poultry farm animal fats and wastes to biodiesel: Parametric sensitivity and fuel quality assessment,” Renewable and Sustainable Energy Reviews, 29 pp. 120-134.

[38]Takase, M., Zhao, T., Zhang, M., Chen, Y., Liu, H., Yang, L., Wu, X., 2015, “An expatiate review of neem, jatropha, rubber and karanja as multipurpose non-edible biodiesel resources and comparison of their fuel, engine and emission properties,” Renewable and Sustainable Energy Reviews, 43 pp. 495-520.

[39]Abedin, M., Masjuki, H., Kalam, M., Sanjid, A., Rahman, S.A., Fattah, I.R., 2014, "Performance, emissions, and heat losses of palm and jatropha biodiesel blends in a diesel engine," Industrial crops and products, 59 pp. 96-104.

[40]Atabani, A., and da Silva César, A., 2014, "Calophyllum inophyllum L.–A prospective non-edible biodiesel feedstock. Study of biodiesel production, properties, fatty acid composition, blending and engine performance," Renewable and Sustainable Energy Reviews, 37 pp. 644-655.

[41]Abedin, M., Masjuki, H., Kalam, M., Sanjid, A., Ashraful, A., Combustion, performance, and emission characteristics of low heat rejection engine operating on various biodiesels and vegetable oils," Energy Conversion and Management, 85 pp. 173-189

[42]https://www.esrl.noaa.gov/gmd/ ccgg/trends/monthly.html

[43]Tangöz, S., Akansu, S.O., Kahraman, N., Malkoç, Y., 2015, "Effects of compression ratio on performance and emissions of a modified diesel engine fueled by HCNG," International Journal of Hydrogen Energy, 40 pp. 15374-15380

[44]Kopyscinski, J., Schildhauer, T.J., Biollaz, S.M.A., 2010, "Production of synthetic natural gas (SNG) from coal and dry biomass—a technology review from 1950–2009," Fuel, 89 pp. 1763-1783

[45]Teng, H., and McCandless, J.C., 2006, "Can heavy-duty diesel engines fueled with DME meet US 2007/2010 emissions standard with a simplified aftertreatment system?," SAE Technical Paper, pp. 2006-01-0053.

[46]Kumar, S., Cho, J.H., Park, J., Moon, I., 2013, "Advances in diesel–alcohol blends and their effects on the performance and emissions of diesel engines," Renewable and Sustainable Energy Reviews, 22 pp. 46-72.

[47]Papagiannakis, R.G., Rakopoulos, C.D., Hountalas, D.T., Rakopoulos, D.C., 2010, "Emission characteristics of high speed, dual fuel, compression ignition engine operating in a wide range of natural gas/diesel fuel proportions," 7th International Symposium on Alcohol Fuels, 89(7) pp. 1397-1406

[48]Johnson, F.X., Silveira, S., 2014, "Pioneer countries in the transition to alternative transport fuels: comparison of ethanol programmes and policies in Brazil, Malawi and Sweden," Environmental Innovation and Societal Transitions, 11, pp.1-24.

[49]Walter, A., Rosillo-Calle, F., Dolzan, P., Piacente, E., Borges da Cunha, K., 2008, "Perspectives on fuel ethanol consumption and trade," Biomass and Bioenergy, 32 (8) pp. 730-748.

[50]Tibaquirá, J.E., Huertas, J.I., Ospina, S., Quirama, L.F., Niño, J.E., 2018, "The effect of using ethanol-gasoline blends on the mechanical, energy and environmental performance of in-use vehicles," Energies, 11(221) pp. 1-17

[51]Foong, T.M., Morganti, K.J., Brear, M.J., da Silva, G., Yang, Y., Dryer, F.L., 2014, "The octane numbers of ethanol blended with gasoline and its surrogates," Fuel, 115 pp. 727-739

[52]Li, Y., Zhao, H., Brouzos, N.P., 2008, "CAI combustion with methanol and ethanol in an airassisted direct injection SI engine," SAE technical paper, pp. 2008-01-1673. http://dx.doi.org/10.4271/2008-01-1673

[53]Xie, H., Wei, Z., He, B., Zhao, H., 2006, "Comparison of HCCI combustion respectively fueled with gasoline, ethanol and methanol through the trapped residual gas strategy," SAE technical paper, pp. 2006-01-0635. http://dx.doi.org/10.4271/ 2006-01-0635

[54]Nigam, P.S., Singh, A., 2011, "Production of liquid biofuels from renewable resources," Progress in Energy and Combustion Science, 37 pp. 52–68.

[55]Jeuland, N., Montagne, X., Gautrot, X., 2004, “Potentiality of Ethanol As a Fuel for Dedicated Engine,” Oil & Gas Science and Technology-revue De L Institut Francais Du Petrole, 59 pp. 559-570. https://doi.org/10.2516/ogst:2004040

[56]Ilhak, M.I., Tangoz, S., Akansu, S.O., Kahraman, N., 2019, “Alternative Fuels for Internal Combustion Engines, The Future of Internal Combustion Engines,” Antonio Paolo Carlucci, IntechOpen, DOI: 10.5772/intechopen.85446. Available from: https://www.intechopen.com/books/the-future-of-internal-combustion-engines/alternative-fuels-for-internal-combustion-engines

[57]Shapouri, H., Duffield, J. A., and Graboski, M. S., 1995, “Estimating the Net Energy Balance of Corn Ethanol,” USDA Economic Research Service Report No. AER-721, Washington, D.C.

[58]Shapouri, H., Duffield, J. A., and Wang, M., 2003, “The Energy Balance of Corn Ethanol Revisited,” Trans. ASAE, 46 (4) pp. 959–968.

[59]Flowers, D.L., Aceves, S.M., Frias, J.M., 2007, “Improving Ethanol Life Cycle Energy Efficiency by Direct Utilization of Wet Ethanol in HCCI Engines,” SAE Technical Paper, pp. 2007-01-1867.

[60]Frias, J.M., Aceves, S.M., Flowers, D.L., 2007, “Improving ethanol life cycle energy efficiency by direct utilization of wet-ethanol in HCCI engines,” J. Energy Resour. Technol., 129(4) pp. 332-337. https://doi.org/10.1115/1.2794768

[61]Kumar, P., Rehman, A., 2016, “Bio-diesel in homogeneous charge compression ignition (HCCI) combustion,” Renew Sustain Energy Rev., 56 pp. 536–50.

[62]Duan, X., Liu, J., Yuan, Z., Guo, G., Liu, Q., Tang, Q., 2018, “Experimental investigation of the effects of injection strategies on cycle-to-cycle variations of a DISI engine fueled with ethanol and gasoline blend,” Energy, 165 pp. 455–70.

[63]Jung, D., 2018, “Autoignition and Chemical-Kinetic Mechanisms of Homogeneous Charge Compression Ignition Combustion for the Fuels with Various Autoignition Reactivity,” Advanced Chemical Kinetics. doi:10.5772/intechopen.70541

[64]Najt, P.M., and Foster, D. E., 1983, “Compression-ignited homogeneous charge combustion,” SAE Technical Paper, pp. 830264.

[65]Dec, J.E., and Yang, Y., 2010, “Boosted HCCI for High Power Output without Engine Knock and with Ultra-Low NOx Emissions – using Conventional Gasoline,” SAE Technical Paper, pp. 2010-01-1086. doi: 10.4271/2010-01-1086

[66]Dec., J.E., and Sjöberg, M., 2004, “Isolating the Effects of Fuel Chemistry on Combustion Phasing in an HCCI Engine and the Potential for Fuel Stratification for Ignition Control,” SAE Technical Paper, pp. 2004-01-0557. doi: 10.4271/2004-01-0557.

[67]Yang, Y., Dec, J., Dronniou, N., Simmons, B., 2010, “Characteristics of Isopentanol as a Fuel for HCCI Engines,” SAE Technical Paper, pp. 2010-01-2164. doi: 10.4271/2010-01-2164.

[68]Saxena, S., Chen, J-Y, Dibble, R., 2011, “Maximizing power output in an automotive scale multi-cylinder homogeneous charge compression ignition (HCCI) engine,” SAE Technical Paper, pp. 2011-01-0907. doi: 10.4271/2011-01-0907.

[69]Bedoya, I.D., Saxena, S., Cadavid, F.J., Dibble, R.W., 2011, “Exploring Strategies for Reducing High Inlet Temperature Requirements and Allowing Optimal Operating Conditions in a Biogas Fueled HCCI Engine for Power Generation,” ASME IC Engine Conference, Morgantown, WV, Oct. 2011, ICEF2011-60198.

[70]Bendu, H., Murugan, S., 2014, “Homogeneous charge compression ignition (HCCI) combustion: mixture preparation and control strategies in diesel engines,” Renew Sustain Energy Rev., 38, pp. 732–46.

[71]Canova, M., Garcin, R., Midlam-Mohler, S., Guezennec, Y., Rizzoni, G., 2005, "A control - oriented model of combustion process in a HCCI diesel engine," Proc. 2005, Am. Control Conf. 2005., IEEE; 2005, p. 4446–51. doi:10.1109/ACC.2005.1470696.

[72]Maurya, R.K., Agarwal, A.K., 2011, "Experimental study of combustion and emission characteristics of ethanol fuelled port injected homogeneous charge compression ignition (HCCI) combustion engine," Appl Energy, 88, pp. 1169–80. doi:10.1016/j.apenergy.2010.09.015.

[73]Iida, N., 1994, "Combustion Analysis of Methanol-Fueled Active Thermo-Atmosphere Combustion (ATAC) Engine Using a Spectroscopic Observation," SAE Technical Paper, pp. 940684. doi:10.4271/940684.

[74]Dunn-Rankin, D., 2008, "Lean combustion: technology and control," Academic Press.

[75]Onishi, S., Hong Jo, S., Shoda, K., Do Jo, P., Kato, S., "Active Thermo-Atmosphere Combustion (ATAC) – A New Combustion Process for Internal Combustion Engines," SAE790501

[76]Yamaguchi, J., 1997, "Honda readies Activated Radical Combustion two-stroke engine for production motorcycle," Automotive Engineering.

[77]Ishibashi, Y., and Asai, M., 1998. "A Low Pressure Pneumatic Direct Injection Two-Stroke Engine by Activated Radical Combustion Concept," SAE Technical Paper, pp. 980757.

[78]Noguchi, M., Tanaka, Y., Tanaka, T., Takeuchi, Y., 1979, "A Study on Gasoline Engine Combustion by Observation of Intermediate Reactive Products during Combustion," SAE Technical Paper, pp. 790840. doi:10.4271/790840

[79]Thring, R. H., 1989, “Homogeneous charge compression ignition (HCCI) engines,” SAE Technical Paper, pp. 892068.

[80]Lavy, J., Dabadie, J., Angelberger, C., Duret, P., Willand, J., Juretzka, A., Schaflien, J., Ma, T., Lendress, Y., Satre, A., Shultz, C., Kramer, H., Zhao, H., Damiano, L., 2000, “Innovative ultra-low NOx controlled auto-ignition combustion process for gasoline engines: the 4-SPACE project,” SAE Technical paper, pp. 2000-01-1837.

[81]Zhao, H., Li, J., Ma, T., Ladommatos, N., 2001, “Performance and analysis of a 4-stroke multi-cylinder gasoline engine with CAI combustion,” SAE Technical paper, pp. 2002-01- 0420.

[82]Koopmans, L., and Denbratt, I., 2001, “A four-stroke camless engine, operated in homogeneous charge compression ignition mode with a commercial gasoline,” SAE Technical paper, pp. 2001-01-3610.

[83]Law, D., et al., 2000, “Controlled combustion in an IC-engine with a fully variable valve train,” SAE Technical paper, pp. 2000-01-0251.

[84]Nishijima, Y., Asaumi, Y., Aoygi, Y., 2001, “Premixed Lean Diesel Combustion (PREDIC) using Impingement Spray System,” SAE Technical paper, pp. 2001-01-1892.

[85]Kimura, S., et al., 1999, “New Combustion Concept for Ultra-clean and High Efficiency Small DI Diesel Engines,” SAE Technical paper, pp. 1999-01-3681.

[86]Yanagihara, H., Satou, Y., Mizuta, J., 1996, “A simultaneous reduction of NOx and soot in diesel engines under a new combustion system (Uniform Bulky Combustion System – UNIBUS),” 17th Int. Vienna Motor Symposium.

[87]Yang, J., Culp, T., Kenny, T., 2002, “Development of a Gasoline Engine System using HCCI Technology – the Concept and the Test Results,” SAE Technical paper, pp. 2002-01-2832.

[88]Aoyama, T. et al., 1996, “An experimental study on premixed-charge compression ignition gasoline ,” SAE Technical paper, pp. 960081.

[89]Zhao, H., 2007, “HCCI and CAI Engines for the Automotive Industry,” 1st Edition, Woodhead Publishing Limited, Cambridge, England.

[90]Dec, J.E, 2009, “Advanced compression-ignition engines—understanding the in-cylinder processes,” Proceedings of the Combustion Institute, 32 (2) pp. 2727-2742. doi: 10.1016/j.proci.2008.08.008.

[91]Kim, D. S., and Lee, C. S., 2006, “Improved emission characteristics of HCCI engine by various premixed fuels and cooled EGR,” Fuel, 85 pp. 695–704.

[92]Lu, X., Han, D., Huang, Z., 2011, “Fuel design and management for the control of advanced compression-ignition combustion modes,” Prog. Energy Combust. Sci., 37 (6) pp. 741–783. https://doi.org/10.1016/j.pecs.2011.03.003

[93]Reitz, R.D., Duraisamy, G., 2015, “Review of high efficiency and clean reactivity controlled compression ignition (RCCI) combustion in internal combustion engines,” Prog. Energy Combust. Sci., 46 pp.12–71.

[94]Gowthaman, S., Sathiyagnanam, A., 2017, “Analysis the optimum inlet air temperature for controlling homogeneous charge compression ignition (HCCI) engine,” Alexandria Eng. J., 57 pp. 2209–2214.

[95]Calam, A., Solmaz, H., Yılmaz, E., İçingür, Y., 2019, “Investigation of effect of compression ratio on combustion and exhaust emissions in A HCCI engine,” Energy, 168 pp. 1208–1216.

[96]Dubreuil, A., Foucher, F., Mounaim-Rousselle, C., Dayma, G., Dagaut, P., 2007, "HCCI combustion: effect of NO in EGR," Proceedings of the Combustion Institute, 31 pp. 2879–2886.

[97]Mack, J. H., 2007, "Investigation of homogeneous charge compression ignition (HCCI) engines fuelled with ethanol blends using experiments and numerical simulations," Berkeley, USA: University of California.

[98]Manofsky, L., Vavra, J., Assanis, D., Babajimopoulos, A., 2011, "Bridging the gap between HCCI and SI: spark-assisted compression ignition," SAE Technical Paper, pp. 2011-01-1179.

[99]Nguyen, Q. L., 2007, "The effects of operating parameters on combustion and emissions of si engine—a pre study of hcci combustion," Southern Taiwan University.

[100]Gharehghani, A., 2019, "Load limits of an HCCI engine fueled with natural gas, ethanol, and methanol," Fuel, 239 pp. 1001-1014. https://doi.org/10.1016/j.fuel.2018.11.066

[101]Yao, M., Zheng, Z., Liu, H., 2009, "Progress and Recent Trends in Homogeneous Charge Compression Ignition (HCCI) Engines," Progress in Energy and Combustion Science, 35 (5) pp. 398–437. doi:10.1016/j.pecs.2009.05.001

[102]Olsson, J.-O., Tunestål, P., Haraldsson, G., Johansson, B., 2001, "A Turbo Charged Dual Fuel HCCI Engine," SAE Technical Paper.

[103]Christensen, M., and Johansson, B., 1998, "Influence of Mixture Quality on Homogeneous Charge Compression Ignition," SAE Technical Paper.

[104]Wang, Z., Wang, J.-X., Shuai, S.-J., Tian, G.-H., An, X., Ma, Q.-J., 2006, "Study of the Effect of Spark Ignition on Gasoline HCCI Combustion. Proceedings of the

Institution of Mechanical Engineers," Part D: Journal of Automobile Engineering, 220 (6) pp. 817–825.

[105]Yang, D.-b., Wang, Z., Wang, J.-X., Shuai, S.-J., 2011, "Experimental Study of Fuel Stratification for HCCI High Load Extension," Applied Energy, 88 (9) pp. 2949–2954.

[106]Yang, J., 2004, "HCCI Engine Intake/Exhaust Systems for Fast Inlet Temperature and Pressure Control with Intake Pressure Boosting," Google Patents.

[107]Yoshioka, S., Matsuoka, T., Hamada, S., Hinatase, H., 1987, "Engine Intake System Having a Pressure Wave Supercharger," Google Patents.

[108]Hyvönen, J., Haraldsson, G., Johansson, B., 2003, "Operating Range in a Multi Cylinder HCCI Engine Using Variable Compression Ratio," SAE Technical Paper.

[109]Olsson, J.-O., Tunestål, P., Johansson, B., 2004, "Boosting for High Load HCCI," SAE Technical Paper.

[110]Cairns, A., and Blaxill, H., 2005, "The effects of combined internal and external exhaust gas recirculation on gasoline controlled auto-ignition," SAE Technical Paper.

[111]Osborne, R., Li, G., Sapsford, S., Stokes, J., Lake, T., Heikal, M.R., 2003, "Evaluation of HCCI for future gasoline powertrains," SAE Technical Paper.

[112]Hyvönen, J., Haraldsson, G., Johansson, B., 2005, "Operating conditions using spark assisted HCCI combustion during combustion mode transfer to SI in a multi-cylinder VCR-HCCI engine," SAE Technical Paper.

[113]Kalian, M., Zhao, H., Qiao, J., 2008, " Investigation of transition between spark ignitionand controlled auto-ignition combustion in a V6direct-injection engine with cam profile switching," Proc IMechE D: J Automobile Eng., 222 pp. 1911–26.

[114]Urushihara, T., Yamaguchi, K., Yoshizawa, K., Itoh, T., 2005, “A study of a gasoline-fueled compression ignition engine-Expansion of HCCI operation range using SI combustion as a trigger of compression ignition,” SAE Technical Paper.

[115]Milovanovic, N., Blundell, D., Pearson, R., Turner, J., Chen, R., 2005, “Enlarging the operational range of a gasoline HCCI engine by controlling the coolant temperature,” SAE Technical Paper.

[116]Yao, M., Zheng, Z., Liu, H., 2009, “Progress and recent trends in homogeneous charge compression ignition (HCCI) engines,” Prog Energy Combust Sci., 35 pp. 398–437. doi:10.1016/j.pecs.2009.05.001

[117]Angelos, J.P., Puignou, M., Andreae, M., Cheng, W., Green, W., Singer, M., 2008, “Detailed chemical kinetic simulations of homogeneous charge compression ignition engine transients,” Int J Engine Res., 9 pp. 149–64.

[118]Lü, X., Hou, Y., Zu, L., Huang, Z., 2006, “Experimental study on the auto-ignition and combustion characteristics in the homogeneous charge compression ignition (HCCI) combustion operation with ethanol/n-heptane blend fuels by port injection,” Fuel, 85 pp. 2622–31.

[119]Flowers, D., Dibble, R., Aceves, S., Westbrook, C., Smith, J., 2001, “Detailed chemical kinetic simulation of natural gas HCCI combustion: gas composition effects and investigation of control strategies,” J Eng Gas Turbines Power, 123 pp. 433–9.

[120]Chintala, V., and Subramanian, K.A., 2016, “Experimental Investigation on Effect of Enhanced Premixed Charge on Combustion Characteristics of a Direct Injection Diesel Engine,” International Journal of Advances in Engineering Sciences and Applied Mathematics, 6 (1-2) pp. 3–16. doi:10.1007/s12572-014-0109-7

[121]Schleppe, M. N., 2011, “SI-HCCI mode switching optimization using a physics based model [M.S. thesis],” University of Alberta.

[122]Olsson, J. O., Tunestål, P., Johansson, B., 2001, “Closed-loop control of an HCCI engine,” SAE Technical paper.

[123]Furutani, M., Ohta, Y., Kono, M., Hasegawa, M., 1998, “An ultra-lean premixed compression-ignition engine concept and its characteristics” The Fourth International Symposium COMODIA, 98 pp. 173-177.

[124]Akagawa, H., Miyamoto, T., Harada, A., Sasaki, S., Shimazaki, N., Hashizume, T., 1999, “Approaches to solve problems of the premixed lean diesel combustion,” SAE Technical paper.

[125]Yap, D., Megaritis, A., Peucheret, S., Wyszynski, M., Xu, H., 2004, “Effect of hydrogen addition on natural gas HCCI combustion,” SAE Technical paper.

[126]Xu, H., Wilson, T., Richardson, S., Wyszynski, M., Megaritis, T., Yap, D., 2004, “Extension of the boundary of HCCI combustion using fuel reforming technology,” JSAE Annual Cong Proc., pp. 23–6.

[127]Hosseini, V., Neill, W.S., Checkel, M.D., 2009, “Controlling n-heptane HCCI combustion with partial reforming: experimental results and modeling analysis,” J Eng Gas Turbines Power, 131 pp. 052801.

[128]Liu, H., Zheng, Z., Yao, M., Zhang, P., Zheng, Z., He, B., 2012, “Influence of temperature and mixture stratification on HCCI combustion using chemiluminescence images and CFD analysis,” Appl Therm Eng., 33 pp. 135–43.

[129]Yang JED, Y., Dronniou, N., Sjӧ Oberg, M., 2011, “Tailoring HCCI heat-release rates with partial fuel stratification: comparison of two-stage and single-stage-ignition fuels,” Proc Combust Inst., 33 pp. 2026–38.

[130]Jennische, M., 2003, “Closed-loop control of start of combustion in a homogeneous charge compression ignition engine (MSc Thesis),” Lund Institute of Technology.

[131]Caton, P.A., Simon, A.J., Gerdes, J.C., Edwards, C.F., 2003, “Residual-effected homogeneous charge compression ignition at a low compression ratio using exhaust reinduction,” Int J Engine Res., 4 pp. 163–77.

[132]Yamaoka, S., Kakuya, H., Nakagawa, S., Okada, T., Shimada, A., Kihara, Y., 2005, “HCCI operation control in a multi-cylinder gasoline engine,” SAE Technical paper.

[133]Christensen, M., Hultqvist, A., Johansson, B., 1999, “Demonstrating the multi fuel capability of a homogeneous charge compression ignition engine with variable compression ratio,” SAE Technical paper.

[134]Olsson, J.O., Tunestål, P., Johansson, B., Fiveland, S., Agama, R., Willi, M., 2002, “Compression ratio influence on maximum load of a natural gas fueled HCCI engine,” SAE Technical Paper.

[135]Hyvönen, J., Haraldsson, G., Johansson, B., 2003, “Supercharging HCCI to extend the operating range in a multi-cylinder VCR-HCCI engine,” SAE Technical paper.

[136]Chen, R., Milovanovic, N., Turner, J., Blundell, D., 2003, “The thermal effect of internal exhaust gas recirculation on controlled auto ignition,” SAE Technical paper.

[137]Fathi, M., Saray, R.K., Checkel, M.D., 2011, “The influence of Exhaust Gas Recirculation (EGR) on combustion and emissions of n-heptane/natural gas fueled Homogeneous Charge Compression Ignition (HCCI) engines,” Appl Energy, 88 pp. 4719–24.

[138]Haraldsson, G., Tunestål, P., Johansson, B., Hyvönen, J., 2004, "HCCI closed-loop combustion control using fast thermal management," SAE Technical paper.

[139]Maurya, R. K., Agarwal, A.K., 2011, "Experimental investigation on the effect of intake air temperature and air–fuel ratio on cycle-to-cycle variations of HCCI combustion and performance parameters," Appl Energy, 88 pp. 1153–63.

[140]Milovanovic, N., Blundell, D., Pearson, R., Turner, J., Chen, R., 2005, "Enlarging the operational range of a gasoline HCCI engine by controlling the coolant temperature," SAE Technical paper.

[141]Christensen, M., Johansson, B., 1999, "Homogeneous charge compression ignition with water injection," SAE Technical paper.

[142]Takeda, Y., Keiichi, N., Keiichi, N., 1996, "Emission characteristics of premixed lean diesel combustion with extremely early staged fuel injection," SAE Technical paper.

[143]Nakagome, K., Shimazaki, N., Niimura, K., Kobayashi, S., 1997, "Combustion and emission characteristics of premixed lean diesel combustion engine," SAE Technical Paper.

[144]Handford, D., Checkel, M., 2009, "Extending the load range of a natural gas HCCI engine using direct injected pilot charge and external EGR," SAE Technical paper.

[145]Ramesh, N., and Mallikarjuna, J.M., 2016, "Engineering Science and Technology, an International Journal Evaluation of incylinder mixture homogeneity in a diesel HCCI engine – A CFD analysis," Eng. Sci. Technol. an Int. J., 19(2), pp. 917–925.

[146]Harada, A., Shimazaki, N., Sasaki, S., Miyamoto, T., Akagawa, H., Tsujimura, K., 1998, "The effects of mixture formation on premixed lean diesel combustion engine," SAE Technical paper.

[147]Iwabuchi, Y., Kawai, K., Shoji, T., Takeda, Y., 1999, "Trial of new concept diesel combustion system-premixed compression-ignited combustion," SAE Technical paper.

[148]Aoyama, T., Hattori, Y., Mizuta, Ji., Sato, Y., 1996, "An experimental study on premixedcharge compression ignition gasoline engine," SAE Technical paper, pp. 960081. https://doi.org/10.4271/960081

[149]Christensen, M., Johansson, B., Einewall, P., 1997, "Homogeneous charge compression ignition (HCCI) using isooctane, ethanol and natural gas-a comparison with spark ignition operation," SAE Technical paper, pp. 972874. https://doi.org/10.4271/972874

[150]Kotas, T. J., 2013, "The exergy method of thermal plant analysis," Elsevier.

[151]Descamps, C., Bouallou, C., Kanniche, M., 2008, "Efficiency of an Integrated Gasification Combined Cycle (IGCC) power plant including $CO_2$ removal," Energy, 33(6) pp. 874-881.

[152]Chiesa, P., and Macchi, E., 2002, "A thermodynamic analysis of different options to break 60% electric efficiency in combined cycle power plants," In ASME Turbo Expo: Power for Land, Sea, and Air, pp. 987-1002.

[153]Maizza, V., and Maizza, A., 2001, "Unconventional working fluids in organic Rankine-cycles for waste energy recovery systems," Applied thermal engineering, 21(3) pp. 381-390.

[154]Bejan, A., 2016, "Advanced engineering thermodynamics," 4th ed. John Wiley & Sons, Inc.

[155]Moran, M. J., 1982, "Availability analysis: a guide to efficient energy use," New Jersey: Prentice-Hall.

[156]Moran, M. J., Shapiro, H. N., Boettner, D. D., Bailey, M. B., 2010, “Fundamentals of engineering thermodynamics,” John Wiley & Sons.

[157]Dincer, I., and Rosen, M. A., 2012, “Exergy: energy, environment and sustainable development,” Newnes.

[158]Hung, T. C., Wang, S. K., Kuo, C. H., Pei, B. S., Tsai, K. F., 2010, “A study of organic working fluids on system efficiency of an ORC using low-grade energy sources,” Energy, 35(3) pp. 1403-1411.

[159]Mahabadipour, H., 2017, “Second Law Analysis of Dual Fuel Low Temperature Combustion in a Single Cylinder Research Engine,” Mississippi State University.

[160]Nakonieczny, K., 2002, “Entropy generation in a diesel engine turbocharging system,” Energy, 27(11) pp. 1027-1056.

[161]Koroneos, C., Spachos, T., Moussiopoulos, N., 2003, “Exergy analysis of renewable energy sources,” Renewable energy, 28(2) pp. 295-310.

[162]Caliskan, H., Tat, M. E., Hepbasli, A., Van Gerpen, J. H., 2009, “Exergy analysis of engines fuelled with biodiesel from high oleic soybeans based on experimental values,” International Journal of Exergy, 7(1) pp. 20-36.

[163]Mahabadipour, H., and Ghaebi., 2013, “Development and comparison of two expander cycles used in refrigeration system of olefin plant based on exergy analysis,” Applied Thermal Engineering, 50 (1) pp. 771-780.

[164]Morosuk, T., and Tsatsaronis, G., 2008, “A new approach to the exergy analysis of absorption refrigeration machines,” Energy, 33(6) pp. 890-907.

[165]US DOE, 2017, “SuperTruck II, Vehicle Technologies Office Program Wide Selections to Accelerate the Development of Innovative Technologie,” https://www.energy.gov/articles/energy-department-announces-137-millioninvestment-commercial-and-passenger-vehicle

[166]Saad, D., Saad, P., Kamo, L., Mekari, M., Bryzik, W., Schwarz, E., Tasdemir, J., 2007, “Thermal barrier coatings for high output turbocharged diesel engine,” SAE Technical Paper, pp. 2007-01- 1442.

[167]Wakisaka, Y., Inayoshi, M., Fukui, K., Kosaka, H., Hotta, Y., Kawaguchi, A., Takada, N., “Reduction of heat loss and improvement of thermal efficiency by application of “temperature swing” insulation to direct-injection diesel engines,” SAE International Journal of Engines, 9(3) pp. 1449-1459.

[168]Pazek, T.W., 2004, “Thermodynamics of corn-ethanol bio-fuel cycle,” Crit Rev Plant Sci., 23(6) pp. 519-567. https://doi.org/10.1080/07352680490886905

[169]Mack, J.H., Aceves, S.M., and Dibble, R.W., 2009, “Demonstrating direct use of wet-ethanol in a homogeneous charge compression ignition engine,” Energy 34 (6) pp. 782-787. https://doi.org/10.1016/j.energy.2009.02.010

[170]Boldaji, M.R., Gainey, B., O’ Donnell, P., Gohn, J., Lawler, B., 2020, “Investigating the effect of spray included angle on thermally stratified compression ignition with wet ethanol using computational fluid dynamics,” Appl Therm Eng., 170 pp. 114964.

[171]Mack, J.H., Dibble, R.W., Buchholz, B.A, and Flowers, D.L., 2005, “The effect of the di-tertiary butyl peroxide (DTBP) additive on HCCI combustion of fuel blends of ethanol and di-ethyl ether,” SAE Technical Paper No. 2005-01-2135. https://doi.org/10.4271/2005-01-2135

[172]Lang, L., Colonna, P., and Almbauer, R., 2013, “Assessment of waste recovery from a heavy-duty truck engine by means of an ORC turbogenerator,” ASME *J. Eng. Gas Turbines Power,* 135 (4), pp. 042313. https://doi.org/10.1115/1.4023123

[173]Saidur, R., Rezaei, M., Muzammil, W.K., Hassan, M.H., Paria, S., Hasanuzzaman, M., 2012, "Technologies to recover exhaust heat from internal combustion engines," Renew Sust Energy Rev., 16 pp. 5649-5659.

[174]Saxena, S., Schneider, S., Aceves, S., and Dibble, R., 2012, "Wet ethanol in HCCI engines with exhaust heat recovery to improve the energy balance of ethanol fuels," Appl. Energy, 98 pp. 448-457, https://doi.org/10.1016/j.apenergy.2012.04.007

[175]Lodwig, E., 1970, "Performance of a 35 HP organic Rankine cycle exhaust gas powered system," SAE Paper pp. 700160. https://doi.org/10.4271/700160

[176]Di Nanno, L.R., Di Beilla, F.A., Koplow, M.D., 1983, "An RC-1 Organic Rankine bottoming cycle for an adiabatic diesel engine," Report DOE/NASA/0302-1, NASA CR-168256, December.

[177]Yu, G., Shu, G., Tian, H., Wei, H., Liu, L., 2013, "Simulation and thermodynamic analysis of a bottoming organic Rankine cycle (ORC) of diesel engine (DE)," Energy, 51 pp. 281-290.

[178]Wei, D, Lu, X., Lu, Z., Gu, J., 2007, "Performance analysis and optimization of organic Rankine cycle for waste heat recovery," Energy Convers Manage., 48 (4) pp. 1113-1119. https://doi.org/10.1016/j.enconman.2006.10.020

[179]Zhang, S.J., Wang, H.X., Guo, T., 2011, "Performance comparison and parametric optimization of subcritical organic Rankine cycle and transcritical power cycle system for low temperature geothermal power station," Appl Energy, 88 (8) pp. 2740-2754.

[180]Schuster, A., Karellas, S., Aumann, R., 2010, "Efficiency optimization potential in supercritical organic Rankine cycles," Energy, 35 (2) pp. 1033-1039.

[181]Tchanche, B.F., Lambrinos, G.R., Frangoudakis, A., Papadakis, G., 2011, "Low-grade heat conversion into power using organic Rankine cycles- a review of various applications," Renew Sust Energy Rev., 15 (8) pp. 3963-3979.

[182]Srinivas, K.K., Mago, P.J., and Krishnan, S.R., 2010, "Analysis of exhaust waste heat recovery from a dual fuel low temperature combustion engine using an organic Rankine cycle," Energy, 35(6), pp. 2387-2399, https://doi.org/10.1016/j.energy.2010.02.018

[183]Vaja, I., Gambarotta, A., 2010, "Internal combustion engine (ICE) bottoming with organic Rankine cycles (ORCs)," Energy, 35 pp. 1084-1093.

[184]Khaliq, A., Trivedi, S.K., Dincer, I., 2011, "Investigation of a wet ethanol fuelled HCCI engine based on first and second law analysis," Appl Therm Eng., 31(10), pp. 1621-1629.

[185]Saxena, S., Bedoya, I.D., Shah, N., Phadke A., 2013, "Understanding loss mechanisms and identifying areas of improvement for HCCI engines using detailed exergy analysis," ASME J. Eng. Gas Turbines Power, 135 (9) pp. 091505. https://doi.org/10.1115/1.4024589

[186]Khaliq, A., and Trivedi, S.K., 2012, "Second law assessment of a wet-ethanol fueled HCCI engine combined with organic Rankine cycle," ASME J. Energy Resour. Technol., 134(2) pp. 022201. https://doi.org/10.1115/1.4005698

[187]Qin, F., Chen, J., Lu, M., Chen, Z., Zhou, Y., Yang, K., 2007, "Development of a metal hydride refrigeration system as an exhaust gas driven automobile air conditioner," Renew Energy, 32 pp. 2034-2052.

[188]Najafi, M., Javahardeh, K., Liravinia, B., 2012, "Exergy analysis of a trigeneration system driven by an internal combustion engine with a steam ejector refrigeration system," Int J Adv Des Manuf Tech., 5(3) pp. 61-71.

[189]Unal, S., Yilmaz, T., 2015, “Thermodynamic analysis of the two-phase ejector air conditioning system for buses,” Appl Therm Eng., 79 pp. 108-116.

[190]Dai, Y., Wang, J., Gao, L., 2009, “Exergy Analysis, Parametric Analysis and Optimization for a Novel Combined Power and Ejector Refrigeration Cycle,” Appl Therm Eng., 29 pp. 1983-1990.

[191]Elakhdar, M., Landoulsi, H., Tashtoush, B., Nehdi, E., Kairouani, L., 2019, “A combined thermal system of ejector refrigeration and organic Rankine cycle for power generation using a solar parabolic trough,” Energy Convers Manage., 199 pp. 111947. https://doi.org/10.1016/j.enconman.2019.111947

[192]Habibzadeh, A., Rashidi, M.M., Galanis, N., 2013, “Analysis of a Combined Power and Ejector Refrigeration Cycle Using Low Temperature Heat,” Energy Convers Manage., 65 pp. 381-391. https://doi.org/10.1016/j.enconman.2012.08.020

[193]Manzela, A.A., Hanriot, S.M., Cabezas-Gomez, L., and Sodre, J.R., 2010, “Using engine exhaust gas as energy source for an absorption refrigeration system,” Appl. Energy, 87 (4) pp. 1141-1148. https://doi.org/10.1016/j.apenergy.2009.07.018

[194]Xia, J., Wang, J., Lou, J., Zhao, P., and Dai, Y., 2016, “Thermo-economic analysis and optimization of a combined cooling and power (CCP) for engine waste heat recovery,” Energy Convers. Manage., 128, pp. 303-316. https://doi.org/10.1016/j.enconman.2016.09.086

[195]Khaliq, A., Islam, S., Dincer, I., 2019, “Energy and exergy analyses of a HCCI engine-based system running on hydrogen enriched wet-ethanol fuel,” Int J Exergy, 28 (1) pp. 72-95. https://doi.org/10.1504/IJEX.2019.097272

[196]Parvez, M., Khaliq, A., 2014, “Exergy analysis of syngas fuelled cogeneration cycle for combined production of power and refrigeration,” Int J Exergy, 14(1) pp. 1-21.

[197]Rostamzadeh, H., Ebadollahi, M., Ghaebi, H., Amidpour, M., Kheiri, R., 2017, “Energy and exergy analysis of novel combined cooling and power (CCP) cycles,” Appl Therm Eng., 124 pp. 152-169.

[198]Chen, Y., Han, W., Jin, H., 2017, “Investigation of an ammonia-water combined power and cooling system driven by the jacket water and exhaust gas heat of an internal combustion engine,” Int J Refrigeration, 82 pp. 174-188.

[199]Klein, S.A., 2012, “Engineering Equation Solver (EES) for Microsoft Windows operating systems: Academic professional version: F-chart software,” Madison, W.I. (Available online http://www.fchart.com)

[200]REFPROP, 2013, “NIST Reference Thermodynamic and Transport Properties,” version 9.1.

[201]Somoyaji, C., Mogo, P.J., Chamra, L.M., 2006, “Second law analysis and optimization of organic Rankine cycle,” ASME Power Conference, Atlanta, Georgia, USA, pp. 591-596. https://doi.org/10.1115/POWER2006-88061

[202]Armstead, J.R., Miers, S.A., 2014, “Review of waste heat recovery mechanisms for internal combustion engine,” ASME J. Thermal Sci. Eng. Appl., 6 (1), pp. 014001. https://doi.org/10.1115/1.4024882

[203]Sara, H., Chalet, D., Cormerais, M., 2018, “Different configurations of exhaust gas heat recovery in internal combustion engine: evaluation on different driving cycles using numerical simulations,” ASME J. Thermal Sci. Eng. Appl., 10 (4), pp. 041010. https://doi.org/10.1115/1.4039304

[204]Hill, J., 2007, “Environmental costs and benefits of transportation biofuel production from food and lignocelluloses-based energy crops: a review,” Agron. Sustain. Dev., 27 (1), pp. 1-12, https://doi.org/10.1051/agro:2007006

[205]Ma, F., and Wang, Y., 2008, “Study on the extension of lean operation limit through hydrogen enrichment in a natural gas spark-ignition engine,” Int. J. Hydrogen Energy, 33 (4) pp. 1416-1424. https://doi.org/10.1016/j.ijhydene.2007.12.040

[206]Prashant, D.K., Lata, D.B., and Joshi, P.C., 2016, “Investigation on the effect of ethanol blend on the combustion parameters of dual fuel diesel engine,” Appl. Therm. Eng., 96 pp. 623-631. https://doi.org/10.1016/j.applthermaleng.2015.11.051

[207]Fagundez, J.L.S., Sari, R.L., Mayer, F.D., Martins, M.E.S., and Salau, N.P.G., 2017, “Determination of optimal wet ethanol composition as a fuel in spark ignited engine,” Appl. Therm. Eng., 112 pp. 317-325. https://doi.org/10.1016/j.applthermaleng.2016.10.099

[208]Yao, M.F., Zhang, Z., and Liu, H., 2009, “Progress and recent trends in homogeneous charge compression ignition (HCCI) engines,” Prog. Energy Combust. Sci., 35 (5) pp. 398-437. https://doi.org/10.1016/j.pecs.2009.05.001

[209]Rokopoulos, C.D., and Giakoumis, E.G., 2004, “Parametric study of transient turbocharged diesel engine operation from the second law perspective,” SAE Technical Paper No. 2004-01-1679. https://doi.org/10.4271/2004-01-1679

[210]Caton, J.A., 2012, “Exergy destruction during the combustion process as functions of operating and design parameters for a spark ignition engine, “Int J. Energy Res., 36(3) pp. 368-384. https://doi.org/10.1002/er.1807

[211]Boldaji, M.R., Gainey, B., and Lawler, B., 2019, "Thermally stratified compression ignition enabled by wet ethanol with a split injection strategy: A CFD simulation study," Appl. Energy, 235 pp. 813-826. https://doi.org/10.1016/j.apenergy.2018.11.009

[212]Roman, R., and Hernandez, J.I., 2011, "Performance of ejector cooling systems using low ecological impact refrigerants," Int. J. Refrigeration, 34 (7) pp. 1707-1716. https://doi.org/10.1016/j.ijrefrig.2011.03.006

[213]Galindo, J., Gil, A., Dolz, V., Ponce-Mora, A., 2020, "Numerical optimization of an ejector for waste heat recovery used to cool down the intake air in an internal combustion engine," ASME J. Thermal Sci. Eng. Appl., 12 (5), pp. 051024. https://doi.org/10.1115/1.4046906

[214]Jaruwongwittaya, T., and Chen, G., 2012, "Application of two stage ejector cooling system in a bus," Energy Procedia, 14 pp. 187-197. https://doi.org/10.1016/j.egypro.2011.12.916

[215]Zegenhagen, M.T., and Ziegler, F., 2015, "Feasibility analysis of an exhaust gas waste heat driven jet-ejector cooling system for charge air cooling of turbocharged gasoline engines," Appl. Energy, 160 pp 221-230. https://doi.org/10.1016/j.apenergy.2015.09.057

[216]Unal, S., 2015, "Determination of the ejector dimensions of a bus air-conditioning system using analytical and numerical methods," Appl. Therm. Eng., 90 pp. 110-119. https://doi.org/10.1016/j.applthermaleng.2015.06.090

[217]Zhang, H., Wang, L., Jia, L., and Wang, X., 2018, "Performance investigation of automobile waste heat recovery system for ejector refrigeration cycle" 13th IEEE Conference on Industrial Electronics and Applications (ICIEA): pp. 400-405. Wuhan, China, May 31-June 02. DOI: 10.1109/ICIEA 2018.8397750.

[218]Koehler, J., Tegethoff, W.J., Westphalen, D., and Sonnekalb, M., 1997, "Absorption refrigeration system for mobile applications utilizing exhaust gases," Heat and Mass Transfer 32 pp. 333-340. https://doi.org/10.1007/s002310050130

[219]Turns, S.R., and Kraige, D.R., 2007, "Properties Tables Booklet for Thermal Fluids Engineering," Cambridge University Press, New York.

[220]Khaliq, A., Habib, M.A., and Choudhary, K.A., 2019, "Thermo-environmental evaluation of a modified combustion gas turbine plant," ASME J. Energy Resour. Technol., 141(4) pp. 042004. https://doi.org/10.1115/1.4041898

[221]Steinhilber, T., and Sattelmayer, T., 2006, "The effect of water addition on HCCI diesel combustion," SAE Technical Paper No. 2006-01-3321.

[222]Khaliq, A., 2017, "Energetic and exergetic performance investigation of a solar based integrated system for cogeneration of power and cooling," Appl. Therm. Eng., 112 pp. 1305-1316. https://doi.org/10.1016/j.applthermaleng.2016.10.127

[223]Seckin, C., 2019, "Effect of operational parameters on a novel combined cycle of ejector refrigeration cycle and Kalina cycle, ASME J. Energy Resour. Technol., 142 (1) pp. 012001. https://doi.org/10.1115/1.4044220

[224]Shokati, N., Ranjbar, F., and Yari, M. A., 2018, "Comprehensive exergoeconomic analysis of absorption power and cooling cogeneration cycles based on Kalina part I: Simulation," Energy Convers. Manage., 158 pp. 437-459. https://doi.org/10.1016/j.enconman.2017.12.086

[225]Dhahad, H.A., Hussen, H.M., Nguyen, P.T., Ghaebi, H., and Ashraf, M.A., 2020, "Thermodynamic and thermoeconomic analysis of innovative integration of Kalina and absorption refrigeration cycles for simultaneously cooling and power generation," Energy Convers. Manage., 203 pp. 112241. https://doi.org/10.1016/j.enconman.2019.112241

[226]Chua, H.T., Toh, H.K., Malek, A., Ng K.C., Srinivasan, K., 2000, "Improved thermodynamic property fields of LiBr-$H_2O$ solutions," Int. J. Refrigeration, 23 (6), pp. 412-429. https://doi.org/10.1016/S0140-7007(99)00076-6

[227]Srinivas, K.K., Mago, P.J., and Krishnan, S.R., 2010, "Analysis of exhaust waste heat recovery from a dual fuel low temperature combustion engine using an organic Rankine cycle," Energy, 35(6), pp. 2387-2399, https://doi.org/10.1016/j.energy.2010.02.018

[228]Dolz, V., Novella, R., Garcia, A., and Sanchez, J., 2012, "HD Diesel engine equipped with a bottoming Rankine cycle as a waste heat recovery system. Part 1: study and analysis of the waste energy," Appl. Therm. Eng., 36, pp. 269-278. https://doi.org/10.1016/j.applthermaleng.2011.10.025

[229]Yu, Z., Han, J., Liu, H., and Zhao, H., 2014, "Theoretical Study on a Novel Ammonia-Water Cogeneration System with Adjustable Cooling to Power Ratios," Appl Energy, 122, pp. 53-61.

[230]Yu, W., Xu, Y., Wang, H., Ge, Z., Wang, J., Zhu, D., and Xia, Y., 2020, "Thermodynamic and thermoeconomic performance analyses and optimization of a novel power and cooling cogeneration system fueled by low-grade waste heat," Appl. Therm. Eng., 179, pp. 115667. https://doi.org/10.1016/j.applthermaleng.2020.115667

[231]Ruangtrakoon, K., and Aphornratana, S., 2019, "Design of steam ejector in a refrigeration application based on thermodynamic performance analysis," Sustainable Energy Technologies and Assessments, 31, pp. 369-382. https://doi.org/10.1016/j.seta.2018.12.014

[232]Abdulateef, J.M., Sopian, K., Alghoul, M.A., and Sulaiman, M.Y., 2009, “Review on solar-driven ejector refrigeration technologies,” Renew. Sustain. Energy Rev., 13, pp. 1338-1349.

[233]Alexis, G.K., and Karayiannis, E.K., 2005, “A solar ejector cooling system using refrigerant R134a in the Athens area,” Renew. Energy, 30 (9), pp. 1457–1469. https://doi.org/10.1016/j.renene.2004.11.004

[234]Bourhan, T., Aiman, A., Saja, A., 2015, “Performance study of ejector cooling cycle at critical mode under superheated primary flow,” Energy Convers. Manage., 94, pp. 300-310.

[235]Chandra, V.V., and Ahmed, M.R., 2014, “Experimental and computational studies on a steam jet refrigeration system with constant area and variable area ejectors,” Energy Convers. Manage., 79, pp. 377-386.

[236]Yılmaz, A., and Aktas, A.E., 2019, “Comparative Analysis of Ejector Refrigeration System Powered with Engine Exhaust Heat using R134a and R245fa,” European Mechanical Science, 3(1), pp. 13-17. https://doi.org/10.26701/ems.430831

[237]Kornhauser, A.A., 1990, “The use of an ejector as a refrigerant expander,” International Refrigeration and Air Conditioning Conference. Paper 82. http://docs.lib.purdue.edu/iracc/82

[238]Chaiwongsa, P., and Wongwises, S., 2007, “Effect of throat diameters of the ejector on the performance of the refrigeration cycle using a two-phase ejector as an expansion device,” Int. J. Refrigeration, 30, pp. 601-608.

[239]Pottker, G., Guo, B., and Hrnjak, P.S., 2010, “Experimental investigation of an R410A vapor compression system working with an ejector,” International

Refrigeration and Air Conditioning Conference, Paper 1135. http://docs.lib.purdue.edu/iracc/1135

[240]Lawrence, N.D., 2012, "Analytical and experimental investigation of two-phase ejector cycles using low-pressure refrigerants (MS Thesis)," University of Illinois, Urbana, IL, USA. http://hdl.handle.net/2142/42337

[241]Lawrence, N., and Elbel, S., 2013, "Theoretical and practical comparison of two-phase ejector refrigeration cycles including first and second law analysis," Int. J. Refrigeration, 36, pp. 1220-1232.

[242]Wang, X., and Yu, J., 2016, "An investigation on the component efficiencies of a small two-phase ejector," Int. J. Refrigeration, 71, pp. 26-38.

[243]Siddiqui, M.A., Khaliq, A., and Kumar, R., 2021, "Proposal and analysis of a novel cooling-power cogeneration system driven by the exhaust gas heat of HCCI engine fueled by wet-ethanol," Energy, 232, pp. 120954. https://doi.org/10.1016/j.energy.2021.120954

[244]Yu, W., Wang, H., Ge, Z., 2021, "Comprehensive analysis of a novel power and cooling cogeneration system based on organic Rankine cycle and ejector refrigeration cycle," Energy Convers. Manage., 232, pp. 113898. https://doi.org/10.1016/j.enconman.2021.113898

[245]Djermouni, M., Ouadha, A., 2014, "Thermodynamic analysis of an engine based system running on natural gas," Energy Convers Manage., 88 pp. 723-731. https://doi.org/10.1016/j.enconman.2014.09.033

[246]Zheng, Z.Q., Yao, M.F., Chen, Z., and Zhang, B., 2004, "Experimental study on HCCI combustion of dimethyl ether (DME)/methanol dual fuel," SAE Paper 2004-01-2993.

[247]Mo, Y., 2002, “HCCI heat release rate and combustion efficiency: a coupled kiva multi-zone modeling study,” PhD Thesis, University Michigan, USA.

[248]Soyhan, H.S., Yasar, H., Head, B., Kalghatgi, G.T., and Sorusbay, C., 2009, “Evaluation of heat transfer correlations for HCCI engine modeling,” Appl Therm Eng., 29, pp. 541-549.

[249]Olof, E., 2002, “Thermodynamic simulation of HCCI engine systems,” PhD Thesis, Lund University, Sweden.